

---

# **Guidance of Missiles**

*Debasish Ghose*

*Guidance, Control, and Decision Systems Laboratory  
Department of Aerospace Engineering  
Indian Institute of Science  
Bangalore, India*

*NPTEL COURSE  
March 2012*

---

© Debasish Ghose, 2012

These lecture notes are for the web course offered through NPTEL and should not be reproduced in any medium without explicit permission of NPTEL and the author.

## Foreword

These lecture notes cover material on guidance of missiles. The first few chapters are dedicated to the basic concepts of guidance of missiles. The formulation of guidance problems are developed from the basics and both the classical guidance laws and modern guidance laws are covered. The later chapters focus on specific applications of guided missiles and introduce some advanced guidance laws and their variants.

**Acknowledgements.** These lecture notes have been in the making since 1996 and have gone through several revisions, additions, and changes through class room teaching to master's students at IISc. I am indebted to the students who attended these classes and gave me valuable inputs. The work of my PhD and Master's students also find a place in these notes. However, the two reviewers (Dr. S.E. Talole of DIAT and Dr. A Sinha of IIT-B), who reviewed these specific NPTEL course notes, deserve a special note of thanks for their meticulous review and excellent suggestions.

**Suggestions for Students.** This web course is designed for self reading and learning although you may have an instructor who will teach you. The best way to learn any new subject is to read and understand it yourself. There are several assignments and questions given at the end of almost all the lectures. The assignments are of two types. the first type is descriptive in which you need to collect information from web resources and books and write a descriptive term paper. The second type are those which may require some familiarity with MATLAB to generate the numerical results and are an important part of learning the subject. You will see that these results will supplement the material in the course notes and help you to understand them better. Finally, the questions are those that help you to test your understanding of the subject. These can be descriptive or numerical.

**Suggestions for Instructors.** An important aspect of teaching is a continuous but informal evaluation of how much the student has gained in terms of knowledge. Also, the best teacher is one who can get the students involved in the course. The assignments in this web course is designed to get the students interested and involved. As the course is meant for graduate students or senior undergraduates, some of the material in the course is not covered explicitly but is given in the form of assignments through which the students will be able to get a better understanding of the concepts. When you evaluate the assignments please assign marks not just for the results obtained but also to originality, presentation, and interpretation of the results. Encourage them to discuss the results in the light of the course material. Finally, the list of questions given can be used to set questions for tests and final examinations. Note that many questions are similar and may demand answers that are also similar. This repetition is intentional as it gives the instructors more flexibility in selecting questions and for the student to test his/her knowledge gained in the course. Please do allocate marks for the assignments as well as to answers to questions in the test when you are evaluating the students for their final grades.

Finally, both students and instructors, please feel free to contact me over email if you have any questions and/or suggestions.

**Debasish Ghose** (dghose@aero.iisc.ernet.in)  
Indian Institute of Science, March 2012



# Contents

<b>1</b>	<b>Introduction</b>	<b>1</b>
1.1	What is Guidance? . . . . .	1
1.2	What is a Guided Missile? . . . . .	3
1.2.1	Surface-to-Surface Missiles . . . . .	4
1.2.2	Surface-to-Air Missiles . . . . .	5
1.2.3	Air-to-Surface Missiles . . . . .	5
1.2.4	Air-to-Air Missiles . . . . .	6
1.3	Tactical vs. Strategic Missiles . . . . .	6
1.4	Other of Missiles . . . . .	7
1.5	Peaceful Applications of Guidance . . . . .	7
1.5.1	Applications in Robotics . . . . .	8
1.5.2	Smart Cars on Smart Roads . . . . .	8
1.5.3	Docking of Spacecrafts . . . . .	9
1.5.4	Terrain Avoidance . . . . .	9
<b>2</b>	<b>History of Guided Missiles</b>	<b>11</b>
2.1	Early History . . . . .	11
2.2	Before World War I . . . . .	12
2.3	World War I and After . . . . .	13
2.4	During World War II . . . . .	15
2.5	After World War II . . . . .	15
2.6	The Indian Missile Program . . . . .	17

2.7 Concluding Remarks . . . . .	17
<b>3 Major Components of Tactical Missiles</b>	<b>19</b>
3.1 Airframe . . . . .	19
3.2 Flight Control System . . . . .	26
3.3 Guidance Subsystem . . . . .	32
3.4 Proximity Fuze . . . . .	35
3.5 Propulsion System . . . . .	37
3.6 Warhead . . . . .	37
3.7 Concluding Remarks . . . . .	39
<b>4 Fundamentals of Guidance</b>	<b>41</b>
4.1 Guidance Phases During Missile Flight . . . . .	41
4.2 Different Categories of Homing Guidance . . . . .	44
4.2.1 Active Homing . . . . .	44
4.2.2 Semi-Active Homing . . . . .	45
4.2.3 Passive Homing . . . . .	45
4.3 Some Standard Terminologies in Missile Guidance . . . . .	48
4.4 The Kinematic Equations . . . . .	53
4.5 The Collision Geometry . . . . .	54
4.6 Capturability . . . . .	55
4.7 Concluding Remarks . . . . .	57
<b>5 Basic Results in Interception and Avoidance</b>	<b>59</b>
5.1 Engagement Between Two Point Objects . . . . .	60
5.1.1 Equations of motion . . . . .	60
5.1.2 $(V_\theta, V_R)$ -trajectory . . . . .	61
5.1.3 The collision condition and the collision triangle . . . . .	65
5.1.4 Miss-distance . . . . .	67
5.1.5 Effect of lethal radius . . . . .	68

5.1.6 Asymptotic behaviour of $V_\theta$ and $V_R$ . . . . .	70
5.2 Avoidance . . . . .	70
5.3 Concluding Remarks . . . . .	70
<b>6 A Taxonomy of Guidance Laws</b>	<b>73</b>
6.1 An Overview of Guidance Laws . . . . .	73
6.2 Conceptual Classical Guidance Laws . . . . .	79
6.2.1 Pursuit guidance law . . . . .	79
6.2.2 Constant bearing course . . . . .	81
6.3 Implementable Classical Guidance Laws . . . . .	84
6.3.1 Line-of-Sight (LOS) Guidance . . . . .	84
6.3.2 Proportional Navigation (PN) Guidance . . . . .	88
6.4 Modern Guidance Laws . . . . .	91
6.4.1 Modern Guidance Scheme . . . . .	92
6.4.2 Differential Games Guidance Laws . . . . .	93
6.4.3 Reachable Set Guidance Law . . . . .	94
6.4.4 Predictive Guidance Laws . . . . .	95
6.5 Concluding Remarks . . . . .	96
<b>7 The Pursuit Guidance Law</b>	<b>98</b>
7.1 Pure Pursuit Guidance Law . . . . .	98
7.1.1 The engagement equations . . . . .	98
7.1.2 Trajectory in the $(V_\theta, V_R)$ -space . . . . .	100
7.1.3 The capture region . . . . .	102
7.1.4 Time of interception . . . . .	104
7.1.5 Lateral acceleration history . . . . .	105
7.1.6 Miss-distance . . . . .	106
7.2 Deviated Pursuit Guidance Law . . . . .	110
7.2.1 The engagement equations . . . . .	110
7.2.2 Trajectory in the $(V_\theta, V_R)$ -space . . . . .	111

Good  
for latek  
Github desc


7.2.3	The capture region . . . . .	117
7.2.4	Time of interception . . . . .	118
7.2.5	Lateral acceleration history . . . . .	119
7.3	Implementation . . . . .	119
7.4	Concluding Remarks . . . . .	121
<b>8</b>	<b>The Line of Sight Guidance Law</b>	<b>123</b>
8.1	LOS Guidance . . . . .	124
8.2	Implementation of LOS Guidance . . . . .	128
8.2.1	Beam-Rider (BR) Guidance . . . . .	129
8.2.2	Command to Line-of-Sight (CLOS) Guidance . . . . .	131
8.3	Some Additional Analysis . . . . .	135
8.3.1	The nonlinear engagement block in the BR/CLOS guidance loop	135
8.3.2	Capturability analysis . . . . .	136
8.4	Concluding Remarks . . . . .	137
<b>9</b>	<b>An Introduction to Proportional Navigation</b>	<b>140</b>
9.1	Pure Proportional Navigation (PPN) . . . . .	142
9.2	True Proportional Navigation (TPN) . . . . .	142
9.3	Generalized TPN (GTPN) . . . . .	144
9.4	Ideal Proportional Navigation (IPN) . . . . .	145
9.5	Concluding Remarks . . . . .	145
<b>10</b>	<b>True Proportional Navigation</b>	<b>147</b>
10.1	Original TPN with Non-Maneuvering Target . . . . .	148
10.2	Realistic True Proportional Navigation . . . . .	155
10.3	Comparison of TPN Guidance Laws . . . . .	161
10.4	Miss-Distance Analysis . . . . .	161
10.4.1	Miss-distance analysis for original TPN . . . . .	162
10.4.2	Miss distance analysis for RTPN . . . . .	169

10.5 Concluding Remarks . . . . .	173
<b>11 Pure Proportional Navigation</b>	<b>176</b>
11.1 Non-Maneuvering Target . . . . .	177
11.1.1 An Illustrative Example . . . . .	188
11.1.2 Comments . . . . .	191
11.2 Maneuvering Target . . . . .	192
11.2.1 Missile latax . . . . .	202
11.2.2 Representation in the LOS referenced frame . . . . .	204
11.2.3 Representation of PPN capturability in the relative velocity space	207
11.3 Concluding Remarks . . . . .	210
<b>12 Applications of Guidance</b>	<b>214</b>
12.1 PN Based Impact Angle Constrained Guidance . . . . .	214
12.2 Impact Angles Against a Stationary Target with PN . . . . .	215
12.3 Orientation Guidance . . . . .	217
12.3.1 Orientation guidance command . . . . .	218
12.3.2 Properties of the orientation trajectory . . . . .	218
12.4 Composite Guidance law . . . . .	221
12.5 Simulations Results . . . . .	221
12.5.1 Constant speed missile model . . . . .	222
12.5.2 Realistic missile model . . . . .	224
12.6 Impact Angles Against a Moving Target with Proportional Navigation .	228
12.7 Orientation Guidance . . . . .	231
12.7.1 Orientation guidance command . . . . .	232
12.7.2 Properties of the orientation trajectory . . . . .	232
12.8 The Proposed Guidance law . . . . .	236
12.9 Simulation Results . . . . .	236
12.9.1 Constant speed interceptor . . . . .	236
12.9.2 Realistic interceptor . . . . .	239

<b>13 Optimal Control Based Guidance Laws</b>	<b>244</b>
13.1 Linearized Proportional Navigation . . . . .	244
13.1.1 Heading Error . . . . .	246
13.1.2 Maneuvering target . . . . .	248
13.1.3 Zero Effort Miss . . . . .	249
13.1.4 Augmented proportional navigation . . . . .	249
13.1.5 Comparison between PN and APN . . . . .	251
13.2 Linear Optimal Control . . . . .	253
13.3 Optimal Control Based Guidance Laws . . . . .	260
13.3.1 Case 1: No terminal constraints; Fixed terminal time . . . . .	260
13.3.2 Case II: Some state variables specified at a fixed terminal time . . . . .	265
13.3.3 Case III: Functions of state variables specified at a fixed terminal time . . . . .	267
13.3.4 Case IV: Some State Variables specified at an unspecified terminal time (Including minimum time problems) . . . . .	268
13.4 Conclusions . . . . .	268

# Chapter 1

## Introduction

### Module 1: Lecture 1 What is Guidance?

**Keywords.** Guided missiles, Tactical missiles, Strategic missiles, SAM, AAM, ASM, SSM

#### 1.1 What is Guidance?

Quite often people use the phrase *guidance and control* as a single entity. The reason is that these two aspects almost always go hand-in-hand and there is no sharp distinction between them. The intervening space is a grey area that some call *guidance* and others *control*. But if you look at the overall picture you will realize that *guidance* is distinct from *control*, although textbooks – even those which are specifically written on guidance – fail to give a clear distinctive definition to these two terms. At the beginning of the lecture let me make these definitions clear. I will borrow from one of the leading experts in this field, *Professor Arthur E. Bryson*, who came up with a fairly clear definition of these terms. This he did in a paper published in the *Journal of Guidance, Control, and Dynamics* in the year 1985 [see Bryson (1985)]. Curiously enough, such a clear definition did not exist before Bryson defined these terms, although guidance and control as separate entities has been active areas of research for many years.

A flight vehicle, regardless of whether it is a missile, an aircraft, or a launch vehicle,

needs the help of human intelligence to achieve its mission. This human intelligence manifests itself in various forms like gathering information about flight conditions, generating appropriate commands to the flight vehicle, and designing equipments to interpret these commands and translate them into action on-board. Each flight vehicle has a mode of operation which might differ from another. For example, in a missile or a launch vehicle, information is gathered by various sensors and conveyed to a computer which then takes appropriate decisions. In an aircraft it is usually the human pilot who takes decisions based upon similar information.

Irrespective of the kind of flight vehicle, the theory behind the design and analysis of all these tasks eventually emanates from a branch of applied mathematics called *control theory*. The application of control theory to aerospace may be divided into four areas.

- *Flight path planning:* This refers to the determination of a nominal flight path and associated control histories for a given flight vehicle to accomplish specified objectives with specified constraints.
- *Navigation:* The determination of a strategy for estimating the position of a vehicle along the flight path, given the outputs from specified sensors.
- *Guidance:* The determination of a strategy for following the nominal path in the presence of off-nominal conditions, wind disturbances, and navigational uncertainties.
- *Control:* The determination of a strategy for maintaining the angular orientation of the vehicle during the flight that is consistent with the guidance strategy, and the vehicle, crew, and passenger constraints.

However, it should be kept in mind that the boundaries between these four categories are not very sharp and they often overlap. For example, consider the aircraft velocity and its angular orientation. These are coupled and so the guidance and control of an aircraft must be considered together.

Since the focus of these lectures are mainly on guidance of flight vehicles, let us define the term *guidance* in an intuitively appealing manner:

*When one object, based on information gathered from its environment, moves in such a way that it comes closer and closer to another stationary or moving object (a goal point) then we say that the object is guiding itself toward its goal point.*

The basic questions that a guidance system designer addresses are the following:

- *What information do we need to collect from the environment?*
- *How do we go about collecting this information?*
- *How much can we trust the correctness of this information?*
- *How do we use this information to achieve our goal? (This, in fact, is the main objective of guidance!)*
- *Is our capability sufficient to meet our goal?*
- *How do we know if we have reached our goal or not?*
- *Are there some secondary goals that we must keep in mind while trying to achieve our primary goal? If yes, then how do we go about doing it?*

## 1.2 What is a Guided Missile?

Guided missiles have been in the forefront of modern warfare since the Second World War. Although it is true that guided missiles are mainly used for destructive purposes, one cannot disregard the fact that they are the most outstanding examples of the application of scientific techniques to design, control, and guide remote vehicles without direct human intervention.

A simple definition of a guided missile would be the following [see Locke (1955)]:

*A guided missile is a space-traversing unmanned vehicle which carries within itself the means for controlling its flight path.*

Another definition, based on its operational principle, could be the following [see Garnell and East (1977)]:

*A guided missile is one which is usually fired in a direction approximately toward the target and subsequently receives steering commands from the guidance system to improve its*

*accuracy.*

A number of different classifications of guided missiles are possible. However, the most usual is the one in which the *position of the launch point* and the *position of the target* are used as the basis for classification [see Locke (1955)]. This is the most widely used classification as these positions more or less designate the general requirements or specialities of the missiles used. The four general categories of missiles are :

- *Surface-to-Surface Missiles (SSM)*
- *Surface-to-Air Missiles (SAM)*
- *Air-to-Air Missiles (AAM)*
- *Air-to-Surface Missiles (ASM)*

### 1.2.1 Surface-to-Surface Missiles

These missiles are launched from some point on the surface of the earth to another point on the surface of the earth. They could also be launched from a ship. These missiles are usually employed against *large and stationary targets*. The range of the missile and the type of warhead it uses depends on the kind of targets. The target could be a small factory or a big city. The range could be as low as a few kilometers to as high as thousands of kilometers. Though the terminal accuracy required of the missile guidance system is usually not much, the accuracy required for targets at long range must be high compared to those required for short ranges. However, many recently designed surface-to-surface missiles demand very high terminal accuracy. The accuracy of such missiles depends, to a large extent, on the accuracy of determining the position of the target with reference to some standard frame.

Missiles of this kind, by the very nature of their use, are *offensive missiles*. Missiles employed for long-range targets are also known as *strategic missiles*. Short Range, Intermediate Range, and Inter-Continental Ballistic Missiles (*SRBM*, *IRBM*, and *ICBM*) are some of the generic names (based on the range performance) of these missiles. Some examples of this type of missiles are : *CSS-3 ICBM* (Country of origin : China, Maximum range : 7000 km), *SS-18 Satan ICBM* (CIS-formerly USSR, 12000 km), *Minuteman ICBM* (USA, 12500 km).

There could be a further classification of SSMs as *ballistic missiles* (those which leave the atmosphere after launch and fly in a ballistic trajectory till re-entry into the atmosphere) and *cruise missiles* (which fly at a relatively low altitude within the atmosphere).

### 1.2.2 Surface-to-Air Missiles

Any guided missile launched from a point on the surface of the earth to destroy a target in the air qualifies for this category. The launch point, however, could be either a ship or land. Here the targets are always in motion and quite often have considerable maneuvering capability. The guidance system must be accurate since the targets are usually *small in size, move at high speeds, and/or are capable of executing complicated maneuvers* (e.g., fighter aircraft, helicopters, SSMs). Thus, these missiles have support equipments which continuously collect information about the current position and velocity of the target. The *time available* for the missile to destroy a flying target is *usually small* and so the guidance system must be able to take appropriate actions in a short period of time.

These missiles are normally used as *defensive weapons*. Some examples of such missiles are : *Gremlin SA-14* (CIS, 6 km), *MANPADS* (France, 4-6 km), *Stinger* (USA, 45 km), *Patriot* (USA, 160 km).

### 1.2.3 Air-to-Surface Missiles

These missiles are usually launched from an aircraft to destroy targets on the surface of the earth. The targets could be moving (not at very high speeds) but are normally *stationary*. The launch point (aircraft) is in motion. Hence, it is possible to *search and seek out* targets whose positions or movements are not known beforehand. In other words, the targets for such missiles are seldom predetermined as in the case of SSMs, which means that the missile must have some means of seeking out these targets. This causes the additional problems of avoiding spurious signals from the ground. Since it is possible to come close to the target, accuracy can also be improved. However, the launch point itself moves, and so the velocity and other dynamic properties of the aircraft must be taken into account in the guidance system.

These missiles are primarily *offensive weapons* but can also be considered a *defen-*

sive weapon system depending on their actual use. Some examples are : *Gabriel MK-III* (Israel, 40 km), *HARM AGM-88A* (USA, 25 km).

#### 1.2.4 Air-to-Air Missiles

Here, both the launch point and the target are aircraft. These missiles are perhaps the *most difficult to design and build*. Both aircraft are in motion at high speeds. They are also capable of *high maneuverability*. Targets are small and difficult to locate. The guidance system has to take into account all the factors mentioned for SAMs at the target end, and those mentioned for ASMs at the launch end. In addition, the guidance system should be such that it should not prevent the aircraft which launches the missile from taking evasive actions for its own survival after the missile has been launched.

These missiles can be used both as *offensive* and *defensive* weapon systems. Some examples are : *Super 530* (France, 25 km), *Ash AA-5* (CIS, 5-20 km), *Sidewinder AIM-9* (USA, 5-15 km).

### 1.3 Tactical vs. Strategic Missiles

*Tactical missiles* are those which are used for achieving some *short-term missions*. By the very nature of their function they are *small in size*, have *short ranges*, and have *limited destructive power*. The short missions could be that of destroying a penetrating enemy aircraft using a SAM or an AAM, destroying a small ground target (for example, an enemy tank or an enemy supply base) using an ASM. Seldom are large SSMs used for this kind of missions. Again, judging by their mission, tactical missiles are *mainly defensive weapons* with limited capability for offence.

*Strategic missiles* are those that are used to achieve *long term goals* – the kind of goals that will make a strategic difference to the outcome of a war. By the very nature of their function they are *large in size*, have *long ranges*, and have *vast destructive capabilities*. These are mainly SSMs and their missions could be destruction of a huge military-industrial complex in the enemy territory or even big cities. These weapons are mainly *offensive weapons*.

*In these lectures we will restrict our attention only to the guidance of tactical missiles which are mainly used for defensive purposes – for example, SAM category of missiles. We shall*

*study the guidance laws that are used to guide these missiles and also study how these guidance laws and the fundamental principles behind them can be used for building many systems that have predominantly peaceful uses.*

#### 1.4 Other of Missiles

Some terms referring to some special types of missiles are also used in common parlance. For instance, anti-satellite missiles (used to destroy military satellites), anti-radiation missiles (that detects the presence of active radars by identifying their radiations and destroys them), submarine launched missiles (these are missiles that are launched from a submarine from the depths of the ocean and emerges into the atmosphere, and may continue on to exit the atmosphere and follow a ballistic trajectory, ending with re-entry), anti-tank missiles (specially designed to penetrate tank armours), etc.

#### 1.5 Peaceful Applications of Guidance

It is a proven fact of history that the most rapid advancement in modern science and technology took place during the First and the Second World War and its aftermath in the era of the cold war. The intense research and development activities that took place during the Second World War spilled over into the second half of this century and by its sheer momentum spawned an innumerable number of scientific inventions that ultimately contributed to give us the modern society that we live in.

One of the lesser known facts is the contributions that the defence aerospace engineering industry in the US has made to nurture the infant computer technology in the fifties and give it a firm footing. Similarly, missile research has given rise to many advanced technologies like small, compact, and light-weight antennas, efficient and robust control systems, propulsion technology, among many others, that have a much larger domain of important peaceful applications than those for which they were originally intended.

Equally important is the fact that, contrary to popular belief, there are numerous *peaceful applications of guidance theory* that are emerging in the present day scenario of a modern society based on rapid technological progress. The theory of guidance pro-

vides the basic framework for solving these important and practical problems in engineering. Below we shall list some of them.

### 1.5.1 Applications in Robotics

One of the major problems in robotics is that of *path planning of robots to avoid stationary or moving obstacles* as robots move about in their work environment. Avoidance of obstacles basically involves the *detection of the obstacle, prediction of its trajectory, and taking corrective actions* to ensure that there is no collision. The first two can be directly identified with the intermediate goals in a guidance problem. The last is diametrically opposite to what guidance has as a goal – in fact, it is so diametrically opposite that the principles of guidance are also applicable to it. We shall show how this is so toward the end of these lectures.

But apart from collision avoidance, guidance also has applications in another sense in the robotics path planning. Automated guided vehicles, often have the goal of going from a *start point* to a *goal* or *destination point*. This also requires guidance. But note that the guidance that an automated guided vehicle will require will be based on a different kind of system model. When we talk of missiles we are talking about a flight vehicle where we do not have much control over the longitudinal velocity of the vehicle but only on its lateral motions through aerodynamic control. Whereas, when we speak of an automated guided vehicle we are talking about a vehicle which moves on ground, is subject to both longitudinal and lateral control, and accordingly requires guidance which can be expressed in terms of a larger number of parameters.

### 1.5.2 Smart Cars on Smart Roads

One of the major problems faced in the western industrialized countries is the problem of transportation of people and goods over the surface of the globe [Varaiya (19993)]. The need to transport people will reduce, to a large extent (and will hopefully cease to be a problem!), by the tremendous technological advancements in telecommunications and the creation of the information superhighway. This will most probably become a workable reality by the turn of this century. But transportation of goods by the conventional means of railroad and highways will remain a necessary reality in the foreseeable future. To improve the system of surface transportation there are massive projects being

undertaken to create what are known as smart cars on smart roads. The essential idea behind these projects is to transfer the major part of the control of a car to an automatic controller that will ensure that vehicles can move at tremendous speeds with very little separation between them across long distances, on roads equipped with smart sensors. For this we need sensors and other systems that can detect imminent collisions and take fast corrective actions. These are objectives that are at the core of guidance theory and its applications.

#### **1.5.3 Docking of Spacecrafts**

Docking is an operation by which one object fixes itself in a certain way on to a larger object. For example, docking of a ship in its wharf involves this kind of maneuvers. In futuristic space stations docking of a spacecraft will be one of the most intricate maneuvers that will be performed. A spacecraft as well as a space station normally has many appendages (antennas, solar panels, solar shields, and so on) which give them a somewhat unwieldy shape. These appendages make the docking operation more complicated as the spacecraft has to avoid collision between two appendages and at the same time perform maneuvers that would make the docking operation successful. This problem is related to the path planning problem in robotics but combines the features of space operations along with conventional robotics.

#### **1.5.4 Terrain Avoidance**

Helicopters and other low-flying vehicles have to detect and avoid the underlying terrain. They have to pass through mountain ranges where there is possibility of frontal collision. To help the pilot in detecting and avoiding such collisions automatic pilot advisory systems are built and put in the helicopter. There is considerable scope of guidance theory being used, and is indeed being explored, for this kind of applications.

### *Assignment*

1. Collect data about one missile each of the four category of missiles (AAM, ASM, SAM, SSM). Do this for each of the following countries: India, USA, China, Rus-

sia, France, Germany, Pakistan. The data should cover standard information like airframe configuration, size, weight, range, type of propulsion, etc.)

Use internet resources for this purpose. Wikipedia, Jane's, etc., are standard web resources. However, please mention the source from which you collect data. Always acknowledge the web source from which you have taken a picture to illustrate your data. This is ethical practice that must be followed.

### *Questions*

1. Define (a) SAM (b) SSM (c) ASM (d) AAM.
2. What are tactical missiles and how are they different from strategic missiles.
3. Define the terms (a) Flight path planning (b) Navigation (c) Guidance (d) Control.
4. Describe a scenario involving a Air to Surface Missile (ASM) attacking a surface target where all the above four components can be identified.
5. What is a guided missile?

### *References and Further Reading*

1. A.E. BRYSON: New concepts in control theory, 1959-1984, *Journal of Guidance, Control, and Dynamics*, Vol. 8, No. 4, pp. 417-425, July-August 1985.
2. P. GARNELL AND D.J. EAST: *Guided Weapon Control System*, Pergamon Press, 1977.
3. A.S. LOCKE: *Guidance*, D. Van Nostrand Co., 1955.
4. R.G. LEE, C.A. SPARKES, D.E. JOHNSON: *Guided Weapons*, Brassey's Inc, 3rd Edition, 2000.
5. P. VARAIYA: Smart cars on smart roads: Problems of control, *IEEE Transactions on Automatic Control*, Vol. 38, No. 2, February 1993, pp. 195-207.

## Chapter 2

# History of Guided Missiles

## Module 1: Lecture 2 History of Guided Missiles

**Keywords.** History, First World War, Second World War, IGMDP

Use of guided missiles has become an essential feature of modern warfare. Though such missiles have been in use only during the past few decades, their evolution from more primitive weapons has taken place over a period of many centuries. This evolution can be traced through history under various periods of development.

### 2.1 Early History

The idea of using *arrows and spears*, which can be thrown from a distance for hunting or warfare, has been there since pre-historical times. Such weapons served only a limited purpose since their range and destructive power was limited. Obviously enough, to increase the effectiveness of these weapons, subsequent developments concentrated on the task of overcoming these limitations. It is a historical fact that the *Greeks* used *flaming arrows* against the *Arabs* in the *war of Constantinople* in the 7th century. These were essentially arrows or spears with lighted torches tied to them. The *Chinese*, in the 10th century, were known to use *bamboo tubes filled with explosive powder* which was used to propel the tubes to some distance. This is perhaps the first recorded instance of

*solid-propellant rockets* being used in warfare. These rockets were later used in Europe in the 14th century in the *war between Venice and Genoa*. During this time people like *Albert Magnus* in Germany and *Roger Bacon* in England, in the 13th century, and *Leonardo da Vinci* and *Giovanni da Fontana*, both from Italy, in the 15th century, had begun investigating the design of such rockets. Some documents and drawings testifying to their imaginative approach to the problem still survive. Subsequently, a German engineer *Conrad Haas*, in the 16th century, sketched a *multi-stage rocket* in which the first stage burns itself out, thus saving the trouble of separating this stage from the missile body. Haas also proposed a *swept-back fin arrangement* to improve the stability of the rocket.

## 2.2 Before World War I

In the 18th century the *British and French forces* were battling the *armies of various kingdoms in India*. During this time the Indian soldiers were reported to be using *incendiary rockets* which caused much discomfort to the European soldiers. These rockets weighed about 3 to 6 kgs and could be fired either in a *ballistic path* or in a *horizontal path* close to the ground. This kind of rocket essentially had a cylinder filled with gunpowder and a stick attached to the side and extending to the rear (Figure 2.1(a)). The destructive capability of these rockets was somewhat limited but they provided a *certain strategic advantage* to the Indians since the weapons were new to the enemy and in addition to scaring the horses in the cavalry they also created a fear among the soldiers. These rockets were of *simple design*, could be *easily transported, easily operated*, and were *readily producible* - properties which are desirable even for modern missiles.

A British army colonel, *William Congreve*, was impressed by these Indian rockets and began experimenting with them in the early 19th century. He was able to stabilize the rockets further by *extending the stick to the rear and later moving it to the center of the cylinder* (see Figure 2.1(b)), so that the rockets could be inserted into a tube and launched. He was also able to increase their weight to about 150 kgs, and designed them to carry a warhead of about 25 kgs at the nose-end. He recognised the fact that the weight and the center of gravity of these rockets change during flight and a good design must account for these changes. The *Congreve rockets* became popular with the British and were used extensively against the French in the *Napoleonic wars* in the beginning of the 19th century. It is reported that in 1807 the *city of Copenhagen* was completely

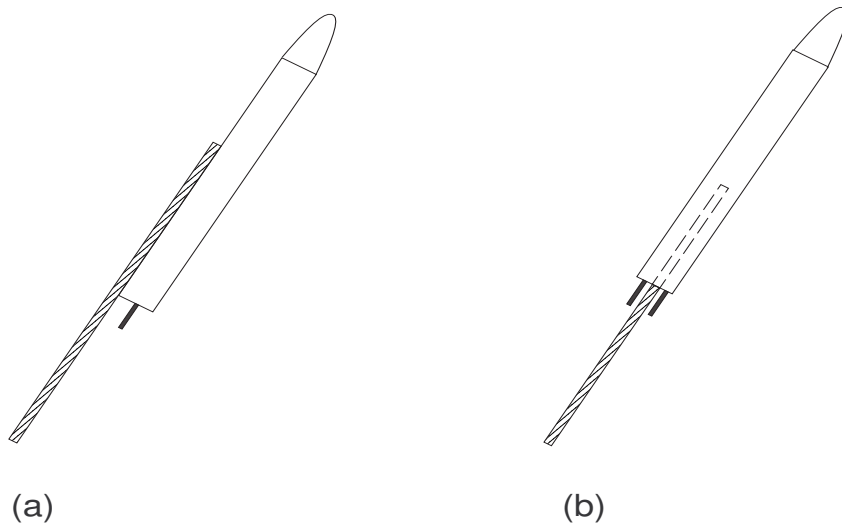


Figure 2.1: (a) Indian rocket (b) Centrally mounted stick in Congreve rockets

destroyed by about 25,000 to 40,000 such rockets fired during a three day siege.

Further developments in these rockets occurred in 1839 when *William Hale*, an Englishman, discovered that the stick, which was the cause of serious problems during launch, could be entirely eliminated and stability can be achieved by *spinning the rocket*. This was done by *directing the propellant exhaust through some slanted exit holes at the rear of the rocket*. During the end of the 19th century *Wilhelm Unge*, a Swedish engineer, carried out extensive research on rocket designs and propellant fuels. His research was financed by *Alfred Nobel*, the inventor of dynamite. Unge also found that spinning stabilizes a rocket in its flight, but in his design the spin was imparted to the rockets by *spinning the launcher tube itself*. In spite of these advances in rocket design the Swedish army did not show any interest in Unge's work and in 1908 the German company Krupp bought all of Unge's patents.

### 2.3 World War I and After

Towards the end of the 19th century interest in rockets had almost died down since these weapons were losing their *novelty* value and the consequent *psychological advantage* they gave to an army. However, the beginning of the *first world war* (1914-1918) changed everything and rockets were found to be useful against small but strategic tar-

gets. The French did successful air launchings, especially against enemy balloons and *German Zeppelins*.

During this time a British professor *A.M. Low* designed a small radio controlled monoplane called the *Flying Target* or *FT*. These were to be launched from a lorry using compressed air catapults. The Royal Aircraft Factory produced six of these *FTs*. They were found to perform satisfactorily but for some inexplicable reasons they were never used. Low is also credited with the design of *radio-controlled rockets* during this time. In 1918, *Charles Kettering* in the USA designed a similar *unmanned airplane* intended to serve as an *aerial torpedo*. Nicknamed the *Bug*, it had a range of 100 kms and flew at a speed of about 150 kmph. The flight direction was controlled by *preset vaccum relays* and after a certain time, when the Bug was expected to be above the intended target, its engine was automatically shut off and the wings were released so that the Bug with its payload fell onto the target in a ballistic trajectory. Experiments with the Bug were quite successful but again it was never used in any war.

Soon after the end of World War I and the defeat of Germany, the primary center of activity in rocket research shifted to Germany. Perhaps the reason for this was the *Treaty of Versailles* which had imposed a number of overly restrictive conditions on German research and development activities relating to military weapons. The Germans soon realised that rocket research was one of the areas which did not find an explicit mention in the treaty and could be carried out without attracting too much attention. Consequently, they started a top secret research establishment at *Kummersdorf* in 1932 and the 20 years old *Werner von Braun*, the famous German rocket scientist, was made its chief. Apart from rocket development, he was also given permission to write his doctoral thesis in physics which he completed in 1934 and was awarded a doctorate degree by the *University of Berlin*.

Apart from von Braun, many other famous German scientists contributed to rocket research during this time. They were *Hermann Oberth*, *Johannes Winkler*, and *Rudolf Nebel*, who had first inducted von Braun into his research team. During this time *Robert H. Goddard* in America and *Tsander* and *Kondryatyuk* in Russia had also begun research in this direction.

## 2.4 During World War II

*Adolf Hitler* came to power in Germany in 1933. He recognized the potential of rocket research and set up a top secret research establishment at *Peenemunde*. Von Braun was made the technical director of the establishment at the age of 25. The Peenemunde laboratories were equipped with a number of wind tunnels and other elaborate test facilities. This was perhaps the first time when such a systematic and concerted research effort was devoted to the development of a flight vehicle. This intensive research activity, prior to the World War II, led to the development of the famous *vengeance* missiles V-1 and V-2. The V-1 missile had an *inertial guidance system* to guide it on its path. The V-2 missiles were the weapons which laid waste vast portions of the *city of London* during the war. The Germans used to launch these missiles from France across the English channel. In October 1942, during an experiment, one of these V-2 missiles achieved a height of 116 miles and left the atmosphere. This was perhaps the first instance of a *man-made object penetrating the atmosphere* and enter space. During this time, a winged version of V-2 called A-9 was also developed.

Apart from the famous vengeance missiles, a number of other missile programmes were initiated and some of them completed successfully. A number of surface-to-air missiles were produced and flight experiments conducted with them proved to be successful. The *Wasserfall* surface-to-air missile, designed by *Ludwig Roth*, was one such missile which reached the stage of test flights but was never actually used in the war. Another such missile was the *Henschel HS-293* missile which was a *radio-controlled air-to-surface missile* and was used in August 1943 to sink the British warship *HMS Egret*. This incident is believed to be the first instance of a guided missile being used in war successfully. The Henschel missile weighed about 1200 Kg and had a length of 3.7 meters.

During this time the USA, UK, and the USSR did carry out developmental activities in this area but these were not as successful as the German missile programmes.

## 2.5 After World War II

During the spring of 1942, when the defeat of Germany and its allies became inevitable, and the Russian army was poised to occupy Peenemunde, von Braun and his team of

scientists escaped from there and were later captured by the Americans. The Americans were delighted with their catch and they flew the whole team of scientists back to the USA where they were persuaded to continue their experiments.

The first US missile programme *Hermes* was conducted by von Braun in association with the *General Electric Company*. The design of this missile was based on the *Wasserfall* missile. *Hermes* was a surface-to-air missile with a range of 250 kms and carried a warhead weighing almost 450 kg. Although a number of test flights were conducted the missile never came to the operational stage. However, it served as the base level design for many ballistic missiles developed later. The German scientists were also involved in developing many surface-to-surface missiles, e.g., *Corporal* (Range 130 kms, length 15 m, launch weight 5500 kgs), *Sergeant* (Range 40-140 kms, length 11 m, launch weight 4500 kgs), and *Redstone* (Range 400 kms, length 22 m, launch weight 30,000 kgs). Both the *Sergeant* and the *Redstone* carried an *onboard inertial guidance system*. About a 1000 *Redstone* missiles were produced and deployed in the West Germany till about 1963 when they were replaced by the *Pershing* missiles. The *Redstone* also provided the basic system which launched the first American astronaut into sub-orbital flight in May 1961. One of the first guided missiles to be built and tested in the US was the *Convair MX-774* which was modelled on the German V-2. Its testing gave valuable data which was used in the development of *Atlas*, the first ICBM to be built in the west.

The Russians were not far behind in this race. They too used the basic V-2 design to build a missile called *M-101* which in turn was the forerunner of many huge Russian ICBMs. The booster rocket that placed the world's first satellite, *Sputnik*, in space in October 1957, was also based on this initial design.

The design of the German V-1 missiles were also exploited by both the Soviet Union and the US to develop *cruise missiles* - the *JB (jet-bomb)* series of cruise missiles were developed by the US, while the *J-1, J-2*, and *J-3* cruise missiles were developed by the Russians.

From 1950 to 1970 several missile programmes were launched in the USA and many were successfully completed. Notable among them were the *Gorgon* series of missiles, *Firebird* (AAM), *Kingfisher* (anti-ship/anti-submarine), the *Bumblebee* programme (under which were developed the *Terrier/Tartar* shipbased SAMs, *Talos* air defense SAM,

*Triton* SSM, and the *Typhon* shipbased area defense SAMs), *Sparrow* (AAM), the *Nike* family of air defense SAMs, *Hercules* (SAM), *Falcon* (AAM), *Phoenix* (long range AAM), *Maverick* (ASM), *Sidewinder* (AAM), *Chaparral* (SAM), *Northrop SM-62 Snark* (cruise missile), *SM-64 Navaho* (cruise missile with nuclear warhead), *Pershing* (SSM), *Hawk* (SAM), and the *Patriot* (SAM - made famous by its much trumpeted performance in the recent Gulf war).

Subsequent research and development on missiles involved a multitude of R&D defence organisations in the US and some reputed institutions like the *Jet Propulsion Laboratory* at *California Institute of Technology*, and the *Applied Physics Laboratory* at the *Johns Hopkins University*.

## 2.6 The Indian Missile Program

The Integrated Guided Missile Development Program (IGMDP) was launched by the Indian Government in 1983 under the stewardship of A.P.J. Abdul Kalam with the intention of indigenously developing several missiles of various types. These were the *Akash* [Length 6.5m, Launch Weight 700 kg, Range > 20km] and *Trishul* [Length 3m, Launch Weight 130 kg, Range > 8km] surface-to-air missiles, the *Nag* anti-tank missile, and the *Prithvi* [Length 8m, Launch Weight 14500 kg, Range > 120km] and *Agni* [Length 20m, Launch Weight 16000 kg, Range > 1400km] surface-to-surface missiles. Some of these missiles have been successfully test-flown and some have reached the deployment stage as well.

## 2.7 Concluding Remarks

The above account of the major events in the history of guided missiles is somewhat slanted towards the American contributions, especially in the period after the Second World War. This does not mean that the European, Russian, and the Chinese contributions were not significant. In fact, these countries also took up and successfully completed a number of missile programs of their own. The erstwhile Soviet Union was, till very recent times, the world leader in the production of ICBMs. However, the devel-

opments that took place in the US are much better documented and easily available.

### *Assignment*

1. Collect information about the Indian missile program that started in the early eighties. There are books and internet resources that provide information on this program. Write a term paper (something like a magazine article) of about 5-6 pages in your own words consolidating this information and data. Make the presentation as attractive as you can with pictures of missiles, organizations, and people involved in the program. As in the earlier assignment, please do not forget to credit sources from where the material has been obtained. This is an absolute must. Also, make sure that the writing is your own and not copied.

### *References*

1. M.W. FOSSIER: The development of radar homing missiles, *Journal of Guidance, Control, and Dynamics*, Vol. 7, No. 6, November-December 1984, pp. 641-651.
2. M.W. FOSSIER: Development of low-altitude air defense systems, *Journal of Guidance, Control, and Dynamics*, Vol. 11, No. 2, March-April 1988, pp. 97-102.
3. M.L. SPEARMAN: History of guided missile developments, in *Tactical Missile Aerodynamics, Part I: General Topics*, M.J. Hemsch (ed.), AIAA Inc., Washington, 1992.
4. S.J. ZALOGA: Momentum in the missile market, *Aviation week & Space Technology*, January 13, 1997, pp. 137-157.

## Chapter 3

# Major Components of Tactical Missiles

## Module 2: Lecture 3 Airframe

**Keywords.** Airframe, Control Sequence

A tactical missile comprises of many components or subsystems. Each of them are important in their own right and require considerable care and expertise to design. In this lecture we shall discuss those components which have a direct bearing on the guidance of the missile. In particular, we will study the following subsystems: *Airframe*, *Flight Control System*, *Guidance System*, *Fuze*, *Warhead*, and *Propulsion System*. The usual locations of these subsystems in a tactical missile are shown in the schematic diagram in Figure 3.1.

### 3.1 Airframe

The airframe is the structure that houses all the missile subsystems. In general, tactical missile airframes can be classified as,

- Cruciform
- Planform

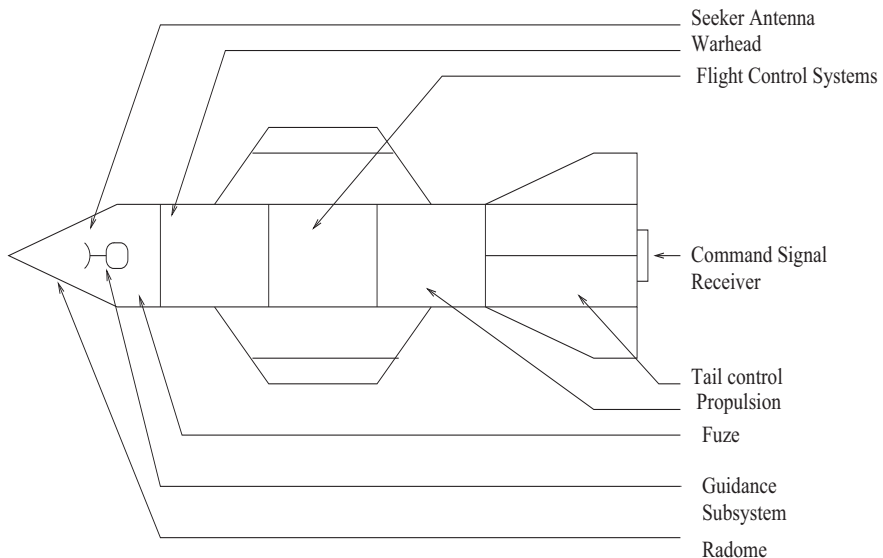


Figure 3.1: *Tactical Missile Subsystems*

*Cruciform* missiles are those that have control surfaces and/or lifting surfaces at 90 degrees from each other. In *planform* missiles these surfaces are located at 180 degrees from each other (see Figure 3.2).

Based on the source of lift and the location of the control surfaces a further classification of the basic missile airframe is possible. For this we follow the following set of notations:  $B$  (body),  $T$  (tail),  $W$  (wing),  $C$  (canard),  $l$  (lift),  $c$  (control).

An airframe designated by  $B_lT_lC_c$  will indicate an airframe that generates lift using its body and its tail surfaces, and in which the control is provided by forces acting on the canards. Below, we list five such airframes in Figure 3.3, along with the names of some existing missiles which have these airframe configurations.

The cause-and effect sequence by which a missile generates the lateral acceleration from a guidance command is as follows: The guidance computer generates the guidance command. This guidance command is fed into the flight control system which deflects the control surfaces by an appropriate amount. The control surface deflection produces a small lift force which, in turn, deflects the lifting surfaces and the body of the missile about its CG and changes the angle of attack. This produces a large lift force that is responsible for the lateral acceleration needed to turn the missile or cause it to

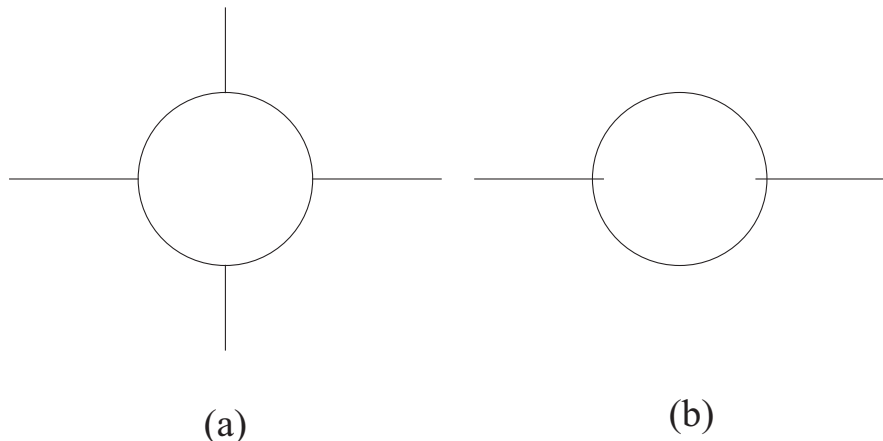


Figure 3.2: (a) Cruciform (b) Planform

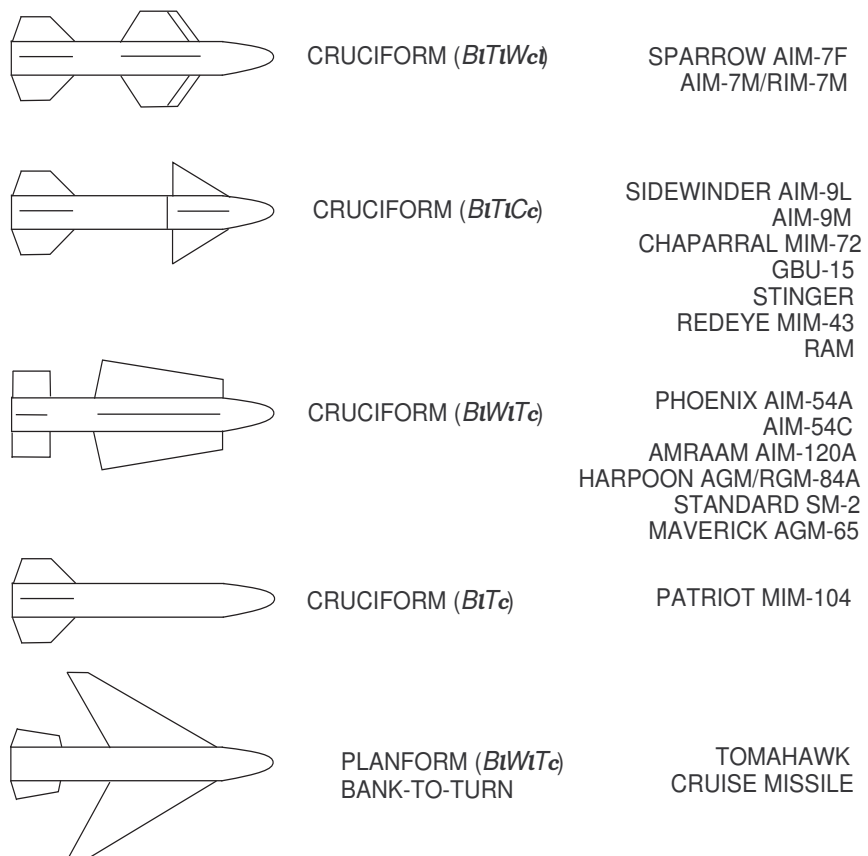


Figure 3.3: Airframe configurations

maneuver. This cause and effect sequence is shown below in the form of a functional block diagram in Figure 3.4.

In  $B_lT_lW_{cl}$  type of airframe lift is generated by the body, tail, and the wings. The wings also act as control surfaces. A deflection of the wings produces a force which moves the missile laterally and causes a change in its angle of attack. This causes a lift to be generated by the body, tail, and the wings themselves. This kind of airframe has a reasonably fast response. Since the wings are placed close to the moment center, a large control force is required to cause the required lateral movement of the body. This means that large servos need to be placed inside the body very close to the wings.

In  $B_lT_lC_c$  configuration the canards are the control surfaces and their deflection produces the desired control force to cause a change in the angle of attack of the missile. This in turn produces the required lift on the body and tail of the missile. Because of the large distance between the canards and the moment center, the servos used are small. This is fortuitous since these servos have to be placed next to the canards and close to the guidance subsystem where very little space is available.

In  $B_lT_c$  and  $B_lW_lT_c$  configuration the tail acts as the control surface. When the tail is deflected the force causes the missile to rotate and change its angle of attack. Lift is produced by the body and/or the wings. Here too the servos used to deflect the control surfaces are small, but the response of this type of airframe is quite slow.

The lift generated by the airframe has the effect of a lateral acceleration (latax) on the missile. This causes the missile to turn in the direction in which lift is generated. It is customary to express the guidance command, which deflects the control surfaces and generates lift, as a lateral acceleration command on the missile. This guidance command is usually a step input to the control surfaces and is influenced by the dynamics of the autopilot, the flight control system, and the airframe. The resulting latax is therefore not a step function but contains oscillations. For usual amount of damping in these dynamical systems, the response is quite fast (see Figure 3.5).

Thus, the actual achieved latax is different from the commanded latax. This fact should be taken into account during any realistic design and analysis of the guidance subsystem. Another aspect that needs to be taken into account is the *saturation effect*

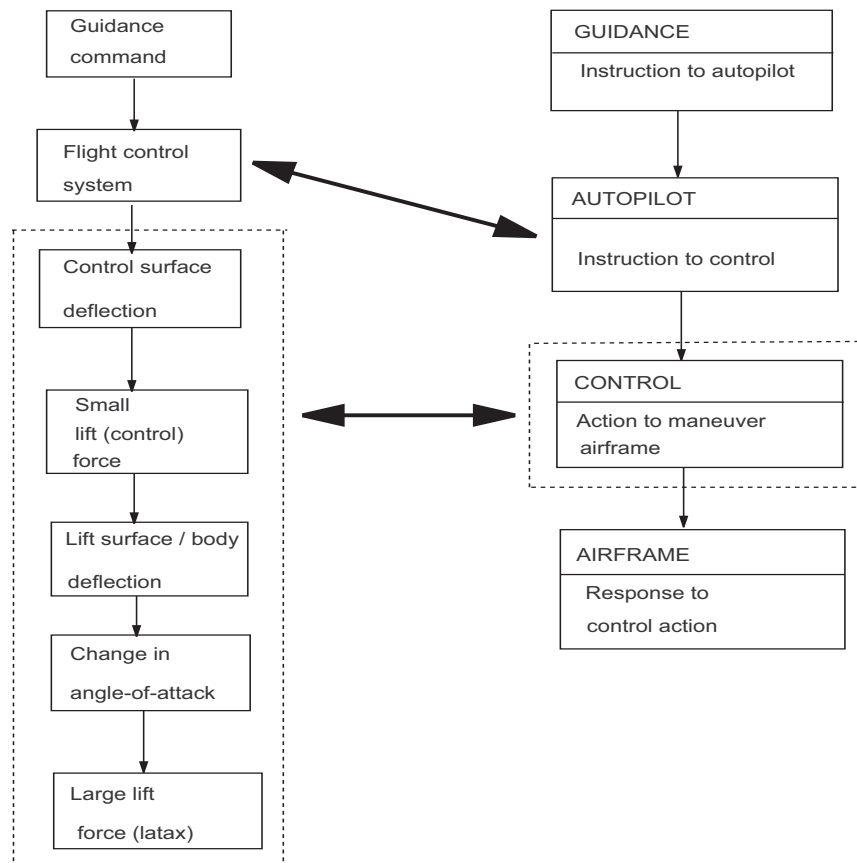


Figure 3.4: The cause-and-effect sequence by which latax is generated in a tactical missile

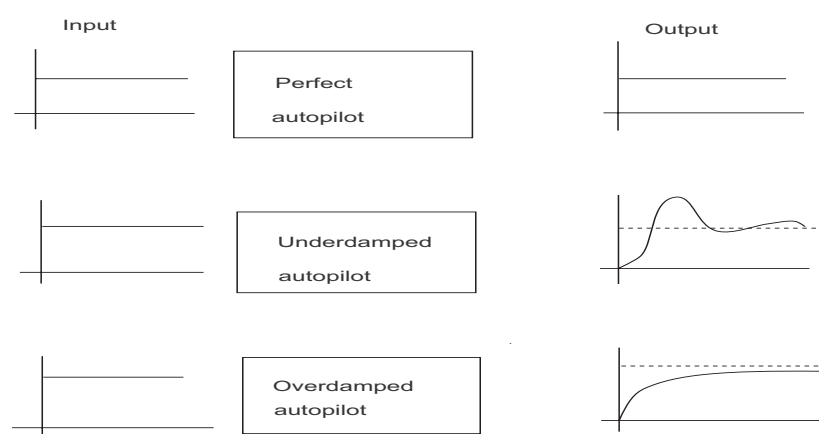


Figure 3.5: Commanded and achieved latax

on the lateral acceleration. At higher altitudes, the amount of lift that can be generated is limited by various considerations and so the actual lateral force that can be pulled by the missile may be different from that which is demanded by the guidance law.

*Assignment*

1. For those missiles for which you have collected data in the previous assignment, find out their airframe configurations. Identify their lifting and control surfaces.
2. Find out what the following terms mean (a) Skid-to-turn (b) Bank-to-turn (c) Tail control (d) Forward or canard control (e) Wing control (f) Preferred orientation control (g) Thrust vector control

*Questions*

1. Sketch a tactical missile and identify the important subsystems.
2. What are the major types of airframes and what kind of missiles use them?
3. How are airframes classified in terms of the way the lateral acceleration is generated? Give a couple of examples.
4. What is the normally used airframe for tactical air-to-air missiles?
5. What type of airframe does a cruise missile use.
6. What kind of airframe uses bank-to-turn control strategy?
7. What kind of airframes uses lift-to-turn control strategy?
8. Define the cause-and-effect sequence by which lateral acceleration is generated in a cruciform tactical missile. Also, do the same for a planform missile.

9. Describe how lift is generated in the following types of airframes (a)  $B_l T_l C_c$  (b)  
 $B_l T_l W_{cl}$  (c)  $B_l W_l T_c$  (d)  $B_l T_c$ .

## Module 2: Lecture 4

### Flight Control System

**Keywords.** Roll, Pitch, Yaw, Lateral Autopilot, Roll Autopilot, Gain Scheduling

#### 3.2 Flight Control System

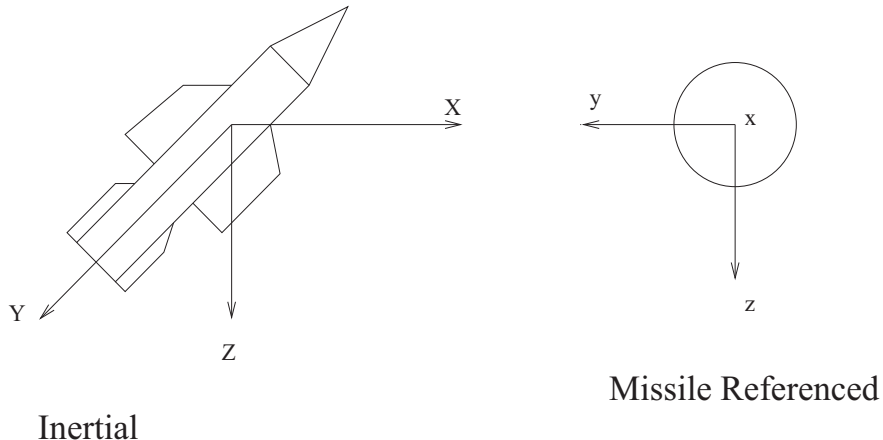
The flight control system is responsible for

- *stabilizing the missile*
- *controlling the missile in its flight and*
- *ensuring that the missile airframe responds effectively to guidance commands.*

To understand the exact function of the missile flight control system let us define some co-ordinate axes, which will be useful to describe missile motions.

The co-ordinate axes, denoted by the  $x$ ,  $y$ , and  $z$  coordinates, are defined with respect to the missile itself. The  $x$  axis points directly along the longitudinal axis of the missile. In the case of a cruciform missile, the  $y$  and  $z$  axis are parallel to the control surfaces, while for the planform missile the  $y$  axis is parallel to the control surfaces and the  $z$  axis is normal to the  $x - y$  plane. Usually a right-handed co-ordinate system is used. The angular motions of the missile about the  $x$ ,  $y$ , and  $z$  axes are called *roll*, *pitch*, and *yaw*. These coordinate axes are shown in Figure 3.6. Note that the figure on the left shows a right handed coordinate system. The figure on the right shows a left handed coordinate system, if the missile, and the  $x$ -axis, is pointing towards you. Since the right handed coordinate system is the more usual form, how do you think the figure needs to be changed to represent a right-handed coordinate system?

Airframe motions about the  $x$ ,  $y$ , and  $z$  axes are controlled by automatic feedback control systems and are commonly known as *autopilots*. Motion about the  $y$  and  $z$  axes produces forces which cause a change in the angular orientation of the missile, which manifests itself as a change in the direction of flight of the missile. The autopilot which controls motion about the  $x$ -axis is called the *roll autopilot*, that which controls motion

Figure 3.6: *Missile coordinate systems*

about the  $y$ -axis is called the *pitch autopilot*, and the one which controls motion about the  $z$ -axis is called the *yaw autopilot*, respectively.

The pitch and yaw autopilots are, in principle, similar since they control the same kind of missile motion. They are functionally identical and go under the common name of *lateral autopilots*. A block diagram of the basic lateral autopilot is shown in Figure 3.7.

Note that there are three feedback loops in a lateral autopilot. Let us try to understand why each of them is necessary and the role they play in the overall functioning of the autopilot.

The innermost loop is the *attitude (angle) feedback loop*. This essentially feeds back the *attitude angle*, either in the *pitch plane* or in the *yaw plane*, of the missile. To generate a lateral in one of these planes the missile needs to have a certain *angle of attack* in the respective plane. This, in turn, requires a change in the angular attitude of the missile. The output of the angle feedback loop is the achieved angle. This is subtracted from the desired angle and the difference is used to generate the command which serves to reduce this gap. The angular orientation of the missile is measured using an *attitude gyroscope*.

The *attitude rate feedback loop* feeds back the angular rate at which the missile is changing its *angular orientation*. This feedback is used to *damp* the output of the system and drive the angular rate to zero as the required angular orientation is achieved. Rate

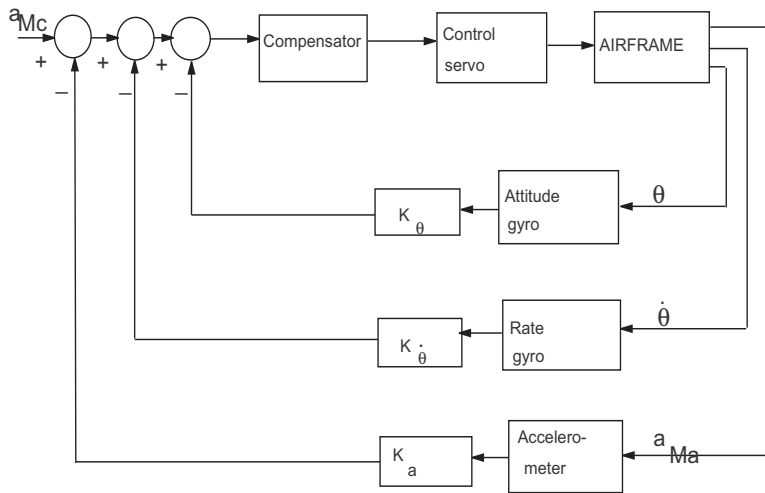


Figure 3.7: Lateral Autopilot

feedback improves the stability of a missile. The angular rate is measured using a *rate gyroscope*.

The *latax feedback* is used to establish when the commanded latax has been achieved and to generate appropriate inputs using the difference between the achieved and desired latax till they become equal.

One of the main concerns during the design of a tactical missiles is its weight which has to be kept at a minimum. One way to achieve some *weight reduction* is to *eliminate the attitude gyroscope* and use the rate feedback itself to generate the angle information. This is done by integrating the angular rate over time.

*Roll autopilots* are somewhat different in design from lateral autopilots. They always use the *roll angular rate feedback* to generate *roll angle information*. The functional block diagram for a roll autopilot using rate feedback is shown below in Figure 3.8.

Note that here we do not have any latax feedback simply because the roll autopilot only changes the roll orientation of the missile. No latax is desired or generated in this process. The *rate feedback improves stability*. This is important in those missiles in which *roll stabilization* is required. There are some missiles in which roll stabilization is not so

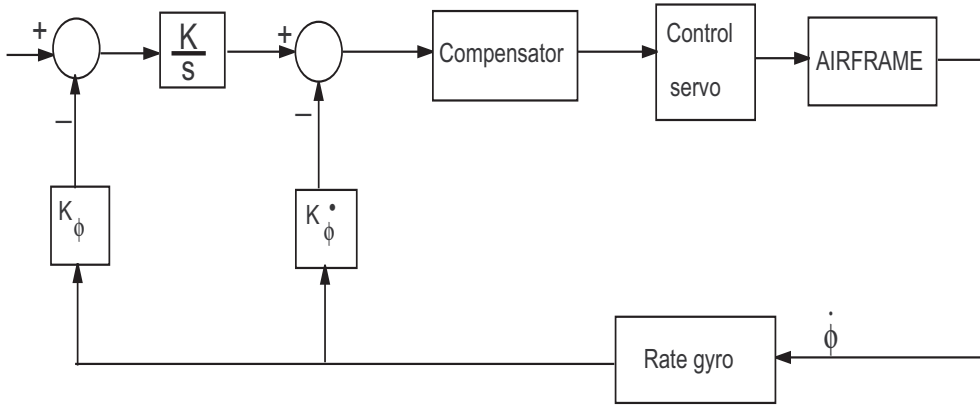


Figure 3.8: Roll autopilot with rate feedback

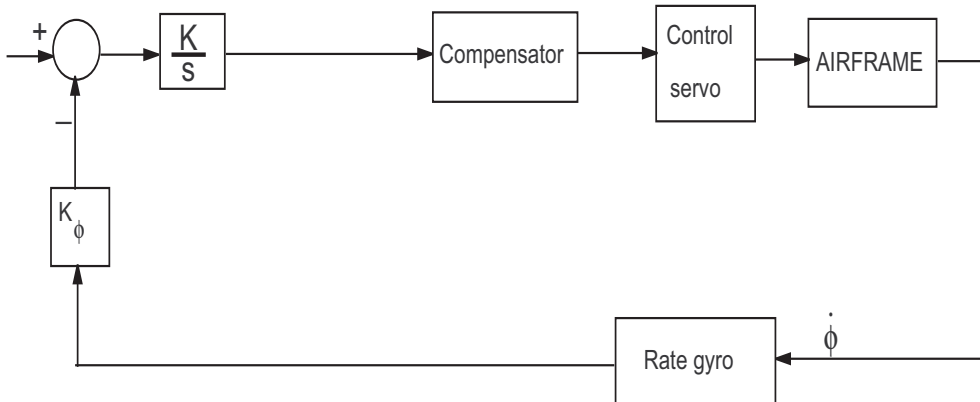


Figure 3.9: Roll autopilot without rate feedback

important. These missiles use roll autopilots which do not use rate feedback. This is shown in Figure 3.9 below. However, note that though a rate gyro is still employed, its output is not fed back directly. Rather, it is first *integrated* to extract the roll angle information.

In the block diagrams for lateral and roll autopilots given above nothing was said about the *nature of the gain terms*. Automatic feedback control systems which undergo minor or no parameter variations during operation usually perform satisfactorily with constant gains. But missile autopilots are expected to perform in different environments, sometimes during a single engagement. For example, a surface-to-air missile

may experience considerable *change in altitude* which, in turn, causes *drastic change in aerodynamic conditions*. A missile at very *high altitude* will require a *higher gain* to produce a *larger deflection* of the control surfaces to generate a given latax when compared to the same missile at a *low altitude*. Other important parameters which change during flight and thus necessitate a change in gain are *missile's velocity* and *weight*, and the *atmospheric temperature* and *pressure*. These changes are usually taken care of by an *adaptive gain control system* which can be designed in a variety of ways.

One of the ways to do this is known as the *dither technique*, also known as the *response measurement technique*. A *low frequency* and *low amplitude square wave*, called a *dither*, is injected into the autopilot. Its response, in the form of control surface deflection, is measured and compared with a reference obtained from the input dither itself. The difference signal is used to modify the autopilot gains.

Another technique, known as the *inertial reference adaptive gain control*, uses the *missile velocity and altitude*, obtained by integrating the output of the accelerometer situated in an inertial platform in the missile. This information is used to determine suitable gains from a *look-up table*. Obviously, it is more difficult to mechanize this technique than the dither technique, since this requires an inertial navigation unit inside the missile. This technique also falls under the broad category of *gain scheduling* techniques used widely by researchers.

### *Questions*

1. What are the major functions of a flight control system?
2. What are the different autopilots used in a missile and what are their functions?
3. Draw the block diagram of a lateral autopilot and explain the components.
4. What are the functions of the (a) Attitude loop (b) Attitude rate feedback loop (c) Latax feedback loop?
5. What modifications can be made to the lateral autopilot to keep its weight down?

6. Give the block diagram of a roll autopilot and describe its functioning. Write a note on the requirement of roll stabilization.
7. What are the techniques used for taking into account variations in altitude and its effects?
8. Write notes on (a) Need of adaptive gain control systems (b) Dither technique (c) Inertial reference adaptive gain control system.

## Module 2: Lecture 5

### Guidance Subsystem

**Keywords.** Tracking, Seeker Stabilization

#### 3.3 Guidance Subsystem

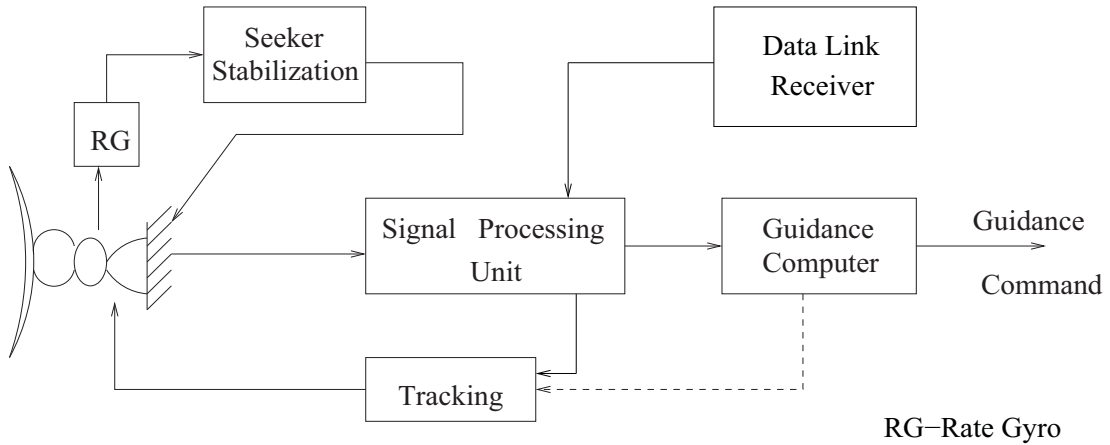
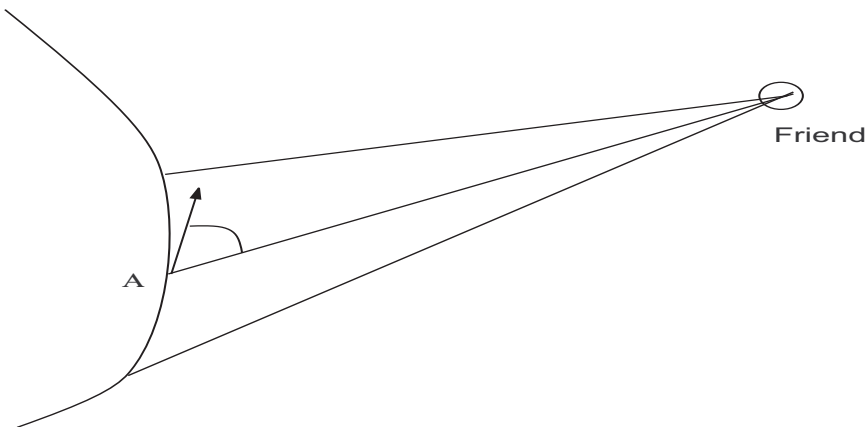
The guidance subsystem constitutes the *sensory organs* and the *brain* of the tactical missile. It performs several necessary functions.

- The guidance subsystem *acquires* and subsequently *tracks* the target.
- During tracking it *decouples the seeker motion from the missile body motion and disturbances*, thus improving the *stability of the seeker system*.
- It *collects information about the target and generates appropriate guidance commands* to guide the missile to an intercept.

The components of the guidance subsystem are the *seeker antenna*, the *gimbal system* which is attached to the missile body and on which the seeker is mounted, a *rate gyroscope* for measuring the *angular rate* of the seeker head, a *signal processing unit*, and a *guidance computer* which computes the guidance command.

A functional block diagram of the guidance subsystem is given in Figure 3.10. The *seeker stabilization loop* decouples the seeker from the body motions which is fed back at an appropriate position in the loop.

Let us try to understand each of these components and their functions in the light of our everyday experience. Suppose while walking you spot a friend some distance away on your right (Figure 3.11). Your eyes focus on the person, registers the person's image, and recognises him as an acquaintance (*target acquisition*). As you walk down the road you keep your eyes on this person (*target tracking*) who might be standing still (*stationary target*) or walking (*moving target*). Your neck (the *gimbal system*) allows your head to turn in such a way that your eyes (the *seeker*) keeps looking at this person. When you are at point *A* you have to turn your head by a certain angle from the direction in

Figure 3.10: *Guidance subsystem*Figure 3.11: *Take a walk!*

which you are moving. In other words you are subconsciously decoupling the motion of your head from the motion of your body. Suppose you decide to turn off the road and walk up to your friend. Your brain decides the best way (i.e., where to start turning off the road and by how much) to reach your friend. This is precisely what the missile guidance computer does.

The *guidance law* of the missile is *encoded into the memory* of the guidance computer. As the missile starts tracking the target, guidance commands are generated by the computer at periodic intervals. These are suitably transformed and fed into the autopilots. In later chapters we shall describe various forms of guidance laws and evaluate them

in terms of their performance.

*Questions*

1. What are the major functions of the guidance subsystem?
2. What are the major sub-components of the guidance subsystem? Explain with a block diagram.
3. Devise a situation from your own day-to-day experience (apart from the one given in the lecture notes here) that explains how the guidance sub-system works.

## Module 2: Lecture 6

### Proximity Fuze; Propulsion System; Warhead

**Keywords.** RF Proximity Fuze, Laser Proximity Fuze, Warhead, Detonator, Booster, Sustainer

#### 3.4 Proximity Fuze

The proximity fuze is a vital component of the missile since it seldom so happens that a missile actually hits the target. The more likely occurrence is that the missile comes very close to the target. This event is *sensed* by the missile and its warhead is detonated. The proximity fuze performs precisely this function. The kind of proximity fuze which is used in most tactical missiles are of the *active* kind.

The *RF proximity fuze* consists of two CW radars placed diametrically opposite on two sides of the missile, a little behind the guidance subsystem. The mainlobes generate a saucer-shaped pattern around the missile (Figure 3.12).

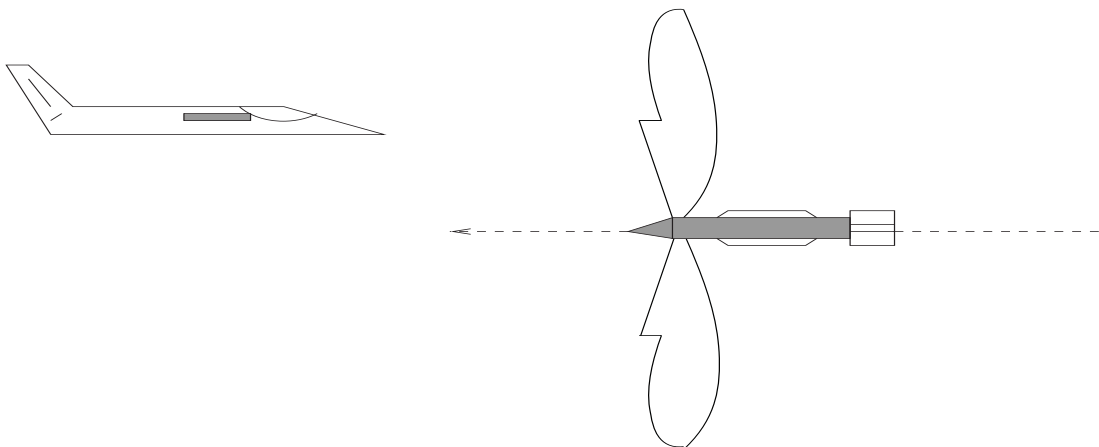


Figure 3.12: The RF fuze pattern

When the target enters this pattern, the reflected energy is received by the receiving antennas. The *doppler frequency* is extracted from this signal and is used to generate the *fuze pulse*. There is an *in-built range cut-off*, implemented through a *delay reference*, which suppresses reflected signals from objects at larger distance than the *lethal radius*.

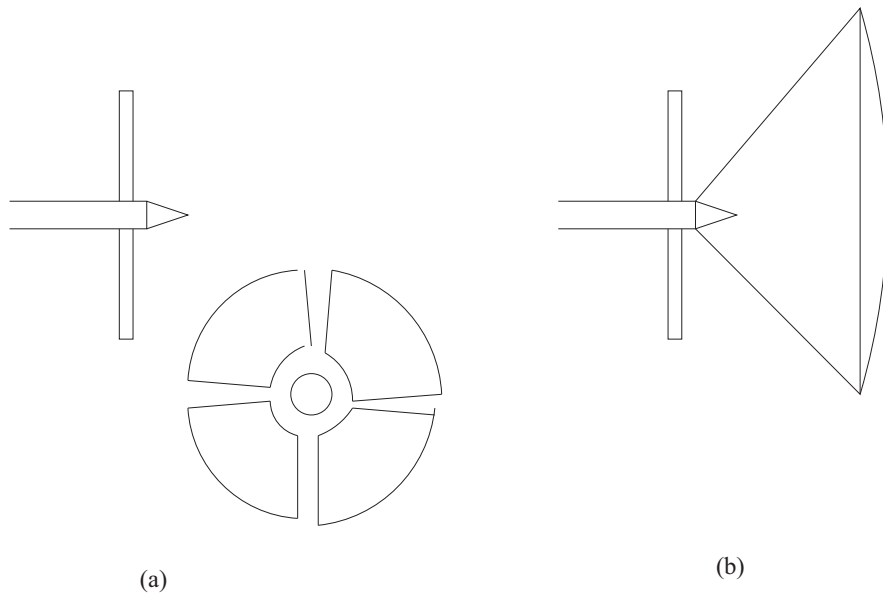


Figure 3.13: The Laser Fuze Pattern (a) Circular (b) Circular-Conical

of the warhead (the maximum distance at which the warhead is effective). This ensures that no fuze pulse is generated for signals reflected from the ground or the sea or from other nearby objects like foliage, buildings, etc. There are two other checks which help in preventing a false alarm. The doppler signal is passed through a *bandpass filter* to ascertain whether the signal is within a specified bandwidth, and then through a *threshold detector* to check if it satisfies the minimum level of reflected signal which identifies a target. The threshold detector also suppresses the *second-time-around echoes* and eliminates the possibility of *ambiguous range measurements*.

The *laser proximity fuze* uses a laser source as the *active transmitter* and an *infrared detector* as the *receiver*. The high frequency energy helps in obtaining very accurate information about the target position. *Four emitters* are mounted on the missile at 90 degrees from each other. Each produces a *sector-shaped pattern* with 90 degrees angular spread. The combination of the four patterns produces a *circular pattern* of a definite radius and very small thickness (Figure 3.13(a)).

A *receiver* is mounted next to each emitter. The signal received from the target is passed through some simple circuitry to extract the necessary information to generate the fuze pulse. Due to its inherent accuracy the *possibility of false alarm in laser fuzes is*

*very small* compared to the RF fuze.

Using a *different number and arrangement* of transmitters, various other laser beam patterns can be obtained. One of these is shown in Figure 3.13(b). The advantage of having these patterns is that the warhead explosion can be timed suitably to ensure that the blast occurs nearer to the center of the target. This can be done by using the time instants at which the target intercepts the two beams.

### 3.5 Propulsion System

The propulsion system of the missile provides the required initial thrust to the missile to enable it to fly with sufficient velocity during the subsequent engagement period with the target. There are two phases in missile propulsion:

- *Boost*
- *Sustain*

During *boost* the propulsion system provides a high level of missile acceleration over a relatively short period of time (1-15 secs). The purpose of *sustain* propulsion is to maintain the missile at a desired velocity for the majority of the remaining missile flight. Various combinations of boost and sustain propulsion (like *all-boost*, *boost-sustain*, *all sustain*) may be used in different missile systems. However, in principle, the all-sustain configuration is never used, since it usually requires a very short boost phase. An example is the air-to-air missile which does not have a booster motor but a short boost is provided by the sustainer motor itself. The thrust and velocity profiles of various propulsion systems are shown in Figure 3.14.

The booster motor is typically a *solid propellant motor* while the sustainer motor could either be a *solid propellant* one or a *jet engine*. Some modern missiles nowadays use *integrated rocket-ramjet propulsion*.

### 3.6 Warhead

The warhead is the payload of the missile and consists of a *shell*, *explosives*, and a *detonator*. The weight of the warhead depends on the size of the missile. The fuze pulse

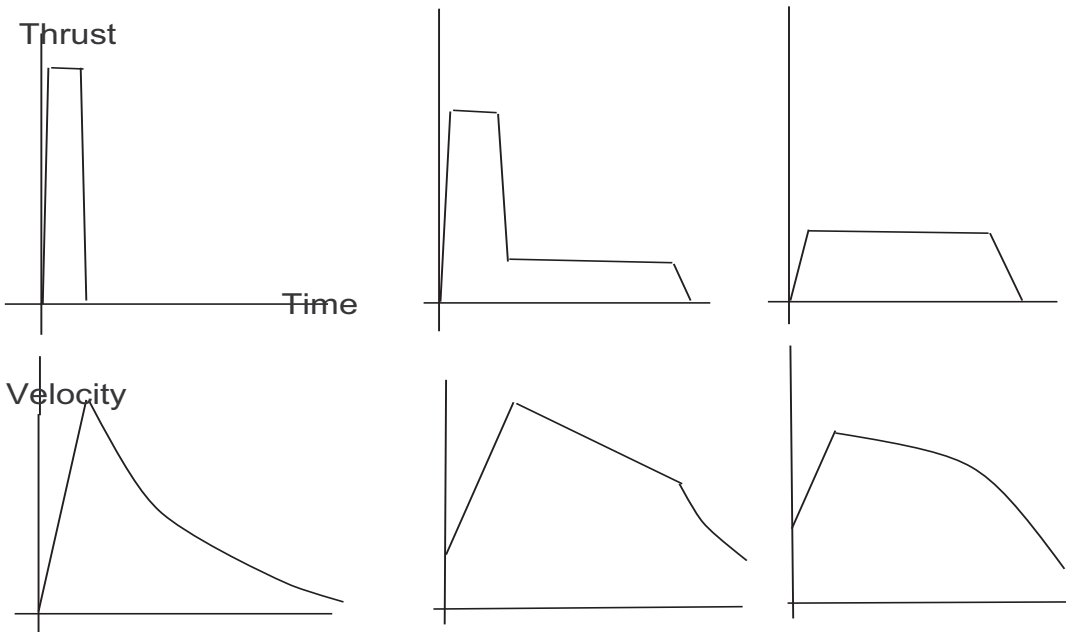


Figure 3.14: Thrust and velocity profiles

activates the detonator which in turn triggers the explosive. The shell breaks into numerous fragments which are propelled outward in a 60-90 degrees spread and achieves target kill by penetrating target components. Apart from the basic *fragmentation* type of warhead the other kinds of warheads are: *continuous-rod* warhead, *annular blast fragmentation* warhead, *selectively aimable* warhead.

In the selectively aimable warhead, four detonators are embedded in the explosive. The fuze pulse is first sent to the detonator which is closest to the target or in the direction of the target. The fuze pulse to the other detonators are slightly delayed. Because of this the warhead explosive around the first detonator explodes first, bursting or weakening the outer shell at this point. When the explosive in the rest of the warhead explodes, the effect of the explosion rushes out through the weakened spot in the shell and the full force of the explosion hits the target. This way the effectiveness of the warhead is increased many times over the conventional warhead in which the effect of the explosion is dispersed in all directions and is wasted (see Figure 3.15).

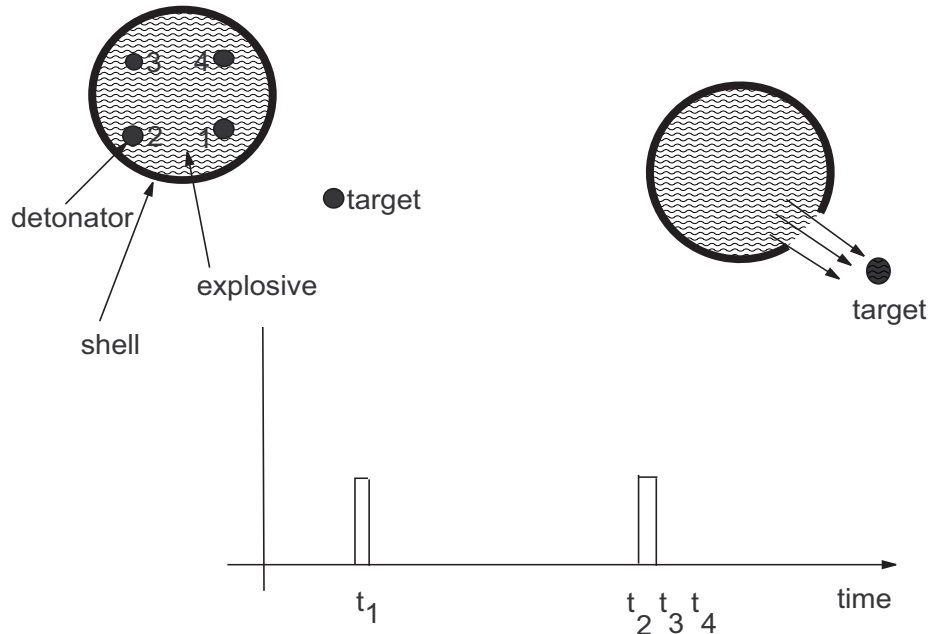


Figure 3.15: Selectively aimable warhead

### 3.7 Concluding Remarks

In this chapter we gave a brief overview of the various components of a tactical missile which together aid in the functioning of the guidance system and ultimately help in achieving the mission of a tactical guided missile. The level of discussions was kept at a fairly elementary level since it is important to understand the exact contribution that each of these subsystems makes in the overall functioning of the missile, without getting involved in the intricate details.

### *Questions*

1. What is a proximity fuze?
2. How does a RF proximity fuze work?
3. How does a laser proximity fuze work?

4. What are the different types of propulsion systems used in tactical missiles? What are the corresponding missile velocity profiles?
5. What are the different types of warheads used in a tactical missile?
6. Describe the operation of a selectively aimable warhead.

*References*

1. *E.J. Eichblatt: Test and Evaluation of the Tactical Missile*, AIAA Inc., Washington DC, 1989.
2. *M.J. Hemsch: Tactical Missile Aerodynamics Part I: General Topics*, AIAA Inc., Washington DC, 1992.

## Chapter 4

# Fundamentals of Guidance

### Module 3: Lecture 7 Guidance Phases; Categories of Homing Guidance

**Keywords.** Command Guidance, Three-point Guidance, Homing Guidance, Two-point Guidance, Active Homing, Passive Homing, Semi-active Homing

#### 4.1 Guidance Phases During Missile Flight

The basic difference between an unguided projectile and a guided missile is the generation of guidance commands which attempts to change the missile's flight direction. This guidance command is in the form of a lateral acceleration command which the autopilot translates into the amount of lift necessary to produce the desired turn rate (or maneuver).

Portions of missile trajectory for SAMs and AAMs can be classified into several *guidance phases* based either on their function or on the mode of guidance employed. For example, in an air-to-air missile, the first part of the trajectory is called a *programmed maneuver phase*, which is independent of target information and is executed solely to ensure that the missile clears the launch aircraft. At the completion of this maneuver, *midcourse guidance phase* is initiated. The function of the midcourse guidance phase is to place the missile within the *terminal acquisition range* of its seeker with the missile

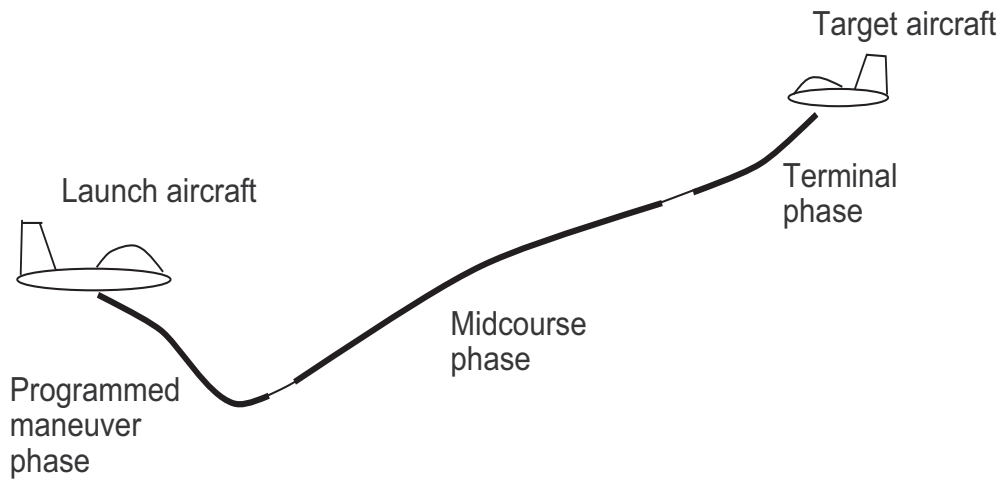


Figure 4.1: Guidance phases for an air-to-air missile

seeker pointed at the target. The last few seconds of the engagement constitutes the *terminal guidance phase*, which is the most crucial since its success or failure determines the success or failure of the entire mission. In the terminal phase the missile locks on to the target and attempts to close the distance to the target as quickly as possible under the constraints of energy availability and maneuver limitations. The intercept seldom takes place by the missile directly hitting the target. Usually the missile passes close to the target and the proximity fuze explodes the warhead. Hence, the effectiveness of the terminal guidance phase is solely judged on how close the missile can get to the target (i.e., the *miss-distance*). These phases are shown in Figure 4.1.

The missile trajectory for SAMs is almost the same except the initial phase which is called the *boost phase*. In this phase the missile's booster provides the required velocity to the missile. Since this phase occurs for a very short time during which the missile is marginally stable and has high longitudinal acceleration, no guidance commands are normally given to the missile. However, some modern missiles under development consider the incorporation of a *boost phase guidance scheme* to improve overall performance. Figure 4.2 shows these phases in the trajectory of a SAM.

Missile trajectories can also be classified according to the nature of the guidance scheme. This will be discussed in the context of surface-to-air missiles. In the *com-*

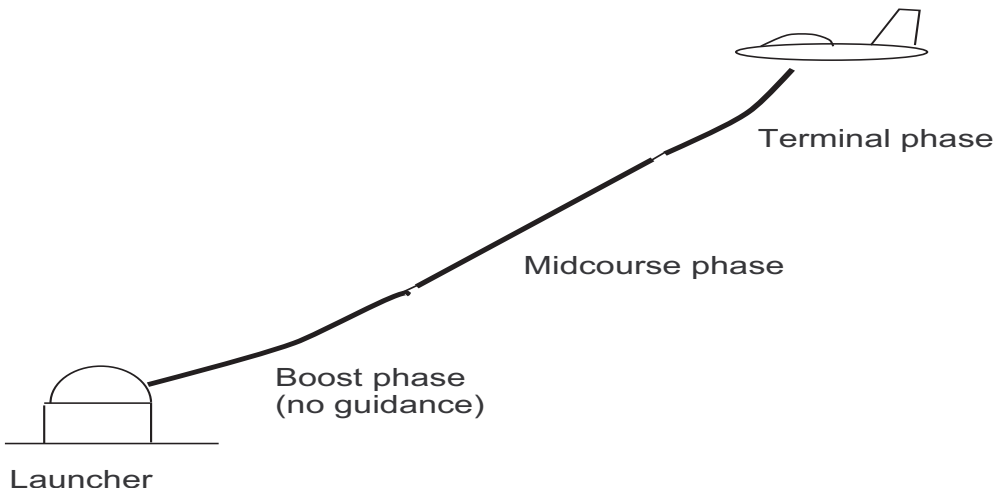


Figure 4.2: Guidance phases for a surface-to-air missile

*mand guidance* scheme the target and missile positions and velocities are measured by a tracking radar situated at the ground station. This information is processed and given to the guidance computer which generates the steering or guidance commands using some guidance law. The guidance computer is also situated at the ground station. The guidance commands are then communicated to the missile via a data uplink. Based on these inputs the missile flight control system takes action. Thus, the computers and other equipment at the ground station *command* the missile to behave in a certain fashion. This kind of guidance is also known as *three-point guidance* since there are three major points of reference : the *missile*, the *target*, and the *ground station*. The part of the trajectory in which the missile is command guided is called the *command guided phase*. Usually in purely command guided missiles there are three phases: *boost phase*, *command guidance phase*, and the *terminal phase*. The last phase is for a short duration in which the missile is very close to the target and hence normally it either does not maneuver or uses some constant maneuver level obtained from previous guidance commands. The reason for this is that the missile during this phase is so close to the target that there is little time to generate new guidance commands and consequently update the maneuver level. This kind of trajectory is shown in Figure 4.3(a). *Homing guidance* scheme does not depend on any ground station for the generation of guidance commands. This is also called *two-point guidance*. Though some homing guidance

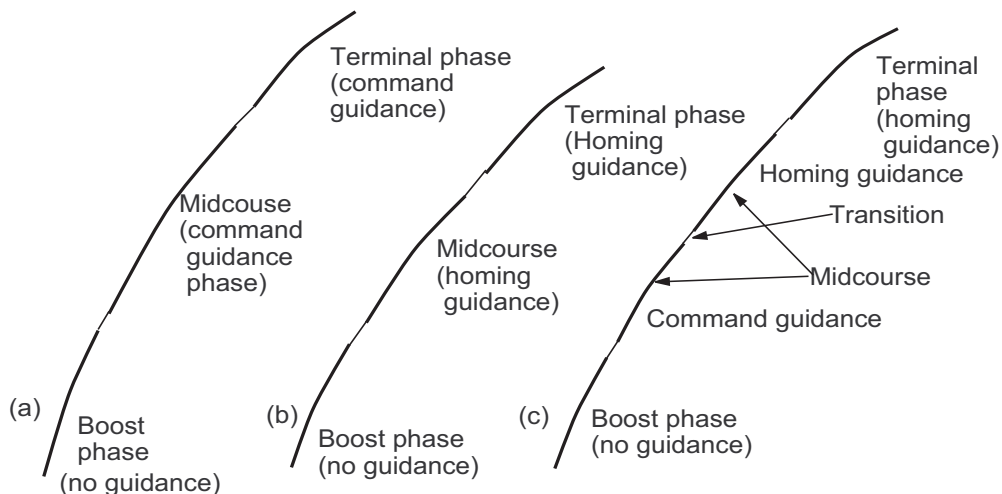


Figure 4.3: Trajectories for (a) Command guidance (b) Homing guidance (c) Mixed guidance

schemes need assistance from a ground station, the guidance commands themselves are generated inside the missile itself. Here too we have a *boost phase*, a *homing guidance phase*, and a *terminal phase*. This is shown in Figure 4.3(b). One can also have a mixed guidance scheme in which after the boost phase the missile is command guided from a ground station till the target comes within the acquisition range of the missile seeker antenna. Then the missile uses homing guidance till the terminal phase. This is shown in Figure 4.3(c).

## 4.2 Different Categories of Homing Guidance

Homing guidance schemes are desirable from the point of view that they require less control from a ground station and once launched, could be more or less autonomous in guiding themselves. These are also called *fire-and-forget* missiles. However, there are many categories of homing guidance which invest varying degrees of autonomy to the missile. Some of these categories are discussed below.

### 4.2.1 Active Homing

An active homing guidance system is one in which both the source of energy to illuminate the target and the receiver of the energy reflected from the target are carried in the missile. Hence, the missile contains a *transmitting antenna*, a *receiving antenna*, and a *re-*

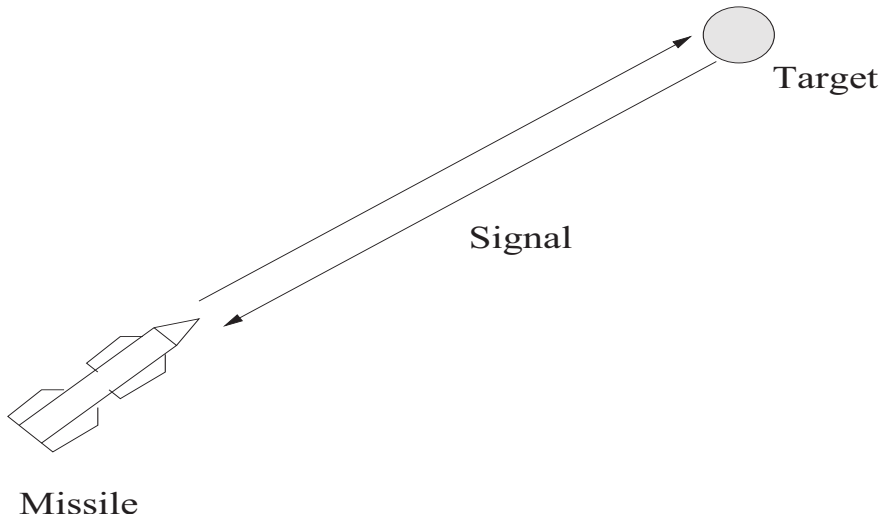


Figure 4.4: Active homing guidance

*ceiver*. It also carries within it the signal processor and the guidance computer. Missiles employing active homing are *fully autonomous*. Such a system is shown in Figure 4.4.

#### 4.2.2 Semi-Active Homing

A system wherein the transmitter of the energy is at a point external to the missile, but the receiver is inside the missile is called a semi-active homing system. The energy is reflected from the target and is received by the missile. The missile contains a *receiving antenna*, a *signal processor*, and a *guidance computer*. Since the transmitting antenna is located externally (either land-based or ship-based), it has *less autonomy* than active homing guidance. This system is shown in Figure 4.5.

#### 4.2.3 Passive Homing

A system in which the receiver, placed inside the missile, utilizes the energy emanating from the target is called a passive homing system. It does not require a transmitter. A *heat seeking missile* uses such a system. The missile contains the *receiver* appropriate for the kind of energy that the target emanates, a *signal processor*, and a *guidance computer*. These missiles may appear to be as autonomous as missiles using active homing but are actually less autonomous, since they have to depend on the target to emanate the necessary energy. If the target stops emanating this energy, the missile stops functioning.

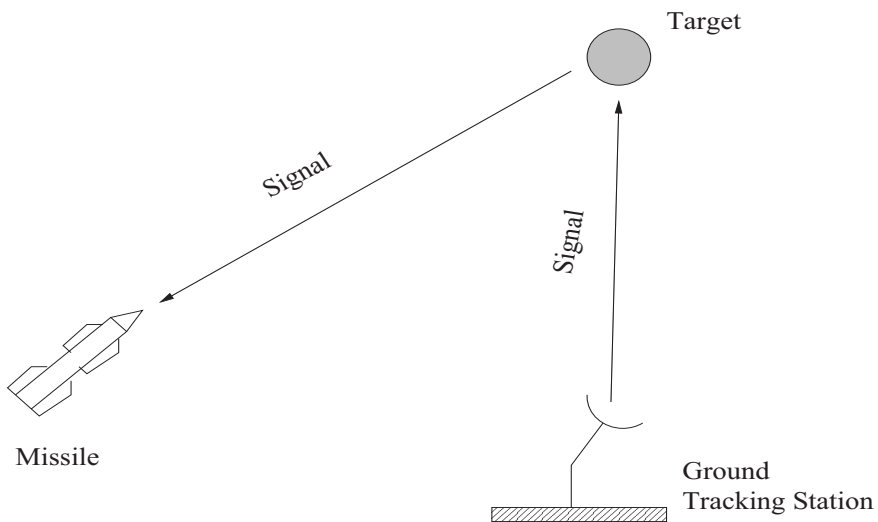


Figure 4.5: Semi-active homing guidance

Passive homing system is shown in Figure 4.6.

### *Questions*

1. What are the guidance phases of a (a) Surface-to-air-missile (b) Air-to-Air missile?  
Sketch figures to explain.
2. What are two point and three point guidance schemes?
3. Define command guidance and homing guidance.
4. Describe the following phases of the missile trajectory (a) Programmed maneuver phase (b) boost phase (c) midcourse phase (d) terminal phase.
5. What are the different category of homing guidance schemes?
6. Sketch figures and describe the following (a) Active homing (b) Semi-active homing (c) passive homing.

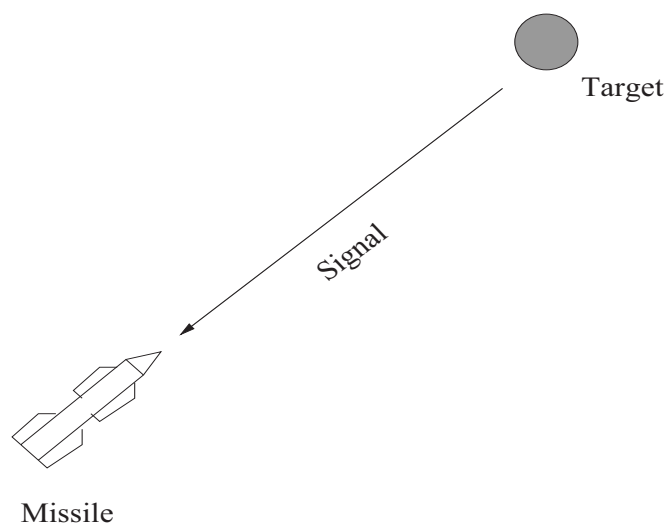


Figure 4.6: *Passive homing guidance*

## Module 3: Lecture 8

### Standard Terminologies in Missile Guidance

**Keywords.** Latax, Line-of-Sight (LOS), Miss-Distance, Time-to-Go, Fire-and-Forget, Glint Noise, Collision Triangle

#### 4.3 Some Standard Terminologies in Missile Guidance

One often comes across a number of standard terms in the literature on missile guidance. In this section we will define many of these terms precisely.

*Lateral Acceleration:* This is also known as *latax*. This is the acceleration that the missile needs to apply in order to achieve a desired turn rate. It is called lateral acceleration since it is usually applied in a direction close to the normal to the missile longitudinal axis or the missile velocity vector. In fact, the guidance command generated by the guidance law is usually expressed as a lateral acceleration term. This is called the *commanded latax* and is given as an input to the lateral autopilots. Since the autopilots are essentially dynamical systems subject to time delay, the actual *achieved latax* is a time-varying quantity and is different from the commanded latax at any moment in time. This difference may also occur due to the *saturation effect* since the missile may not be able to pull a very high commanded latax.

*Line-of-Sight (LOS) Rate:* During a missile-target engagement the imaginary line joining the missile and the target at any given instant in time is called the instantaneous *line-of-sight* or the *LOS*. This line changes in length and orientation as the engagement proceeds. The change in its angular orientation is given by its angular velocity or rate of turn and is usually expressed in units of radians/sec. This is called the *LOS rate*.

*Closing Velocity:* This is the velocity with which the missile closes on to the target. Obviously this is given by the rate at which the length of the LOS or the *LOS separation* shrinks. Hence, it is the negative of the rate of change of the LOS separation or *range*

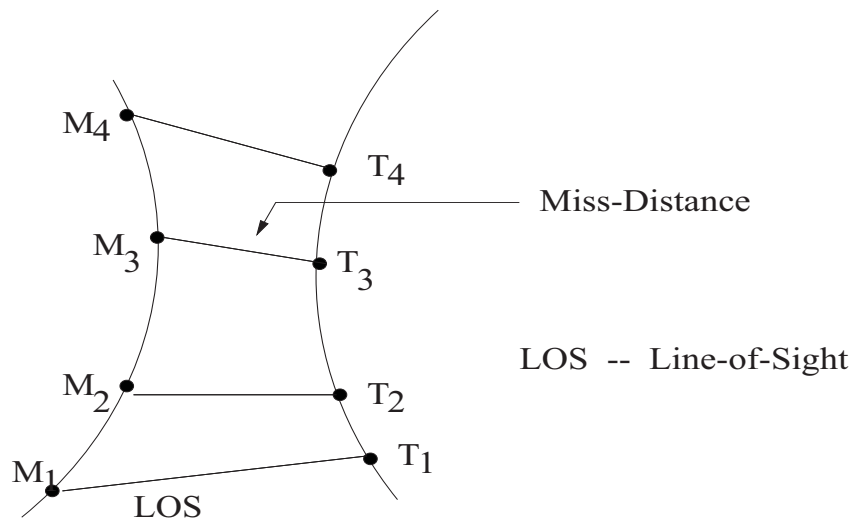


Figure 4.7: Miss-distance

rate. It is also the *doppler relative velocity* of the target with respect to the missile along the line-of-sight. Note that the doppler relative velocity is positive when the target is approaching and negative when it is receding.

**Miss Distance:** This is the *distance of closest approach* of the missile to the target. When the missile directly hits the target, the miss distance is zero. But when the missile passes close to the target the miss distance is non-zero. In this case the proximity fuze detonates the warhead and the engagement comes to an end. Obviously, the primary objective of a guidance system is to minimize the miss-distance. Also note that the miss-distance is a non-negative quantity. Consider Figure 4.7 which shows the trajectories of a missile and a target, and also the miss-distance. It also shows the LOS at different instants in time, including the LOS at the *instant of closest approach*. The length of the LOS at this instant gives the miss-distance. Now, what distinguishes this LOS from all the other LOSs? It can be easily deduced that the closing velocity at this instant is zero. The closing velocity before this instant is positive and after this instant is negative.

**Time-to-Go :** The time-to-go is an important trajectory parameter which is used for the

implementation of many advanced guidance laws. Suppose we record the trajectory data of a missile-target engagement and find that the engagement ends with an interception at time  $t_f$  (*final time*). Note that interception is assumed to have taken place when either the missile directly hits the target or at the time of closest approach. Now, at any given instant in time  $t$  during the engagement the time-to-go is defined as the time remaining till interception and is given by  $(t_f - t)$ . It is usually denoted as  $t_{go}$ . This value is the actual time-to-go which is known only after the engagement is over. But, to implement the guidance law, we need to estimate the  $t_{go}$  during the engagement. There are many ways by which this can be done. One of the ways, based on the available instantaneous information, is to use the formula,

$$\hat{t}_{go} = \frac{R}{(-\dot{R})} \quad (4.1)$$

where,  $\hat{t}_{go}$  is the estimated time-to-go and  $R$  is the LOS separation or the distance between the target and the missile at that instant in time. This is not a very accurate method of estimating the  $t_{go}$ , but for some limited cases it is satisfactory. For instance, it is accurate when we consider the collision triangle. There are other more accurate, but complicated, ways of finding the  $t_{go}$  also.

*Blind Zone:* In a homing guidance system the seeker has to keep pointing towards the target in order to track it. However, during the last part of the terminal phase the missile could be pointing in such a direction that the seeker has to turn by a very large angle to keep the target within its field of view. However, seeker turn angle is subject to mechanical limitations. Hence, it may not be possible for the seeker to turn by such a large angle. In this case the seeker loses track of the target and cannot *see* it any more. This part of the missile trajectory is called the *blind zone* for the missile. This is shown in Figure 4.8. There is no information input from the seeker during this phase and the guidance system has to depend on previous information.

*LOBL - Lock On Before Launch:* In this mode the launch platform radar performs the search and acquisition functions and sends target position information to the missile seeker, directing it to lock on to the target before the missile is launched. However, this is normally an impractical procedure because of the following factors:

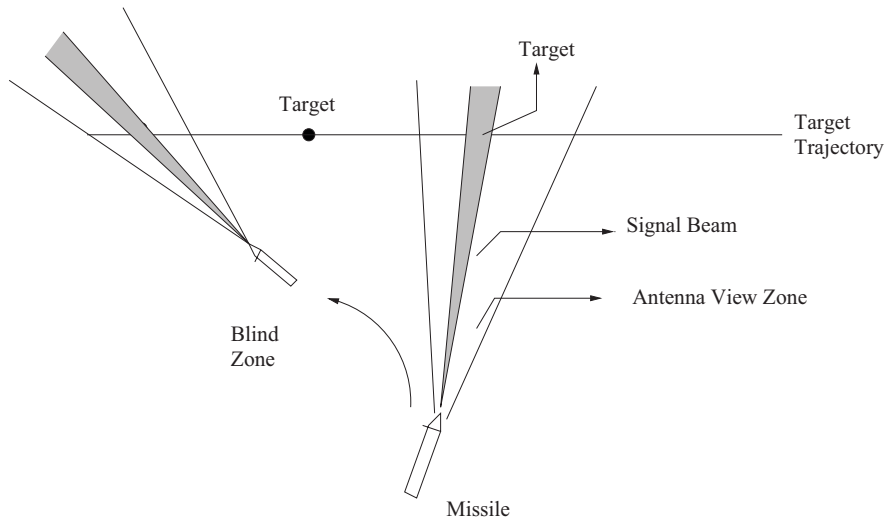


Figure 4.8: Blind zone in the terminal homing phase

- The missile seeker may suffer interference due to the signals emanating from the launch platform radar.
- It is difficult for the missile guidance system to track the target when the missile is experiencing a high acceleration during the boost phase that occurs immediately after the launch.
- The target may not be in the field-of-view of the missile seeker before launch.

*LOAL - Lock On After Launch:* This is a more complex procedure than LOBL. The missile has to be provided with the target information to enable the missile seeker to acquire the target. Even then the missile must go through the process of search and acquisition.

*Fire-and-Forget or Launch-and-Leave:* This refers to those missiles that have the capability to reach their targets after launch in the absence of any support from the launch platform or the operator.

*Glint Noise:* A target such as an aircraft has many radar reflector surfaces. The net return from these surfaces can be modelled as a movement of the apparent radar

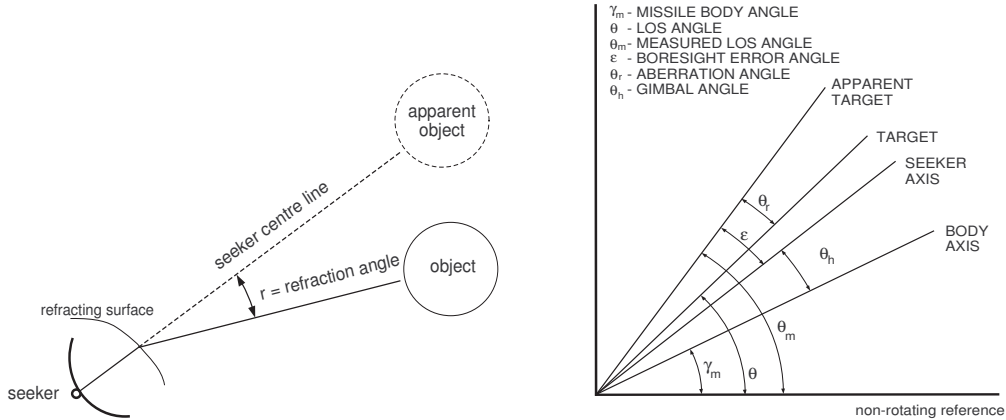


Figure 4.9: Radome error and the virtual target

position and is typically modelled as a Gaussian random variable with zero mean and some non-zero variance. This is called *glint noise*.

**Radome Error:** The missile seeker is used to track the target by processing the reflected signal from it. The radome that covers the missile seeker (in a homing guided missile) causes deterioration to the angle of the incoming signal due to refraction (in fact, due to this the radome has to be designed not only from the aerodynamic point of view but also from the viewpoint of electromagnetic considerations). Because of this the missile seeker actually tracks a *virtual target* whose position is shifted from the actual position of the target. This can be seen from Figure 4.9.

**Heading Error:** The heading error is the difference in angle between the actual missile velocity vector and the angle required by the missile velocity vector to satisfy the collision geometry conditions. This parameter is an important performance measure for missiles that follow the mixed guidance scheme and have to transit from a command phase to a homing phase.

**Factors affecting miss-distance:** There are many factors that affect the performance of the missile and its guidance law in terms of miss-distance. The main among these are

- Target maneuver

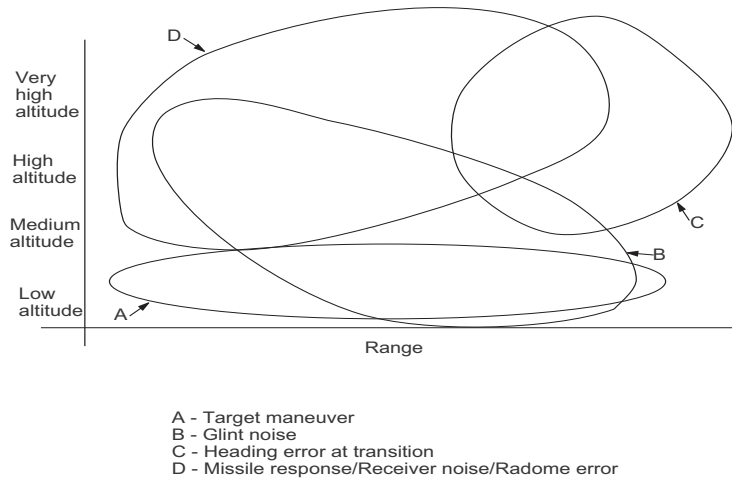


Figure 4.10: Factors affecting miss-distance

- Glint noise
- Heading error at transition
- Missile response
- Receiver noise
- Radome error

These factors affect miss-distance differently depending on the altitude and range of the target. This is shown in Figure 4.10.

#### 4.4 The Kinematic Equations

The kinematic equations for the missile-target engagement, assuming point mass models for the missile and the target, are given below with reference to Figure 4.11.

$$V_R = \dot{R} = V_T \cos(\alpha_T - \theta) - V_M \cos(\alpha_M - \theta) \quad (4.2)$$

$$V_\theta = R\dot{\theta} = V_T \sin(\alpha_T - \theta) - V_M \sin(\alpha_M - \theta) \quad (4.3)$$

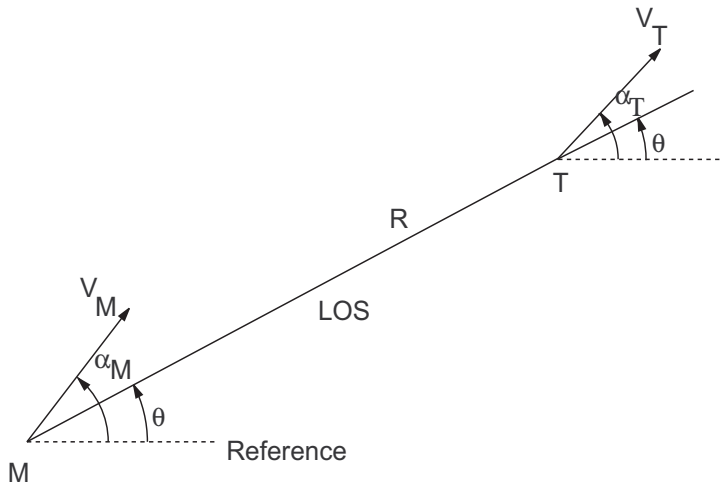


Figure 4.11: *Missile-target engagement geometry*

Here,  $V_T$  and  $V_M$  are the target and missile velocities, and  $R$  is the distance from the missile to the target (LOS separation). Usually  $V_M > V_T$ . The quantities  $V_R$  and  $V_\theta$  are very important for us – they are the components of the relative velocity (of the target with respect to the missile) along the LOS and normal to the LOS, respectively. We shall have occasion to use these quantities quite often in the later part of our lectures. The missile employs a lateral acceleration  $a_M$  to turn the missile in an appropriate direction. Note that  $\dot{\theta}$  is the LOS rate and  $\dot{R}$  is the rate of change of the LOS separation. Also, the closing velocity  $V_c$  is given by,

$$V_c = -\dot{R} \quad (4.4)$$

Equations (4.2) and (4.3) do not form the complete set of kinematic equations. The complete set will consist of equations modelling the variations in  $\alpha_M$ ,  $\alpha_T$ ,  $\theta$ ,  $V_M$ , and  $V_T$ . Integrating these equations with respect to time from some given initial conditions will give the complete trajectory of this system of equations.

#### 4.5 The Collision Geometry

The *collision geometry* or the *collision triangle* is the most fundamental concept in guidance law design. In this section, we will take a closer look at it and try to pin down what the collision triangle means in terms of some basic guidance parameters. See Figure 4.12 which shows the collision triangle.

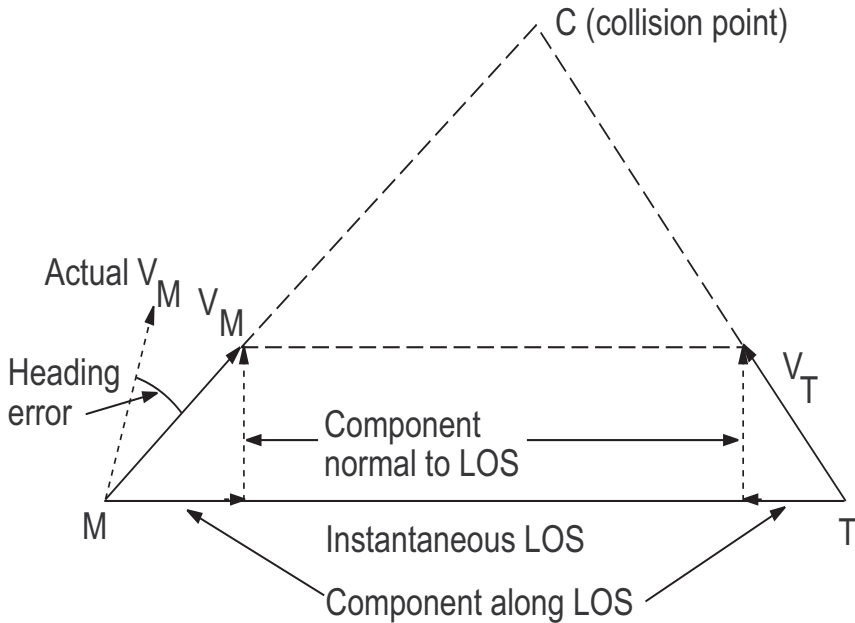


Figure 4.12: The collision triangle

Essentially the collision triangle defines the trajectories of the missile and the target when they culminate in an intercept, while both the vehicles are moving with constant speeds and in straight-line trajectories. This implies that the LOS does not rotate in space and so in (4.3) we have  $V_\theta = 0$ . Also, since the missile and target speeds and directions of flight are constant, in (4.2)  $V_R$  remains a constant negative quantity. These two together ensure that the engagement ends up in a successful interception of the target by the missile. So, for the conditions of the collision geometry to be satisfied we must have

$$V_\theta = 0, \quad V_R < 0 \quad (4.5)$$

Note also that  $V_\theta = 0$  implies that the component of the target velocity perpendicular to the LOS is equal to the component of the missile velocity perpendicular to the LOS.

#### 4.6 Capturability

*Capturability* or interceptability is another fundamental notion in the performance evaluation of guidance laws. The primary objective of any missile is to intercept the target, all other performance measures are secondary to it. So it stands to reason that we

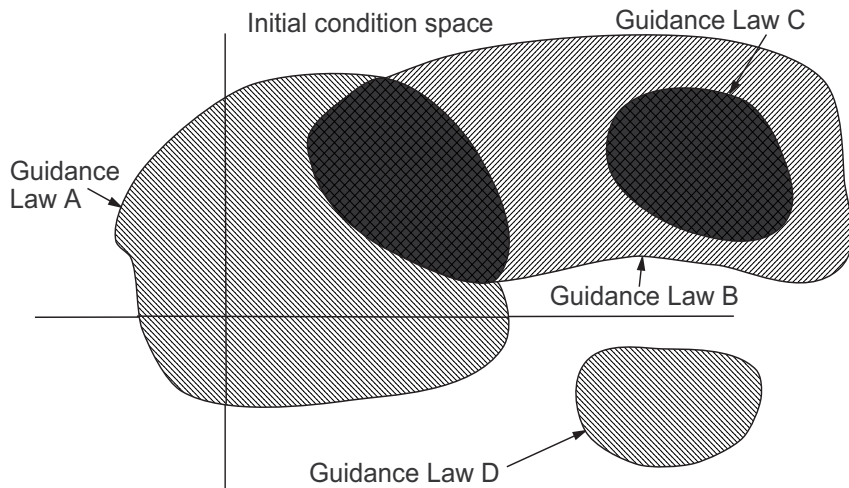


Figure 4.13: *The capture region*

would like to identify all the initial conditions in the state space from which a missile can capture the target using a given guidance law. As we shall see in later chapters, the performance of guidance laws are limited by many factors. Because of this, a particular guidance law may be able to capture from a given set of initial conditions while it may fail to do so from another. A schematic representation of this is given in Figure 4.13.

The region in the state space or initial condition space, from which the missile is able to capture the target with a given guidance law (that is, the collection of those points in the initial condition space which satisfy the requirements of *capturability*) is called the *capture region*. The capture regions of two guidance laws may intersect, may form a subset or superset of each other, or may be totally disjoint. But based on the shape and size of the capture region we can derive many important observations regarding the suitability of the guidance law.

In our subsequent analysis we will try to express the capture region in the initial condition space of the relative velocities  $V_R$  and  $V_\theta$ . We shall also show that this is the most natural representation of capturability, from the viewpoint of kinematics. I should also point out that the capture region we will obtain are those which will be based on purely theoretical considerations. Although they help us to draw many important and useful conclusions the actual capture region will be modified further (and will

be perhaps smaller) if we take into account other realistic factors like latax saturation, constraints on fuel, and atmospheric conditions.

#### 4.7 Concluding Remarks

In this chapter I have tried to introduce some of the fundamental concepts and terminologies used in the guidance literature. These will help us to go deeper into the design and actual working of several guidance laws and help us to understand them better.

#### *Questions*

In all the following questions, sketch a figure, if it helps you to explain the concept better.

1. Define commanded lateral acceleration and achieved lateral acceleration. Why are they different?
2. Define LOS angular rate. Write down the expression.
3. Define closing velocity. Write down the expression. When is the closing velocity positive and when is it negative?
4. What is miss distance?
5. What is time-to-go? How is it usually computed? When is this computation accurate?
6. What is blind zone and when does it occur?
7. Define (a) LOBL (b) LOAL (c) Fire-and-forget (d) Glint noise.
8. What are radome error and heading error?
9. What are the factors that affect miss distance? What values of altitude and range make these factors relatively more important?
10. Sketch a missile-target engagement geometry and write down the kinematic equations that govern the evolution of this system in time.

11. What is the relative velocity space?
12. What is a collision triangle and what are its features?
13. Define capturability in general and capturability in the relative velocity space.

### *References*

1. C.-F. Lin: *Modern Navigation, Guidance, and Control Processing*, Prentice Hall, Englewood Cliffs, NJ, 1991.

## Chapter 5

# Basic Results in Interception and Avoidance

## Module 4: Lecture 9 Engagement between Two Point Objects

**Keywords.** Avoidance, Interception, Capture, Capturability

The main objective of guidance is to direct one object to move in such a way as to enable it to come as close as possible to another object. In missile guidance this is equivalent to the missile *intercepting* or *capturing* the target. By definition, an *interception* or *capture* is said to have taken place if the positions of the two objects coincide. Of course, in a practical situation (especially when one considers missile guidance) it seldom happens that the positions of the two objects coincide in an exact sense. What normally happens is that the objects come *close* to each other. Can we call this as interception? That would depend on how close is considered to be close enough. In case of missiles, normally the missile would carry a warhead and this warhead would have a certain lethal range in the sense that a target located within this lethal range when the warhead explodes is likely to be destroyed. If we have a definite value for this lethal range then we may say that interception has occurred if the missile approaches the target within this range.

Although at first sight the primary objective of guidance is to enable an object to

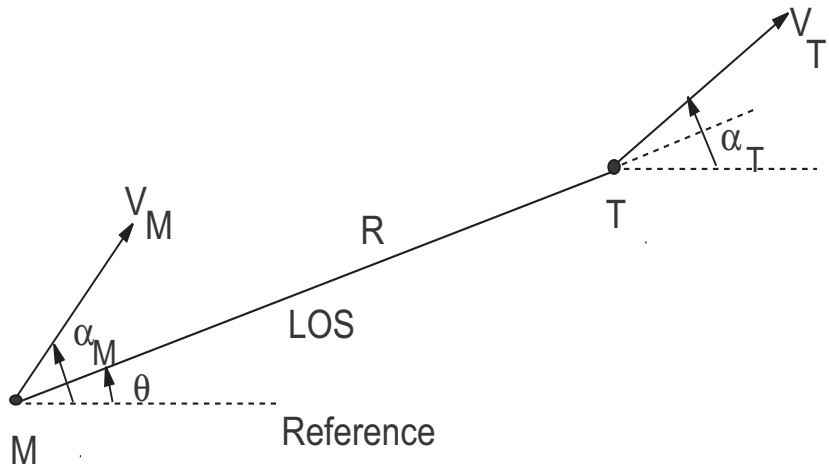


Figure 5.1: Engagement between two point objects

intercept another, another related objective is to enable an object to move in such a way as to enable it to *avoid* another object. Robotics literature yields numerous examples of this kind of application. *Avoidance* and *Interception* are two sides of the same coin and the philosophy that enables us to arrive at a viable guidance law for interception can also be used to obtain a guidance law for avoidance.

All these definitions of capture and avoidance are ultimately related to the movement of an object under the influence of a guidance law. To understand how a guidance law affects the trajectory of an object we must first look at the kinematics of the interception problem. We will see that *relative velocities* between objects play a very important role in deciding whether an interception has occurred or not. In this chapter we will first look at the various possibilities when two objects move with constant velocities without any guidance being applied to them. The results obtained will give us a good idea about how guidance laws should be designed, what are the major parameters that need to be used, and also the major issues in a guidance problem.

## 5.1 Engagement Between Two Point Objects

### 5.1.1 Equations of motion

Consider the two point objects to be denoted as M and T. See Figure 5.1. These objects

have constant velocities  $V_M$  and  $V_T$ . This means that both objects move in straight lines with constant speeds. The line joining the two objects is called the *line-of-sight* or LOS. The distance between the two objects is denoted by  $R$  and is also referred to as the *LOS separation*. Note that angles are measured with respect to some fixed reference and the angle that the LOS makes with the reference is denoted by  $\theta$  and is called the *LOS angle*. The direction of movement of the objects are given by the angles  $\alpha_M$  and  $\alpha_T$ . Note that since  $V_M$ ,  $V_T$ ,  $\alpha_M$ , and  $\alpha_T$  are constants, the states of the system are only  $R$  and  $\theta$  since these are the only quantities that vary with time. The equations of motion are then given by,

$$V_R = \dot{R} = V_T \cos(\alpha_T - \theta) - V_M \cos(\alpha_M - \theta) \quad (5.1)$$

$$V_\theta = R\dot{\theta} = V_T \sin(\alpha_T - \theta) - V_M \sin(\alpha_M - \theta) \quad (5.2)$$

Note that  $V_R$  and  $V_\theta$  are components of the relative velocity of the target with respect to the missile. Here  $V_R$  is the component along the LOS and  $V_\theta$  is the component normal to the LOS. We shall see that these two relative velocity components will play a crucial role in defining the *Capturability* of an engagement scenario or that of a guidance law. Since  $V_M$  and  $V_T$  are constants and so are  $\alpha_M$  and  $\alpha_T$ , it means that both the objects continue moving with constant velocities (that is, constant speed and constant direction). There is no guidance applied here.

### 5.1.2 $(V_\theta, V_R)$ -trajectory

The behaviour of  $V_\theta$  and  $V_R$  with respect to time will reveal several interesting facts. To study these we differentiate them with respect to time to yield,

$$\begin{aligned} \dot{V}_R &= -V_T \sin(\alpha_T - \theta)(-\dot{\theta}) + V_M \sin(\alpha_M - \theta)(-\dot{\theta}) \\ &= \dot{\theta} \{V_T \sin(\alpha_T - \theta) - V_M \sin(\alpha_M - \theta)\} \\ &= \dot{\theta} V_\theta \end{aligned} \quad (5.3)$$

$$\begin{aligned} \dot{V}_\theta &= V_T \cos(\alpha_T - \theta)(-\dot{\theta}) - V_M \cos(\alpha_M - \theta)(-\dot{\theta}) \\ &= -\dot{\theta} \{V_T \cos(\alpha_T - \theta) - V_M \cos(\alpha_M - \theta)\} \\ &= -\dot{\theta} V_R \end{aligned} \quad (5.4)$$

Note that (5.3) and (5.4) are obtained by substituting from (5.2) and (5.1).

From (5.3) and (5.4) we obtain,

$$\begin{aligned}\dot{\theta} &= \frac{\dot{V}_R}{V_\theta} = -\frac{\dot{V}_\theta}{V_R} \\ \Rightarrow V_R \dot{V}_R &= -V_\theta \dot{V}_\theta \\ \Rightarrow V_R \dot{V}_R + V_\theta \dot{V}_\theta &= 0\end{aligned}$$

Integrating both sides of the above equation we get,

$$V_R^2 + V_\theta^2 = c^2 \text{ (A constant)} \quad (5.5)$$

which is the equation of a circle in the  $(V_\theta, V_R)$ -space. This circle has radius equal to  $c$  and center at the origin. If the initial values of  $V_R$  and  $V_\theta$  are,

$$\begin{aligned}V_R(t=0) &= V_{R0} \\ V_\theta(t=0) &= V_{\theta0}\end{aligned}$$

then

$$c = \sqrt{V_{R0}^2 + V_{\theta0}^2} \quad (5.6)$$

This circle is shown in Figure 5.2. This shows that with time the  $(V_\theta, V_R)$ -point moves in a circle in the  $(V_\theta, V_R)$ -space. The circle itself gets determined by the initial values  $V_{\theta0}$  and  $V_{R0}$ .

Note that in this figure we have shown some arrows that indicate the direction in which the  $(V_\theta, V_R)$ -point moves with time. How did we get these directions? For this let us look at (5.3) and (5.4). If we multiply  $R$  on both sides of these equations and substitute  $V_\theta = R\dot{\theta}$  and  $V_R = \dot{R}$  then we get,

$$R\dot{V}_R = V_\theta^2 \quad (5.7)$$

$$R\dot{V}_\theta = -V_\theta V_R \quad (5.8)$$

Since  $R$  is always a positive quantity, i.e.,  $R > 0$ , we have

$$\dot{V}_R > 0 \text{ always}$$

$$\dot{V}_\theta > 0 \text{ if } \{V_R > 0 \text{ and } V_\theta < 0\} \text{ OR } \{V_R < 0 \text{ and } V_\theta > 0\}$$

$$\dot{V}_\theta < 0 \text{ if } \{V_R > 0 \text{ and } V_\theta > 0\} \text{ OR } \{V_R < 0 \text{ and } V_\theta < 0\}$$

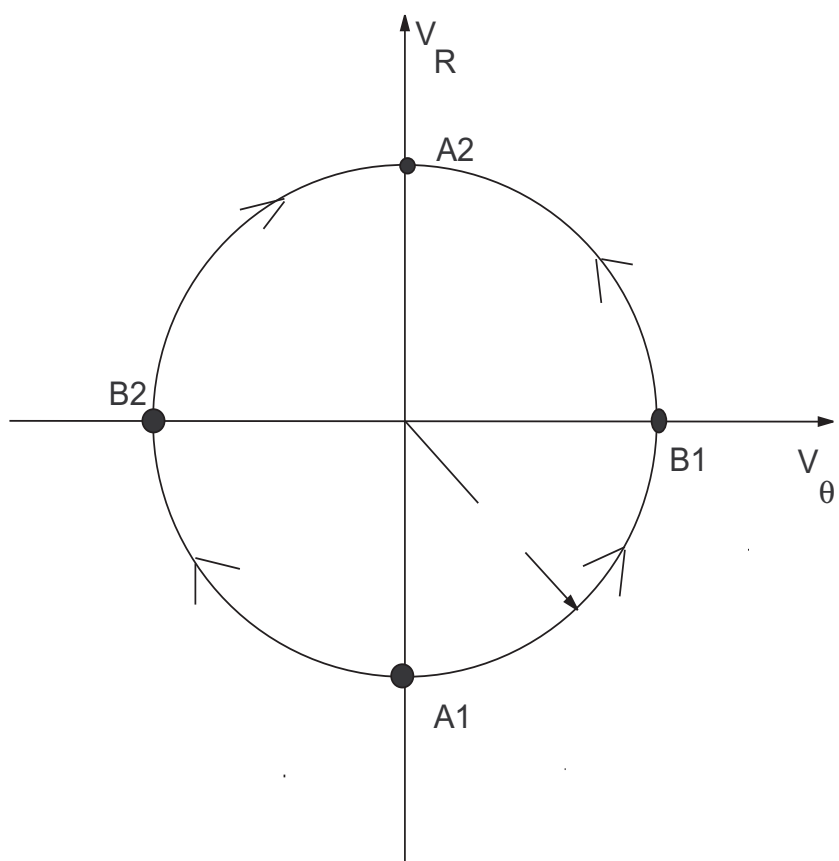


Figure 5.2: Engagement trajectory in  $(V_\theta, V_R)$ -space

These are sufficient to determine the direction of movement of the  $(V_\theta, V_R)$ -point.

*Questions*

1. Show that the trajectory in the relative velocity space of two unguided objects moving in straight lines on a plane is a circle.
2. Show that a point in the relative velocity space representing the components of the relative velocity always moves upwards.
3. In the figure below, the two objects M and T are moving in straight lines. Obtain the equation of the trajectory in the relative velocity space.

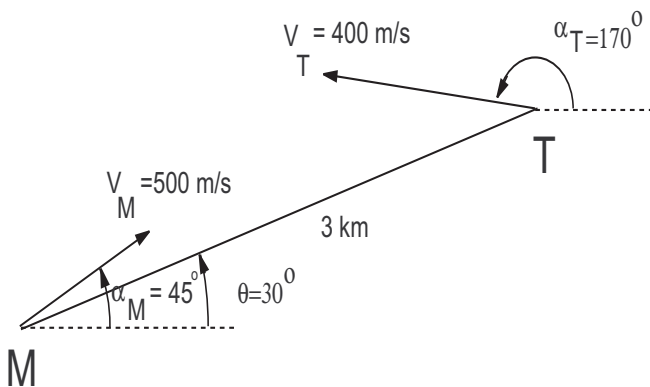


Figure 5.3: Initial engagement geometry for Question 3

## Module 4: Lecture 10

### Collision Condition and Collision Triangle

**Keywords.** Collision triangle, Miss-distance, Inverse collision triangle

#### 5.1.3 The collision condition and the collision triangle

Note that when  $V_\theta = 0$ , from (5.8) we have  $\dot{V}_\theta = 0$ , which implies that points A1 and A2 shown in Figure 5.2 are stationary points. So, states corresponding to these points are invariant with time. At A1 and A2,

$$V_\theta = 0 \quad (5.9)$$

and so, from (5.8) and (5.7), since  $R > 0$  always,

$$\begin{aligned}\dot{V}_R &= 0 \\ \dot{V}_\theta &= 0\end{aligned}$$

which implies that at these points both  $V_R$  and  $V_\theta$  remain constant thus proving the stationarity of the points A1 and A2. Let us now examine point A1 where,

$$V_R < 0 \quad (5.10)$$

which implies that the LOS separation between the two objects shrinks at a constant rate if the state is on A1. Hence, after a finite time the two objects collide with each other. Thus, (5.9) and (5.10) together form the *collision condition*.

Since  $V_\theta = R\dot{\theta} = 0$ , it also implies that  $\theta$  remains constant with time, i.e., the LOS does not rotate in space with time. This is the condition for the *collision triangle*, so called because if we consider the trajectories of M and T for some time before the actual collision takes place, we will get a triangle in which the two objects move in a straight line and the LOS remains parallel for all time. The collision triangle is shown in Figure 5.4.

At point A2, we have  $V_\theta = 0$  and  $V_R > 0$  which is the inverse of the collision triangle in the sense that, although the LOS does not rotate in space, the objects move away from each other with constant LOS rate. This situation is shown in Figure 5.5.

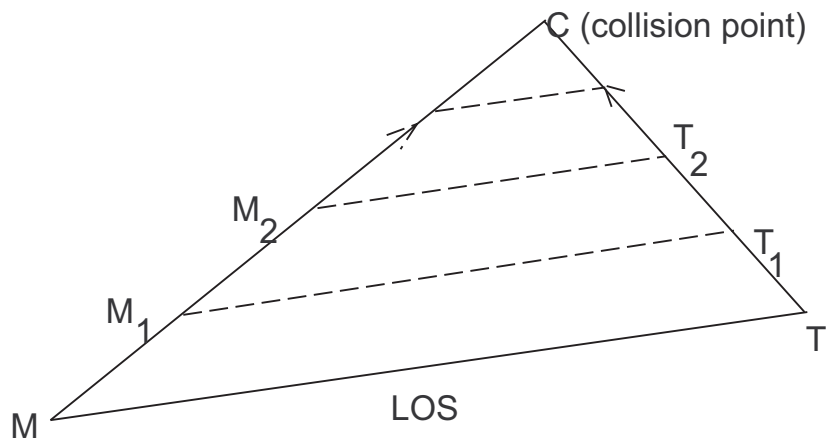


Figure 5.4: The collision triangle – Point A1

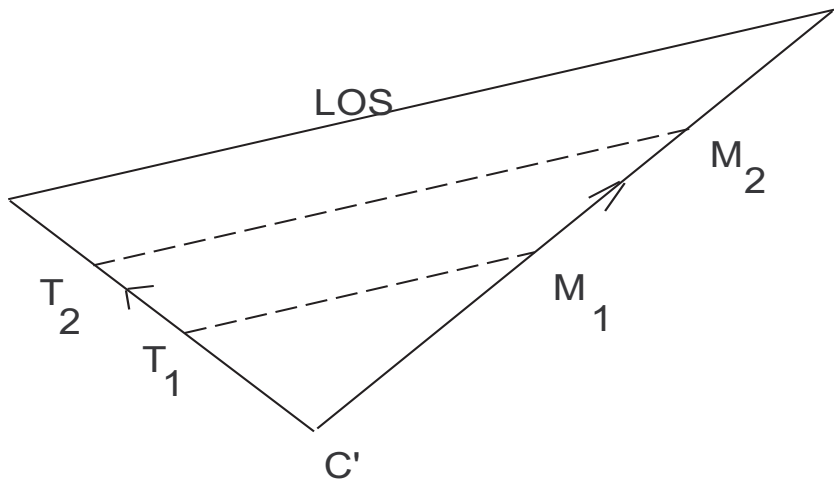


Figure 5.5: The inverse collision triangle – Point A2

### 5.1.4 Miss-distance

Let us now examine Points B1 and B2 where,

$$V_R = 0$$

$$V_\theta \neq 0$$

Looking at the trajectory in the neighbourhood of these points we see that  $V_R < 0$  just prior to these points and  $V_R > 0$  immediately after these points. This implies that the LOS separation  $R$  attains a minimum at the points B1 and B2. Hence, the *miss-distance* or the *distance of closest approach* occurs at these points. Can we get a closed-form expression for the miss-distance ( $R_{\text{miss}}$ ) and the time ( $t_{\text{miss}}$ ) at which the miss-distance occurs? For this we have to use (5.5),

$$V_R^2 + V_\theta^2 = c^2$$

Since, according to (5.7)  $RV_R' = V_\theta^2$ , we have

$$\begin{aligned} V_R^2 + RV_R' &= c^2 \\ \Rightarrow \dot{R}^2 + R\ddot{R} &= c^2 \end{aligned}$$

Since  $d/dt(R\dot{R}) = \dot{R}^2 + R\ddot{R}$ , the above equation, on integration, yields

$$R\dot{R} = c^2 t + b \quad (5.11)$$

where,  $b$  is a constant equal to,

$$b = R_0 V_{R0} \quad (5.12)$$

obtained by putting  $t = 0$  in (5.11) so that  $R_0$  is the initial LOS separation and  $V_{R0}$  is the initial value of  $V_R$ . Now, at points B1 and B2 we have  $V_R = \dot{R} = 0$ ,  $R = R_{\text{miss}}$ , and  $t = t_{\text{miss}}$ , substituting which in (5.11) we obtain,

$$\begin{aligned} 0 &= c^2 t_{\text{miss}} + b \\ \Rightarrow t_{\text{miss}} &= \frac{-b}{c^2} \end{aligned} \quad (5.13)$$

$$\Rightarrow t_{\text{miss}} = \frac{-R_0 V_{R0}}{V_{R0}^2 + V_{\theta0}^2} \quad (5.14)$$

Equation (5.11) can be further integrated to yield,

$$\frac{1}{2}R^2 = \frac{c^2 t^2}{2} + bt + a \quad (5.15)$$

where,

$$a = \frac{R_0^2}{2} \quad (5.16)$$

From (5.15) we obtain,

$$R = \sqrt{c^2 t^2 + 2bt + 2a} \quad (5.17)$$

So, the miss-distance  $R_{\text{miss}}$  is obtained by substituting  $t = t_{\text{miss}}$  in (5.17).

$$\begin{aligned} R_{\text{miss}} &= \sqrt{c^2 t_{\text{miss}}^2 + 2bt_{\text{miss}} + 2a} \\ &= R_0 \sqrt{\frac{V_{\theta 0}^2}{V_{\theta 0}^2 + V_{R0}^2}} \end{aligned} \quad (5.18)$$

Thus, the above equation allows us to compute the miss-distance that occurs given the initial configuration of the two objects. This result can be further extended to yield other interesting results.

### 5.1.5 Effect of lethal radius

When we consider M to be a missile and T to be a target, it is quite likely in practice that the missile does not actually hit the target, but passes close to it. The proximity fuze in the missile, on detecting the nearness of the target, activates the detonators and explodes the warhead. The warhead has a certain range of effectiveness given by its lethal radius ( $R_{\text{lethal}}$ ), so that any target within this range will be destroyed when the warhead explodes. So, a target should be considered as *captured* or *intercepted* if the miss-distance is less than the lethal radius, i.e.,

$$\begin{aligned} R_{\text{miss}} &\leq R_{\text{lethal}} \\ \Rightarrow R_0 \sqrt{\frac{V_{\theta 0}^2}{V_{\theta 0}^2 + V_{R0}^2}} &\leq R_{\text{lethal}} \\ \Rightarrow R_0^2 V_{\theta 0}^2 &\leq R_{\text{lethal}}^2 (V_{\theta 0}^2 + V_{R0}^2) \\ \Rightarrow (R_0^2 - R_{\text{lethal}}^2) V_{\theta 0}^2 &\leq R_{\text{lethal}}^2 V_{R0}^2 \\ \Rightarrow V_{\theta 0}^2 &\leq \left( \frac{R_{\text{lethal}}^2}{R_0^2 - R_{\text{lethal}}^2} \right) V_{R0}^2 \\ \Rightarrow |V_{\theta 0}| &\leq \sqrt{\frac{R_{\text{lethal}}^2}{R_0^2 - R_{\text{lethal}}^2}} |V_{R0}| \end{aligned} \quad (5.19)$$

The inequality (5.19) is now the *collision condition* or the *capturability condition* in lieu of (5.9). Note that if we put  $R_{\text{lethal}} = 0$  in (5.19), we get (5.9). But what about (5.10)? This remains as it is.

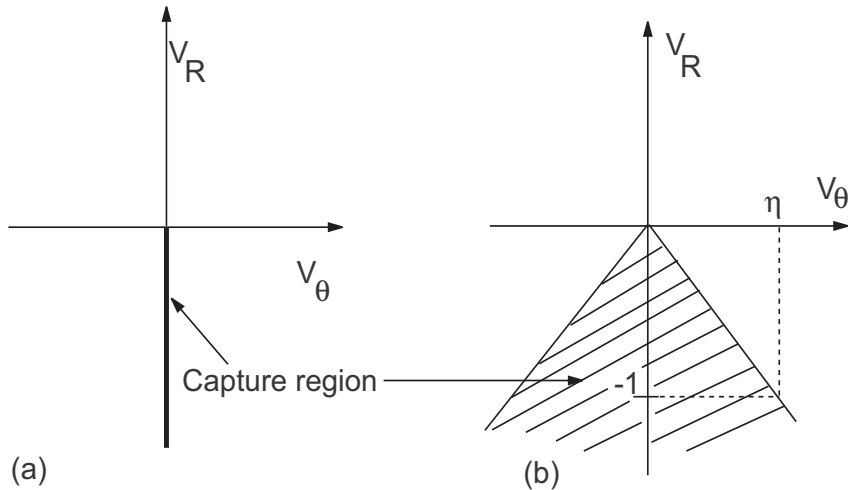


Figure 5.6: *Capture region in the  $(V_\theta, V_R)$ -space* (a) Zero miss-distance (b) Non-zero miss-distance

So, when intercept is defined as zero miss-distance the collision or capturability condition is given by,

$$V_{\theta 0} = 0$$

$$V_{R0} < 0$$

Whereas, when intercept is defined as non-zero miss-distance less than a given value  $R_{\text{lethal}}$ , collision or capturability condition is given by,

$$|V_{\theta 0}| \leq \eta |V_{R0}|$$

$$V_{R0} < 0$$

where,

$$\eta = \sqrt{\frac{R_{\text{lethal}}^2}{R_0^2 - R_{\text{lethal}}^2}} \quad (5.20)$$

The above equations define intercept and collision conditions in a sufficiently general way. Using (5.19) we can demarcate the *capture region* in the  $(V_\theta, V_R)$ -space. This is shown in Figure 5.6 for both zero and non-zero miss-distances.

### 5.1.6 Asymptotic behaviour of $V_\theta$ and $V_R$

Figure 5.2 shows the behaviour of  $V_\theta$  and  $V_R$  in the  $(V_\theta, V_R)$ -space. But what happens to these relative velocity components with respect to time? From (5.11), we have

$$\begin{aligned} RV_R &= c^2 t + b \\ \Rightarrow V_R &= \frac{c^2 t + b}{R} \\ \Rightarrow V_R &= \frac{c^2 t + b}{\sqrt{c^2 t^2 + 2bt + 2a}} \end{aligned} \quad (5.21)$$

So, from (5.5),

$$V_\theta = \sqrt{c^2 - V_R^2} \quad (5.22)$$

From these equations we obtain,

$$\lim_{t \rightarrow \infty} V_R = c = \sqrt{V_{R0}^2 + V_{\theta0}^2} \quad (5.23)$$

$$\lim_{t \rightarrow \infty} V_\theta = 0 \quad (5.24)$$

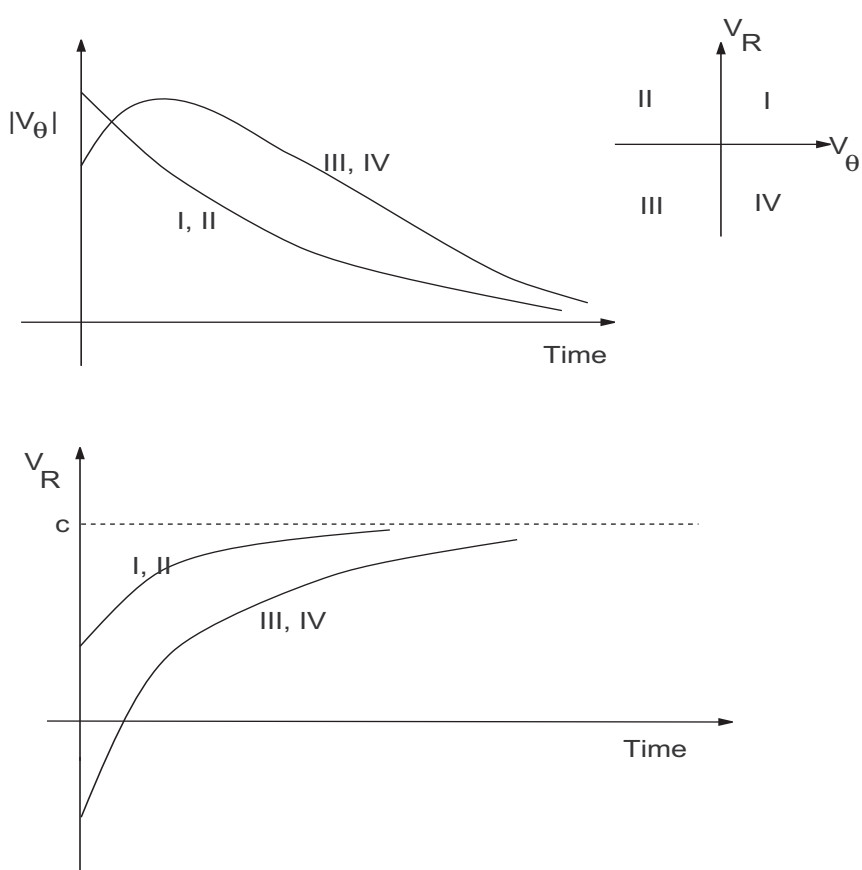
which implies that as time tends to infinity the point  $(V_\theta, V_R)$  asymptotically approaches the point A2 shown in Figure 5.2. The variation of these relative velocities with respect to time starting from different quadrants in the  $(V_\theta, V_R)$ -space is shown in Figure 5.7.

## 5.2 Avoidance

The above results can also be used to conceptualize the idea of avoidance. We will not go into details at this juncture, but it is interesting to note that the violation of the capture conditions given in the previous section leads to a *no capture* situation. Consider that the  $R_{\text{lethal}}$  is the radius of the circular object T. Then, by violating the capture condition we can ensure that M avoids T. We will have more to say about this in a later lecture where we will show how these concepts can be utilized to formulate avoidance strategies.

## 5.3 Concluding Remarks

In this chapter we discussed some fundamental ideas behind the kinematics of interception or capture between two bodies moving with constant velocities. We did not

Figure 5.7: Variation of  $V_\theta$  and  $V_R$  against time

discuss guidance strategies at all, but we shall see later how the ideas discussed here naturally lead to guidance strategies.

### Questions

1. What is a collision triangle and inverse collision triangle?
2. Derive the expression for miss-distance between two objects moving in a straight line. Also, obtain the expression for the time at which the miss-distance occurs.
3. What is the capture region when capture is defined by one object hitting the other object. What is it when one object is carrying a lethal warhead which has some definite range of effectiveness?
4. To what values do the relative velocity components converge when the two objects are not on collision course.
5. For the following initial engagement geometry determine the miss distance, the time of closest approach, and the capture region when M carries a warhead of lethal range 30 m.

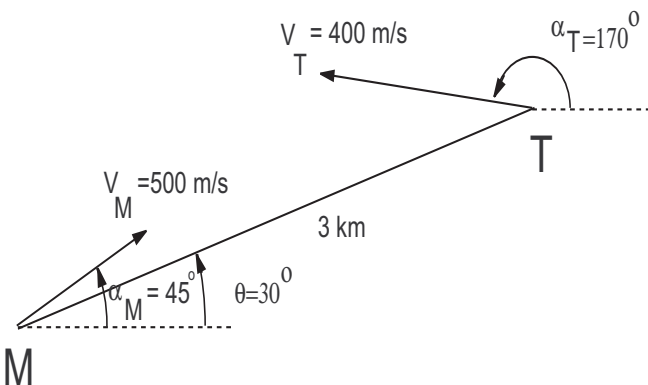


Figure 5.8: Initial engagement geometry for Question 5

## Chapter 6

# A Taxonomy of Guidance Laws

## Module 5: Lecture 11 An Overview of Guidance Laws

**Keywords.** Classical Guidance, Modern Guidance

### 6.1 An Overview of Guidance Laws

As mentioned in the previous lecture the primary objective of the guidance subsystem in a tactical missile is to generate suitable commands so that the missile comes closer and closer to its target. This is a very broad definition and it is somewhat unsatisfactory when you consider the fact that there are many physical constraints under which a missile has to perform. The major constraint is that of *time*. Tactical missiles of the SAM or AAM category seldom have a flight time of more than 50 seconds. In this short time the guidance system has to generate a sufficient number of commands to enable the missile to fly in the proper intercept course and intercept the target. So the main concern here is the following : *How can a guidance subsystem utilize the information available to it to generate proper guidance commands within the time limitations imposed upon it?*

This was the concern of the guidance system designers in the early days of guided missile design. Of course, in those days it was more vital to design a proper propulsion

system that could carry the missile and its payload to the desired distance rather than to design a guidance system that can accurately intercept a target. The reasons for this were two-fold. The first was that guided missiles were used mainly for the psychological advantage that they gave to an army rather than for their accuracy (to be frank, this seems to be an important factor even now – if you go by the track record of the Patriot missiles during the recent gulf war!). The second reason was that the targets in those days were somewhat clumsy and slow moving – for example, Zeppelins during the First World War (these were more like huge balloons that you could hit by throwing a stone – well, almost!), or low-flying and low-speed aircraft. However, soon after the Second World War, all this changed and demand on the guidance system went up. They needed to be more *accurate* and more *reliable*. So well-defined guidance laws with a firm grounding on a theoretical framework was essential. Even then, the *Classical Guidance Laws*, which were proposed and tried out, were based on very simple ideas. We will look at some of them in a short while. These simple ideas were intuitively appealing but did not initially have any firm theoretical basis. In fact, they were rather *empirical* in nature. However, their major advantages were:

- They were easy to understand,
- easy to implement,
- needed simple information inputs, and
- by their very simplicity instilled a sense of confidence in their designers (which is perhaps the most important – and quite often the least understood – aspect of all pioneering and successful design activities).

It was not until the 1960s that a rigorous mathematical framework for these guidance laws began to emerge with the rapid developments in the area of *Optimal Control Theory* and its applications, which basically dealt with problems of *dynamic optimization*. The kind of problems in which optimal control theory found applications were related to the optimization of some performance criterion by a dynamical system working under well-specified constraints. It is easy to see that many missile-target engagement problems can be quite obviously formulated in this framework. However, formulation of a problem is one thing and the solution of it is another. It was soon found that with

the available computing resources it was almost impossible to obtain a solution to a realistically formulated non-linear guidance problem. The obvious next step was to adopt a linearized formulation and hope for a solution that can be implemented easily and yield a close-to-optimal solution when implemented in a closed-loop manner. The fundamental principle behind this approach was that when you break up a real-life dynamical system into smaller time-frames then, within that time frame, it can be approximated as a linear system. This approach yielded rich results in more ways than one. The so-called linear quadratic formulation gave a simpler solution to the problem with the hope of achieving partial implementation at some future time when computing capability go up. But the more important benefit of this exercise was the realization that many of the empirical guidance laws could actually be shown to have a very good theoretical basis. In other words, it was found that the so-called empirical guidance laws were optimal under some simplified assumptions.

From the above discussion we can now classify guidance laws as:

- *Classical or Empirical guidance laws*
- *Modern or Theoretically-rigorous guidance laws*

Further, we can also classify guidance laws from the point of view of their *implementability*. This classification is not much different from what I have mentioned above. It is easy to see that most *classical* guidance laws were “fairly easy” to implement since they all arose from simple ideas.

You may wonder why I have put the words *fairly easy* under quotes. This is because the implementation of these guidance laws were easy from a conceptual viewpoint in the sense that all the necessary hardware were available or could be produced with little effort. But the actual implementation took many thousands of man-hours of intense effort by some of the best engineering brains of the time. If you want to catch a glimpse of the hard work, the euphoria, and the sense of serendipity that pervaded the dedicated team of people who handled these projects in the Raytheon Company in the USA then I suggest that you read an account of it in Mike Fossier’s 1984 paper that appeared in the *Journal of Guidance, Control, and Dynamics* and which I have referred to in my first lecture.

Coming back to the issue of implementability, the modern guidance laws were extremely elegant and, in computer simulations, gave wonderful performance results. But, alas, their requirement of large amount of time to complete all the intricate computations, and also their hunger for extra information which was impractical to obtain with sufficient accuracy, made them totally unimplementable. Even now, notwithstanding the tremendous strides made in harnessing vast computing powers in the space of a small silicon chip, these laws still remain unimplementable due to the strict time constraints imposed by the short flight time of a tactical missile. Optimal control theory was instrumental in putting man on the moon, sending space crafts on interstellar missions covering mind-boggling distances, and huge satellites in orbit in space, but when it came to tactical missiles, it still did not, and indeed even now does not, have the capability to deliver the performance that it promised in computer simulations.

In subsequent sections we will briefly discuss the several *classical* and *modern* guidance laws for tactical missiles. Our discussion will be confined to explain the working of these guidance laws, the fundamental principles behind them, and why they perform well or fail to perform at all. We will not go into any complicated mathematical framework or analysis to do this. The emphasis will be more on intuition and understanding rather than on rigorous analysis. A taxonomy of guidance laws for tactical missiles is given in Figure 6.1. From this figure you can see that the classical guidance laws have been further sub-divided into *conceptual* and *implementable* categories. In the following sections we will look at these separately.

### Questions

1. Why are the classical guidance laws favoured by missile system designers?
2. What benefits did the modern guidance laws bring to the guidance law performance?
3. What was the motivation behind formulating guidance problems in the optimal control framework?
4. What are the drawbacks of the modern guidance laws as against the classical or

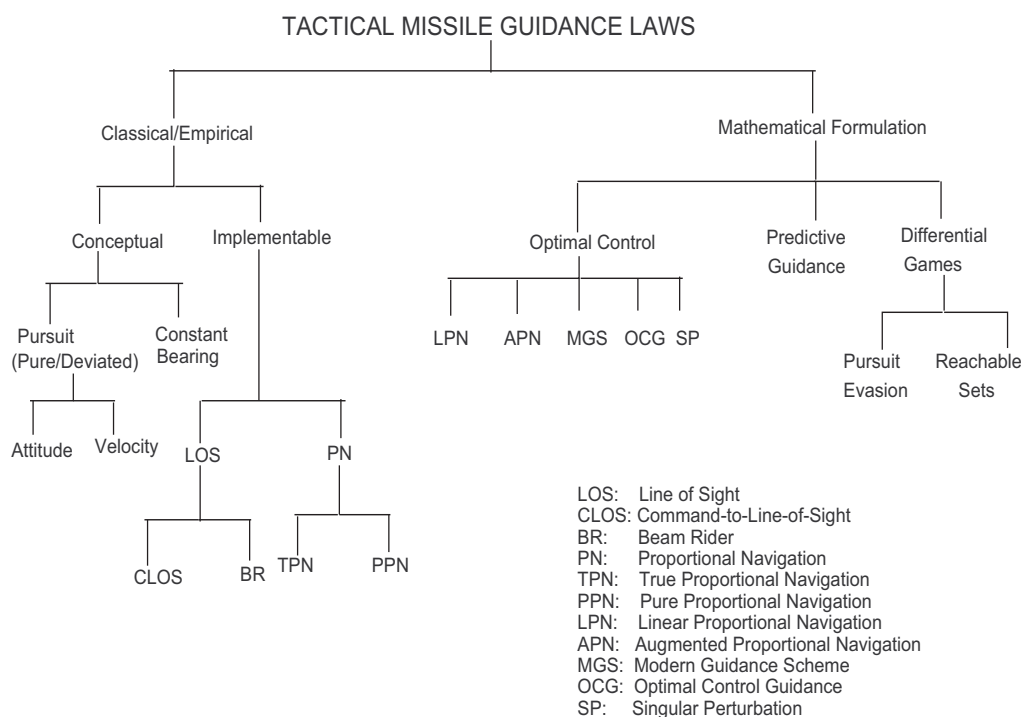


Figure 6.1: A taxonomy of tactical missile guidance laws

empirical guidance laws?

5. Draw a flowchart depicting the taxonomy of guidance laws.

## Module 5: Lecture 12

### Conceptual Classical Guidance Laws

**Keywords.** Pursuit Guidance, Deviated Pursuit, Constant Bearing Course, Proportional Navigation (PN)

#### 6.2 Conceptual Classical Guidance Laws

These guidance laws are the ones that were conceptually sound and attracted quite a bit of attention in the early days of guidance law development but very quickly they revealed several drawbacks, mainly in terms of performance and implementability. But, because the concepts on which their initial premise was based were quite logical, they reveal a lot about how guidance schemes work in reality. So we shall discuss some of these conceptual guidance laws next.

##### 6.2.1 Pursuit guidance law

The pursuit guidance law was based on the simplest of all ideas. It is also called the *dog-and-rabbit* guidance law. When a dog – which is known for its friendliness to the human species, but is seldom commended for its intelligence – chases a rabbit, it tries to keep pointing its muzzle at the rabbit as it runs toward it. Logically speaking, this should be considered an excellent guidance strategy since only a moment's thought will convince you that if you keep on pointing towards a moving target and continue to come closer and closer to it, then after some time you are bound to hit the target. But, if you have ever had an occasion to watch such a chase you would have noticed that quite often towards the end of the chase the dog, while taking a sharp turn, misses a step, slips, and falls. By the time it gets up, the rabbit is gone! This is precisely the major problem with pursuit guidance too. The reason the dog misses its step is because it tries to take too sharp a turn. Look at the next figure (Figure 6.2).

Notice that at every instant in time the missile is pointing towards the target (a low-flying incoming aircraft – also called a crossing target) which is flying in a straight line. At point A on the trajectory the missile has to take a very sharp turn if it is to continue pointing towards the target. Now, a missile cannot take any arbitrary turn. It has a

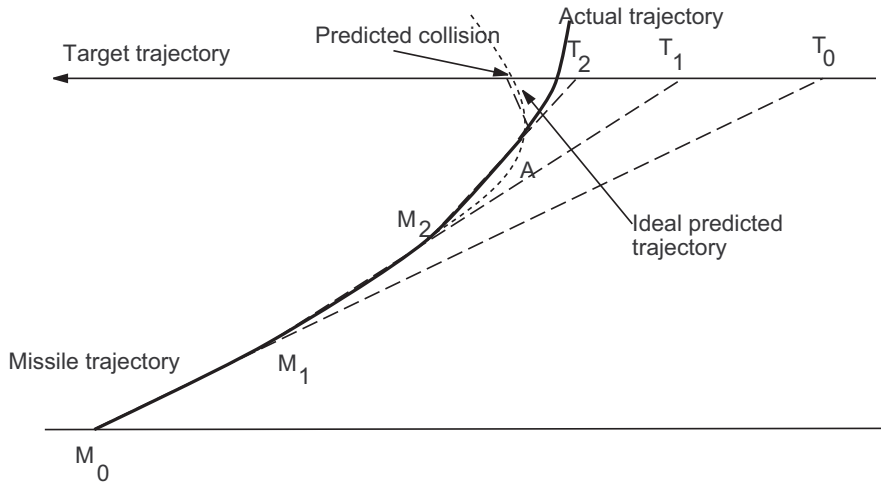


Figure 6.2: Why the pursuit guidance law fails!

minimum turn radius below which it cannot turn (just the way your motor vehicle has – you cannot make your vehicle turn in a circle of 1 meter radius). So, it can no longer keep pointing towards the target and ultimately misses it. The broken line after point A is the trajectory which the missile would have followed and ultimately hit the target, had it been capable of taking sharp turns. The solid line shows the actual trajectory of the missile when it is constrained by a minimum turn radius. This trajectory causes the missile to miss the target. Note that the missile missed the target in spite of the target not trying to maneuver at all. It would have been worse if the target had actually maneuvered.

This guidance law is actually called the *pure pursuit* guidance law. A natural question that comes to mind is, *what happens if we train the dog to display a little more intelligence by taking advantage of the information that the rabbit is running in a particular direction?* The next stage in the development of this guidance law was precisely this and it was called the *deviated pursuit* guidance law. Here, the missile does not point toward the target but at a point slightly ahead of it. This scheme does reduce the demand on the guidance system in terms of the turn radius but has other kind of problems. One obvious problem is the fact that if the target changes its direction of flight (a maneuvering target – for example, one which executes a circular maneuver) then the angular deviation needed must also change accordingly. It is not a very trivial matter to carry out an implementa-

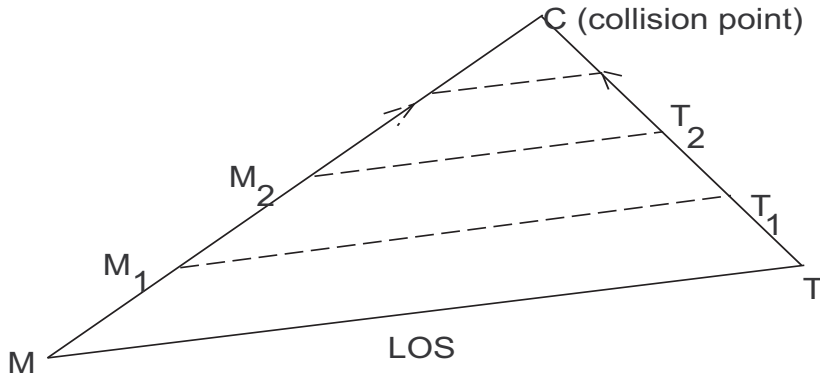


Figure 6.3: The constant bearing course engagement geometry

tion of this aspect. Other variations of the pursuit guidance are the *attitude pursuit* and the *velocity pursuit*. In *attitude pursuit* the missile's centerline or the longitudinal axis is made to point toward the target, whereas in the *velocity pursuit* the velocity vector of the missile is made to point toward the target. Note that these two are different since the velocity vector of a missile lags its longitudinal axis by the *angle-of-attack*.

It is actually not correct to say that pursuit guidance is unimplementable. It is an inefficient guidance law so far as aircraft target are concerned, where the target velocity is quite high. But this guidance law works fine with slowly moving targets like ships and tanks, and realistic simulations have reported excellent performance. However, since our objective was to understand the guidance philosophy here rather than the carrying out of a detailed study we shall stop our discussion here.

### 6.2.2 Constant bearing course

This is conceptually the best guidance law that one can think of. All guidance laws actually try to achieve the performance of the *Constant Bearing Course Guidance Law*. It is based upon the concept of *collision triangle* described in the previous chapter. To explain how this guidance law works look at the next figure (Figure 6.3).

Consider the triangle  $CMT$ . Initially the missile is at  $M$  and the target is at  $T$ . Suppose they move at constant speeds in the directions shown by the arrows and ultimately collide at point  $C$ . Then it implies that the time taken by the missile to cover

the distance  $MC$  was the same as the time taken by the target to cover the distance  $TC$ . Which, in turn, implies that the velocity ratio of the missile and the target is the same as the ratio  $\frac{MC}{TC}$  between the sides of the triangle. This is called the *collision triangle*. Now look at the other positions of the missile and the target: When the missile is at position  $M_1$  the target is at position  $T_1$ , when the missile is at position  $M_2$  the target is at position  $T_2$ , and so on. The line joining the missile position and the target position is called the *instantaneous line-of-sight (LOS)*. A little thought will convince you that under the given conditions the LOS does not rotate at all. In other words,  $MT$  is parallel to  $M_1T_1$ , which in turn is parallel to  $M_2T_2$ , and so on. Thus, the line-of sight does not rotate in space. It turns out that this is a necessary condition for collision to occur when the missile and the target are both flying in straight line paths and with constant speed. If, in addition, the rate of change of the *LOS separation* is negative, i.e., the length of the LOS is decreasing in time, then these two conditions together constitute a necessary and sufficient condition for intercept to occur. This is a very important and fundamental result in guidance theory and we will have occasion to use it quite often in our analysis in the subsequent lectures.

Now, coming back to the constant bearing course, it appears that the constant bearing guidance law is the solution to all our guidance problems. Theoretically this guidance law indeed gives the best performance with respect to reasonable performance measures but, in practice, neither the missile nor the target flies at a constant speed. Moreover, the target is quite likely to maneuver. This means that the LOS will tend to rotate in space and to implement the constant bearing guidance law the guidance system must be able to take corrective actions for every such change instantaneously. Only then will the guidance law give satisfactory performance results. But this is too much to expect from any guidance law. No physical system has such fast response. Added to it is the fact that the measurement errors are also quite high. Hence, an exact implementation of the constant bearing course is next to impossible. So, what is the alternative? It turns out that the alternative is the *Proportional Navigation (PN)* guidance law, which tries to implement the constant bearing guidance law in the most practical way possible, and that is the reason why PN has been found to give such good performance even at the face of serious odds. We shall discuss and study the performance of the PN guidance law and its important variants in a series of subsequent lectures.

*Questions*

1. Describe the basic philosophy behind the pure pursuit guidance laws.
2. With a sketch show the trajectory of a missile guided by the pure pursuit guidance law against a level incoming target and explain why the pursuit guidance law is likely to fail.
3. Explain deviated pursuit and its philosophy.
4. Explain attitude pursuit and velocity pursuit.
5. Explain constant bearing guidance law and why is it difficult to implement

## Module 5: Lecture 13

# Implementable Classical Guidance Laws

**Keywords.** LOS Guidance, CLOS Guidance, Beam Rider, Proportional Navigation

### 6.3 Implementable Classical Guidance Laws

In this section we shall talk about some classical/empirical guidance laws which are not only based upon very simple concepts but were also actually implemented in many missiles during the early days of tactical missile development. Some of these missiles are being used even now and continue to give excellent performance.

#### 6.3.1 Line-of-Sight (LOS) Guidance

The *LOS Guidance* also works on a simple philosophy. According to it, if the missile remains on the line-of-sight joining the launch station and the target, and it is fired in the direction of the target then the missile must hit the target. The basic idea behind this guidance law is that the line-of-sight from the launch station to the target is basically some kind of a reference which defines the position of the missile at any given instant in time. The missile guidance system acts in such a way that the missile attempts to remain on this line. Also note that the missile has to turn in such a way that it has to match the LOS rate, that is, its velocity normal to the line-of-sight should equal the LOS velocity at that point. This is shown in Figure 6.4.

Before we look into the actual implementation of this guidance law let us see how the guidance law performs. Let us consider a scenario similar to the one in pursuit guidance, that is, we consider an incoming target which is flying low and at a reasonably high speed. The next figure (Figure 6.5) shows the resulting trajectory. You can see that a problem similar to the one in pursuit guidance occurs even here. That is, towards the end of the engagement the missile needs to take a very sharp turn.

In spite of this drawback, LOS guidance has been used quite extensively for many types of missiles. It is basically mechanized in two forms: *Command-to-Line-of-Sight (CLOS)* and *Beam Rider (BR)*. Their basic principle remains the same. They differ only

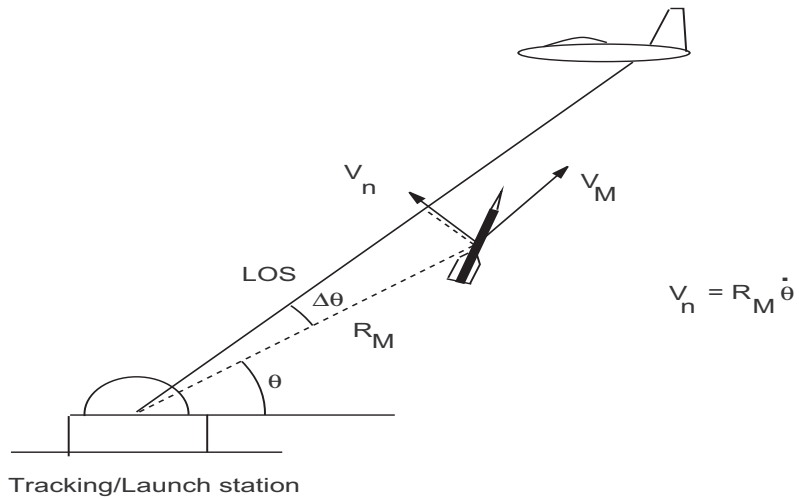


Figure 6.4: The LOS guidance principle

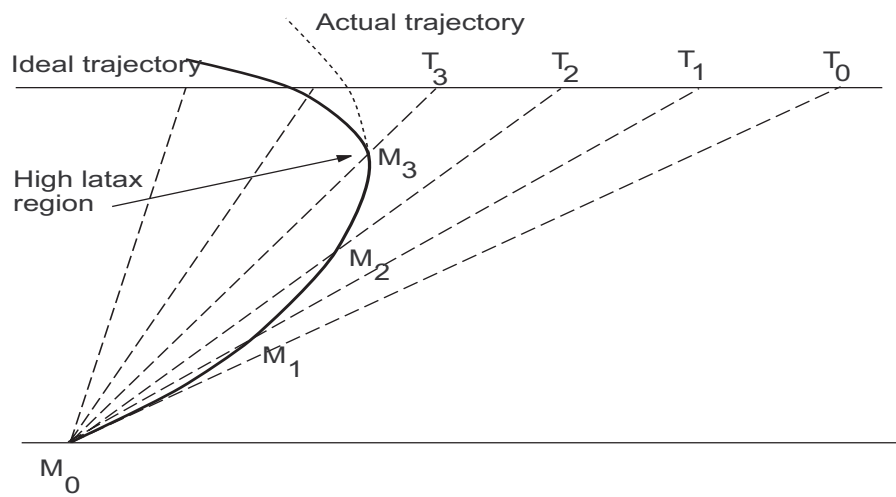


Figure 6.5: The LOS guidance trajectory

in their mechanization.

*Command-to-Line-of-Sight:* In this kind of guidance, an uplink is used to transmit guidance commands from a guidance computer, situated on the ground station or the launch platform, to the missile. The ground station tracks the missile and the target, computes the guidance command which would enable the missile to remain on the LOS joining the ground station (tracking radar) and the target, and transmits this guidance command to the missile via an uplink which could be a radio link or a wire link. Since the ground station tracks the missile, the missile's position is known to it, and so the guidance command compensates for the missile position before transmission of the command to the missile. Normally the guidance command is proportional to the angular error between the LOS and the line joining the ground station and the missile, and the distance of the missile from the ground station. Note that this quantity is the linear displacement of the missile from the LOS and normal to it. A compensation term is added to this guidance command in a feedforward mode. We will not go into details.

*Beam-Rider:* There is an electro-optical beam that joins the ground station with the target. The missile guidance system which is located inside the missile senses the deviation of the missile position from the beam and generates guidance commands to enable the missile to stay inside the beam. Figure 6.6 explains the working of the beam-rider missile.

The beam may be a radar beam or a laser one and the source of the beam is attached to the launcher itself. The missile carries a receiver at its rear end which receives the beam signal and helps the missile to determine how far away from the beam axis the missile is. The beam signal is reflected by the target and is in turn received by the ground radar. This signal is used to track the target. One problem here is that as the missile turns, its axis has a large angular deviation with respect to the beam axis. So, if the receiver at the rear end of the missile does not have sufficient beam width then it can easily miss the signal from the beam. This situation is likely to occur when the target is a high-speed approaching or crossing aircraft and is illustrated in Figure 6.7.

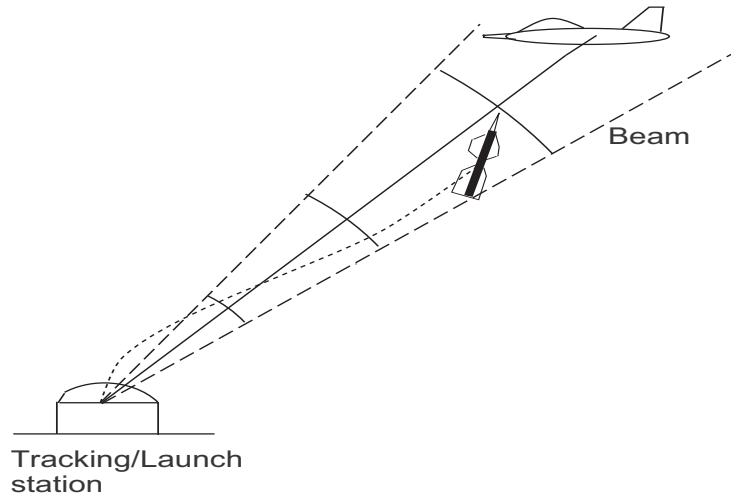


Figure 6.6: Beam-rider guidance

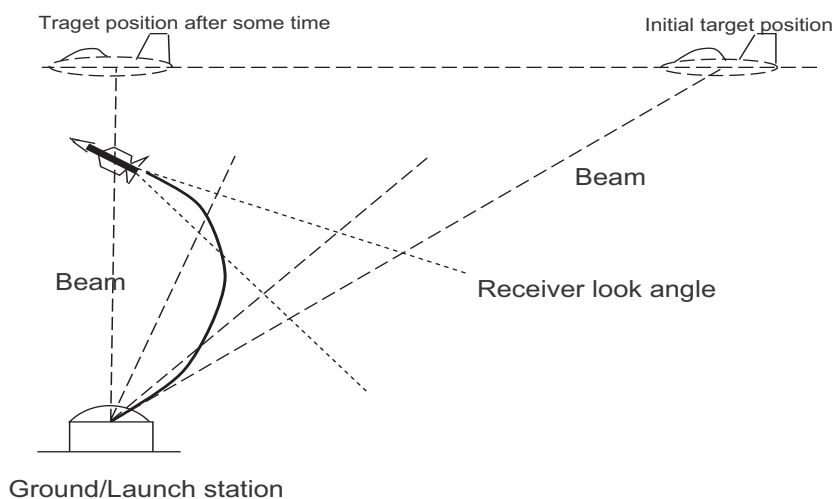


Figure 6.7: How the missile receiver may miss the beam signal

The beam-rider missile requires on-board autopilot compensation since in this case (unlike the CLOS case) the ground tracker does not know the position of the missile once the missile has been fired. The *Talos* beam-rider missile is an example of an early missile which uses this principle.

### 6.3.2 Proportional Navigation (PN) Guidance

Now we come to the most important guidance law of all the classical guidance laws. This guidance law tries to emulate the principle of the *constant bearing guidance law* in the most logical way. Before we try to understand how the PN guidance law is formulated let us go back in history to the genesis of the PN law.

In olden days when mariners did not have sophisticated instruments to help them, one of the main problems for a ship entering the harbour was to avoid colliding with other ships. The detection of collision well in advance was crucial since if avoidance maneuvers are not put into execution with sufficient time to spare, the ships tended to collide since achieving even a slight change in the course of a ship takes a fairly long time. The mariners used a very practical thumb rule for detecting collisions between ships.

*When a neighbouring ship appears to be stationary, and also seems to be growing in size, a collision is imminent.*

This is the time when they immediately began avoidance maneuvers by changing the course of their ship.

If we analyse the observations made by the sailors and compare them with the constant bearing course that we have discussed earlier we will see that there is a close analogy between the two. When another ship appears to be stationary with respect to your own ship it implies that the line-of-sight between the two ships is not rotating. If the other ship appears to grow larger and larger, it implies that the distance between the two ships is reducing, that is, the LOS separation between the two ships is reducing. These are precisely the two conditions (necessary and sufficient) which ensures interception of the target by the missile.

Proportional Navigation (PN) uses this observation to design a guidance law. To

obtain a collision the LOS rotation rate (also called the LOS rate) must be kept at zero, while the separation must be reduced with time. It is easy to ensure the latter by launching the missile approximately in the direction of the target (or a predicted collision point), but to ensure zero LOS rate the missile has to make its own turn rate proportional to the LOS rate. This implies that if the missile carried sensors to measure the line-of-sight rate then this information can be used to easily generate a proper guidance command.

Note that the phrase *proportional navigation* is a misnomer since it has nothing to do with navigation (which is the determination of the position of a vehicle). The reason why this name has stuck is that when proportional navigation was first invented, the difference between guidance and navigation was not a clearly understood concept and every activity related to the task of moving a vehicle from one point to another was termed as *navigation*. Also, this kind of work in those days was influenced by naval terminologies where, again, navigation was a word that encompassed a whole lot of activities. Because of this the name has remained and, out of respect for its historical legacy, is used even now. The word proportional, of course, comes from the fact that the missile turn rate is made proportional to the LOS rate.

It is interesting to note that the proportional navigation guidance law was known to the German scientists during the World War II in the Peenemunde research laboratories, and a considerable amount of research had been carried out by them, although, fortunately for the allies' warplanes, it was never implemented by the Germans in any missiles during the Second World War<sup>1</sup>.

We will not go into the details of how the PN guidance law works since we are going to deal with it in greater detail in our subsequent lectures anyway. But let me stress that of all the guidance laws that we have discussed till now, and even among those that we are going to discuss later, PN stands apart in terms of its implementability, elegance, simplicity, and its wide applicability. Later we shall show how most of the so called modern guidance laws are just logical extensions and variants of the PN philosophy and a study of them can be easily carried out under the unified framework of the PN philosophy.

---

<sup>1</sup>There is some controversy about the historical origin of PN with some scientists claiming that that there is no evidence of the Germans being aware of this law, and that it was the result of an American research effort [see Shneydor (1998)]

*Questions*

1. Explain the philosophy of line-of-sight guidance law.
2. Sketch a figure to show the trajectory of a LOS law guided missile against an incoming target and explain why it is likely to fail.
3. Explain command-to-line-of-sight guidance law.
4. Explain beam rider guidance law.
5. Under what circumstances can the BR guided missile miss the beam signal.
6. What is the basic philosophy behind the proportional navigation guidance law?
7. How did ancient sailors determine if their ship is in collision course with another ship?

## Module 5: Lecture 14

### Modern Guidance Laws

**Keywords.** Modern Guidance, Differential Game Guidance, Predictive Guidance, Reachable Sets based Guidance

#### 6.4 Modern Guidance Laws

Lastly, we will discuss the so-called modern guidance laws. These have mainly evolved out of the applications of *optimal control theory* to missile guidance problems. Without going into the mathematical formulation let me try to explain the steps through which this evolution took place.

First, the kinematic equations for the missile-target engagement were considered as the state space model of a dynamical system. The guidance problem was formulated in many different ways depending on the requirements of the mission. Some of them are listed below:

- The performance criterion was the *integral square control effort* which was minimized. This, in turn, served to minimize the *maneuver induced drag* on the missile. The *final time* was assumed to be *fixed* and the *constraint of zero miss-distance* was imposed. There was *no constraint on the lateral acceleration* capability of the missile. In other words, the missile was assumed to have *infinite lateral acceleration* capability.
- The performance criterion was the *minimization of the miss-distance*. The *time of flight was fixed*, and a *constraint on the lateral acceleration* that can be pulled by the missile was imposed.

These two were the basic formulations relevant to missile guidance problems. Several variations of both these formulations were considered in the literature in which the performance criterion was considered as a weighted sum of the miss distance, integral square control effort, and the time for interception. This performance measure was coupled with constraints on the lateral acceleration capability of the missile.

Unfortunately, most of these problems, or at least the ones that have some practical bearing, did not have a closed form solution, mainly because the kinematic equations were non-linear. They gave rise to very complicated *Two Point Boundary Value Problems* that were solved with great difficulty due to the sensitivity of the terminal conditions with respect to the initial conditions on the Lagrange multipliers or co-state variables. Even when it was possible to come up with robust algorithms it was found that the time taken to compute the exact guidance command using these algorithms was large even when powerful computers were used. This was unacceptable as these guidance laws had to be either implemented on-board on microprocessors or solved by portable minicomputers on ground. The next logical step was to linearize the state equations and try to obtain simpler and quicker solutions, with the hope that a closed-loop implementation will take care of the approximations inherent in linearization. However, it soon became apparent that the simple solutions so obtained were no different from what has already been proposed as the PN guidance law.

#### 6.4.1 Modern Guidance Scheme

The *modern guidance scheme* is basically the guidance law obtained from a linearized system model. The performance index considered is the integral square control effort. It is assumed that the final time of interception is known. It is also assumed that the missile autopilot can be approximated as a first-order system. With all these assumptions the guidance law can be obtained as a closed form expression, a representation of which is given below,

$$\begin{aligned} \text{Missile Latax} &= \text{PN Component} + \text{Target Maneuver Component} \\ &\quad + \text{Autopilot Lag Component} \end{aligned}$$

The PN component is nothing but the lateral acceleration that would be generated by the proportional navigation guidance law. The second part is the lateral acceleration component that gets added provided you have an accurate knowledge of the maneuver the target is executing perpendicular to the LOS. Now, there is a catch here. Firstly, it is very difficult to measure target acceleration or any of its specific components. Secondly, and more seriously, if the measurement of target acceleration is noisy then, as has been shown through analysis and simulations, the effect of using an inaccurate target acceleration will *deteriorate* the guidance law's performance rather than improve it.

So you might have been better off just using the PN law.

The last term compensates for the lag in the guidance system and is definitely an improvement over the PN law.

The major disadvantage that Modern Guidance Scheme has is its non-implementability. It requires not only the accurate estimate of the target maneuver, it also requires an accurate estimate of the time-to-go (that is, the time remaining till interception) and to implement the component due to the autopilot lag, it requires the knowledge of the current maneuver level of the missile, which again is a difficult quantity to measure.

But the main contribution of the Modern Guidance Scheme was to show that the classical PN law indeed has a very strong theoretical basis. In fact, in a linearized geometry, it gives optimal performance against non-maneuvering target. In the absence of any target maneuver information, it is also the best that you can do against maneuvering target as well. It also spawned a number of other guidance laws which were interesting in their own right. The foremost among them was the *Augmented Proportional Navigation* - which is an optimal guidance law against a maneuvering target if you assume that the missile autopilot is a perfect one. But remember that an actual implementation of this law would again suffer from any inaccuracies in the target maneuver measurement.

#### 6.4.2 Differential Games Guidance Laws

The fundamental idea behind optimal control theory, applied to the guidance problems in missile-target engagement, is that of a target which is assumed to move in some specified way (the specification is basically obtained from its current position, velocity, and acceleration). Based on this information the missile or the *pursuer* tries to come up with a strategy by which it can intercept the target. If you look at this closely you will realize that the specification of the target's future behaviour is important for this method to work. The current position, velocity, and acceleration of the target is used to completely specify its future trajectory, and the pursuer's job is now to decide at which point on the trajectory should it intercept the target (provided of course that intercept is possible).

Differential game theory extends this framework to what is known as the *pursuit-evasion problem* where the target is called the *evader* and is assumed to have as much intelligence as the missile. What would such an intelligent target do? Obviously, it would try to come up with an optimal way of evading the pursuer. Now, the pursuer can no longer predict the target's behaviour and so cannot apply optimal control theory any more! So now we enter the domain of *differential game theory* which helps us to handle exactly this kind of situations where a dynamic game is played between two intelligent opponents (the word "differential" comes from the fact that the motion of the two players are represented by differential equations). How does this help us in solving a missile-target problem? Think of a surface-to-air-missile being used against a piloted fighter aircraft. If the pilot can detect the firing of the missile then obviously the missile cannot any longer expect that the aircraft will continue to proceed in the same way as before. It will start taking evasive actions and its trajectory cannot be predicted any more based on the current position, velocity, or acceleration of the aircraft. And therefore optimal control theory fails and this is where differential game theory comes to your rescue.

But this works fine as long as you remain in the theoretical domain. But, the moment you try to obtain workable solutions for a nonlinear system, you face the same kind of computational difficulty that arose when trying to apply optimal control theory. However, there is quite a bit of literature on how differential games guidance laws are formulated from a linear framework. Differential games also has one advantage over the optimal control guidance laws in the sense that it does not use target maneuver information as this is a quantity that cannot be predicted. But the computational problems still remain. Although in recent years there has been quite a bit of work in trying to see whether this type of guidance law can actually be used or not, the studies so far have not yet yielded any results that can be brought to the implementation stage.

#### 6.4.3 Reachable Set Guidance Law

Another class of guidance laws is based on what is known as the *reachable set theory*. This, in turn, was based on game-theoretic ideas. Without going into details let me just mention that it involved predicting the reachable sets of the missile and the target. The reachable sets are the subsets of the state-space which is reachable by the vehicle

states in a given time. An intersection of these two sets mapped onto the physical space gave an idea of the set of feasible guidance commands that the missile can use to capture the target. The best guidance command was chosen from this set based on some performance measure. Although theoretically elegant, the implemetability of this kind of guidance law remained doubtful.

#### 6.4.4 Predictive Guidance Laws

There are quite a few other guidance laws which were proposed at different times during the last couple of decades. Most of them can be grouped under the broad name of *predictive guidance laws*. The essential idea behind them was to predict the future position of the target based on some understanding of the target trajectory and then design the best guidance strategy to intercept this target. Although logically sound, these guidance laws suffered from two serious drawbacks. The first is the obvious one of not knowing what the target is actually going to do next. And the second was that the amount of computations required to make these predictions and then come up with a suitable guidance law required an enormous amount of computations with prohibitive times associated with them. To alleviate the computational burden in the predictive guidance laws, an attempt was made to simplify them through linearization or other simplifying assumptions. But the corresponding guidance laws turned out to be no different from the PN law and its many variants! A notable exception was a guidance law called *Maximum Acceleration Design Digital Optimal Guidance* which has the interesting abbreviation *MADDOG!* In this guidance law the target position, velocity, and acceleration was used to predict a future position of the target in 3-D space. The simplification was in terms of keeping the velocity and acceleration constant so that the trajectory of the target was a circular one. A future position C of the target was predicted based on a fixed interception time assumption. Then a maneuver plane was defined which contained the missile velocity vector and this future point C. The missile was assumed to maneuver in this plane with maximum acceleration till the missile velocity vector points towards C. Then the missile was assumed to fly in a straight line trajectory. It is a simple matter to calculate the actual time that the missile takes to reach this point C. If this time is different from the previously assumed time to predict the position of C then an average of the two times is taken as the new time and the process is repeated. A few iterations (usually 2 to 3 were enough after the first cycle) later the solution con-

verges. The guidance law had an advantage from two points. The first was that all the calculations could be done by using closed-form expressions, and the other was that it was also a time optimal guidance law in a nonlinear setting. However, I am not aware if the guidance law was actually used for any realistic simulations. But some extensions of this guidance law have been examined in the literature. For example, there is one which examines what happens when instead of using maximum acceleration the missile spreads the acceleration over the whole engagement period. This minimizes the integral square control effort and also reduces the possibility of chattering.

## 6.5 Concluding Remarks

In this chapter I have tried to give you an overview of the major guidance laws which have appeared in the guidance literature in the past forty years. I have avoided complicated mathematics and tried to convey to you the basic principles behind these guidance laws. I have also tried to illustrate the subtle points which distinguished one guidance law from another. Another message that I tried to convey to you is the fact that in the area of guidance laws, as indeed in most other areas, there are certain concepts which are elegant, theoretically sound, and are academically of great interest. But it is quite possible that when we consider engineering applications these elegant theories may fall by the wayside, whereas some not-so-elegant methods actually manage to deliver the goods.

### *Questions*

1. What were the considerations that lead to the development of modern guidance laws?
2. What were the major advantages of the optimal control based guidance schemes?
3. What motivated the development of differential games based guidance laws?
4. What is the basic philosophy behind reachable sets based guidance laws?
5. What are predictive guidance laws?

### *References*

1. R. Isaacs: *Differential Games*, Wiley, New York, 1965.
2. C.-F. Lin: *Modern Navigation, Guidance, and Control Processing*, Prentice Hall, Englewood Cliffs, NJ, 1991.
3. F.W. Nesline and P. Zarchan: A new look at classical vs. modern homing missile guidance, *Journal of Guidance and Control*, Vol. 4, No. 1, January-February 1981, pp. 78-85.
4. H.L. Pastrick, S.M. Seltzer, and M.E. Warren: Guidance laws for short-range tactical missiles, *Journal of Guidance and Control*, Vol. 4, No. 2, March-April 1981, pp. 98-108.
5. P. Zarchan: *Tactical and Strategic Missile Guidance*, AIAA Inc., Washington DC, 1990.

## Chapter 7

# The Pursuit Guidance Law

## Module 6: Lecture 15 Pure Pursuit Guidance Law

**Keywords.** Pure pursuit; Capture Region

As discussed earlier, pursuit guidance law is one of the most logical guidance laws to be used for missile guidance. The basic philosophy behind this guidance law is, if the missile continues to point towards the target then it is guaranteed that after a finite time the missile will intercept the target. Intuitively speaking this must be true if the missile has a higher speed than the target. In this chapter we will formulate the equations of motion for the pursuit guidance law and analyze those equations to obtain a few important and significant results. First we will address the *pure pursuit guidance law* and then subsequently the *deviated pursuit guidance law*.

### 7.1 Pure Pursuit Guidance Law

#### 7.1.1 The engagement equations

Consider the engagement geometry given in Figure 7.1. Note that if the missile is using a perfect pursuit guidance law, then at all instants in time,  $V_M$  should point towards the current target position. This is shown in Figure 7.1. The target is assumed to be a

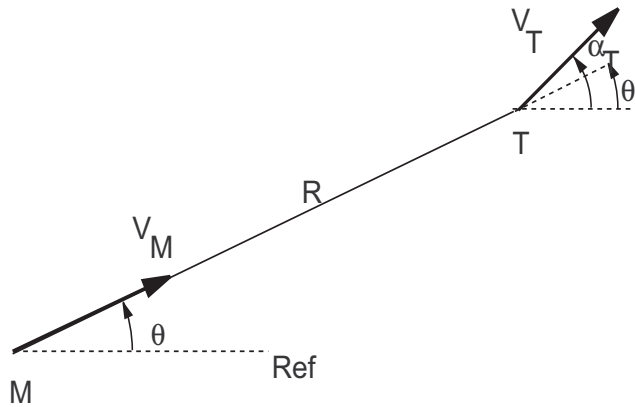


Figure 7.1: Engagement geometry for pure pursuit

non-maneuvering one. The equations of motion are given by,

$$V_R = \dot{R} = V_T \cos(\alpha_T - \theta) - V_M \quad (7.1)$$

$$V_\theta = R\dot{\theta} = V_T \sin(\alpha_T - \theta) \quad (7.2)$$

Note that here too  $V_R$  and  $V_\theta$  are the two components of the relative velocity between the target and the missile, along the LOS and normal to the LOS. Dividing the first equation by the second and with some manipulation we get,

$$\frac{1}{R} dR = \{\cot(\alpha_T - \theta) - \nu \csc(\alpha_T - \theta)\} d\theta \quad (7.3)$$

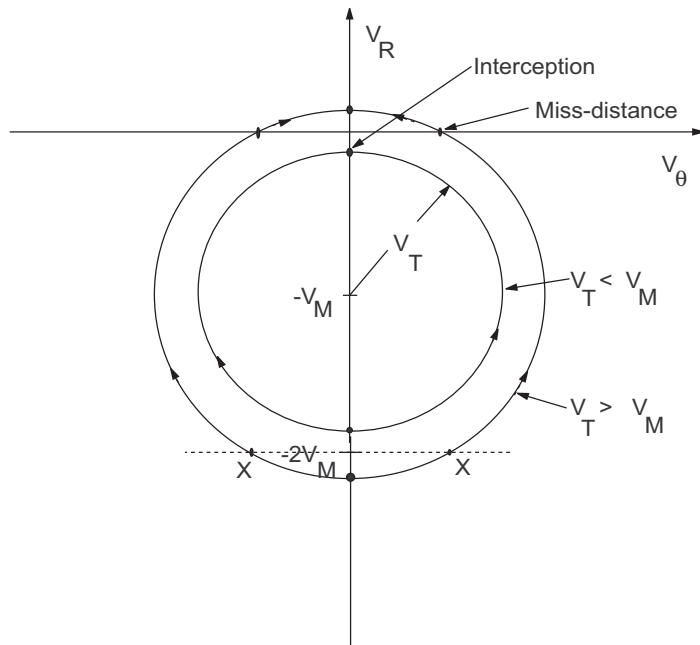
where

$$\nu = \frac{V_M}{V_T} \quad (7.4)$$

Integrating this equation, we get,

$$R = f(\theta) \quad (7.5)$$

But this equation does not help us much since  $R$  is expressed as a function of  $\theta$  and not as a function of time  $t$ . Of course, as shown in Locke (1955), it is possible to manipulate this complicated equation further and obtain some interesting results. But we will not follow this route since the complexity of the resulting equations cause a loss in clarity. As we did in Chapter 4, we will study the behaviour of the relative velocity components.

Figure 7.2: The  $(V_\theta, V_R)$  trajectory

### 7.1.2 Trajectory in the $(V_\theta, V_R)$ -space

To obtain the engagement trajectory in the  $(V_\theta, V_R)$ -space let us rewrite (7.1) and (7.2) as,

$$\begin{aligned} V_R + V_M &= V_T \cos(\alpha_T - \theta) \\ V_\theta &= V_T \sin(\alpha_T - \theta) \end{aligned}$$

Squaring both equations and summing we obtain,

$$(V_R + V_M)^2 + V_\theta^2 = V_T^2 \quad (7.6)$$

This is the equation of a circle in the  $(V_\theta, V_R)$ -space with center at  $(0, -V_M)$  and radius equal to  $V_T$ . It shows that the  $(V_\theta, V_R)$  point remains on the circumference of this circle as the engagement proceeds. The circle is shown in Figure 7.2. The arrows in Figure 7.2 denote the direction in which the  $(V_\theta, V_R)$  point moves from different positions in the  $(V_\theta, V_R)$ -space with respect to time. These directions are obtained as follows: Differen-

tiating (7.1) and (7.2), we obtain,

$$\dot{V}_R = -V_T \sin(\alpha_T - \theta)(-\dot{\theta}) = \dot{\theta}V_\theta \quad (7.7)$$

$$\dot{V}_\theta = V_T \cos(\alpha_T - \theta)(-\dot{\theta}) = -\dot{\theta}(V_R + V_M) \quad (7.8)$$

Multiplying  $R$  on both sides of both the above equations, we get,

$$R\dot{V}_R = V_\theta^2 \quad (7.9)$$

$$R\dot{V}_\theta = -V_\theta(V_R + V_M) \quad (7.10)$$

Since  $R > 0$ , (7.9) implies that  $\dot{V}_R > 0$  always. If we analyze (7.10) we find that,

$$\dot{V}_\theta > 0 \text{ if } \{V_\theta > 0 \text{ and } V_R < -V_M\} \text{ OR } \{V_\theta < 0 \text{ and } V_R > -V_M\}$$

$$\dot{V}_\theta < 0 \text{ if } \{V_\theta > 0 \text{ and } V_R > -V_M\} \text{ OR } \{V_\theta < 0 \text{ and } V_R < -V_M\}$$

These two conditions are sufficient to determine the direction of movement of the  $(V_\theta, V_R)$  point.

The points where the circle cuts the  $V_R$ -axis are stationary points since at these points  $V_\theta = 0$  and so from (7.7) and (7.8) we see that  $\dot{V}_\theta = 0$  and  $\dot{V}_R = 0$ .

The points on the  $V_R$  axis are interesting because those on the negative  $V_R$  axis correspond to the collision triangle and those on the positive  $V_R$  axis correspond to the inverse collision triangle. However, when we talk of the collision triangle in the case of pure pursuit, the missile is required to always point towards the current position of the target, and so collision can take place either in the *tail-chase* mode (missile pursuing the target with both the velocity vectors aligned along the LOS) or in the *head-on* mode (missile and target approaching each other with both the velocity vectors aligned along the LOS). Further, in the tail-chase mode collision occurs only if  $V_M > V_T$ , whereas in the head-on mode collision is possible for all values of  $V_T$  and  $V_M$ . The collision triangle in the pure pursuit case is actually a straight line since the missile and target velocity vectors are both aligned along the LOS. Similarly, points on the positive  $V_R$  axis may correspond to missile and target travelling in opposite directions away from each other, or in a tail-chase mode when  $V_M \leq V_T$ . The main idea is that a point on the  $V_R$  axis essentially corresponds to the situation when both the missile and target velocities are aligned with the LOS. This we can also see by using the condition that on

the  $V_R$  axis we have  $V_\theta = 0$ , which implies that,

$$\begin{aligned} V_\theta &= V_T \sin(\alpha_T - \theta) = 0 \\ \Rightarrow \quad \alpha_T &= \theta \text{ or } \theta + \pi \end{aligned}$$

With the above discussion in mind, in Figure 7.2 we have shown two circles. The smaller one corresponds to the case when  $V_T < V_M$  and the larger one corresponds to the case when  $V_T > V_M$ . The smaller circle (corresponding to  $V_T < V_M$ ) shows that the trajectory of  $(V_\theta, V_R)$  ends up on a point on the negative  $V_R$ -axis and thus leads to collision. By the very nature of pure pursuit guidance we can see that any engagement whose initial condition does not correspond to a head-on situation will ultimately end up in the tail-chase mode. And if  $V_T < V_M$  then collision is also guaranteed.

Whereas, when  $V_T > V_M$  the missile will continue to close on to the target till time  $t_{\text{miss}}$  when the miss-distance  $R_{\text{miss}}$  occurs. Obviously, this happens at the point where the  $(V_\theta, V_R)$  point crosses the  $V_\theta$  axis or when  $V_R = 0$ . Afterwards, the missile and target asymptotically approach the tail-chase configuration but without collision taking place since the target is faster than the missile.

A last point I would like to mention is that if the initial point is on the negative  $V_R$  axis then the engagement is either a head-on or a tail-chase, whereas, if  $V_T < V_M$  and the initial point is not on the negative  $V_R$  axis then the engagement ends in a tail-chase collision.

### 7.1.3 The capture region

Based on the above discussion we can now identify the *capture region* of the pure pursuit guidance law. By definition, the capture region is such that if the initial point lies inside it then the engagement leads to a successful capture or interception. In Figure 7.3 we show the capture region for the pure pursuit law and also the capture region for the case when the missile is unguided. For the latter case the capture results were obtained in Chapter 4 earlier. However, note that the capture region is obtained here with  $V_T$  as the free parameter and the initial geometry restricted to the cases where  $V_M$  points towards the target. The figure shows that the use of pure pursuit guidance has expanded the

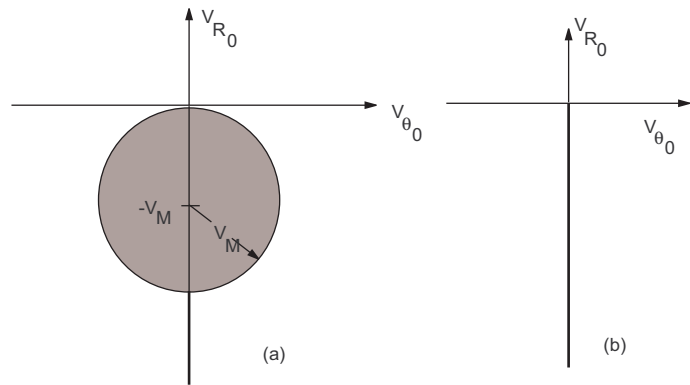


Figure 7.3: Capture region for (a) Pure pursuit (b) Unguided missile

capture region considerably over the unguided case.

## Module 6: Lecture 16

### Time of Interception; Miss Distance

**Keywords.** Pure Pursuit, Time of Interception; Miss Distance

#### 7.1.4 Time of interception

Is it possible to obtain the time at which interception occurs when the initial state is within the capture region? For this, let us consider (7.6).

$$\begin{aligned} (V_R + V_M)^2 + V_\theta^2 &= V_T^2 \\ \Rightarrow V_R^2 + V_M^2 + 2V_M V_R + V_\theta^2 &= V_T^2 \\ \Rightarrow \dot{R}^2 + R\ddot{R} + 2V_M \dot{R} &= V_T^2 - V_M^2 \end{aligned} \quad (7.11)$$

Note that we have used the relations  $V_R = \dot{R}$  and  $V_\theta^2 = R\dot{V}_R$  from (7.9) in the above equation. Integrating (7.11), we obtain

$$R(V_R + 2V_M) = (V_T^2 - V_M^2)t + b \quad (7.12)$$

where,

$$b = R_0(V_{R0} + 2V_M) \quad (7.13)$$

Interception occurs at  $t = t_f$  when  $R = 0$ . Substituting this in (7.12), we get,

$$t_f = \frac{R_0(V_{R0} + 2V_M)}{V_M^2 - V_T^2} \quad (7.14)$$

Note that when  $V_M > V_T$ , i.e., when the initial condition lies inside the capture region, we have  $t_f > 0$  and finite automatically. However, we should also note that when  $V_M < V_T$ , even then  $t_f > 0$  provided that

$$V_{R0} < -2V_M$$

Does it mean that interception occurs at this value of  $t_f$ ? Actually this is not so. Observe that the equation for the final time was obtained by setting the LHS of (7.12) to zero, with the implicit assumption that the LHS becomes zero when  $R = 0$ . But note that the LHS can also become zero when  $V_R = -2V_M$ . This condition never arises when

$V_T < V_M$  but does occur at point X marked in Figure 7.2 when  $V_T > V_M$  and the initial condition lies below the line  $V_R = -2V_M$ . Thus, when  $V_T > V_M$  and  $V_{R0} < -2V_M$ , (7.14) only gives the time at which the  $(V_\theta, V_R)$  point crosses the point X.

### 7.1.5 Lateral acceleration history

In the above analysis we have studied the capture region and the time of interception for a perfectly implemented pursuit guidance law. But what about the lateral history of the missile following the pursuit guidance law? For this we need to look at the rate at which the missile velocity vector has to turn in order to satisfy the requirements of pure pursuit. If  $\alpha_M$  denotes the velocity direction of the missile then in the case of pure pursuit,

$$\begin{aligned}\alpha_M &= \theta \quad \Rightarrow \quad \dot{\alpha}_M = \dot{\theta} \\ &\Rightarrow V_M \dot{\alpha}_M = V_M \dot{\theta} \quad \Rightarrow \quad a_M = V_M \dot{\theta} \\ &\Rightarrow a_M = \frac{V_M V_T}{R} \sin(\alpha_T - \theta)\end{aligned}\tag{7.15}$$

In principle this expression can be used to implement the pure pursuit guidance law, provided that initially the missile points directly towards the target. So, if we know  $R$  and  $\theta$  then we can immediately obtain the lateral acceleration  $a_M$  of the missile. To obtain  $R$  as a function of  $\theta$  we must then go back to (7.5) the explicit expression for which is obtained by solving (7.3) as,

$$\begin{aligned}\frac{1}{R} dR &= \{\cot(\alpha_T - \theta) - \nu \operatorname{cosec}(\alpha_T - \theta)\} d\theta \\ \Rightarrow R &= K \frac{\{\tan(\frac{\alpha_T - \theta}{2})\}^\nu}{\sin(\alpha_T - \theta)} = K \frac{\{\sin(\alpha_T - \theta)\}^{\nu-1}}{\{1 + \cos(\alpha_T - \theta)\}^\nu}\end{aligned}\tag{7.16}$$

where,  $K$  is a constant obtained from the initial conditions as,

$$K = R_0 \frac{\sin(\alpha_T - \theta_0)}{\{\tan(\frac{\alpha_T - \theta_0}{2})\}^\nu} = R_0 \frac{\{1 + \cos(\alpha_T - \theta_0)\}^\nu}{\{\sin(\alpha_T - \theta_0)\}^{\nu-1}}\tag{7.17}$$

If we substitute  $R$  from the above into (7.15) then we obtain the lateral as a function of  $\theta$  as:

$$a_M = \frac{V_M V_T}{K} \frac{\sin^2(\alpha_T - \theta)}{\{\tan(\frac{\alpha_T - \theta}{2})\}^\nu}\tag{7.18}$$

This does not give us the lateral history directly since we do not have any explicit expression that gives  $a_M$  as a function of time. However, there is an indirect relationship

through another function that relates  $R$  and  $\theta$  with  $t$  as follows: Consider (7.12), from which we get,

$$t = \frac{b - R(V_R + 2V_M)}{V_M^2 - V_T^2} \quad (7.19)$$

Substituting from (7.13) and (7.1),

$$t = \frac{R_0\{V_T \cos(\alpha_T - \theta_0) + V_M\} - R\{V_T \cos(\alpha_T - \theta) + V_M\}}{V_M^2 - V_T^2} \quad (7.20)$$

The equations (7.16) and (7.20) together can be used to obtain  $R$  and  $\theta$  as functions of time. Substituting these values in (7.18) we can obtain  $a_M$  as a function of time.

Note that at interception the engagement geometry is a tail-chase one, and so when the initial condition lies inside the capture region and interception is guaranteed, as  $t \rightarrow t_f$  we have  $\theta \rightarrow \alpha_T$ . So the terminal value of  $a_M$  can be obtained from (7.18) by evaluating,

$$\lim_{t \rightarrow t_f} a_M = \lim_{\theta \rightarrow \alpha_T} a_M \quad (7.21)$$

This yields the following results: As  $t \rightarrow t_f$ , if

$$\begin{aligned} 1 < \nu < 2 & \quad a_M \rightarrow 0 \\ \nu = 2 & \quad a_M \rightarrow \frac{4V_M V_T}{K} \\ \nu > 2 & \quad a_M \rightarrow \infty \end{aligned} \quad (7.22)$$

The above result is illustrated in Figure 7.4.

### 7.1.6 Miss-distance

In the case when  $V_T > V_M$ , interception does not take place and the corresponding miss-distance  $R_{\text{miss}}$ , which occurs at  $t_{\text{miss}}$ , is obtained as follows:

From Figure 7.2, the point at which miss-distance occurs, we have

$$\begin{aligned} V_R = 0 & \Rightarrow V_T \cos(\alpha_{T_{\text{miss}}} - \theta_{\text{miss}}) = V_M \\ & \Rightarrow \alpha_{T_{\text{miss}}} - \theta_{\text{miss}} = \cos^{-1} \nu \end{aligned}$$

From (7.16), we get,

$$R_{\text{miss}} = K \frac{\left\{ \tan \left( \frac{\cos^{-1} \nu}{2} \right) \right\}^\nu}{\sin(\cos^{-1} \nu)} = K \frac{\{\sin(\cos^{-1} \nu)\}^{\nu-1}}{(1+\nu)^\nu} \quad (7.23)$$

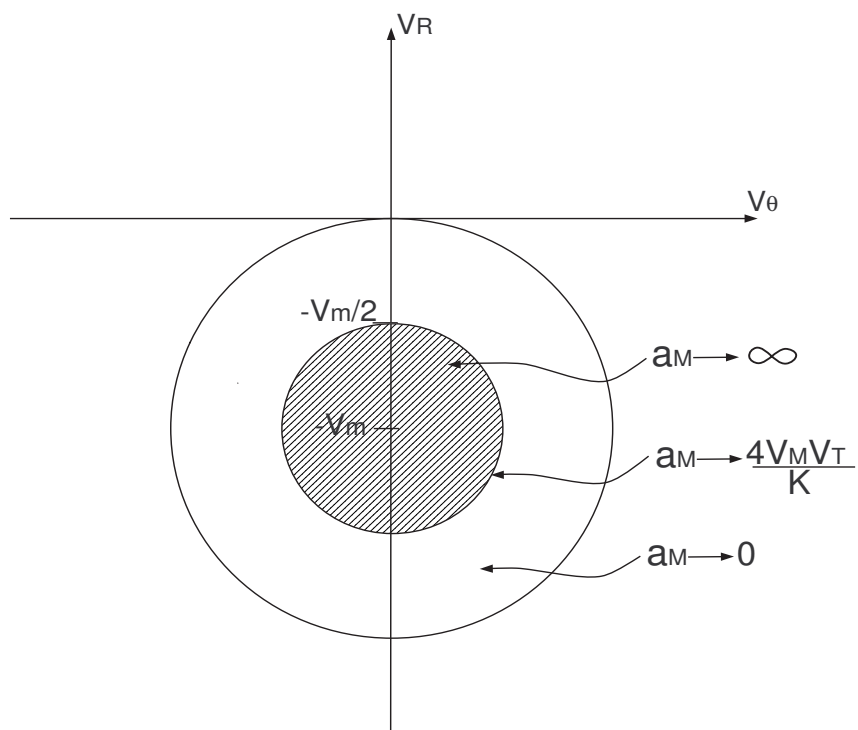


Figure 7.4: Limits of lateral acceleration in the pure pursuit guidance law

where,  $K$  is given by (7.17).

Now, from (7.12), we can write

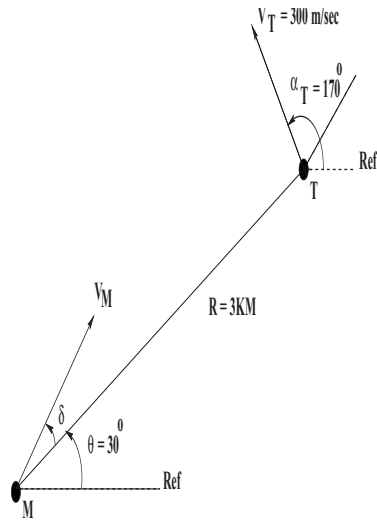
$$2V_M R_{\text{miss}} = (V_T^2 - V_M^2) t_{\text{miss}} + b \quad (7.24)$$

So,

$$t_{\text{miss}} = \frac{2V_M R_{\text{miss}} - b}{V_T^2 - V_M^2} \quad (7.25)$$

### Questions

1. Show that the trajectory in the relative velocity space when the missile uses a pure pursuit guidance law right from the beginning of the engagement, is a circle. Determine the direction of movement of a point on this trajectory.
2. Obtain the capture region of the pure pursuit guidance law in the relative velocity space.



#### 3. PART A: Pure Pursuit, $\delta = 0^\circ; \alpha_T \in [0^\circ, 180^\circ]$

- A1. Integrate the equations of motion and plot  $R$ ,  $\theta$ ,  $V_\theta$ ,  $V_R$ , and  $a_M$  against time for  $\nu = 0.9, 1.5, 3$ . Note that  $\nu = V_M/V_T$ .
- A2. Also plot the missile and target trajectories for each case.

- A3. Check if interception occurs. If yes, then find  $t_f$ . If no then find  $t_{\text{miss}}$  and  $R_{\text{miss}}$ .
- A4. Plot  $(V_\theta, V_R)$  in  $(V_\theta, V_R)$ -space.
- A5. Interpret the simulation results in the light of the analytical results discussed in the notes.

**PART B: Implementation** *This part will be discussed in the next lectures, but the question is given here for completeness.*

- C1. Use the implementation of pure pursuit as

$$a_M = V_M \dot{\theta} - k(\alpha_M - \theta)$$

when, in the above figure, the initial missile velocity vector lags the LOS by  $10^\circ$ .

Plot  $R, \theta, V_\theta, V_R, \alpha_M$  and  $a_M$  against time for  $\nu = 0.9, 1.5, 3; k = 1, 5, 10$ .

Plot  $(V_\theta, V_R)$  in  $(V_\theta, V_R)$ -space.

Plot the missile and target trajectories for each case.

## Module 6: Lecture 17

### Deviated Pursuit Guidance Law

**Keywords.** Deviated pursuit guidance

#### 7.2 Deviated Pursuit Guidance Law

As in the previous section we will carry out a similar analysis for the deviated pursuit guidance law.

##### 7.2.1 The engagement equations

Consider the engagement geometry given in Figure 7.5. Since the missile is using a

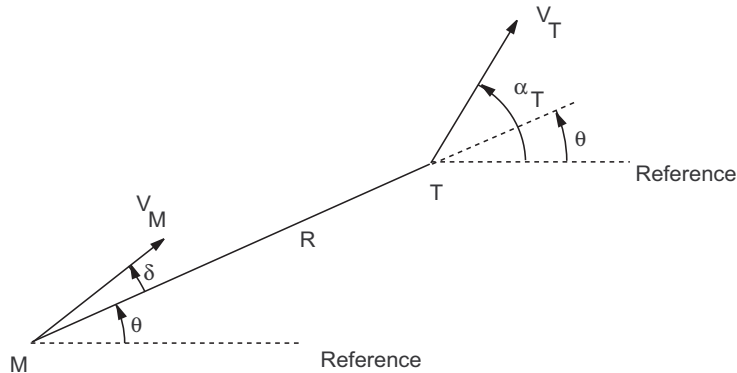


Figure 7.5: Engagement geometry for deviated pursuit

deviated pursuit guidance law, at all instants in time,  $V_M$  should be directed towards a point that deviates from the current target position by a constant angle  $\delta$ . This is shown in Figure 7.5. The target is assumed to be a non-maneuvering one. The equations of motion are given by,

$$V_R = \dot{R} = V_T \cos(\alpha_T - \theta) - V_M \cos \delta \quad (7.26)$$

$$V_\theta = R\dot{\theta} = V_T \sin(\alpha_T - \theta) - V_M \sin \delta \quad (7.27)$$

Note that here too  $V_R$  and  $V_\theta$  are the two components of the relative velocity between the target and the missile, along the LOS and normal to the LOS. As in the pure pursuit

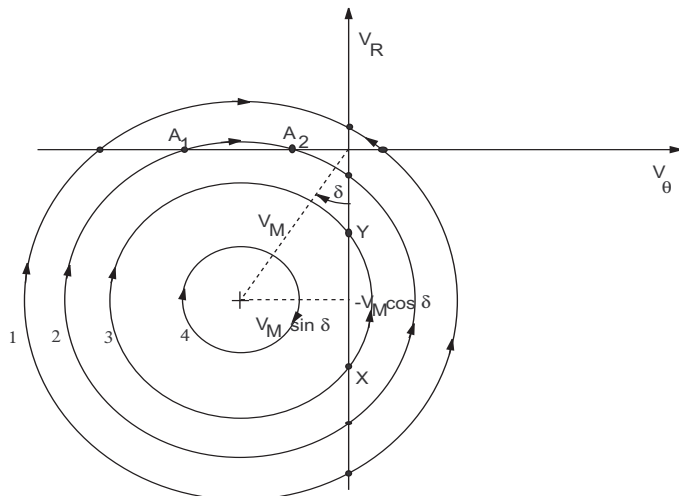


Figure 7.6: The  $(V_\theta, V_R)$  trajectories for deviated pursuit with  $\delta < \pi/4$

case, we will first study the behaviour of the relative velocity components.

### 7.2.2 Trajectory in the $(V_\theta, V_R)$ -space

To obtain the engagement trajectory in the  $(V_\theta, V_R)$ -space let us rewrite (7.26) and (7.27) as,

$$V_R + V_M \cos \delta = V_T \cos(\alpha_T - \theta)$$

$$V_\theta + V_M \sin \delta = V_T \sin(\alpha_T - \theta)$$

Squaring both equations and summing we obtain,

$$(V_R + V_M \cos \delta)^2 + (V_\theta + V_M \sin \delta)^2 = V_T^2 \quad (7.28)$$

This is the equation of a circle in the  $(V_\theta, V_R)$ -space with center at  $(-V_M \sin \delta, -V_M \cos \delta)$  and radius equal to  $V_T$ . It shows that the  $(V_\theta, V_R)$  point remains on the circumference of this circle as the engagement proceeds. This circle is shown in Figure 7.6 for the case when  $\delta < \pi/4$ . The arrows in Figure 7.6 denote the direction in which the  $(V_\theta, V_R)$  point moves from different positions in the  $(V_\theta, V_R)$ -space with respect to time. These directions are obtained as follows: Differentiating (7.26) and (7.27), we obtain,

$$\dot{V}_R = -V_T \sin(\alpha_T - \theta)(-\dot{\theta}) = \dot{\theta}(V_\theta + V_M \sin \delta) \quad (7.29)$$

$$\dot{V}_\theta = V_T \cos(\alpha_T - \theta)(-\dot{\theta}) = -\dot{\theta}(V_R + V_M \cos \delta) \quad (7.30)$$

Multiplying  $R$  on both sides of both the above equations, we get,

$$R\dot{V}_R = V_\theta(V_\theta + V_M \sin \delta) \quad (7.31)$$

$$R\dot{V}_\theta = -V_\theta(V_R + V_M \cos \delta) \quad (7.32)$$

Since  $R > 0$ , (7.31) implies that

$\dot{V}_R > 0$  if  $\{V_\theta > 0 \text{ and } V_\theta > -V_M \sin \delta\}$  OR  $\{V_\theta < 0 \text{ and } (V_\theta < -V_M \sin \delta)\}$   
 $\dot{V}_R < 0$  if  $\{V_\theta > 0 \text{ and } V_\theta < -V_M \sin \delta\}$  OR  $\{V_\theta < 0 \text{ and } (V_\theta > -V_M \sin \delta)\}$

(7.33)

Analyzing (7.32) we find that,

$\dot{V}_\theta > 0$  if  $\{V_\theta > 0 \text{ and } V_R < -V_M \cos \delta\}$  OR  $\{V_\theta < 0 \text{ and } V_R > -V_M \cos \delta\}$   
 $\dot{V}_\theta < 0$  if  $\{V_\theta > 0 \text{ and } V_R > -V_M \cos \delta\}$  OR  $\{V_\theta < 0 \text{ and } V_R < -V_M \cos \delta\}$

(7.34)

These two conditions determine the direction of movement of the  $(V_\theta, V_R)$  point.

The points where the circle cuts the  $V_R$ -axis are stationary points since at these points  $V_\theta = 0$  and so from (7.29) and (7.30) we see that  $\dot{V}_\theta = 0$  and  $\dot{V}_R = 0$ .

The points on the negative  $V_R$  axis correspond to the collision triangle and those on the positive  $V_R$  axis correspond to the inverse collision triangle. This collision triangle for deviated pursuit is defined by the requirement that the missile has to always point at an angle deviated by  $\delta$  from the current LOS, and so is given by that value of  $\alpha_T$  that satisfies,

$$V_\theta = 0 \Rightarrow V_T \sin(\alpha_T - \theta) = V_M \sin \delta \quad (7.35)$$

and the corresponding  $V_R < 0$ . There are two possibilities for the collision triangle at the point of interception and these are shown in Figure 7.7. Note that, when  $\delta = 0$  (pure pursuit), the first one corresponds to a head-on geometry and the second one corresponds to a tail-chase geometry.

In Figure 7.6 we have shown four circles marked as 1, 2, 3, and 4. They correspond to the following conditions:

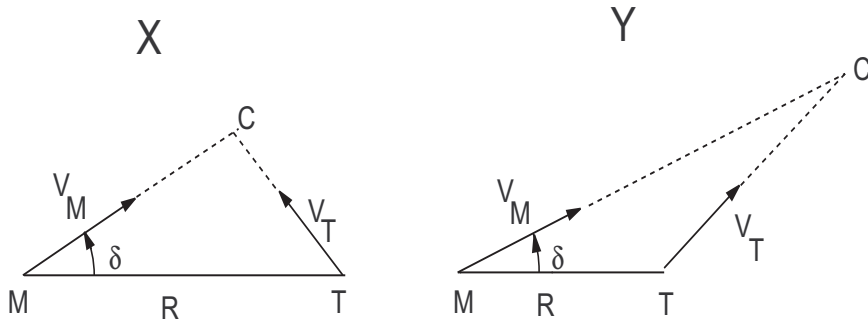
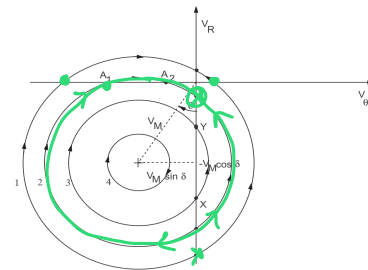


Figure 7.7: The two possible collision triangles at interception

- 1 :  $V_T > V_M$
- 2 :  $V_M \cos \delta < V_T < V_M$
- 3 :  $V_M \sin \delta < V_T < V_M \cos \delta$
- 4 :  $V_T < V_M \sin \delta$

Figure 7.6: The  $(V_\theta, V_R)$  trajectories for deviated pursuit with  $\delta < \pi/4$ 

Hence these circles are defined for various values of  $V_T$  in relation to  $V_M$  and  $\delta$ . Normally,  $\delta$  is a small angle and so it is logical to consider  $\delta < \pi/4$ . However, for the sake of completion we will also consider below the case when  $\delta > \pi/4$ . The corresponding trajectories are shown in Figure 7.8.

The discussion that follows will be with reference to Figure 7.6 when  $\delta < \pi/4$ , unless otherwise mentioned.

The largest circle (Circle 1) corresponds to  $V_T > V_M$  and, except for those initial conditions which are on the negative  $V_R$  axis, all other points end up on the positive  $V_R$  axis showing that there is no interception. The miss-distance occurs at the points marked on the figure.  $V_R = 0$

Points corresponding to Circle 2 lead to interception because they end up on the negative  $V_R$  axis. However, note that initial conditions in the third quadrant first move into the positive  $V_R$  region and then come back to the negative  $V_R$  region before hitting the negative  $V_R$  axis. Thus, point A1 on the trajectory is the point of closest approach before the missile overshoots the target, turns at point A2, and then intercepts the tar-

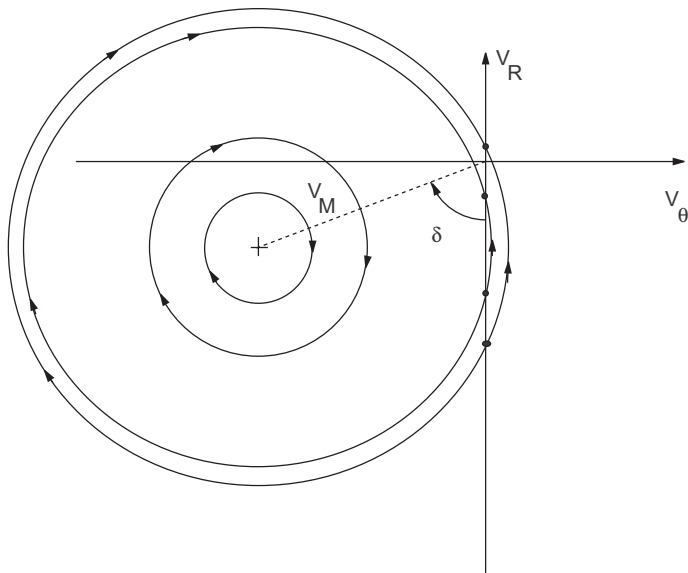


Figure 7.8: The  $(V_\theta, V_R)$  trajectories for deviated pursuit with  $\delta > \pi/4$

get. A representative trajectory is shown in Figure 7.9.

Points corresponding to Circle 3 also lead to interception, but the trajectory remains in the negative  $V_R$  region.

Points corresponding to Circle 4 also lead to interception, but in this case the interception is somewhat different from the previous cases. If we monitor the rate of rotation of the  $(V_\theta, V_R)$ -point about the center of the circle with respect to time we will

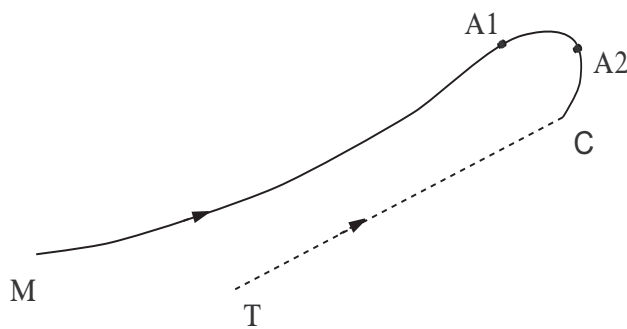


Figure 7.9: A trajectory corresponding to Circle 2

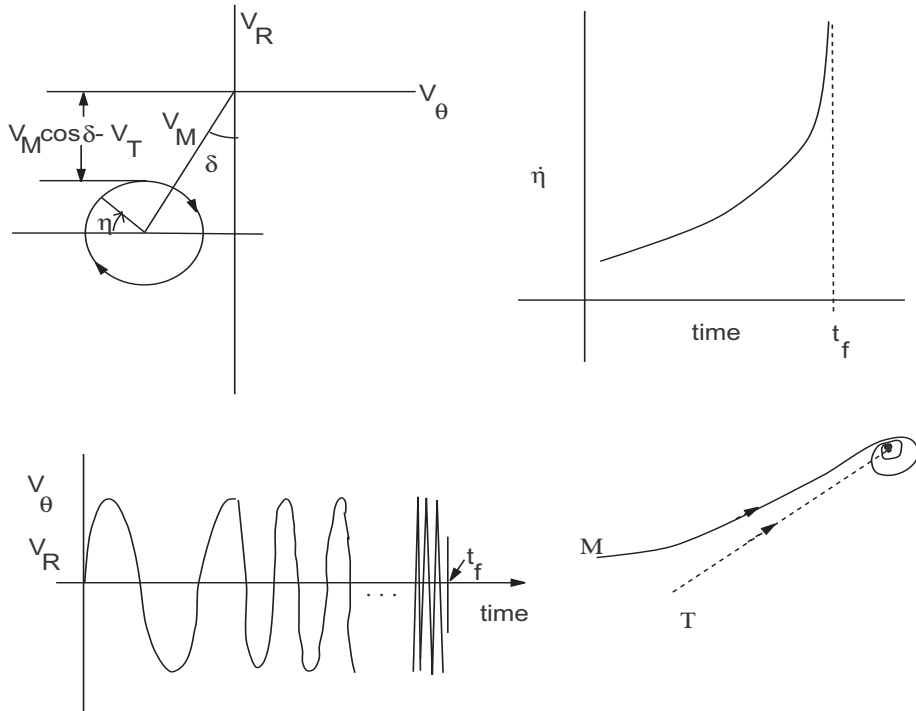


Figure 7.10: Trajectory and angular velocity for Circle 4

see that as time increases the angular velocity of this point also increases and tends toward infinity as the time tends to the interception time value. See Figure 7.10. Here,  $\eta$  denotes the angle of the point  $(V_\theta, V_R)$  from some reference. Then,  $|\dot{\eta}| \rightarrow \infty$  as  $t \rightarrow t_f$ .

The fact that  $|\dot{\eta}| \rightarrow \infty$  can be proved by contradiction. Suppose this is not true. Then interception will occur at some definite point on the circle, given by  $\eta_f$  (say) at some finite time  $t_f$ . Then, from (7.31) and (7.32), this point will be given by

$$V_{\theta f} = -V_M \sin \delta \quad (7.36)$$

$$V_{r f} = -V_M \cos \delta \quad (7.37)$$

Obviously, since the interception point has to be on the circle, both the above conditions cannot be satisfied. The corresponding missile-target engagement trajectory is such that the missile loops around the target an infinite number of times with smaller and smaller radii till it hits the target. Note that although the missile loops for an infinite number of times it still intercepts at a finite time since the radii of looping reduces with

time and becomes zero at  $t_f$ . The fact that the interception occurs in finite time can also be seen from Figure 7.10, where it is shown that at any given time instant the value of  $V_R \leq -(V_M \cos \delta - V_T)$  and so a finite upper bound on the interception time is given by,

$$t_f \leq \frac{R_0}{V_M \cos \delta - V_T} \quad (7.38)$$

$$\begin{aligned}
 & V_R = \underbrace{V_T \cos(\alpha_T - \theta)}_{\leq V_T} - V_M \cos \delta \\
 & \frac{dR}{dt} \leq V_T - V_M \cos \delta \\
 & R_f - R_0 \leq (V_T - V_M \cos \delta) (t_f - t_0) \\
 & t_f \leq \frac{R_0}{V_T - V_M \cos \delta}
 \end{aligned}$$

## Module 6: Lecture 18

### The Capture Region; Implementation

**Keywords.** Deviated pursuit; Capture region; Time of interception, Latax history, Implementation

#### 7.2.3 The capture region

Based on the above discussion we can now identify the *capture region* of the deviated pursuit guidance law. Note that even in this case, if the initial geometry does not satisfy the collision triangle condition (i.e., the initial point is not on the negative  $V_R$  axis) the capture is possible if and only if  $V_T < V_M$ . In Figure 7.11(a) we show the capture region for the deviated pursuit guidance law for a fixed  $\delta > 0$ . The figure shows that for a fixed  $\delta$  the capture region for the deviated pursuit guidance law is of the same size as the pure pursuit guidance law. But the capture circle is now rotated by an angle  $\delta$  clockwise. Another point to note is that a portion of the positive  $V_R$  region has also become a part of the capture region. In this respect the deviated pursuit guidance law performs better than the pure pursuit guidance law.

Since the angle  $\delta$  is a guidance parameter that can be selected by the designer of the guidance algorithm, we can see that by selecting the value of  $\delta$  differently we can demarcate different regions as capture region. If we allow  $\delta$  to vary between  $-\pi/2$  and  $+\pi/2$  the total capture region will be the union of all the individual capture regions for each  $\delta$  and is shown in Figure 7.11(b). Note that for  $\delta < 0$  the capture region is obtained by rotating the capture region for the pure pursuit guidance law ( $\delta = 0^\circ$ ) in the anti-clockwise direction. Thus, if we consider  $\delta$  to be a freely selected guidance parameter then the capture region expands considerably.

Can you guess why I did not consider  $\delta > \pi/2$  or  $\delta < -\pi/2$  to expand the capture region even further?

→ logically  $\vec{V_p}$  would be towards  $\vec{V_T}$  at all (used for evader?)  
 → only region falling in CR would be origin ↗

if  $\delta > \pi/2$ , unstable equilibrium also goes into  $V_R > 0$  region

$\delta = \pi/2 \rightarrow$  stable equilibrium goes into  $V_R > 0$  region

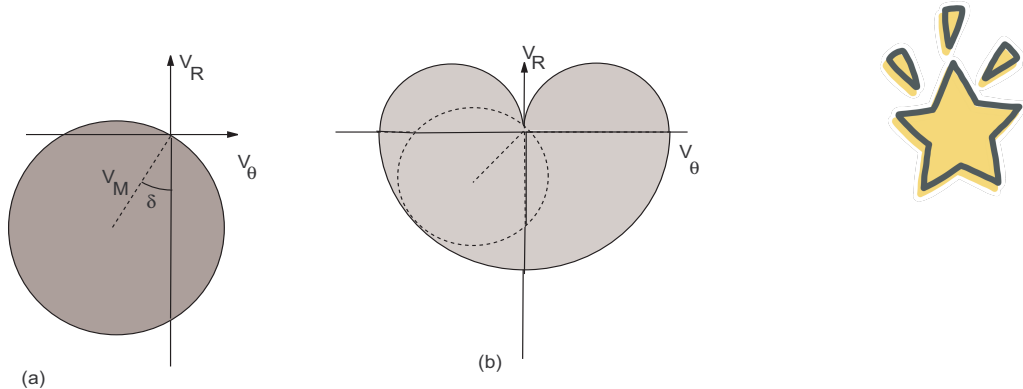


Figure 7.11: Capture region for the deviated pursuit guidance law (a) Fixed  $\delta$  (b)  $-\pi/2 < \delta < \pi/2$

#### 7.2.4 Time of interception

To obtain the interception time when the initial state is within the capture region, let us consider (7.28).

$$\begin{aligned}
 & (V_R + V_M \cos \delta)^2 + (V_\theta + V_M \sin \delta)^2 = V_T^2 \\
 \Rightarrow & V_R^2 + V_M^2 + 2V_M V_R \cos \delta + V_\theta^2 + 2V_M V_\theta \sin \delta = V_T^2 \\
 \Rightarrow & V_R^2 + 2V_M V_R \cos \delta + V_\theta(V_\theta + V_M \sin \delta) + V_M V_\theta \sin \delta = V_T^2 - V_M^2 \\
 \Rightarrow & \dot{R}^2 + R\ddot{R} + 2V_M \cos \delta \dot{R} + V_M V_\theta \sin \delta = V_T^2 - V_M^2
 \end{aligned} \tag{7.39}$$

Note that in the above equation we used (7.31). From (7.32),

$$\begin{aligned}
 R\dot{V}_\theta &= -V_\theta V_R - V_\theta V_M \cos \delta \\
 \Rightarrow V_\theta V_M &= \frac{R\dot{V}_\theta + V_\theta V_R}{-\cos \delta} \\
 \Rightarrow V_\theta V_M \sin \delta &= (R\dot{V}_\theta + V_\theta V_R)(-\tan \delta) = \frac{d}{dt}(RV_\theta)(-\tan \delta)
 \end{aligned}$$

Substituting the above in (7.39), we obtain,

$$\frac{d}{dt}(RV_R) + 2V_M \cos \delta \frac{d}{dt}(R) - \tan \delta \frac{d}{dt}(RV_\theta) = V_T^2 - V_M^2$$

which, on integration, yields

$$R(V_R + 2V_M \cos \delta - V_\theta \tan \delta) = (V_T^2 - V_M^2) t + c \tag{7.40}$$

where,

$$c = R_0 (V_{R0} + 2V_M \cos \delta - V_{\theta0} \tan \delta)$$

If interception occurs, then at  $t = t_f$  we have  $R = 0$ , which yields

$$t_f = \frac{-c}{V_T^2 - V_M^2} = \frac{R_0 (V_{R0} + 2V_M \cos \delta - V_{\theta 0} \tan \delta)}{V_M^2 - V_T^2} \quad (7.41)$$

### 7.2.5 Lateral acceleration history

Exactly as in pure pursuit case, it is possible to derive similar equations for the deviated pursuit case. We omit the details which can be found in [Locke \(1955\)](#). It turns out that if interception occurs the terminal value of  $a_M$  is given by,

$$\begin{aligned} 1 < \nu < 2 & \quad a_M \rightarrow \text{A finite value} \\ \nu \geq 2 & \quad a_M \rightarrow \infty \end{aligned} \quad (7.42)$$

derivation?

## 7.3 Implementation

Here, we start with an assumption that the missile is initially on a pursuit course. but what happens when the missile points in a direction different from the pursuit geometry (pure or deviated) initially? We can examine two alternatives:

1. Missile applies the maximum lateral acceleration till it is on a pursuit course and then applies the pursuit lateral acceleration.
2. If there is no bound on the missile lateral acceleration, then the missile can turn instantaneously and then apply the pursuit acceleration.

However, note that both these alternatives are open-loop in nature and requires an inordinate amount of computations to make them feasible. Thus, errors in measurements, and mismatch between the missile flight angle and the LOS angle, will lead to large miss-distances. Moreover, even if a closed-loop implementation is devised, based upon continuous measurements of the states, latax oscillations will be caused by the high demand on latax. This is bound to occur due to the dynamics of the system.

A practical implementation of the pure pursuit guidance law would be to use a feedback law as follows:

$$a_M = -K(\alpha_M - \theta) \quad (7.43)$$

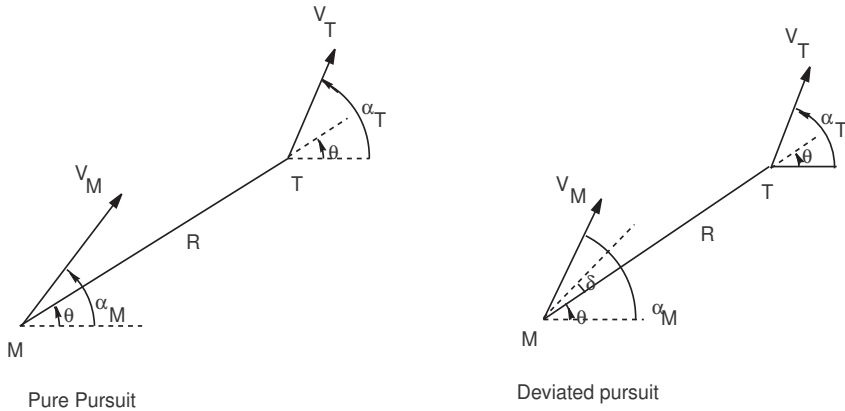


Figure 7.12: Pursuit guidance law: Implementation geometry

with  $K > 0$ . This is with reference to the Figure 7.12. However, this is not enough. For pursuit to be effective, we must have,

$$\dot{\alpha}_M = \dot{\theta} \quad (7.44)$$

Since

$$\dot{\alpha}_M = \frac{a_M}{V_M} \quad (7.45)$$

From which we get,

$$a_M = V_M \dot{\theta} \quad (7.46)$$

Putting (7.43) and (7.46) together, an implementable pure pursuit guidance law would have a form,

$$a_M = V_M \dot{\theta} - K(\alpha_M - \theta) \quad (7.47)$$

The first term equalizes the missile flight path angle rate with the LOS rate and the second term generates a lateral proportional to the angular difference between the flight path and LOS.

We will have occasion to refer to this guidance law again when we discuss the proportional navigation guidance law.

Similarly, the deviated pursuit guidance law may be implemented as,

$$a_M = V_M \dot{\theta} - K(\alpha_M - \theta - \delta) \quad (7.48)$$

In both these cases, the choice of  $K$  is important.

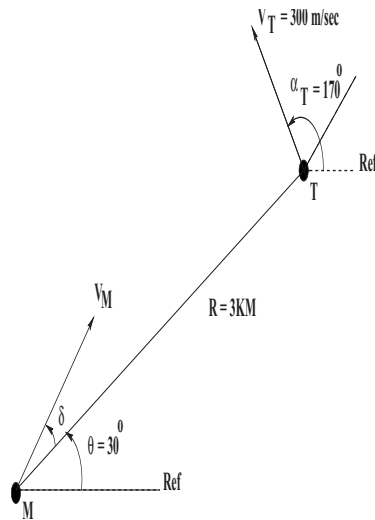
#### 7.4 Concluding Remarks

In this chapter we derived some analytical results about the pursuit guidance law for both pure and deviated versions. In both cases capture is shown to be guaranteed when the missile velocity is higher than the target velocity. It was shown that the capture region for pure pursuit and deviated pursuit is a circle of radius equal to the missile velocity  $V_M$ . However, if the angle of deviation  $\delta$  is considered as a flexible guidance parameter for deviated pursuit, then the deviated pursuit guidance law has a much larger capture region.

The latax history showed that the terminal latax is very high when the missile has more than double the target velocity, but is bounded by a finite value when the missile velocity is more than the target velocity but less than twice the target velocity.

#### *Questions*

1. Show that the trajectory in the relative velocity space when the missile uses a deviated pursuit guidance law right from the beginning of the engagement, is a circle. Determine the direction of movement of a point on this trajectory.
2. Obtain the capture region of the deviated pursuit guidance law in the relative velocity space.
3. **PART A: Deviated Pursuit,  $\delta = 25^\circ$ ;  $\alpha_T \in [0^\circ, 180^\circ]$** 
  - A1. Integrate the equations of motion and plot  $R$ ,  $\theta$ ,  $V_\theta$ ,  $V_R$ , and  $a_M$  against time for  $\nu = 0.9, 1.5, 3$ . Note that  $\nu = V_M/V_T$ .
  - A2. Also plot the missile and target trajectories for each case.
  - A3. Check if interception occurs. If yes, then find  $t_f$ . If no then find  $t_{\text{miss}}$  and  $R_{\text{miss}}$ .
  - A4. Plot  $(V_\theta, V_R)$  in  $(V_\theta, V_R)$ -space.
  - A5. Interpret the simulation results in the light of the analytical results discussed in the class.



### PART B: Implementation

B1. Use the implementation of deviated pursuit, with  $\delta = 8^\circ$ , as

$$a_M = V_M \dot{\theta} - k(\alpha_M - \theta - \delta)$$

when, in the above figure, the initial missile velocity vector lags the LOS by  $10^\circ$ .

Plot  $R$ ,  $\theta$ ,  $V_\theta$ ,  $V_R$ ,  $\alpha_M$  and  $a_M$  against time for  $\nu = 0.9, 1.5, 3; k = 1, 5, 10$ .

Plot  $(V_\theta, V_R)$  in  $(V_\theta, V_R)$ -space.

Plot the missile and target trajectories for each case.

### PART C: Comparisons

Compare the results obtained for pure pursuit in the last section with the results obtained for deviated pursuit.

### References

1. C.-F. Lin: *Modern Navigation, Guidance, and Control Processing*, Prentice Hall, Englewood Cliffs, NJ, 1991.
2. A.S. LOCKE: *Guidance*, D. Van Nostrand Co., 1955.

## Chapter 8

# The Line of Sight Guidance Law

### Module 7: Lecture 19 Introduction; LOS Guidance

**Keywords.** Beam Rider Guidance; CLOS Guidance; LOS Guidance

As mentioned in the previous chapter, the Line-of-sight (LOS) guidance law functions on the philosophy that if the missile remains on the line joining the launch platform and the target then it eventually must hit the target. By its very nature LOS guidance is a three-point guidance. Basically, it may be implemented in two ways:

- *Beam Rider (BR):* Here the missile senses its own deviation from the LOS (defined by an electro-optical beam focussed continuously on the target) and uses this information to generate guidance commands. This can be thought of as similar to semi-active homing but not precisely so since the missile does not use the reflected energy from the target, but rather it uses the beam from the launch platform to the target itself.
- *Command-to-Line-of-Sight (CLOS):* Here the radar at the launch platform tracks both the missile and the target. The deviation is sensed by the tracking radar and the guidance command is computed and sent to the missile through an uplink. This is

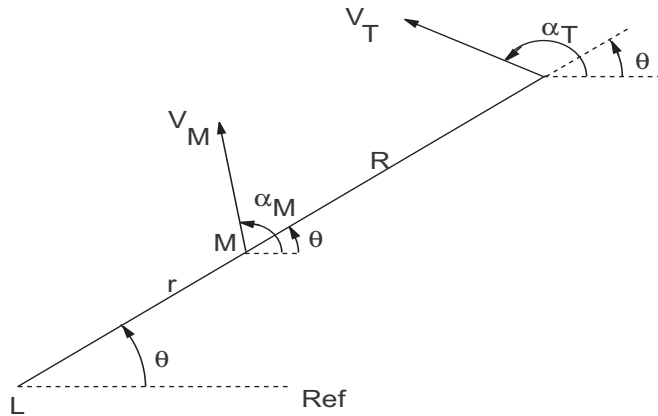


Figure 8.1: Engagement geometry for LOS guidance

similar to *command guidance*.

Essentially BR and CLOS are the two different mechanizations of the basic LOS guidance philosophy. In this chapter we will first study the basic LOS guidance law and then discuss its two mechanizations.

## 8.1 LOS Guidance

In Figure 8.1 we show the engagement geometry of the LOS guidance law. As in earlier cases we restrict our attention to a non-maneuvering target. We assume that  $V_T$ ,  $\alpha_T$ , and  $V_M$  are constants. The distance from the launch platform to the missile is  $LM=r$  and the distance from the missile to the target is  $MT=R$ . In the ideal case, the missile M should always be on the LOS (given by LT) between the launch platform and the target. Note that in LOS guidance the LOS refers to the LOS between points L and T, unlike in pursuit guidance analysis where the LOS was between the missile and the target. We have the following equations of motion,

$$V_r = \dot{r} = V_M \cos(\alpha_M - \theta) \quad (8.1)$$

$$V_R = \dot{R} = V_T \cos(\alpha_T - \theta) - V_M \cos(\alpha_M - \theta) \quad (8.2)$$

$$V_{\theta r} = r \dot{\theta} = V_M \sin(\alpha_M - \theta) \quad (8.3)$$

$$V_{\theta R} = R \dot{\theta} = V_T \sin(\alpha_T - \theta) - V_M \sin(\alpha_M - \theta) \quad (8.4)$$

Note that in this case  $V_r$  is the rate of change of the LOS separation between L and M, and  $V_R$  is the rate of change of the LOS separation between M and T. Similarly,  $V_{\theta r}$  is the angular rate of the LOS between L and M, and  $V_{\theta R}$  is the angular rate of the LOS between M and T.

Now, from (8.3) and (8.4) we can write,

$$\dot{\theta} = \frac{V_M \sin(\alpha_M - \theta)}{r} = \frac{V_T \sin(\alpha_T - \theta) - V_M \sin(\alpha_M - \theta)}{R} = \frac{V_T \sin(\alpha_T - \theta)}{R + r} \quad (8.5)$$

$$\Rightarrow (R + r)V_M \sin(\alpha_M - \theta) = rV_T \sin(\alpha_T - \theta) \quad (8.6)$$

Differentiating (8.6) with respect to time, using the fact that  $\dot{\alpha}_M = a_M/V_M$ , and substituting (8.1)-(8.4) appropriately, we obtain the following sequence of equations,

$$\begin{aligned} & (\dot{R} + \dot{r})V_M \sin(\alpha_M - \theta) + (R + r)V_M \cos(\alpha_M - \theta)(\dot{\alpha}_M - \dot{\theta}) \\ &= \dot{r}V_T \sin(\alpha_T - \theta) + rV_T \cos(\alpha_T - \theta)(-\dot{\theta}) \\ \Rightarrow & V_T \cos(\alpha_T - \theta)V_M \sin(\alpha_M - \theta) + (R + r)a_M \cos(\alpha_M - \theta) - V_T \sin(\alpha_T - \theta)V_M \cos(\alpha_M - \theta) \\ &= V_T \sin(\alpha_T - \theta)V_M \cos(\alpha_M - \theta) - V_T \cos(\alpha_T - \theta)V_M \sin(\alpha_M - \theta) \\ \Rightarrow & (R + r)a_M \cos(\alpha_M - \theta) = 2V_T V_M \sin(\alpha_T - \alpha_M) \\ \Rightarrow & a_M = \frac{2V_T V_M \sin(\alpha_T - \alpha_M)}{(R + r) \cos(\alpha_M - \theta)} \end{aligned} \quad (8.7)$$

substitute based on  $r\dot{\theta}$ ,  
 $(r+R)\dot{\theta}, \dots$

This gives an expression for the missile acceleration  $a_M$  required in an ideal implementation of the LOS guidance law in order to keep the missile on the LOS between the launch platform L and the target T. However, the expression for  $a_M$  given in (8.7) is a function of several time-varying quantities:  $R$ ,  $r$ ,  $\alpha_M$ , and  $\theta$ . Of these, it is possible to express  $\theta$  and  $(R + r)$  as functions of time as follows:

Consider Figure 8.1. From the geometry, since the target moves in a straight line, we can see that,

$$\tan \theta = \frac{(R_0 + r_0) \sin \theta_0 + V_T t \sin \alpha_T}{(R_0 + r_0) \cos \theta_0 + V_T t \cos \alpha_T} \quad (8.8)$$

$$\theta = \tan^{-1} \frac{(R_0 + r_0) \sin \theta_0 + V_T t \sin \alpha_T}{(R_0 + r_0) \cos \theta_0 + V_T t \cos \alpha_T} \quad (8.8)$$

$$R + r = \sqrt{(R_0 + r_0)^2 + (V_T t)^2 + 2(R_0 + r_0)V_T t \cos(\theta_0 - \alpha_T)} \quad (8.9)$$

Where, the subscript '0' denotes the initial values which are known. This gives an expression for the LOS angle  $\theta$  and  $R + r$  as functions of time.

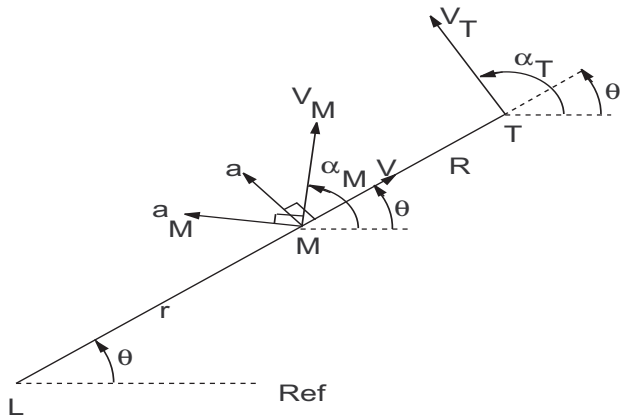


Figure 8.2: Another engagement geometry for LOS guidance

Now, from (8.6), we have,

$$(R + r)V_M \sin(\alpha_M - \theta) = rV_T \sin(\alpha_T - \theta)$$

$$\Rightarrow \sin(\alpha_M - \theta) = \frac{rV_T \sin(\alpha_T - \theta)}{(R + r)V_M}$$

So,  $\alpha_M$  can be finally expressed as a function of  $t$  and the distance  $r$  of the missile from the launch platform. These expressions can be used to generate the missile latax for simulating an LOS guided missile target engagement for a non-maneuvering target.

An alternative way to obtain the missile acceleration, that is usually given in most books is also given below.

Consider the Figure 8.2. In this figure we consider the missile M to be a body moving along a rotating line (actually the LOS between the launch platform L and the target T that rotates at rate  $\dot{\theta}$ ) with speed  $V$ . Then the acceleration experienced by M normal to the rotating line is denoted by  $a$  and is given by,

$$a = 2V\dot{\theta} + r\ddot{\theta} = \frac{d}{dt}(r\dot{\theta}) + \dot{r}\dot{\theta} \quad (8.10)$$

Note that the expression for  $a$  is obtained by adding the Coriolis acceleration  $i\dot{\theta}$  to the rate of change of the angular velocity obtained from  $d/dt(r\dot{\theta})$ .

Now, the actual missile velocity and accelerations are as shown in Figure 8.2.

great  
one

They are related to  $V$  and  $a$  as,

$$\begin{aligned} V &= V_M \cos(\alpha_M - \theta) \\ a &= a_M \cos(\alpha_M - \theta) \end{aligned} \quad (8.11)$$

Substituting in (8.10), we get

$$\begin{aligned} a_M \cos(\alpha_M - \theta) &= 2V_M \cos(\alpha_M - \theta) \dot{\theta} + r \ddot{\theta} \\ \Rightarrow a_M &= 2V_M \dot{\theta} + \frac{r \ddot{\theta}}{\cos(\alpha_M - \theta)} \end{aligned} \quad (8.12)$$

From Figure 8.2,

$$\dot{\theta} = \frac{V_T \sin(\alpha_T - \theta)}{R + r} \quad (8.13)$$

which on rearrangement and differentiation yields,

$$\dot{\theta} \frac{d}{dt}(R + r) + (R + r)\ddot{\theta} = -\dot{\theta}V_T \cos(\alpha_T - \theta) \quad (8.14)$$

Substituting

$$\frac{d}{dt}(R + r) = V_T \cos(\alpha_T - \theta) \quad (8.15)$$

and (8.13), we get

$$\ddot{\theta} = -\frac{2V_T^2 \sin(\alpha_T - \theta) \cos(\alpha_T - \theta)}{(R + r)^2} \quad (8.16)$$

Substituting these expressions for  $\dot{\theta}$  and  $\ddot{\theta}$  in (8.12), we get

$$a_M = \frac{2V_M V_T \sin(\alpha_T - \theta)}{R + r} - \frac{2r V_T^2 \sin(\alpha_T - \theta) \cos(\alpha_T - \theta)}{\cos(\alpha_M - \theta)(R + r)^2} \quad (8.17)$$

Substituting from

$$\dot{\theta} = \frac{V_M \sin(\alpha_M - \theta)}{r} = \frac{V_T \sin(\alpha_T - \theta)}{R + r} \quad (8.18)$$

we get

$$\begin{aligned} a_M &= \frac{2V_M V_T \sin(\alpha_T - \theta)}{R + r} - \frac{2V_M \sin(\alpha_M - \theta) V_T \cos(\alpha_T - \theta)}{\cos(\alpha_M - \theta)(R + r)} \\ \Rightarrow &\frac{2V_M V_T}{(R + r) \cos(\alpha_M - \theta)} [\sin(\alpha_T - \theta) \cos(\alpha_M - \theta) - \sin(\alpha_M - \theta) \cos(\alpha_T - \theta)] \\ \Rightarrow &\frac{2V_M V_T \sin(\alpha_T - \alpha_M)}{(R + r) \cos(\alpha_M - \theta)} \end{aligned} \quad (8.19)$$

which is the same as (8.7) derived earlier.

## Module 7: Lecture 20

### Implementation of LOS Guidance; CLOS; BR

**Keywords.** Beam Rider Guidance; CLOS; BR

#### 8.2 Implementation of LOS Guidance

The implementation of LOS guidance law in an actual missile system differs somewhat from the analytical derivation of the lateral acceleration as obtained in the previous section. The analytical expression for the latax, if implemented, gives perfect results in an ideal situation. But in real-life situation the latax given by (8.7), if implemented in the open-loop mode, may be quite inadequate to achieve an intercept. There are several reasons for this deficiency. Some of them are the following:

1. *Guidance parameters*: The expression for missile latax given in (8.7) or in (8.19) requires the knowledge of  $V_M$ ,  $V_T$ ,  $\alpha_T$ ,  $\alpha_M$ ,  $R + r$  (which is the range to the target from the tracking station), and  $\theta$ . Many of these may not be available, or they may be difficult to obtain, or their measurement or estimation may be prone to severe errors.
2. *Autopilot dynamics*: Autopilot dynamics are not taken into account in the derivation of the missile latax. This will cause the missile to lag behind the LOS between the tracking station and the target. There is no in-built compensation for this lag.
3. *Target maneuver*: The expression for latax was derived based on the assumption of a non-maneuvering target. When the target maneuvers, as it is likely to do in a real-life situation, the latax will not be adequate to ensure the position of the missile on the LOS between the tracking station and the target.
4. *Launch at off-nominal conditions*: Note that for (8.7) to be valid (8.5) must be satisfied for all times, which implies that  $\dot{\theta}_M = \dot{\theta}_T$  (where  $\theta_M$  and  $\theta_T$  are the LOS angles to the missile and the target from the launch platform) must be true at initial time. Only then, by using  $a_M$  in (8.7) we can maintain (8.5) throughout the engagement. In case of off-nominal conditions this will not happen and the missile will deviate

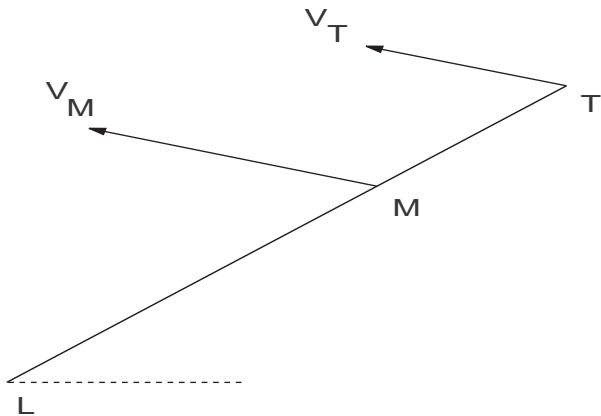


Figure 8.3: Example: Note that the missile and target velocities are parallel, but since  $V_M$  is larger than  $V_T$ , the missile will depart from the LOS. But since  $\alpha_M = \alpha_T$  remains true for all time, according to (8.7), no latax is generated by the missile to correct this situation.

from the LOS. For example, consider a case where  $\alpha_M = \alpha_T$  and  $\theta_M = \theta_T = \theta$ , but (8.5) is not satisfied. This means that the missile will not apply any latax (that is,  $a_M = 0$ ) and will continue in a straight line and will eventually depart from the LOS (see Figure 8.3 for an example of this situation).

In this section we will look at two different implementations of the LOS guidance, namely Beam-Rider (BR) and Command to Line-of-Sight (CLOS) that differ somewhat from the analytical expression for the LOS guidance law.

### 8.2.1 Beam-Rider (BR) Guidance

The objective of beam rider guidance is to fly the missile along a beam focussed on the target. Since the missile attempts to fly along the beam which moves according to the target motion, the missile guidance command must be a function of the angular deviation of the missile from the beam. It is obvious that if the missile stays on the beam (rides the beam) and the beam is kept focussed on the target, an intercept must result.

Consider a BR engagement geometry given in Figure 8.4. The figure shows that the missile is slightly away from the LOS joining the launch platform (or rather, the tracking station) and the target.

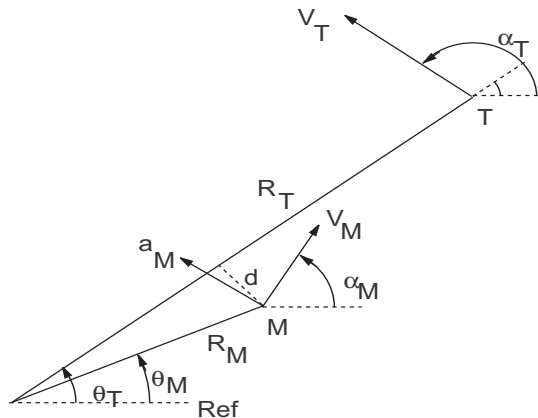


Figure 8.4: Beam rider (BR) engagement geometry

$$d \cong R_M(\theta_T - \theta_M) \quad (8.20)$$

If  $d = 0$  always then the missile follows an ideal LOS course and the missile will ultimately hit the target. Hence, a good guidance law should try to minimize  $d$ . To achieve this, the simplest thing would be to use a commanded acceleration which is proportional to the deviation  $d$ .

$$a_M = Kd = KR_M(\theta_T - \theta_M) \quad (8.21)$$

To implement the BR guidance law, the missile carries a rear-ward looking beam receiver so that the missile can determine its position in the beam (in terms of its deviation from the center line of the beam) and guide itself to the beam axis. Laser beam is used for anti-tank missiles (SSM or ASM), anti-helicopter missiles (AAM), and short range air defense missiles (SAM) because of its high accuracy and high electronic counter-measure resistance property. Radar beam riding is used in older, medium range, SAMs and anti-ship missile systems, for example, the TALOS beam riding system.

Thus, one can see that the on-board sensor of the missile gives it information about its deviation from the center line of the beam, that is, it gives a good estimate of  $\theta_T - \theta_M$  but it has no information about  $R_M$ . So, in the actual implementation of the BR guidance law, a rough estimate of the missile range is used. Accordingly, the commanded acceleration for the BR missile is given by,

$$a_M = K\hat{R}_M(\theta_T - \theta_M) \quad (8.22)$$

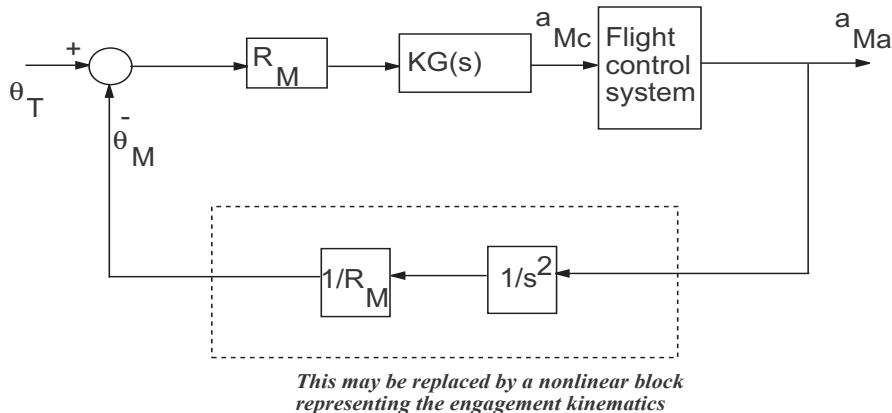


Figure 8.5: Block diagram for beam rider guidance

where,  $\hat{R}_M$  is an estimate of  $R_M$ .

The BR missile still suffers from the inadequacy that it does not take into account the movement of the beam that tracks the target. The BR missile also normally requires on-board autopilot compensation for good performance. The compensation is of the lead-lag type with which the commanded acceleration becomes,

$$a_M = KG(s)\hat{R}_M(\theta_T - \theta_M) \quad (8.23)$$

where,

$$G(s) = \frac{1 + s/a}{1 + s/b} \quad (8.24)$$

A good choice of parameters is that in which  $b$  is about one order of magnitude higher than  $a$  and  $K \cong b/a$ . For example, we may consider  $K = 10$ ,  $b = 20$ ,  $a = 2$ .

A block diagram of the BR guidance is shown in Figure 8.5. The variation of the missile latax for different values of the gain  $K$  with and without compensation is given in Figure 8.6.

### 8.2.2 Command to Line-of-Sight (CLOS) Guidance

In CLOS guidance, both the missile and the target are tracked by the tracking station on the ground or in the launch platform. The guidance command is computed at the ground station and communicated to the missile via an uplink. The engagement ge-

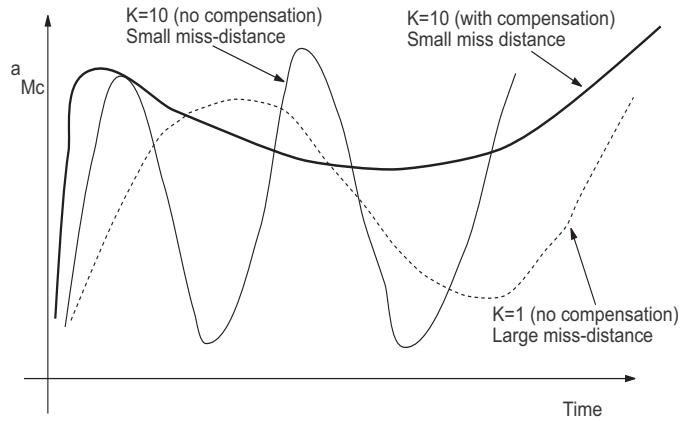


Figure 8.6: Beam rider latrax

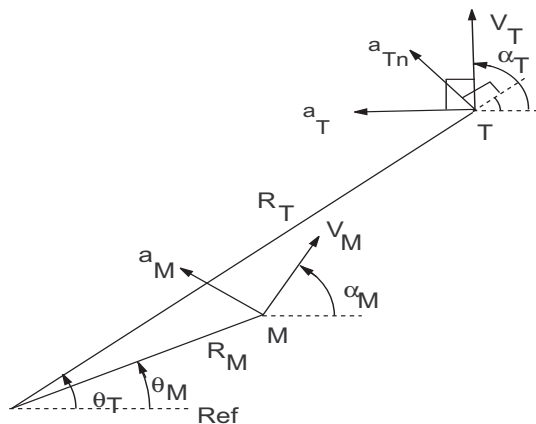


Figure 8.7: Command to line-of-sight (CLOS) engagement geometry

ometry is similar to the one considered in the BR case, but with the additional consideration of target maneuver (see Figure 8.7). Here, we attempt to take into account the motion of the beam. Suppose, the target is maneuvering but, as is often the case, the tracking algorithm is not adequate to give us a good estimate of the target acceleration. But we can have a good estimate of the angular rates of  $\dot{\theta}_T$  from the motion of the tracking radar. Then, the guidance effort should be to ensure that,

$$\begin{aligned}\dot{\theta}_M &= \dot{\theta}_T \\ \ddot{\theta}_M &= \ddot{\theta}_T\end{aligned}\tag{8.25}$$

From Figure 8.7, we have,

$$R_T \dot{\theta}_T = V_T \sin(\alpha_T - \theta_T)$$

which on differentiation with respect to time, yields,

$$\dot{R}_T \dot{\theta}_T + R_T \ddot{\theta}_T = -V_T \dot{\theta}_T \cos(\alpha_T - \theta_T) + V_T \alpha_T \cos(\alpha_T - \theta_T)$$

which, on rearranging and substituting  $a_T = V_T \alpha_T$  and  $\dot{R}_T = V_T \cos(\alpha_T - \theta_T)$ , yields,

$$\begin{aligned} \ddot{\theta}_T &= \frac{-2\dot{R}_T \dot{\theta}_T - a_T \cos(\alpha_T - \theta_T)}{R_T} \\ &= \frac{a_{Tn} - 2\dot{R}_T \dot{\theta}_T}{R_T} \end{aligned} \quad (8.26)$$

where,  $a_{Tn} = a_T \cos(\alpha_T - \theta_T)$  is the target acceleration normal to the LOS between the tracking station and the target. We can rearrange the above equation and write,

$$a_{Tn} = R_T \ddot{\theta}_T + 2\dot{R}_T \dot{\theta}_T \quad (8.27)$$

Similarly, had we carried out a similar analysis for the missile, we would have obtained,

$$a_{Mn} = R_M \ddot{\theta}_M + 2\dot{R}_M \dot{\theta}_M \quad (8.28)$$

If we want  $\dot{\theta}_M = \dot{\theta}_T$  and  $\ddot{\theta}_M = \ddot{\theta}_T$  then  $a_{Mn}$  must satisfy,

$$a_{Mn} = R_M \ddot{\theta}_T + 2\dot{R}_M \dot{\theta}_T \quad (8.29)$$

Ideally we would like to generate a missile acceleration such that its component normal to the LOS between the tracking station and the missile is equal to  $a_{Mn}$ , in reality we directly use this expression in the missile latax command as follows,

$$a_M = KR_M(\theta_T - \theta_M) + R_M \ddot{\theta}_T + 2\dot{R}_M \dot{\theta}_T \quad (8.30)$$

when we use compensation (as in the BR case) we get,

$$a_M = KG(s)R_M(\theta_T - \theta_M) + R_M \ddot{\theta}_T + 2\dot{R}_M \dot{\theta}_T \quad (8.31)$$

with the parameter values similar to the BR case. Note that the second and the third term take into account the movement of the beam and therefore the performance of CLOS is better than that of BR. In fact the miss-distance obtained for CLOS is less than the miss-distance obtained for BR. The block diagram for CLOS guidance loop is given in Figure 8.8. The variation of the missile latax for different values of the gain  $K$  with and without compensation is given in Figure 8.9.

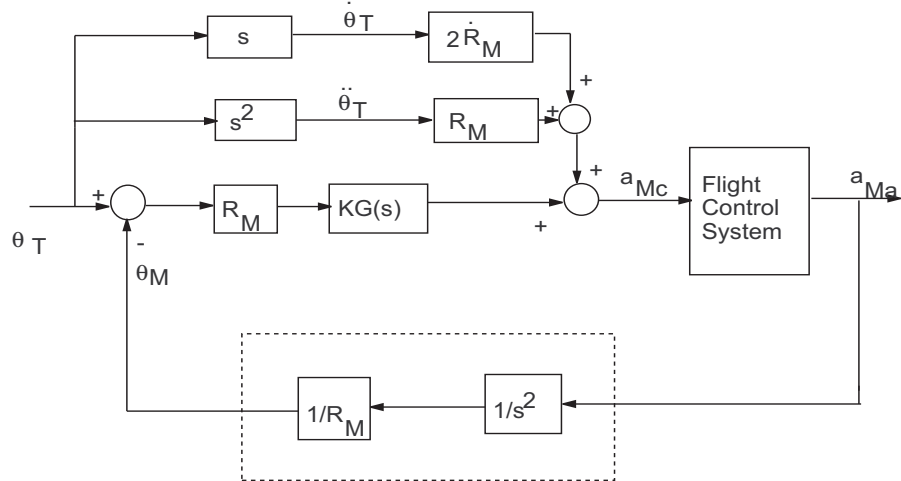


Figure 8.8: Block diagram of CLOS guidance

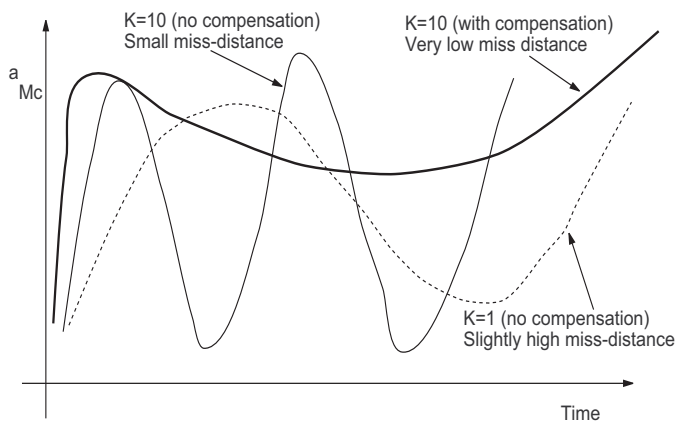


Figure 8.9: CLOS latax

## Module 7: Lecture 21

### Some Additional Analysis

. **Keywords.** Capturability analysis

#### 8.3 Some Additional Analysis

##### 8.3.1 The nonlinear engagement block in the BR/CLOS guidance loop

The block in the guidance loop shown in Figures 8.5 and 8.8 are obtained after making several strong assumptions. We will see this below:

From Figures 8.4 or 8.7, we have

$$R_M \dot{\theta}_M = V_M \sin(\alpha_M - \theta_M) \quad (8.32)$$

Differentiating,

$$\dot{R}_M \dot{\theta}_M + R_M \ddot{\theta}_M = V_M \cos(\alpha_M - \theta_M)(\dot{\alpha}_M - \dot{\theta}_M) \quad (8.33)$$

Since,  $\dot{R}_M = V_M \cos(\alpha_M - \theta_M)$  and  $\dot{\alpha}_M = a_M/V_M$ ,

$$2V_M \cos(\alpha_M - \theta_M) \dot{\theta}_M + R_M \ddot{\theta}_M = a_M \cos(\alpha_M - \theta_M) \quad (8.34)$$

From which, we can write,

$$a_M = 2V_M \dot{\theta}_M + \frac{R_M}{\cos(\alpha_M - \theta_M)} \ddot{\theta}_M \quad (8.35)$$

Since  $V_M \cos(\alpha_M - \theta_M)$  is the component of the missile velocity along the LOS, we can make an assumption that

$$\frac{R_M}{V_M \cos(\alpha_M - \theta_M)} = \tilde{t} \quad (8.36)$$

where,  $\tilde{t}$  maybe an approximation of the time elapsed (which is  $t$ ). This is in the same spirit as that used to compute an approximate value of time-to-go. Then,

$$a_M = 2V_M \dot{\theta}_M + V_M \tilde{t} \ddot{\theta}_M = V_M \tilde{t} \left( \frac{2}{\tilde{t}} \dot{\theta}_M + \ddot{\theta}_M \right) \quad (8.37)$$

If  $\tilde{t}$  is the time elapsed then  $V_M \tilde{t} = \tilde{R}_M$  is the distance covered by the missile. Thus,

$$a_M = \tilde{R}_M \left( \frac{2}{\tilde{t}} \dot{\theta}_M + \ddot{\theta}_M \right) \quad (8.38)$$

Taking Laplace transforms on both sides,

$$\frac{\theta_M(s)}{a_M(s)} = \frac{1}{\tilde{R}_M s \left(\frac{2}{\tilde{t}} + s\right)} \quad (8.39)$$

Now, we make a further strong assumption that the time elapsed is large enough for us to neglect the term  $2/\tilde{t}$  and also that  $\tilde{R}_M \cong R_M$ . (*Note that these are very strong assumptions*). Then,

$$\theta_M(s) = \frac{1}{R_M} \cdot \frac{1}{s^2} a_M(s) \quad (8.40)$$

This is the relationship used to linearize the non-linear block. Hence, while evaluating the guidance law in the loop, we should use the nonlinear engagement geometry rather than the linear representation.

### 8.3.2 Capturability analysis

We can carry out some limited capturability analysis here. For this, we need to first determine the conditions at the initial time and final time. From (8.35), we get an expression for the missile latax,

$$a_M = 2V_M \dot{\theta} + \frac{R_M}{\cos(\alpha_M - \theta)} \ddot{\theta} \quad (8.41)$$

At  $t = 0$ , we have  $R_M = 0$ , and so,

$$a_{M0} = 2V_M \dot{\theta}_0 \quad (8.42)$$

Now, for perfect LOS guidance to be effective, (8.5) has to hold at initial time too. This means that

$$V_M \sin(\alpha_{M0} - \theta_0) = 0 \Rightarrow \alpha_{M0} = \theta_0 \quad (8.43)$$

which implies that initially the missile must point towards the target.

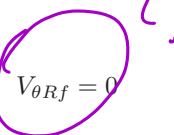
Similarly, suppose at some time  $t = t_f$  interception takes place, then  $R_f = 0$ , and from (8.9),

$$R_{Mf} = \sqrt{R_0^2 + (V_T t_f)^2 + 2R_0 V_t t_f \cos(\theta_0 - \alpha_T)} \quad (8.44)$$

From (8.5),

$$V_M \sin(\alpha_{Mf} - \theta_f) = V_T \sin(\alpha_{Tf} - \theta_f) \quad (8.45)$$

which, from (8.4) implies that

$$\text{?} \quad V_{\theta Rf} = 0 \quad (8.46)$$


which is an obvious condition for interception.

*Theorem 8.1.* If  $V_M > V_T$  then the missile captures the target.

*Proof.* We will prove this by contradiction. Assume that interception does not occur. In that case the target continues to fly for infinite time. Now, as  $t \rightarrow \infty$ , we have  $\theta \rightarrow \alpha_T$  which, from (8.5), implies that  $\alpha_{M\infty} = \theta_\infty = \alpha_T$ . This implies that the missile converges to a tail-chase situation with the target as  $t \rightarrow \infty$ . From (8.2) and (8.4), we have  $V_{\theta\infty} = 0$  and  $V_{R\infty} = V_T - V_M$ . Now, if  $V_M > V_T$ , then the missile will eventually intercept the target. This is a contradiction. And so, the missile will intercept the target in finite time whenever  $V_M > V_T$ .  $\square$

This result can be interpreted as follows: The theorem gives a sufficient condition only. Based on the sufficient condition one can say that the capture region for the LOS guidance is at least as large as that of the pure pursuit guidance law, provided that the initial conditions are the ideal initial conditions for LOS guidance, that is the initial missile velocity vector points directly at the target (note that these initial conditions are the same as that of pure pursuit). However, the theorem does not give a necessary condition and so we cannot say if  $V_M \leq V_T$  implies no interception. There could be conditions under which M may intercept T even when  $V_M \leq V_T$ .

#### 8.4 Concluding Remarks

In this chapter we analyzed another classical guidance law called the LOS guidance law. We also discussed the implementation of the LOS guidance law in two forms: Beam Rider and Command to LOS. Their relative performances were also discussed. However, note that unlike in the previous chapters we did not carry out any detailed

capturability analysis in the relative velocity space. This is because, the LOS guidance equations do not lend themselves very easily to an analysis in the relative velocity space. Moreover, capturability of LOS guidance laws depends on other parameters than just the relative velocity components. In fact, complete capturability results can be obtained only through numerical computations.

### *Questions*

Assume initial position of approaching target: (8 to 12 kms down range, 0.5 to 0.8 km altitude)

1. Consider a BR missile

- Assume that there is no autopilot compensation:

- (A) Guidance law is  $a_M = KR_M(\theta_T - \theta_M)$ . Consider  $K = 1, 5, 10$ .  $V_T/V_M = 0.6$ . Plot the following quantities against time (a) missile latax (b) missile and target trajectories (c)  $R_M(\theta_T - \theta_M)$  (d)  $R$  = Separation between missile and target. Find the miss distance in each case.
- (B) Let  $K = 10$  and  $V_T/V_M = 0.6$ . Assume a pitch up constant target maneuver with  $a_T = 3g$ . Plot against time (a) missile latax (b)  $R$  (c) missile and target trajectories. Find the miss-distance.

- Assume that there is autopilot compensation:

$$G(s) = K \left( \frac{1 + s/2}{1 + s/20} \right)$$

- (C) Assume a non-maneuvering target. Let  $K = 10$ ,  $V_T/V_M = 0.6$ . Plot against time (a) missile latax (b)  $R$  (c) missile and target trajectories. Find the miss-distance.
- (D) Assume a similar maneuvering target. Let  $K = 10$ ,  $V_T/V_M = 0.6$ . Plot against time (a) missile latax (b)  $R$  (c) missile and target trajectories. Find the miss-distance.

2. Consider a CLOS missile:

(A) Without autopilot compensation and  $K = 1, 5, 10$ ,  $V_T/V_M = 0.6$ . The guidance law is given by  $a_M = KR_M(\theta_T - \theta_M) + R_M\ddot{\theta}_T + 2R_M\dot{\theta}_T$ .

For a non-maneuvering target and then for a maneuvering target (3g pitch-up maneuver):

Plot against time (a) missile latax (b) missile target trajectories (c)  $R$ . Find the miss-distance in each case.

(B) Do the same as above for a case with autopilot compensation  $G(s)$  given in the BR case.

Write overall comments comparing the results.

## References

1. C.-F. Lin: *Modern Navigation, Guidance, and Control Processing*, Prentice Hall, Englewood Cliffs, NJ, 1991.
2. A.S. Locke: *Guidance*, D. Van Nostrand Co., 1955.
3. P. Zarchan: *Tactical and Strategic Missile Guidance*, 3rd Ed., AIAA Inc., Washington DC, 1997.

## Chapter 9

# An Introduction to Proportional Navigation

### Module 8: Lecture 22 PPN; TPN; GTPN; IPN

**Keywords.** Proportional Navigation, PPN, TPN, GTPN, IPN

Proportional navigation is, by far, the most important of the classical guidance laws. In this chapter we will give a brief description of the several variants of the PN law that has appeared in the literature.

To explain how the PN law works let us first define an engagement geometry in a 2-D plane. We shall use this engagement geometry or some variants of it in the subsequent lectures. The engagement geometry is two dimensional and is given in Figure 9.1. Point mass models are assumed for both the missile and the non-maneuvering target.

The missile lateral acceleration or latax is given by  $a_M$ . The missile and target

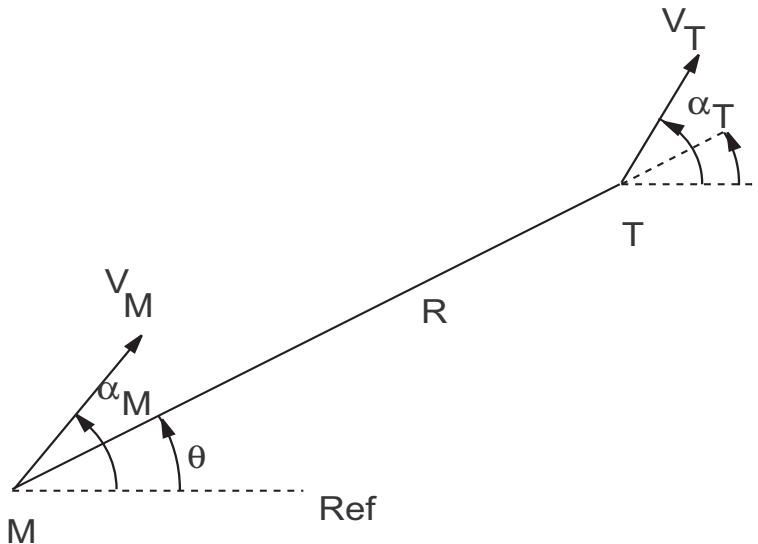


Figure 9.1: Missile-target engagement geometry

velocities are denoted by  $V_M$  and  $V_T$ , respectively. The equations of motion are,

$$V_r = \dot{R} = V_T \cos(\alpha_T - \theta) - V_M \cos(\alpha_M - \theta) \quad (9.1)$$

$$V_\theta = R\dot{\theta} = V_T \sin(\alpha_T - \theta) - V_M \sin(\alpha_M - \theta) \quad (9.2)$$

where,  $V_r$  is the rate of change of the LOS separation (i.e., the component of the relative velocity of the target with respect to the missile along the LOS) and  $V_\theta$  is the angular velocity of the LOS (i.e., the component of this relative velocity perpendicular to the LOS).

Now the *Proportional Navigation (PN)* guidance law is defined as a law that generates a guidance command (or a latax) which ensures that the rate of rotation of the missile velocity vector is proportional to the rate of rotation of the LOS. That is,

$$\dot{\alpha}_M = N\dot{\theta} \quad (9.3)$$

where,  $N$  is the navigation constant. This was the essence of the PN guidance law when it was formulated in the early days of missile guidance research. This innocuous-looking guidance law has, over the years, spawned an enormous variety of guidance laws that have attempted to improve the performance of the basic PN law. These guidance laws are popularly known as PN-variants.

In fact, the PN law is no longer referred to in the form of (9.3). It is expressed in terms of the latax that is prescribed at different instants of time at various points on the trajectory. We shall examine the structure of some of these laws in this lecture.

### 9.1 Pure Proportional Navigation (PPN)

One of the first complete definition of the PN law is what is now known as the *Pure Proportional Navigation (PPN)* guidance law. This is also the most natural definition of the PN law. We know that,

$$\dot{\alpha}_M = \frac{a_M}{V_M} \quad (9.4)$$

So, from (9.3), we get,

$$a_M = NV_M \dot{\theta} \quad (9.5)$$

This is the *PPN* law. But there is one more point to be noted here. We know that (9.4) is valid only when the lateral acceleration  $a_M$  is perpendicular to the velocity  $V_M$  of the missile. So, according to the PPN law, the latax is given by (9.5) and is applied perpendicular to the velocity vector of the missile. If we ignore the angle-of-attack of the missile, then this direction of the latax is also the natural direction of the lift force which is generated by the airframe and the lifting surfaces (as explained earlier) whenever the missile maneuvers. Note that this lift force is responsible for generating the actual lateral acceleration or latax. However, the only problem here is that the angle-of-attack of a missile is never zero and for many highly maneuverable missiles it turns out to be quite high. This is where PPN departs from reality and its elegant results stop being fully applicable. In Figure 9.2(a), the PPN latax is shown.

### 9.2 True Proportional Navigation (TPN)

True proportional navigation is another variant of the proportional navigation guidance law. The logic behind it is as follows: The velocity of interest is actually the closing velocity and not the missile velocity itself, because it is the closing velocity which ultimately drives the LOS separation to zero. Moreover, it is also the LOS rate which we are trying to drive to zero. So, why not apply the missile latax perpendicular to the LOS and also make it proportional to the closing velocity? It isn't a very convincing argument, but the guidance system designers who were desperate to explore ways

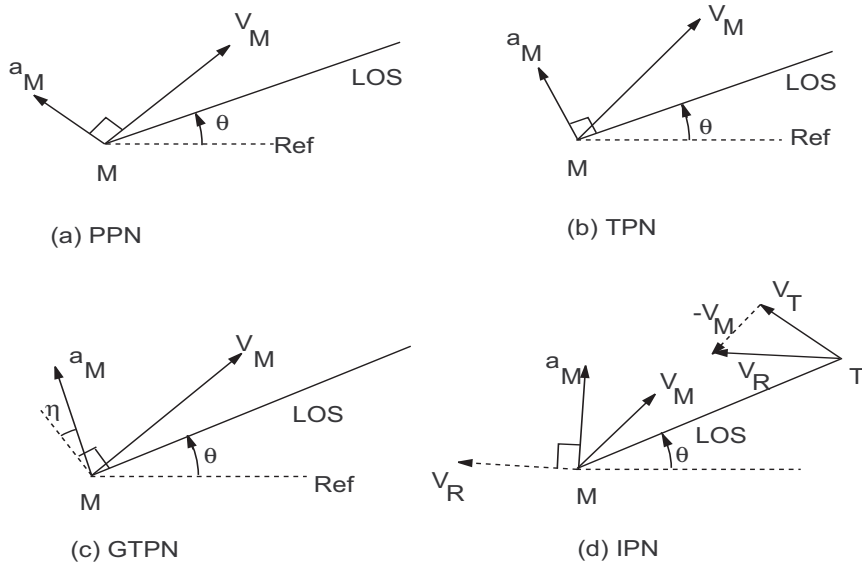


Figure 9.2: (a) PPN Latax (b) TPN Latax (c) GTPN latax (d) IPN Latax

of improving the performance of PN law found this convincing enough to try it out. Another reason was that  $V_M$  is not directly available unless the missile carries an inertial navigation unit, but  $V_c$  is easily available from the doppler data of the seeker. Of course, there were some other arguments regarding the invariance of the latax history with respect to the term  $\frac{NV_M}{V_c}$  ( $= N'$ ) which clinched the argument in favour of true proportional navigation, but we will not go into this at the moment. So the TPN law was born with the following form,

$$a_M = N' V_c \dot{\theta} = -N' V_R \dot{\theta} \quad (9.6)$$

where,  $N'$  is called the *effective navigation ratio* to distinguish it from the navigation constant defined earlier, and  $V_c$  is the *closing velocity*. The word ratio is used to convey the fact that  $N'$  can be interpreted as the navigation constant  $N$  multiplied by the ratio  $V_M/V_c$ . But the main difference between the PPN and the TPN was that here the latax was applied *perpendicular to the LOS* and not to the missile velocity as in PPN (see Figure 9.2(b)). The main problem was that of implementation since this direction of the TPN latax is not a natural direction of the lifting force generated by the missile airframe which is ultimately responsible for the latax. But people came up with the idea of using thrusters which could be fired either in the forward or aft direction to impart

an additional longitudinal acceleration or deceleration. This acceleration coupled with the latax generated by the aerodynamic forces produced the desired latax in the desired direction. But this was not a very practical solution since it was a burden to provide for these extra thrusters. The next argument in favour of TPN was that if we want to use missiles for exo-atmospheric interception then we will have to use thrusters to generate a latax, because aerodynamic forces are non-existent at very high altitudes. So it is only a very little extra effort to deflect the force due to these thrusters in the desired direction. this was quite a convincing argument and quite a lot of work was done in the area of TPN mainly because TPN was found to be more analytically tractable than PPN.

Unfortunately, no matter what was done to make TPN perform better, its performance remained below that of PPN. Actually, this particular fact was not initially realized, because the initial analysis on TPN was done on a linearized geometry and because of the linearization much of the actual performance results were not very reliable. Later, when Guelman (1971, 1972, 1976) carried out a nonlinear analysis of PPN and TPN in a series of classic papers in the seventies, it was proved beyond any conceivable doubt that the performance of TPN was far worse than that of PPN.

### 9.3 Generalized TPN (GTPN)

But the TPN enthusiasts did not give up easily. They generalized the TPN law by saying that if we have the freedom of choosing our lateral acceleration direction, then why not make that a part of the guidance law and define the latax direction as being deviated by some angle from the normal to the LOS? This is shown in Figure 9.2(c). The idea was to increase the capturability performance of the guidance law further and (hopefully!) make it comparable to the PPN law. Well, it did improve matters a little bit, but not much. As an idea, it was indeed an excellent one, but when it came to performance evaluation, it did not measure up to the PPN performance. In fact some recent work in this area has shown that a realistic implementation of TPN or GTPN, that takes into account the fact that the closing velocity term is actually a time-varying one and not constant as assumed by earlier researchers, deteriorated the performance even further.

#### 9.4 Ideal Proportional Navigation (IPN)

A further significant development in this direction occurred when another variant of the PN law called the *Ideal Proportional Navigation* was proposed. Here, the commanded latax was applied perpendicular to the *relative velocity between the missile and the target*. It is easy to see that the arguments in favour of this are similar to the arguments in favour of TPN, given above. But, the performance was significantly different. It was found that the capturability of this law was comparable to that of PPN and much better than that of TPN or its many generalizations. Only problem was that this law was as difficult to implement as TPN or any of its generalizations.

#### 9.5 Concluding Remarks

There were quite a few other variations of the PN law which gave varying performance under various conditions. Their importance arises more from an academic point of view rather than from any real utility in the area of missile guidance. But both TPN and PPN are important – TPN, because of the vast literature that it has generated and consequently gave rise to many fundamental results in capturability which have a wider application than just missile guidance, and PPN, because of its natural application to guidance of missiles.

An important fact is that neither PPN nor TPN are the proper model for the actual performance of the PN guidance law. PPN makes the assumption that the angle-of-attack is zero, which is seldom the case. So the actual PN law is something that lies between the PPN and TPN. In fact, an analytical solution of a variant of PPN law in which the latax is applied at an angle (equal to the angle-of-attack) deviated from the normal to the velocity vector of the missile then this will give the correct performance analysis of the PN law. This is still an open and challenging problem of both academic as well as practical interest.

The earliest reference to the many variants of the PN law, but in a linearized setting, can be found in Murtaugh and Criel (1966). This paper also gives a fairly exhaustive analysis, but in a linearized framework.

Guelman's papers (1971, 1972) were perhaps the first significant results on PPN in

a nonlinear setting.

Guelman's (1976) was again the first significant result on TPN in a nonlinear setting. These results were later extended to a realistic framework with time-varying closing velocity. The generalization to TPN (GTPN) was first proposed by Yang et al. (1989). Ideal PN (IPN) was proposed and analysed by Yuan and Chern (1992).

### *References*

1. *M. Guelman*: A qualitative study of proportional navigation. *IEEE Transactions on Aerospace and Electronic Systems, AES-7*, 4 (July 1971), 637-643.
2. *M. Guelman*: Proportional navigation with a maneuvering target. *IEEE Transactions on Aerospace and Electronic Systems, AES-8*, 3 (May 1972), 364-371.
3. *M. Guelman*: The closed-form solution of true proportional navigation. *IEEE Transactions on Aerospace and Electronic Systems, AES-12*, 4 (July 1976), 472-482.
4. *A.S. Murtaugh, and H.E. Criel*: Fundamentals of proportional navigation. *IEEE Spectrum, 3*, 12 (Dec. 1966), 75-85.
5. *C.D. Yang, F.B. Hsiao, and F.B. Yeh*: Generalised guidance law for homing missiles. *IEEE Transactions on Aerospace and Electronic Systems, AES-25*, 2 (Mar. 1989), 197-211.
6. *P.J. Yuan and J.S. Chern*: Ideal proportional navigation. *Journal of Guidance, Control and Dynamics, 15*, 5 (November-December 1992), 1161-1165.

## Chapter 10

# True Proportional Navigation

### Module 9: Lecture 23 Original TPN with Non-Maneuvering Target

Keywords. Proportional navigation, TPN, Capture region, Capture circle, Capture equation

As mentioned in a previous chapter, the basic PN guidance law has many versions of which the the True Proportional Navigation (TPN) guidance law is one. According to its basic principles, the missile lateral command by it is proportional to the LOS angular rate and is applied *normal to the LOS* (and not normal to the missile velocity vector as in PPN).

In the subsequent sections we will deal with various cases of TPN guidance laws and some of its many variants. The literature shows that the TPN trajectory does admit closed-form solutions. However, these closed-form solutions are quite complex and sometimes implicit in nature. But they have the advantage that we can examine any aspect of the trajectory that we wish without carrying out extensive simulations. We will not spend too much time here to obtain closed-form solutions to TPN. Rather, we will focus our attention on the main capturability results, which can be obtained without actually solving the trajectory equations completely.

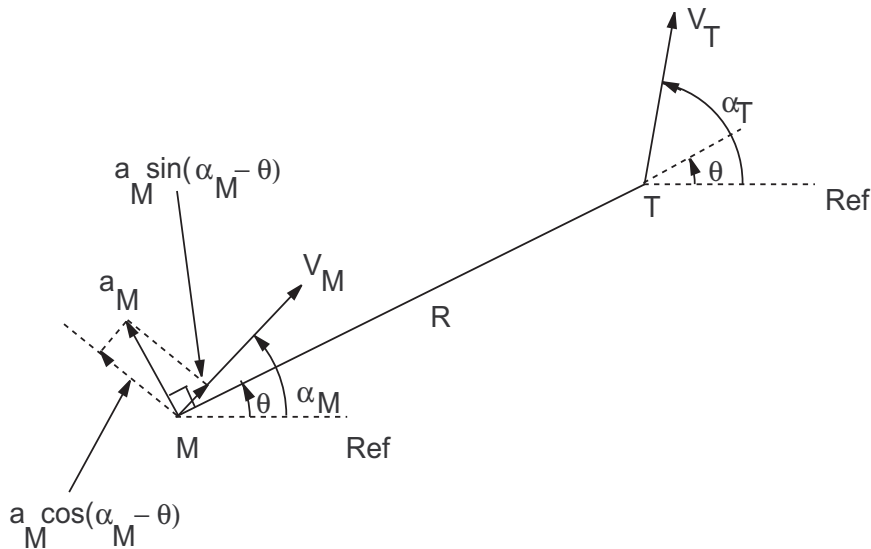


Figure 10.1: Missile-target engagement geometry for TPN

### 10.1 Original TPN with Non-Maneuvering Target

In this section we will consider the TPN law as it was first formulated in the non-linear setting. For our purposes we will call this the *original TPN* law. The missile latax is expressed as,

$$a_M = c\dot{\theta} \quad (10.1)$$

where,  $c > 0$  is a constant. When this law was originally formulated the value of  $c$  was not specified clearly since it was not clear in what way it was related to the other parameters in the system. The idea was to choose a value of  $c$  later that will give the best performance. It could be a function of the missile velocity or of the initial closing velocity or even of the instantaneous closing velocity (in which case it will not be a constant, but a time-varying quantity). We shall explore some of these possibilities later and examine how they affect the performance of the guidance law.

Consider the missile target-engagement geometry given in Figure 10.1. The target is a non-maneuvering one. The equations of motion are,

$$V_R = \dot{R} = V_T \cos(\alpha_T - \theta) - V_M \cos(\alpha_M - \theta) \quad (10.2)$$

$$V_\theta = R\dot{\theta} = V_T \sin(\alpha_T - \theta) - V_M \sin(\alpha_M - \theta) \quad (10.3)$$

$$\dot{V}_M = a_M \sin(\alpha_M - \theta) \quad (10.4)$$

$$\dot{\alpha}_M = \frac{a_M \cos(\alpha_M - \theta)}{V_M} \quad (10.5)$$

Note that unlike in other cases (pursuit and LOS), here the missile velocity is a time-varying quantity. This happens because the missile latax  $a_M$  in this case is not normal to the missile velocity, but is deflected from the normal by a certain angle. Hence, a component of the missile latax is along the missile velocity and changes it with respect to time. This is reflected by (10.4). Also note that in TPN since the closed-form expression for the guidance command ( $a_M$ ) is pre-determined, it can be directly used in the state equations. On the other hand, in the case of LOS and pursuit guidance, the guidance was specified by certain specific requirements (for example, in LOS guidance the guidance command had to be such that the missile had to turn so as to always remain on the LOS, and in pursuit guidance the guidance command had to be such as to keep the missile pointed in a specified direction relative to the current target position). Moreover, in both LOS and pursuit, it was implicitly assumed that the missile latax is normal to the missile velocity.

Now, differentiating (10.2) and (10.3) with respect to time and substituting (10.1), (10.4), and (10.5), we obtain,

$$\begin{aligned} \dot{V}_R &= -V_T \sin(\alpha_T - \theta)(-\dot{\theta}) + V_M \sin(\alpha_M - \theta)(\dot{\alpha}_M - \dot{\theta}) - \dot{V}_M \cos(\alpha_M - \theta) \\ &= \dot{\theta}V_\theta + a_M \sin(\alpha_M - \theta) \cos(\alpha_M - \theta) - a_M \sin(\alpha_M - \theta) \cos(\alpha_M - \theta) \\ &= \dot{\theta}V_\theta \end{aligned} \quad (10.6)$$

$$\begin{aligned} \dot{V}_\theta &= V_T \cos(\alpha_T - \theta)(-\dot{\theta}) - V_M \cos(\alpha_M - \theta)(\dot{\alpha}_M - \dot{\theta}) - \dot{V}_M \sin(\alpha_M - \theta) \\ &= -\dot{\theta}V_R - a_M \cos^2(\alpha_M - \theta) - a_M \sin^2(\alpha_M - \theta) \\ &= -\dot{\theta}V_R - a_M \\ &= -\dot{\theta}(V_R + c) \end{aligned} \quad (10.7)$$

From these two equations we can easily obtain,

$$V_\theta \dot{V}_\theta + V_R \dot{V}_R + c \dot{V}_R = 0 \quad (10.8)$$

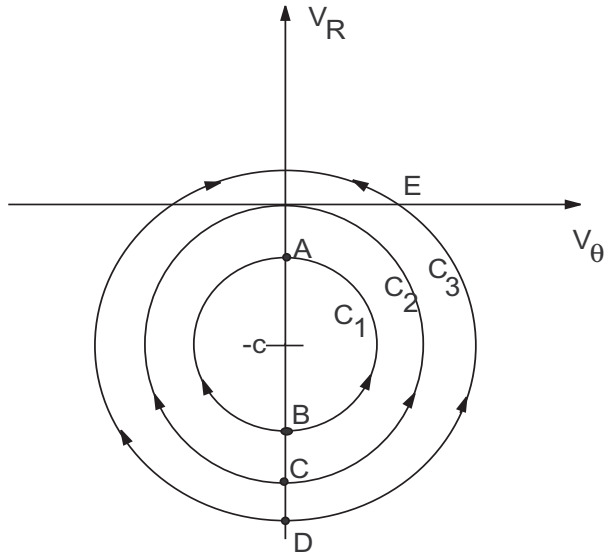


Figure 10.2: Trajectories in the  $(V_\theta, V_R)$  plane

which can be integrated to yield,

$$V_\theta^2 + V_R^2 + 2cV_R = k \quad (10.9)$$

where,

$$k = V_{\theta 0}^2 + V_{R0}^2 + 2cV_{R0} \quad (10.10)$$

So, the above equation can be written as,

$$V_\theta^2 + (V_R + c)^2 = V_{\theta 0}^2 + (V_{R0} + c)^2 \quad (10.11)$$

which is the equation of a circle in the  $(V_\theta, V_R)$ -plane, with center at  $(0, -c)$  and radius equal to  $\sqrt{V_{\theta 0}^2 + (V_{R0} + c)^2}$ . So the point  $(V_\theta, V_R)$  remains on this circle as shown in Figure 10.2. The arrows in the figure show the direction in which the point moves as the engagement proceeds. The direction of these arrows can be easily deduced from (10.6) and (10.7). It is easy to see that the points on the negative  $V_R$ -axis (for example, A, B, C, and D) correspond to the collision geometry and hence they lead to capture. Now, there are three types of circles  $C_1$ ,  $C_2$ , and  $C_3$ . Circles of the type  $C_1$  terminate on the negative  $V_R$ -axis. Circles of type  $C_2$  terminate at the origin. Circles of type  $C_3$  terminate on the positive  $V_R$ -axis. So initial points lying on the  $C_3$  type of circles cannot lead to capture

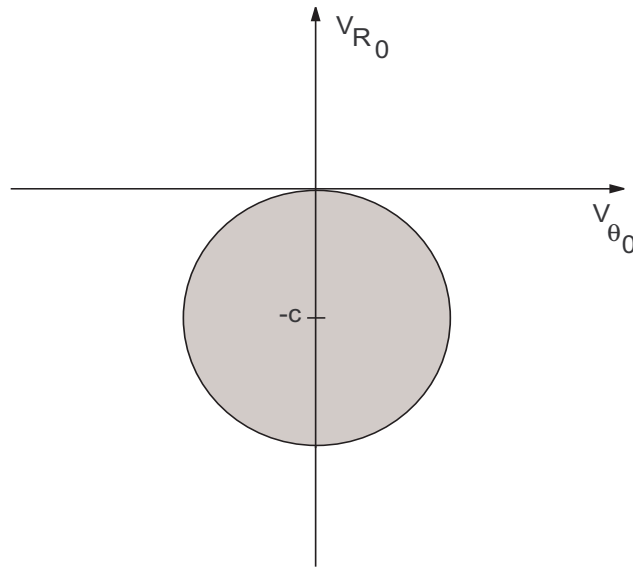


Figure 10.3: Capture region of original TPN

since they end up with  $V_\theta = 0$  and  $V_R > 0$ . This corresponds to a missile which is going away from the target and since  $V_\theta = 0 \Rightarrow \dot{\theta} = 0$ , no lateral is applied by the missile guidance system. The missile therefore continues to go away from the target and no capture is possible. Such trajectories give a non-zero miss-distance which occurs at the point E shown in Figure 10.2, where  $V_R = 0$ .

Points on the  $\mathcal{C}_1$  circle always leads to capture since they end up in the collision geometry. Points on  $\mathcal{C}_2$  are somewhat ambiguous since their capturability depends on the initial range of the missile from the target. In addition, any initial point on the negative  $V_R$ -axis also leads to capture, since it corresponds to the collision geometry right from the beginning. In fact, these points are also *stationary points*. Thus, we have the *capture region* of the original TPN as given in Figure 10.3. Thus the capture region of the original TPN is the interior of a circle of radius  $c$  centered at  $(0, -c)$  (also called the *capture circle*) plus the whole of the negative  $V_R$ -axis. The capture circle is given by  $k < 0$  or,

$$V_{\theta 0}^2 + V_{R0}^2 + 2cV_{R0} < 0 \quad (10.12)$$

This is also called the *capture equation*.

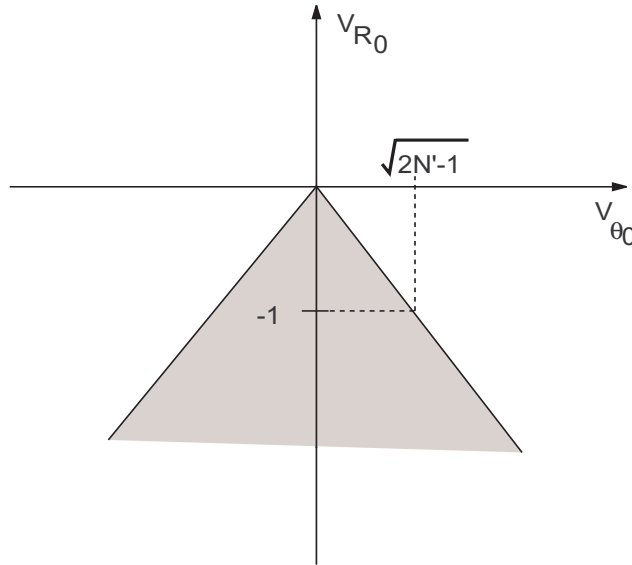


Figure 10.4: Capture region for original TPN using the initial closing velocity for guidance

Note that the parameter  $c$  plays an important role in the determination of the capturability of TPN.

In one of the earlier chapters it was mentioned that the missile latax is considered to be a function of the closing velocity in TPN. We will look at this in detail later. But, for the time being, let us assume that it is a function of the initial closing velocity  $V_{c0} = -V_{R0}$  by letting  $c = -N'V_{R0}$ . The capture equation (10.12) then becomes:

$$|V_{\theta0}|^2 < (2N' - 1)V_{R0}^2 \quad (10.13)$$

This can be written as,

$$|V_{\theta0}| < \sqrt{2N' - 1}|V_{R0}| \quad (10.14)$$

This region is shown in Figure 10.4. Note that the capture region ceases to exist when  $N' < 1/2$ . Of course, the negative  $V_R$ -axis still remains the capture region.

It is possible to integrate (10.9) further as follows: Multiplying  $R$  on both sides of (10.6) and substituting in (10.9) we obtain the following equation:

$$R\dot{V}_R + \dot{R}^2 + 2c\dot{R} = k \quad (10.15)$$

which can be integrated once to yield,

$$R\dot{R} + 2cR = kt + b \quad (10.16)$$

where,  $b = R_0(V_{R0} + 2c)$ . We can obtain the final time of interception from the above equation by setting  $R = 0$  at  $t = t_f$ , and obtain,

$$t_f = -\frac{b}{k} = -\frac{R_0(V_{R0} + 2c)}{V_{\theta 0}^2 + V_{R0}^2 + 2cV_{R0}} \quad (10.17)$$

It is possible to integrate these equations even further and obtain a complete solution to the trajectory equations but these final equations are very complicated and we will not go into the details here.

However, an important result that we can obtain from those equations is the variation of the missile latax with respect to time as the engagement proceeds. It turns out that the capture region can be partitioned into basically six regions (as shown in Figure 10.5(a)) and depending on where the initial condition lies, the corresponding missile LOS rate history is shown in Figure 10.5(b). Note that the LOS rate also represents the qualitative behaviour of the latax since we assume the closing velocity to be positive. It shows that in most cases, except one, the missile latax demand (which is proportional to the LOS rate  $\dot{\theta}$ ) dies down to zero as the missile intercepts the target.

A point that needs to be noted is that unlike the previous guidance laws we do not have any condition on  $V_M$  with respect to  $V_T$ . In other words, so long as the capture conditions are satisfied, the missile can capture the target even if the *initial* missile velocity is less than the target velocity. This may appear to be counter-intuitive but note the stress on the word 'initial'. In TPN the missile velocity changes with time because of the longitudinal acceleration imparted by the latax which is not normal to the missile velocity vector. Due to this, even when the initial  $V_M$  is small, as the engagement proceeds, the missile velocity increases and finally the missile is able to intercept the target.

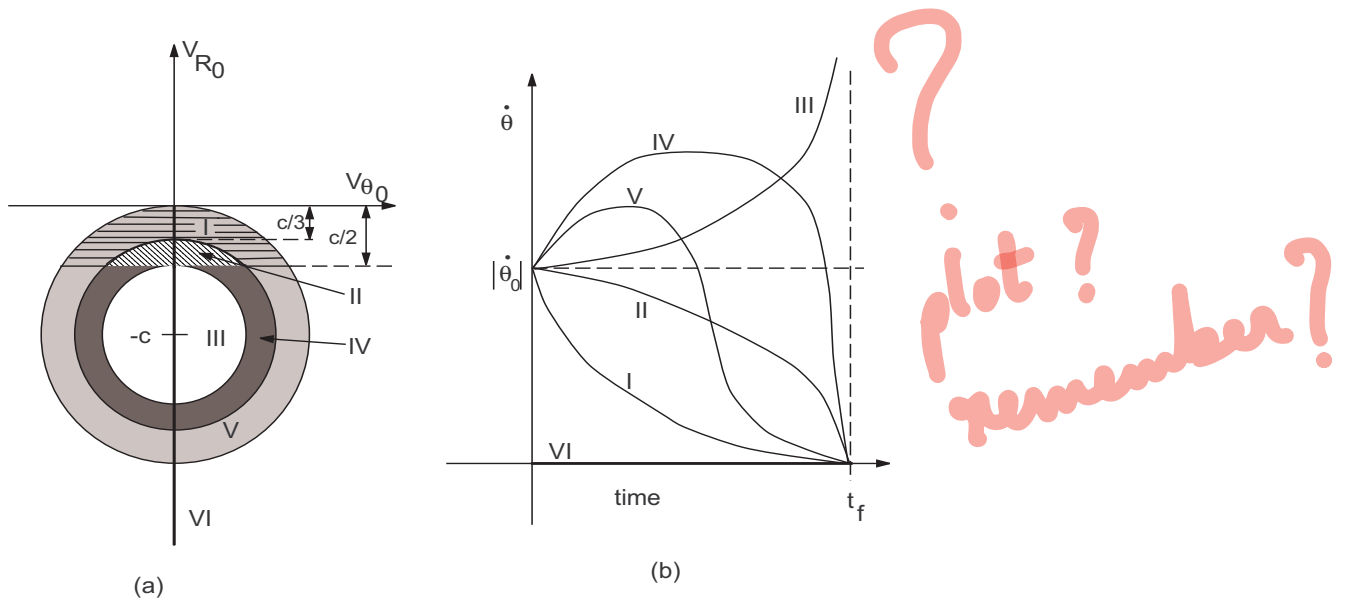


Figure 10.5: (a) Partitioning of the capture region (b) The LOS rate history

## Module 9: Lecture 24

### Realistic True Proportional Navigation

**Keywords.** RTPN, Capture region

#### 10.2 Realistic True Proportional Navigation

In the previous section we defined the TPN law as being a function of the initial closing velocity. But in reality, the closing velocity during the missile-target engagement actually varies with time. In fact, the closing velocity that is measured by the doppler seeker of a homing missile is nothing but the doppler relative velocity between the missile and the target. So, in reality the TPN missile guidance law should be,

$$a_M = -NV_R\dot{\theta} \quad (10.18)$$

which is called the *Realistic True Proportional Navigation (RTPN)* guidance law. Note that we use the navigation constant  $N$  rather than  $N'$  (which was used to define the effective navigation ratio). This is because the navigation constant used here is just a constant and not necessarily derived from the ratio of missile velocity and closing velocity. The symbol  $N'$  was used earlier to emphasize how the navigation constant is interpreted in the context of TPN. We will continue using  $N$  in subsequent chapters too. A performance analysis of this law is expected to give a much better representation of the capturability of the TPN law.

The equation (10.6) remains unchanged while (10.7) has to be obtained by substituting (10.18) rather than (10.1) to give:

$$\dot{V}_R = \dot{\theta}V_\theta \quad (10.19)$$

$$\dot{V}_\theta = -\dot{\theta}(1-N)V_R \quad (10.20)$$

$$\dot{V}_R = \dot{\theta}V_\theta$$

$$\dot{V}_\theta = -\dot{\theta}(V_R + C)$$

From which we can write,

$$\begin{aligned} \dot{\theta} &= \frac{\dot{V}_R}{V_\theta} = -\frac{\dot{V}_\theta}{(1-N)V_R} \\ \Rightarrow V_\theta \dot{V}_\theta + (1-N)V_R \dot{V}_R &= 0 \\ \Rightarrow V_\theta^2 + (1-N)V_R^2 &= k = V_{\theta 0}^2 + (1-N)V_{R0}^2 \end{aligned} \quad (10.21)$$

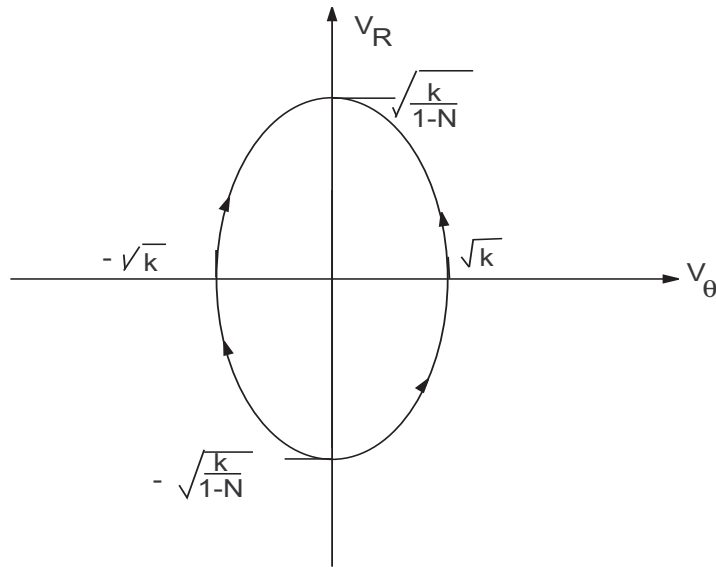


Figure 10.6: Trajectory in the  $(V_\theta, V_R)$ -space when  $0 < N < 1$

To obtain the trajectory in the  $(V_\theta, V_R)$ -space we consider the following cases:

*Case 1:  $0 < N < 1$ .*

Then,

$$k = {V_{\theta 0}}^2 + (1 - N){V_{R0}}^2 > 0 \quad (10.22)$$

When  $V_\theta = 0 \Rightarrow V_R^2(1 - N) = k \Rightarrow V_R^2 = k/(1 - N)$ ,

When  $V_R = 0 \Rightarrow V_\theta^2 = k$ .

This is the equation of an ellipse (shown in Figure 10.6). The trajectory direction is obtained from the fact that  $R\dot{V}_R = V_\theta^2 \Rightarrow \dot{V}_R > 0$  throughout the engagement.

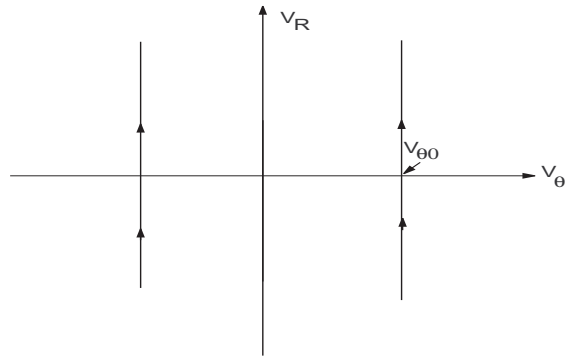
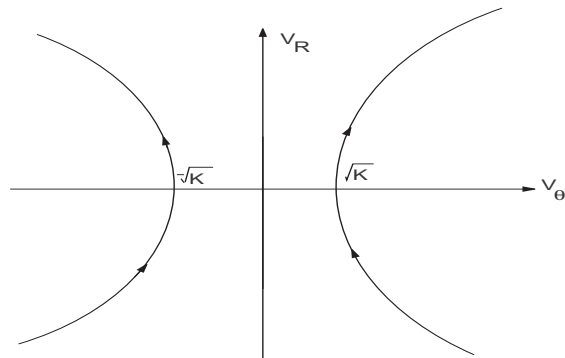
This figure also shows that when  $0 < N < 1$ , capture is not possible from any point on the  $(V_\theta, V_R)$ -space except the negative  $V_R$ -axis.

*Case 2:  $N = 1$ .*

In this case,

$$V_\theta^2 = k = {V_{\theta 0}}^2 \quad (10.23)$$

The corresponding trajectory is shown in Figure 10.7. This again shows that when

Figure 10.7: Trajectory in the  $(V_\theta, V_R)$ -space when  $N = 1$ Figure 10.8: Trajectory in the  $(V_\theta, V_R)$ -space when  $N > 1$  and  $k > 0$ 

$N = 1$ , capture is not possible from anywhere except from initial conditions on the negative  $V_R$ -axis.

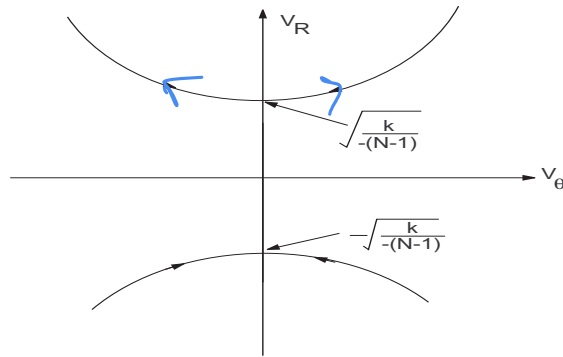
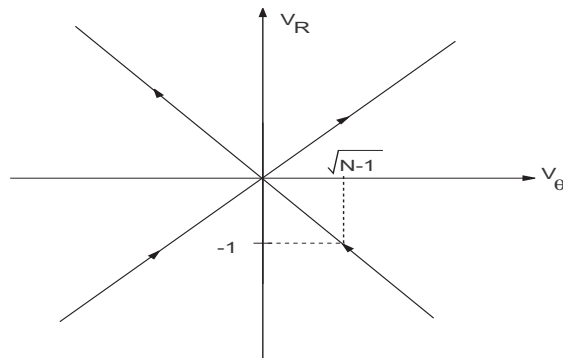
*Case 3:  $N > 1$ .*

In this case,

$$V_\theta^2 - (N-1)V_R^2 = k = V_{\theta 0}^2 - (N-1)V_{R0}^2 \quad (10.24)$$

*Case 3A:* If  $k > 0$ , then  $V_R = 0 \Rightarrow V_\theta^2 = k$ . But there is no value of  $V_R$  for which  $V_\theta = 0$ . Hence the corresponding trajectories are as shown in Figure 10.8. Even in this case, interception is not possible.

*Case 3B:* If  $k < 0$ , then  $V_\theta = 0 \Rightarrow V_R = \pm\sqrt{-k/(N-1)}$ . But there is no value of  $V_\theta$  for which  $V_R = 0$ . Hence the corresponding trajectories are as shown in Figure 10.9. In this case, interception occurs when  $V_{R0} < 0$ .

Figure 10.9: Trajectory in the  $(V_\theta, V_R)$ -space when  $N > 1$  and  $k < 0$ Figure 10.10: Trajectory in the  $(V_\theta, V_R)$ -space when  $N > 1$  and  $k = 0$ 

*Case 3C:* If  $k = 0$ , we have

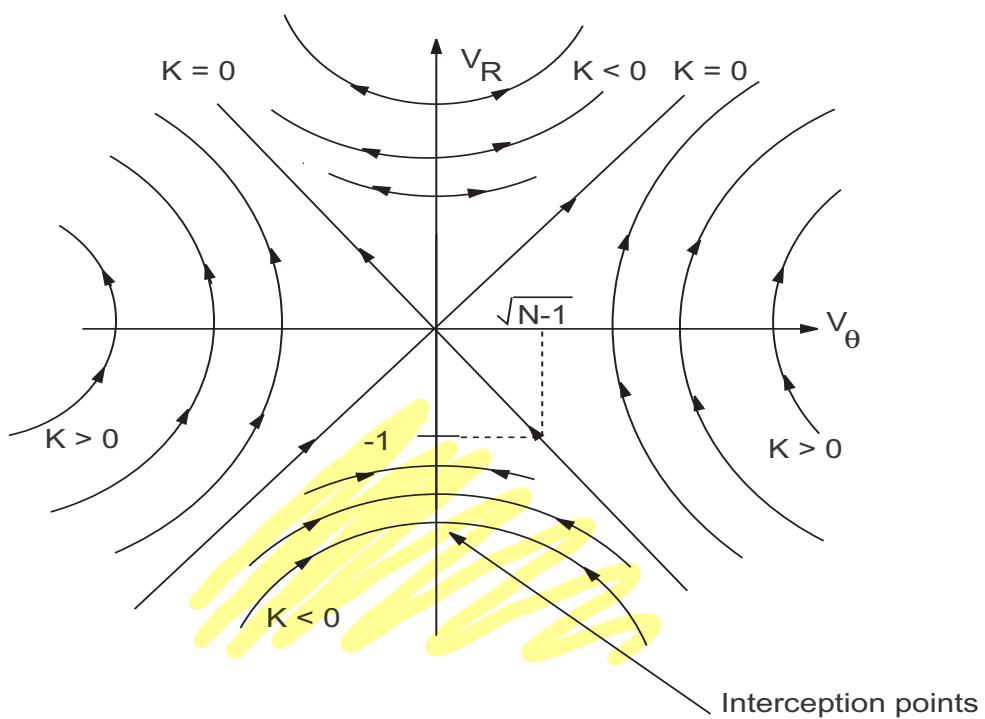
$$V_\theta^2 = (N - 1)V_R^2 \quad (10.25)$$

and the corresponding trajectories are shown in Figure 10.10. Obviously interception does not occur from the positive  $V_R$  region, and nothing can be said about interception from initial conditions in the negative  $V_R$  region.

Putting all the above results together, for the case when  $N > 1$ , we obtain the complete family of trajectories as shown in Figure 10.11.

From the above we can get the capture region for RTPN as shown in Figure 10.12. Hence, the capture region can be expressed through,

$$V_{\theta 0}^2 + (1 - N)V_{R0}^2 < 0, \quad V_{R0} < 0 \quad (10.26)$$

Figure 10.11: Trajectory in the  $(V_\theta, V_R)$ -space when  $N > 1$

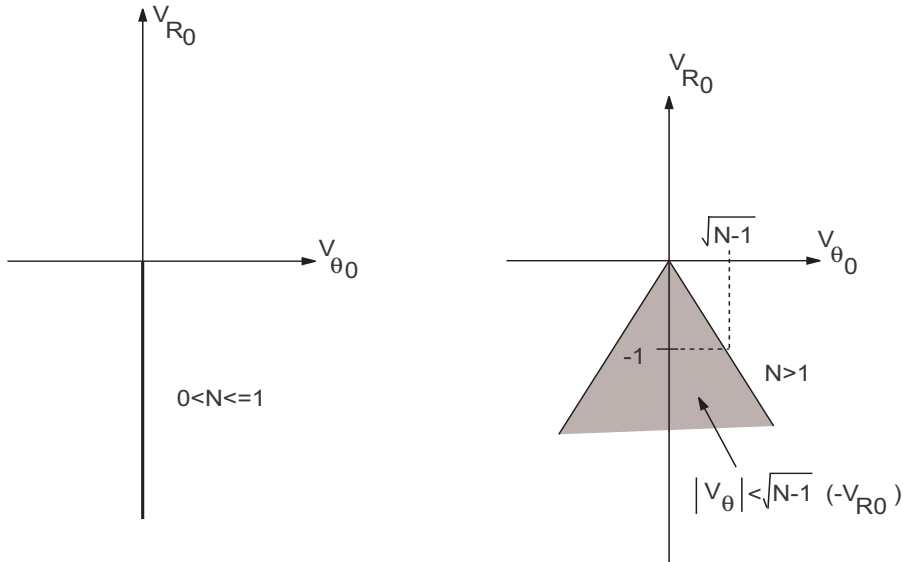


Figure 10.12: Capture region for RTPN

This can be written as,

$$|V_{\theta 0}| < \sqrt{(N-1)(-V_{R0})}, \quad V_{R0} < 0 \quad (10.27)$$

which defines the capture region and is shown in Figure 10.12. Note that the capture region shrinks to the negative  $V_R$ -axis when  $N < 1$ . Also, note that the capture region for RTPN is smaller than the capture region for the original TPN.

As in the original TPN case, RTPN also does not require that the initial missile velocity should be larger than the target velocity.

## Module 9: Lecture 25

### Comparison of TPN Guidance Laws

**Keywords.** TPN, Miss-distance

#### 10.3 Comparison of TPN Guidance Laws

A proper comparison between the capture regions of the different types of the TPN guidance laws require some modifications to the guidance law equation. We do this by using the following expression:

$$a_M = - \left( -\frac{c}{V_{R0}} \right) V_R \dot{\theta} \quad (10.28)$$

That is, we replace  $N$  with  $-c/V_{R0}$  in the RTPN expression of  $a_M = NV_R \dot{\theta}$ . Note that if we put  $V_R = V_{R0}$  in (10.28), we get the original TPN. The block diagram shown in Figure 10.13 clarifies the relationships between the various TPN class of guidance laws. In all these equations we implicitly assume that the engagement starts from the negative  $V_R$  region.

From (10.26), the capture region is defined through,

$$V_{\theta0}^2 < (N - 1)V_{R0}^2 \quad (10.29)$$

with  $N > 1$  and  $V_{R0} < 0$ . Now, replacing  $N = -c/V_{R0}$ , we get

$$V_{\theta0}^2 < \left( -\frac{c}{V_{R0}} - 1 \right) V_{R0}^2 \quad (10.30)$$

$$\Rightarrow V_{\theta0}^2 + V_{R0}^2 + cV_{R0} < 0 \quad (10.31)$$

$$\Rightarrow V_{\theta0}^2 + \left( V_{R0} + \frac{c}{2} \right)^2 < \left( \frac{c}{2} \right)^2 \quad (10.32)$$

which gives a capture region of radius  $c/2$  and centered at  $(0, -c/2)$  in the relative velocity space, as shown in Figure 10.14.

The next figure (Figure 10.15) compares the capture regions of TPN and RTPN.

#### 10.4 Miss-Distance Analysis

TPN lends itself to easy analytical solutions, which is one of the reasons for its popularity. One of the important analytical solutions is the expansion of the capture region

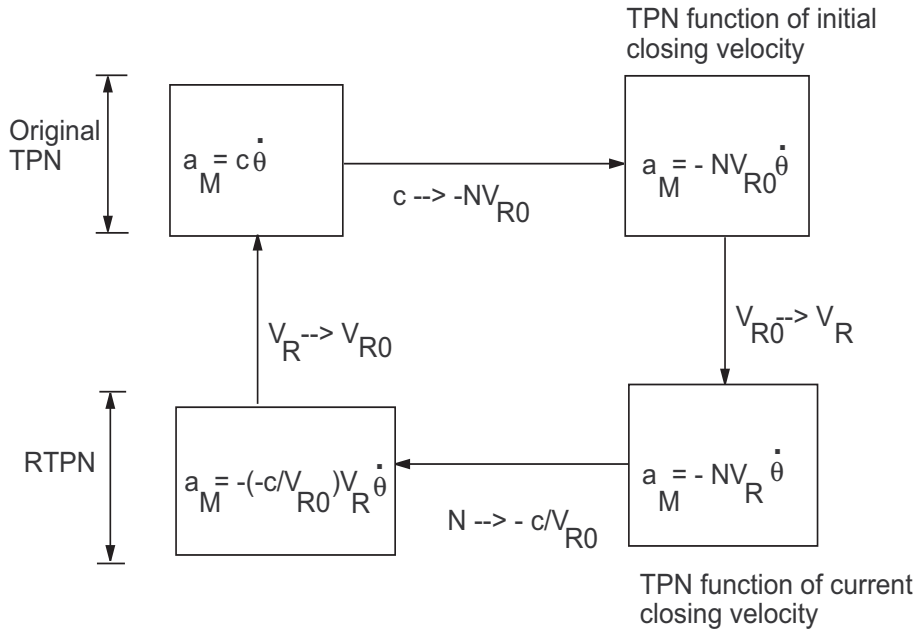


Figure 10.13: Relationship between the TPN class of guidance laws

that occurs due to tolerance in the acceptable miss-distance.

#### 10.4.1 Miss-distance analysis for original TPN

Consider the trajectory equation (10.9) in the relative velocity space as,

$$V_R^2 + V_\theta^2 + 2cV_R = R\ddot{R} + (\dot{R})^2 + 2c\dot{R} = k \quad (10.33)$$

which is obtained by substituting  $V_\theta^2 = R\dot{V}_R = R\ddot{R}$ . We can write,

$$\ddot{R} = \frac{dV_R}{dt} = \frac{dV_R}{dR} \frac{dR}{dt} = V_R \frac{dV_R}{dR} \quad (10.34)$$

Using which, (10.33) can be written as,

$$RV_R \frac{dV_R}{dR} + (V_R)^2 + 2cV_R = k \quad (10.35)$$

Separating the variables we get,

$$\begin{aligned} \frac{V_R}{k - (V_R)^2 - 2cV_R} dV_R &= \frac{dR}{R} \\ \Rightarrow \quad \frac{V_R}{(k + c^2) - (V_R + c)^2} dV_R &= \frac{dR}{R} \end{aligned} \quad (10.36)$$

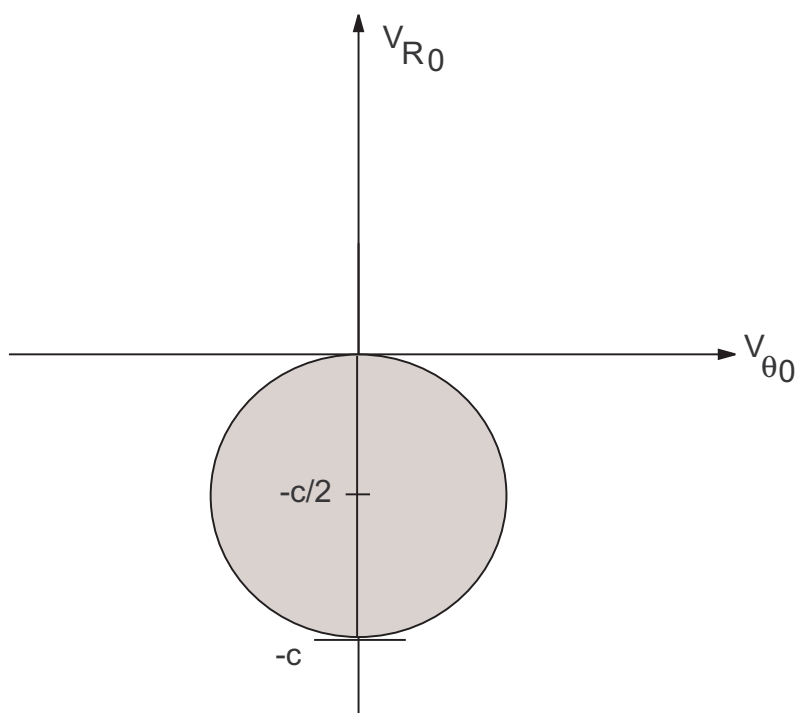


Figure 10.14: Capture region of RTPN with modified navigation constant

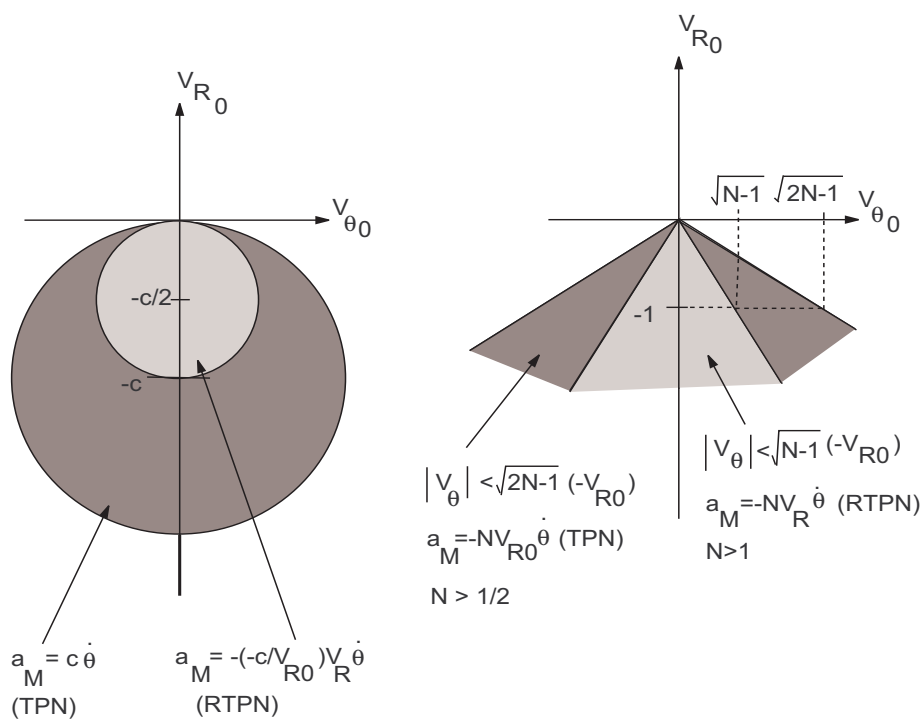


Figure 10.15: Comparison of capture regions of RTPN and TPN

Let

$$\mu^2 = k + c^2, \quad y = V_R + c \quad (10.37)$$

One can interpret  $\mu$  and  $y$  as follows:

$$k = V_R^2 + V_\theta^2 + 2cV_R \quad (10.38)$$

and so,

$$\mu = k + c^2 = V_R^2 + V_\theta^2 + 2cV_R + c^2 = (V_{R0} + c)^2 + V_\theta^2 \quad (10.39)$$

So,  $\mu$  is the radius of the circle on which the  $(V_\theta, V_R)$  point moves in the relative velocity space. Also,  $y$  is the distance of the  $(V_\theta, V_R)$  point, projected on the  $V_R$  axis, from the point  $(0, -c)$ .

Substituting in the above we get,

$$\frac{y - c}{\mu^2 - y^2} dy = \frac{dR}{R} \quad (10.40)$$

This can be integrated to get,

$$\left(\frac{\mu}{c}\right) \ln(\mu^2 - y^2) + \ln\left(\frac{\mu + y}{\mu - y}\right) + \frac{2\mu}{c} \ln R = k_1 \quad (10.41)$$

where,

$$k_1 = \left(\frac{\mu}{c}\right) \ln(\mu^2 - y_0^2) + \ln\left(\frac{\mu + y_0}{\mu - y_0}\right) + \frac{2\mu}{c} \ln R_0 \quad (10.42)$$

and

$$\mu^2 - y^2 = k + c^2 - (V_R + c)^2 = k - V_R^2 - 2cV_R = V_\theta^2 \quad (10.43)$$

Substituting these values we get,

$$\begin{aligned} & \left(\frac{\mu}{c}\right) \ln V_\theta^2 + \ln\left(\frac{\mu + y}{\mu - y}\right) + \frac{2\mu}{c} \ln R = \left(\frac{\mu}{c}\right) \ln V_{\theta0}^2 + \ln\left(\frac{\mu + y_0}{\mu - y_0}\right) + \frac{2\mu}{c} \ln R_0 \\ & \Rightarrow (V_\theta^2)^{\mu/c} \left(\frac{\mu + y}{\mu - y}\right) R^{2\mu/c} = (V_{\theta0}^2)^{\mu/c} \left(\frac{\mu + y_0}{\mu - y_0}\right) R_0^{2\mu/c} \\ & \Rightarrow (V_\theta^2)^{\mu/c} \frac{(\mu + y)^2}{\mu^2 - y^2} R^{2\mu/c} = (V_{\theta0}^2)^{\mu/c} \frac{(\mu + y_0)^2}{\mu^2 - y_0^2} R_0^{2\mu/c} \\ & \Rightarrow (V_\theta^2)^{\mu/c} \frac{(\mu + y)^2}{V_\theta^2} R^{2\mu/c} = (V_{\theta0}^2)^{\mu/c} \frac{(\mu + y_0)^2}{V_{\theta0}^2} R_0^{2\mu/c} \\ & \Rightarrow (V_\theta^2)^{\mu/c-1} (\mu + y)^2 R^{2\mu/c} = (V_{\theta0}^2)^{\mu/c-1} (\mu + y_0)^2 R_0^{2\mu/c} \\ & \Rightarrow (\mu + y)^2 (V_\theta^2)^{\mu/c-1} = (\mu + y_0)^2 (V_{\theta0}^2)^{\mu/c-1} \left(\frac{R_0}{R}\right)^{2\mu/c} \end{aligned} \quad (10.44)$$

This equation holds for all points on the state trajectory. If  $V_{\theta 0} \neq 0$ , then the RHS of the above equation tends to  $\infty$  as  $R \rightarrow 0$ , for all values of  $\mu$  and  $c$ . But the LHS can go to  $\infty$  only if  $\mu < c$  and  $V_\theta \rightarrow 0$  as  $R \rightarrow 0$ . Hence, the capture condition for zero miss-distance with  $V_{\theta 0} \neq 0$  is,

$$\mu < c \Rightarrow \sqrt{k + c^2} < c \Rightarrow k < 0 \Rightarrow V_{R0}^2 + V_{\theta 0}^2 + 2cV_{R0} < 0 \quad (10.45)$$

which we have already derived earlier.

Now, to obtain the capture region for the case when capture is defined even for a non-zero miss-distance  $R_m$ , we need to consider only those points for which  $\mu > c$ .

Now, at  $R = R_m$ , we have  $V_R = 0$  which implies that  $y = c$  since  $y = V_R + c$ . Substituting in (10.44), we get,

$$(\mu + c)^2 (V_\theta^2)^{\mu/c-1} = (\mu + y_0)^2 (V_{\theta 0}^2)^{\mu/c-1} \left( \frac{R_0}{R_m} \right)^{2\mu/c} \quad (10.46)$$

Since  $\mu^2 - y^2 = V_\theta^2$ , at  $R = R_m$  we have  $V_\theta^2 = \mu^2 - c^2$ . Therefore, at  $R = R_m$ ,

$$\begin{aligned} \left( \frac{R_m}{R_0} \right)^{2\mu/c} &= \frac{(\mu + y_0)^2 (V_{\theta 0}^2)^{\mu/c-1}}{(\mu + c)^2 (\mu^2 - c^2)^{\mu/c-1}} \\ &= \frac{(\mu + y_0)^2 (\mu^2 - y_0^2)^{\mu/c-1}}{(\mu + c)^2 (\mu^2 - c^2)^{\mu/c-1}} \end{aligned} \quad (10.47)$$

So,

$$\frac{R_m}{R_0} = \frac{(\mu + y_0)^{c/\mu} (\mu^2 - y_0^2)^{\frac{1}{2} - \frac{c}{2\mu}}}{(\mu + c)^{c/\mu} (\mu^2 - c^2)^{\frac{1}{2} - \frac{c}{2\mu}}} \quad (10.48)$$

Now, using the following relation,

$$(a + b)^n (a^2 - b^2)^{1/2 - n/2} = (a + b)^{(1+n)/2} (a - b)^{(1-n)/2} \quad (10.49)$$

we get

$$\frac{R_m}{R_0} = \left( \frac{\mu + y_0}{\mu + c} \right)^{l_1} \left( \frac{\mu - y_0}{\mu - c} \right)^{l_2} \quad (10.50)$$

where,

$$l_1 = \frac{1}{2} \left( 1 + \frac{c}{\mu} \right) \quad (10.51)$$

$$l_2 = \frac{1}{2} \left( 1 - \frac{c}{\mu} \right) \quad (10.52)$$

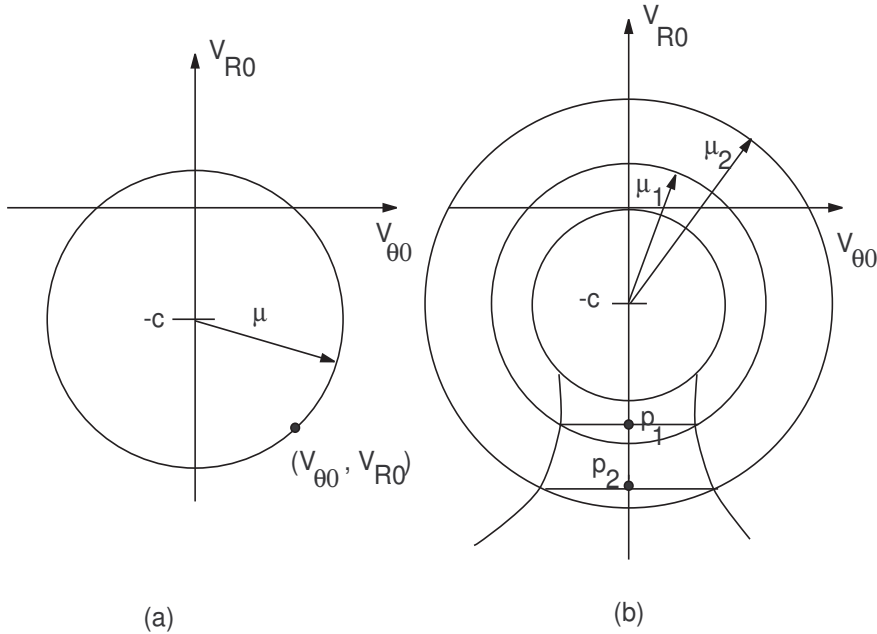


Figure 10.16: Computing the capture region for TPN with non-zero miss-distance

Now,

$$\frac{\mu + y_0}{\mu + c} = 1 + \frac{y_0 - c}{\mu + c} \quad (10.53)$$

$$\frac{\mu - y_0}{\mu - c} = 1 - \frac{y_0 - c}{\mu - c} \quad (10.54)$$

But,  $y - c = V_R$  and  $y_0 - c = V_{R0}$ . So,

$$\frac{R_m}{R_0} = \left(1 + \frac{V_{R0}}{\mu + c}\right)^{l_1} \left(1 - \frac{V_{R0}}{\mu - c}\right)^{l_2} \quad (10.55)$$

$$= \left(1 + \frac{V_{R0}}{\mu + c}\right)^{\frac{1}{2}(1+\frac{c}{\mu})} \left(1 - \frac{V_{R0}}{\mu - c}\right)^{\frac{1}{2}(1-\frac{c}{\mu})} \quad (10.56)$$

This equation can now be used to obtain the capture region for the TPN guidance law with allowable miss-distance. Since we need to look only at those points for which  $\mu > c$ , consider any arbitrary  $\mu$  that satisfies this relation. For a given  $\mu$ , the value of  $\mu$  is actually the radius of the circle drawn with the center at  $(0, -c)$  and radius equal to the distance between  $(0, -c)$  and the initial value  $(V_{\theta 0}, V_{R0})$ . See Figure 10.16(a).

Suppose we assume a value of  $\mu$  so that  $\mu > c$ , and draw this circle. We can then find a value of  $V_{R0} < 0$  such that Equation (10.56) is satisfied for the given  $R_m/R_0$ . Let

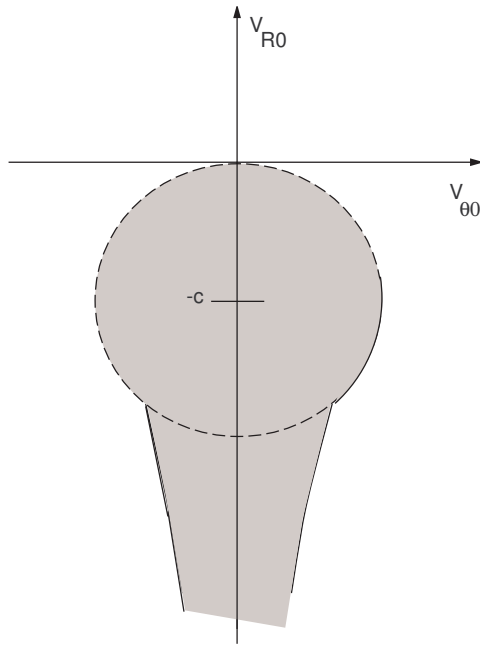


Figure 10.17: Capture region for TPN with non-zero miss-distance

this value of  $V_{R0}$  be equal to  $p$ . In a similar way select  $c < \mu_1 < \mu_2 < \mu_3 < \dots$  in ascending order of magnitudes and compute the corresponding values of  $p_1, p_2, p_3, \dots$ . Joining the intersection of the circles of radius  $\mu_i$  with the horizontal line  $V_{R0} = p_i$  (as shown in Figure 10.16(b)), will produce the capture region for the non-zero miss-distance of  $R_m/R_0$ . In Figure 10.17, we show one such capture region. Note that the lines defining the boundary of the capture region appears to emanate directly from one point on the original circle (which defines the capture region for zero miss-distance). Actually, this is not so. The boundaries emanate from the origin, but the boundary of the non-zero miss-distance capture region and the zero miss-distance capture region are very close together for low values of  $|V_{R0}|$  and they show appreciable separation only for large values of  $|V_{R0}|$ .

## Module 9: Lecture 26

### Miss-Distance Analysis of RTPN

**Keywords.** RTPN, Miss-distance, Capture region

#### 10.4.2 Miss distance analysis for RTPN

Starting with the equation,

$$\begin{aligned} V_\theta^2 - (N-1)V_R^2 &= k = V_{\theta_0}^2 - (N-1)V_{R0}^2 \\ \Rightarrow R\ddot{R} - (N-1)\dot{R}^2 &= k \end{aligned} \quad (10.57)$$

As before

$$\ddot{R} = \dot{V}_R = \frac{dV_R}{dt} = \frac{dV_R}{dR} \frac{dR}{dt} = V_R \frac{dV_R}{dR} \quad (10.58)$$

Substituting the above in (10.57), we get

$$RV_R \frac{dV_R}{dR} - (N-1)V_R^2 = k \quad (10.59)$$

Letting  $\hat{k} = N-1$  and separating the variables, we get

$$\frac{dR}{R} = \frac{V_R}{k + (N-1)V_R^2} dV_R = \frac{V_R}{k + \hat{k}V_R^2} dV_R \quad (10.60)$$

Assuming that  $N \neq 1 \Rightarrow k \neq 0$ , the above equation may be integrated to yield,

$$\ln R + c_1 = \frac{1}{2\hat{k}} \ln(k + \hat{k}V_R^2) \quad (10.61)$$

where,

$$c_1 = \frac{1}{2\hat{k}} \ln(k + \hat{k}V_{R0}^2) - \ln R_0 \quad (10.62)$$

Substituting, we get,

$$\begin{aligned} \ln\left(\frac{R}{R_0}\right) &= \frac{1}{2\hat{k}} \ln\left(\frac{k + \hat{k}V_R^2}{k + \hat{k}V_{R0}^2}\right) \\ \Rightarrow \left(\frac{R}{R_0}\right)^{\frac{2\hat{k}}{k + \hat{k}V_{R0}^2}} &= \frac{k + \hat{k}V_R^2}{k + \hat{k}V_{R0}^2} = \frac{k + \hat{k}V_R^2}{V_{\theta_0}^2} \\ \Rightarrow V_{\theta_0}^2 + \hat{k}(V_R^2 - V_{R0}^2) &= \left(\frac{R}{R_0}\right)^{\frac{2\hat{k}}{k + \hat{k}V_{R0}^2}} V_{\theta_0}^2 \\ \Rightarrow \hat{k}(V_R^2 - V_{R0}^2) &= \left[\left(\frac{R}{R_0}\right)^{\frac{2\hat{k}}{k + \hat{k}V_{R0}^2}} - 1\right] V_{\theta_0}^2 \end{aligned} \quad (10.63)$$

When  $N = 1 \Rightarrow \hat{k} = 0$  (10.60) can be integrated to yield,

$$\ln R + c_2 = \frac{1}{2k} V_R^2 \quad (10.64)$$

with

$$c_2 = \frac{1}{2k} V_{R0}^2 - \ln R_0, \quad k = V_{\theta_0}^2 - (N - 1)V_{R0}^2 = V_{\theta_0}^2 \quad (10.65)$$

Substituting which, we get,

$$\begin{aligned} \ln \left( \frac{R}{R_0} \right) &= \frac{1}{2k} (V_R^2 - V_{R0}^2) \\ \Rightarrow (V_R^2 - V_{R0}^2) &= 2V_{\theta_0}^2 \ln \left( \frac{R}{R_0} \right) \end{aligned} \quad (10.66)$$

Now, putting the above results together in the following two cases:

*Case 1:  $N \neq 1 \Rightarrow \hat{k} \neq 0$ .*

$$\hat{k} (V_R^2 - V_{R0}^2) = \left[ \left( \frac{R}{R_0} \right)^{2\hat{k}} - 1 \right] V_{\theta_0}^2 \quad (10.67)$$

Now, at  $R = R_m$ , we have  $V_R = 0$ . Then,

$$-\hat{k} V_{R0}^2 = \left[ \left( \frac{R_m}{R_0} \right)^{2\hat{k}} - 1 \right] V_{\theta_0}^2 \quad (10.68)$$

$$\Rightarrow \left( \frac{R_m}{R_0} \right)^{2\hat{k}} = 1 - \frac{\hat{k} V_{R0}^2}{V_{\theta_0}^2} \quad (10.69)$$

So, given the initial condition, this equation can be used to compute what the miss-distance would be when the initial condition is in the negative  $V_{R0}$  region. Likewise, given  $R_m/R_0$ , this equation can also be used to define the region for which this miss-distance is achieved as follows:

Since  $R_m/R_0 < 1$ , for  $N > 1$  or  $\hat{k} > 0$ , we have  $(R_m/R_0)^{2\hat{k}} - 1 < 0$ .

Similarly, for  $N < 1$  or  $\hat{k} < 0$ , we have  $(R_m/R_0)^{2\hat{k}} - 1 > 0$ .

Thus, in both cases the boundary of the capture region is given by (10.68) or (10.69).

The capture region itself will be given by,

$$\begin{aligned} |V_{\theta 0}| &< \left[ \frac{\hat{k}}{1 - \left( \frac{R_m}{R_0} \right)^{2\hat{k}}} \right]^{1/2} (-V_{R0}), \quad V_{R0} < 0 \\ \Rightarrow |V_{\theta 0}| &< \frac{\sqrt{N-1}}{\sqrt{1 - \left( \frac{R_m}{R_0} \right)^{2(N-1)}}} (-V_{R0}), \quad V_{R0} < 0 \end{aligned} \quad (10.70)$$

*Case 2:*  $N = 1 \Rightarrow \hat{k} = 0$ .

We have

$$(V_R^2 - V_{R0}^2) = 2V_{\theta 0}^2 \ln \left( \frac{R}{R_0} \right) \quad (10.71)$$

When miss-distance occurs,  $R = R_m$  and  $V_R = 0$ , and so,

$$-V_{R0}^2 = 2V_{\theta 0}^2 \ln \left( \frac{R}{R_0} \right) \quad (10.72)$$

which gives the boundary of the capture region, which itself is given by,

$$|V_{\theta 0}| < \frac{1}{\sqrt{-2 \ln \left( \frac{R_m}{R_0} \right)}} (-V_{R0}), \quad V_{R0} < 0 \quad (10.73)$$

The capture region is shown in Figure 10.18.

To compare with the capture region of the original TPN, substitute

$$N = -\frac{c}{V_{R0}} \quad (10.74)$$

then

$$a_M = - \left( -\frac{c}{V_{R0}} \right) V_R \dot{\theta} \quad (10.75)$$

When  $N \neq 1 \Rightarrow c \neq -V_{R0}$ , we can use (10.69) to obtain,

$$\begin{aligned} \left( \frac{R_m}{R_0} \right)^{2(-c/V_{R0}-1)} &= 1 - \frac{(-c/V_{R0} - 1)V_{R0}^2}{V_{\theta 0}^2} \\ \Rightarrow \left( \frac{R_m}{R_0} \right)^{2(-c/V_{R0}-1)} &= 1 - \frac{(-cV_{R0} - V_{R0}^2)}{V_{\theta 0}^2} \end{aligned} \quad (10.76)$$

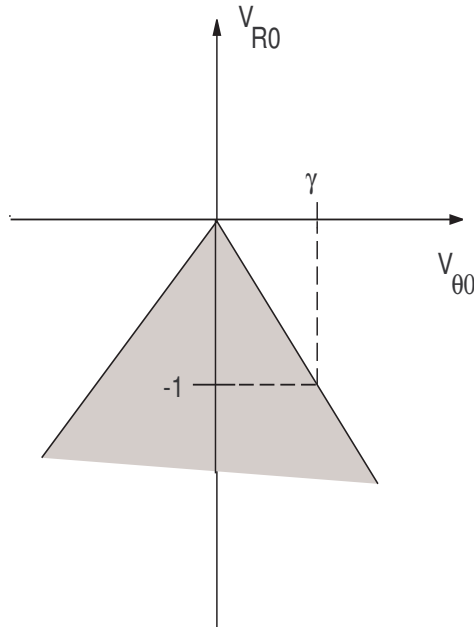


Figure 10.18: The capture region for RTPN with non-zero miss-distance; When  $N \neq 1$ ,  $\gamma = \sqrt{(N-1)/[1 - (R_m/R_0)^{2(N-1)}]}$ ; When  $N = 1$ ,  $\gamma = \sqrt{1/[-2 \ln(R_m/R_0)]}$

Let

$$p = 1 - \left( \frac{R_m}{R_0} \right)^{2(-c/V_{R0}-1)} \quad (10.77)$$

Then we have,

$$pV_{\theta 0}^2 + V_{R0}^2 + cV_{R0} = 0 \quad (10.78)$$

$$\Rightarrow \left( V_{R0} + \frac{c}{2} \right)^2 + pV_{\theta 0}^2 = \left( \frac{c}{2} \right)^2 \quad (10.79)$$

The above equation forms the boundary of the capture region. The capture region itself is given by,

$$\left( V_{R0} + \frac{c}{2} \right)^2 + pV_{\theta 0}^2 < \left( \frac{c}{2} \right)^2 \quad (10.80)$$

for  $V_{R0} \neq -c$ . For  $V_{R0} = -c$ , we have,

$$|V_{\theta 0}| < \frac{c}{\sqrt{-2 \ln(\frac{R_m}{R_0})}} \quad (10.81)$$

The capture region is shown in Figure 10.19.

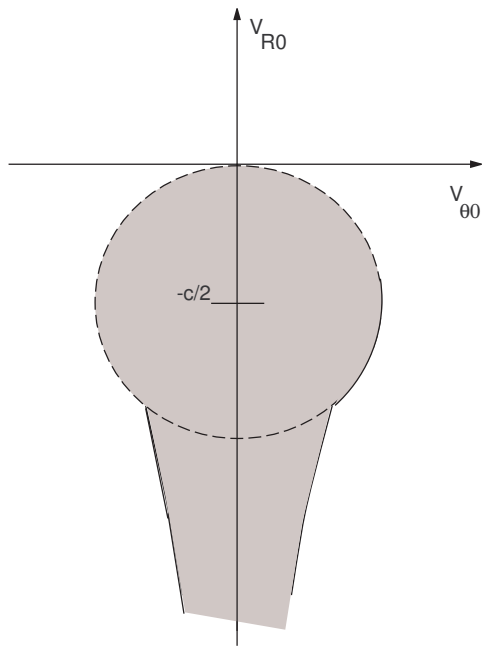


Figure 10.19: The capture region for modified RTPN with non-zero miss-distance

## 10.5 Concluding Remarks

The results discussed here covers many of the important results available in the literature on the analytical evaluation of TPN guidance law in its original form.

A realistic version of TPN is considered in which the time-varying nature of the closing velocity is taken into account. This shows some drastic performance reduction in the capturability of the TPN laws. These are perhaps the most convincing arguments against using TPN as a guidance law.

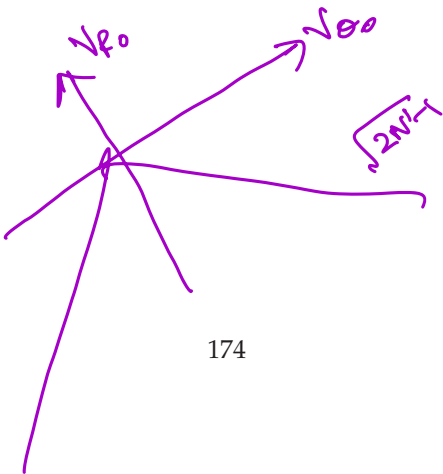
### Assignment

1. **TPN.** Consider an initial geometry as given below. Assume a value of  $V_T$  lying between 0.5 and 0.7 of the value of  $V_M$ .

- (a) The guidance law is given by  $a_M = c\dot{\theta}$  with  $c = -3V_{R0}$ .
  - Find the values of  $\alpha_{M0}$  for which capture is possible.

$$(V_{θ0}) < \sqrt{5} |V_{R0}|$$

$$\begin{aligned}
 0.5 &\leq \angle \theta_0 & \angle \tau_0 &= 60^\circ, \theta_0 = 30^\circ \\
 \angle \rho_0 &= 1 & \angle \rho_0 &= \angle \tau_0 - \angle \theta_0 = 30^\circ \\
 \sqrt{V_{R0}} &= V_T \cos 30^\circ - V_p \cos(\angle \rho_0 - 30^\circ) \\
 \sqrt{V_{θ0}} &= V_T \sin 30^\circ - V_p \sin(\angle \rho_0 - 30^\circ)
 \end{aligned}$$

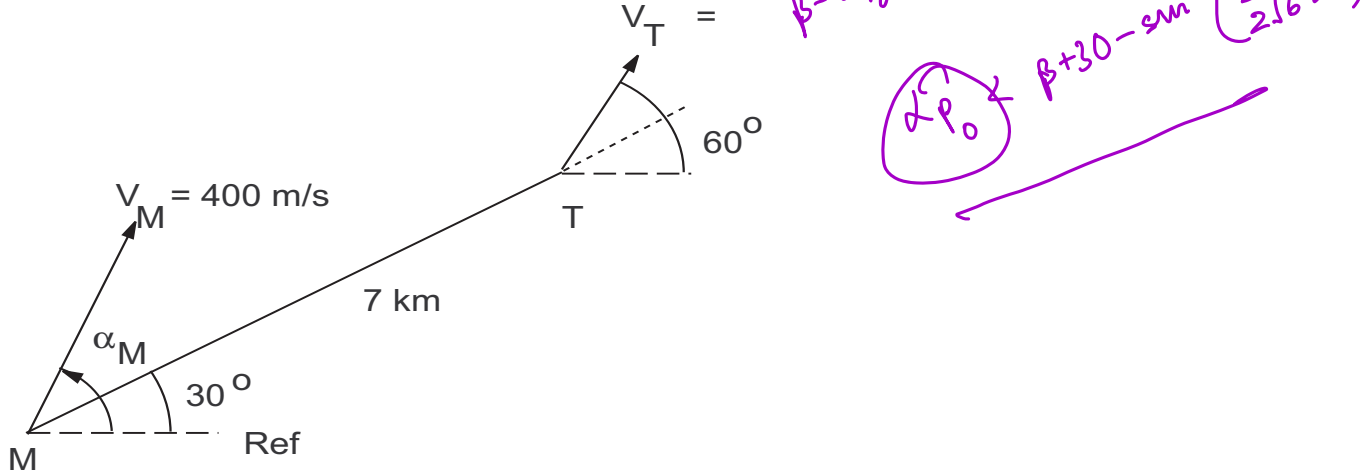


174

$$\begin{aligned}
 & \left| \frac{\sqrt{3}}{2} - v \cos(\alpha_{\theta_0} - 30^\circ) \right| \leq \sqrt{5} \left| \frac{1}{2} - v \sin(\alpha_{\theta_0} - 30^\circ) \right| \\
 & \frac{\sqrt{3} + \sqrt{3}}{2} \leq v \left[ \cos(\alpha_{\theta_0} - 30^\circ) - \sqrt{5} \sin(\alpha_{\theta_0} - 30^\circ) \right] \\
 & \frac{\sqrt{3} + \sqrt{3}}{2} \leq \sqrt{6} v \sin(\beta - \alpha_{\theta_0} + 30^\circ)
 \end{aligned}$$

Guidance of Missiles/NPTEL/2012/D.Ghose

$$\begin{aligned}
 \tan \beta &= \sqrt{5} \\
 \sin \beta &= \frac{\sqrt{5}}{\sqrt{6}}
 \end{aligned}$$



- Plot the corresponding initial conditions in the  $(V_{\theta_0}, V_{R0})$ -space.
  - Compute the interception point for each such point in the capture region and plot  $\alpha_{M0}$  vs.  $t_f$ .
- (b) Simulate the missile target engagement for the above problem and for any two initial values of  $\alpha_{M0}$  (of which one is inside the capture region and the other outside). Plot the following:
- Missile-target trajectories
  - Missile latax against time
  - Trajectory in  $(V_{\theta}, V_R)$ -space
- (c) Same as (b) but assume that the target executes a maneuver with  $a_T = 30 \text{ m/s}^2$  in the clockwise direction.
- (d) Compute and plot the capture region in the  $(V_{\theta_0}, V_{R0})$ -space for the case when capture is defined for a miss-distance less than 20 percent of the initial separation, and  $a_M = c\dot{\theta}$  with  $c = 300$ . Note that only  $V_M$  and  $V_T$  are as given above. All other parameters are free.

## 2. RTPN.

Do exactly the same as before, but with  $a_M = NV_R\dot{\theta}$ , with  $N = 3$ .

For (d) assume  $a_M = -(c/V_{R0})V_R\dot{\theta}$  with  $c = 300$ .

## *References*

1. *M. Guelman*: The closed-form solution of true proportional navigation. *IEEE Transactions on Aerospace and Electronic Systems, AES-12*, 4 (July 1976), 472-482.
2. *P.-J. Yuan and J.-S. Chern*: Solutions of true proportional navigation for maneuvering and non-maneuvering targets, *AIAA Journal of Guidance, Control, and Dynamics*, Vol. 15, No. 1, January-February 1992, pp. 268-271.

## Chapter 11

# Pure Proportional Navigation

### Module 10: Lecture 27 Introduction; Non-maneuvering Target

Keywords. PPN

As mentioned in the previous chapter, the Pure Proportional Navigation (PPN) guidance law generates a guidance command which attempts to make the angular rate of the missile velocity vector equal to the line-of-sight (LOS) angular rate. Moreover, the commanded acceleration is applied in a direction normal to the missile velocity vector. In this chapter we shall analyze the capturability performance of a missile which is guided by the PPN law. Point mass models are assumed for the missile and target. It is also assumed that the angle-of-attack of the missile is negligibly small.

We shall show that the nonlinear kinematic equations obtained for this engagement geometry is too complex to allow a simple closed-form solution, except for very simple cases. Therefore, in this chapter we shall take recourse to what is known as the *qualitative analysis technique* and derive several useful results without actually solving the kinematic equations. Note that the model is nonlinear and therefore the results we obtain are far more realistic than the usual results, based on linearized geometry, that one comes across in the guidance literature.

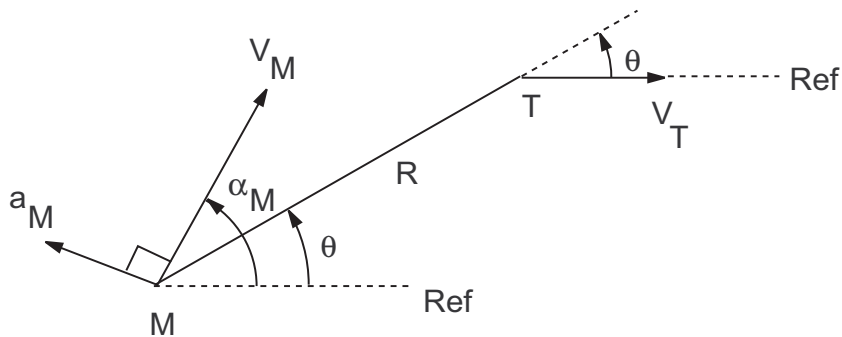


Figure 11.1: Missile-target engagement geometry: Non-maneuvering target

### 11.1 Non-Maneuvering Target

We shall first consider the PPN guidance law being used against a **non-maneuvering target** (that is, one which flies in a straight line with a constant speed). The missile-target engagement geometry is as shown in Figure 11.1.

Note that the reference direction chosen here is not just any arbitrary direction but rather the direction of the target's velocity which, in turn, is a constant since the target is a non-maneuvering one. **Essentially, we are defining a target-centered reference framework where the position of the missile at any instant in time is given with respect to the position of the target.** For example, a given  $(R, \theta)$  will be interpreted as the position of a missile that lies at an angle  $\theta$ , measured anti-clockwise, from the target velocity vector and at a distance  $R$  from the target. Although there is no particular sanctity in choosing this reference framework, it helps in an elegant presentation of the final results. Any other arbitrary reference framework will do equally well so far as the analysis is concerned but may require a little extra algebraic manipulations to present the final results well. Now the equations of motion are given as,

$$V_R = \dot{R} = V_T \cos(-\theta) - V_M \cos(\alpha_M - \theta) \quad (11.1)$$

$$V_\theta = R\dot{\theta} = V_T \sin(-\theta) - V_M \sin(\alpha_M - \theta) \quad (11.2)$$

Here,  $V_R$  and  $V_\theta$  are the relative velocities of the target, along and normal to the, line-of-sight, respectively. Note that the above equations have been written using the conventional LOS angle  $\theta$ .

We may write (11.1) and (11.2) as,

$$V_R = \dot{R} = V_T \cos(\theta) - V_M \cos(\alpha_M - \theta) \quad (11.3)$$

$$V_\theta = R\dot{\theta} = -V_T \sin(\theta) - V_M \sin(\alpha_M - \theta) \quad (11.4)$$

According to the PPN guidance law,

$$\dot{\alpha}_M = N\dot{\theta} \quad (11.5)$$

which, on integration, yields

$$\alpha_M - \alpha_{M0} = N\theta - N\theta_0 \quad (11.6)$$

from which,

$$\alpha_M - \theta = k\theta + \phi_0 \quad (11.7)$$

where,  $k = N - 1$  and  $\phi_0 = -N\theta_0 + \alpha_{M0}$ . Note that  $\phi_0$  is a constant dependent only on the initial conditions. Substituting (11.7) in (11.3) and (11.4), we get the following equations,

$$V_R(\theta) = \dot{R} = V_T \cos(\theta) - V_M \cos(k\theta + \phi_0) \quad (11.8)$$

$$V_\theta(\theta) = R\dot{\theta} = -V_T \sin(\theta) - V_M \sin(k\theta + \phi_0) \quad (11.9)$$

Note that we have used the argument  $\theta$  in the above equations to emphasize the point that after the transformations we have applied, the relative velocity equations can be expressed in terms of a single variable, that is, the LOS angle  $\theta$ . If we now attempt to solve these differential equations, we can write,

$$\frac{\dot{R}}{R\dot{\theta}} = \frac{V_R(\theta)}{V_\theta(\theta)} \quad (11.10)$$

which, in turn, can be written as,

$$\frac{1}{R} \frac{dR}{d\theta} = \frac{V_R(\theta)}{V_\theta(\theta)} \quad (11.11)$$

from which, we get

$$\int \frac{dR}{R} = \int \frac{V_R(\theta)}{V_\theta(\theta)} d\theta \quad (11.12)$$

Partial integration of the above equation yields,

$$R = R_0 \exp \left\{ \int_{\theta_0}^{\theta} \frac{V_R(\theta)}{V_\theta(\theta)} d\theta \right\} \quad (11.13)$$

This equation is completely solvable in the closed-form with little effort for values of  $N = 1$  and partially solvable for  $N = 2$  [Locke(1956)]. It has been recently shown by Becker (1990) that this equation is solvable for all values of  $N$  by using the Mittag-Leffler's theorem in complex analysis. The essential idea is to show that the expression within the integral sign on the RHS is a meromorphic function<sup>1</sup> and hence can be expanded into an uniformly convergent series of rational functions. This operation, in turn, led to an integrable expression. However, the procedure is quite complicated and the ultimate result comes out in the form of a very complex function.

Here, we shall not follow this solution approach but will rather adopt the qualitative analysis technique for differential equations which enables us to obtain many significant results without actually solving the equations of motion. A further advantage of this technique is that it is applicable even in the case of maneuvering targets (as we shall see later), where Becker's approach does not yield any results.

To carry out the qualitative analysis we shall first normalize (11.8) and (11.9) with respect to the target velocity by dividing them by  $V_T$ . This operation yields the following equations,

$$v_R(\theta) = \frac{V_R(\theta)}{V_T} = \frac{\dot{R}}{V_T} = \cos(\theta) - \nu \cos(k\theta + \phi_0) \quad (11.14)$$

$$v_\theta(\theta) = \frac{V_\theta(\theta)}{V_T} = \frac{R\dot{\theta}}{V_T} = -\sin(\theta) - \nu \sin(k\theta + \phi_0) \quad (11.15)$$

where,  $v_R(\theta)$  and  $v_\theta(\theta)$  are the normalized relative velocities; and  $\nu$  is the missile to target velocity ratio, that is,

$$\nu = \frac{V_M}{V_T} \quad (11.16)$$

---

<sup>1</sup>An analytic function whose only singularities in the finite plane are poles is called a *meromorphic function*. For example, rational functions with non-constant denominators like  $\tan z$ ,  $\cot z$ ,  $\sec z$ , and  $\csc z$  are meromorphic functions.

In the following we will state a couple of lemmas which will aid us in carrying out a qualitative analysis of the equations of motion. However, we will not provide any elaborate proof of the lemmas. For the proofs, see Guelman (1971).

*Lemma 11.1.* If  $\nu > 1$  and  $k\nu > 1$ , then the roots of the equations,

$$v_R(\theta) = \frac{V_R(\theta)}{V_T} = \frac{\dot{R}}{V_T} = \cos(\theta) - \nu \cos(k\theta + \phi_0) = 0$$

$$v_\theta(\theta) = \frac{V_\theta(\theta)}{V_T} = \frac{R\dot{\theta}}{v_T} = -\sin(\theta) - \nu \sin(k\theta + \phi_0) = 0$$

alternate along the  $\theta$  axis. □

*Lemma 11.2.* If  $\nu > 1$  and  $k\nu > 1$ ; and  $\theta_\theta$  is a root of the equation  $v_\theta(\theta) = 0$  then,

$$v_R(\theta_\theta) \frac{dv_\theta(\theta_\theta)}{d\theta} > 0 \quad (11.17)$$

□

## Module 10: Lecture 28

### Non-maneuvering Target (Contd...)

**Keywords.** PPN

According to Lemma 11.1, if  $v_R(\theta)$  and  $v_\theta(\theta)$  are plotted against  $\theta$  then these curves intersect the  $\theta$  axis at alternate points. For example, as we plot these quantities from  $\theta = 0$  to  $\theta = 2\pi$  we may find that  $v_\theta$  becomes zero for values of  $\theta$  given by  $\theta_{\theta 1}, \theta_{\theta 2}, \dots, \theta_{\theta i}, \dots$ , and so on. Similarly, we will find that  $v_R$  becomes zero for values of  $\theta$  given by  $\theta_{R1}, \theta_{R2}, \dots, \theta_{Ri}, \dots$ , and so on. Then, according to Lemma 11.1, either

$$\theta_{\theta 1} < \theta_{R1} < \theta_{\theta 2} < \theta_{R2} < \dots < \theta_{\theta i} < \theta_{Ri} < \dots$$

or

$$\theta_{R1} < \theta_{\theta 1} < \theta_{R2} < \theta_{\theta 2} < \dots < \theta_{Ri} < \theta_{\theta i} < \dots \quad (11.18)$$

Note further that the subscripts  $\theta$  and  $R$  are being used to denote whether the roots are that of  $v_\theta$  or of  $v_R$ .

According to Lemma 11.2, if the slope of the  $v_\theta$  curve is negative at one of its roots then the value of  $v_R$  at that point is also negative. Similarly, if the slope of  $v_\theta$  is positive then the value of  $v_R$  is also positive.

Based on Lemmas 11.1 and 11.2, it is easy to determine the shapes of the  $v_R$  and  $v_\theta$  curves and their relative positions in a qualitative sense. This is shown in Figure 11.2. Note that these curves satisfy both the Lemmas. Also note that the curves are bounded above and below by  $\pm(1 + \nu)$ . It is possible to represent the roots of  $v_\theta(\theta)$  and  $v_R(\theta)$  in the polar co-ordinate system as shown in the next figure (Figure 11.3). Using these two figures we will show that the missile will be able to capture the target from almost all initial conditions. Note that a given  $(R, \theta)$  represents the position of the missile with respect to the target in the polar plane (Figure 11.3). Also, this value of  $\theta$  can be used in Figure 11.2 to determine the signs of  $v_R$  and  $v_\theta$  when the missile is at the position given by  $(R, \theta)$ . Now let us consider various initial conditions (with reference to Figures 11.2 and 11.3) for the missile-target engagement.

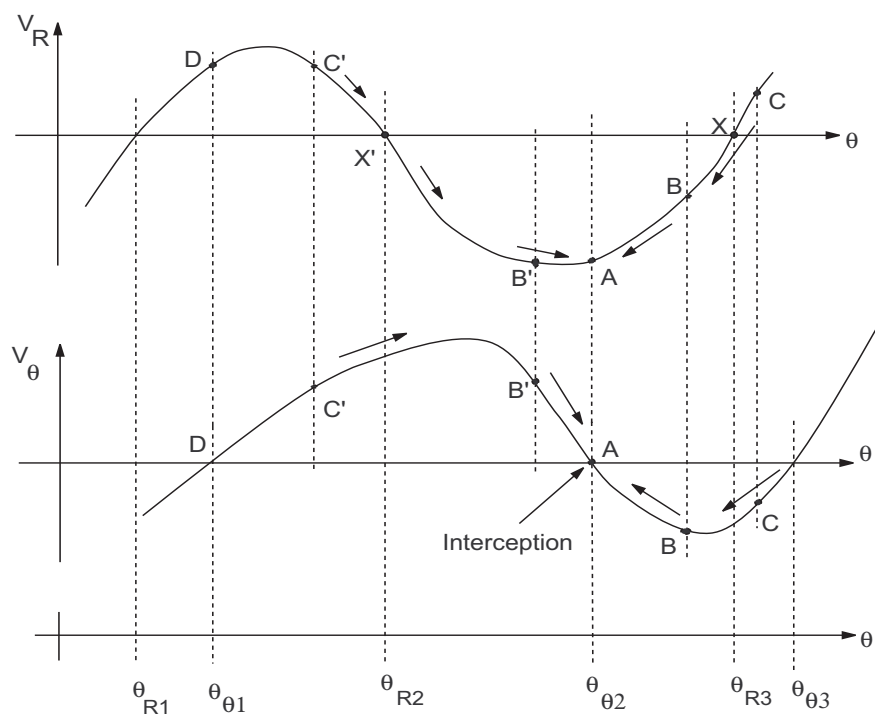
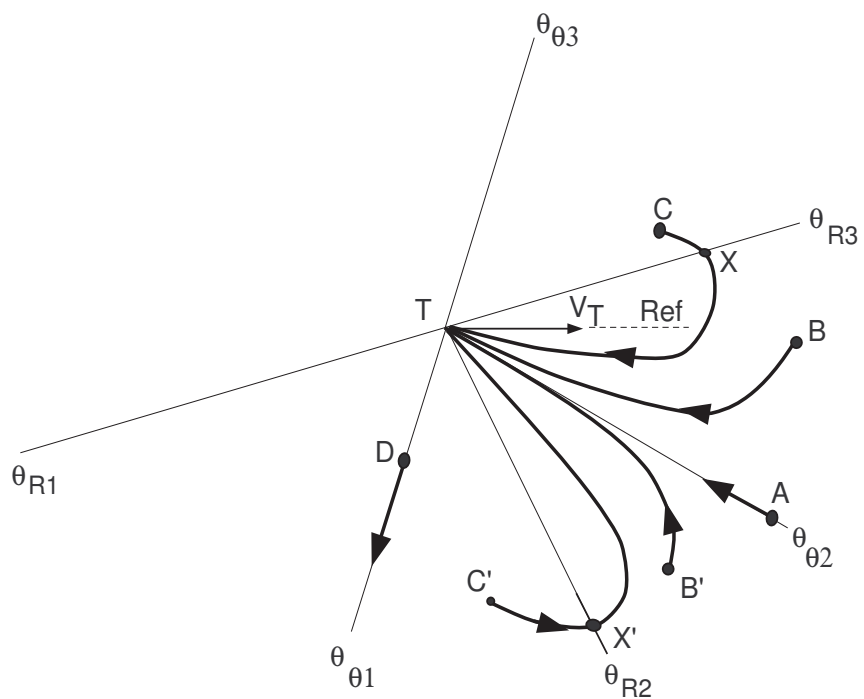


Figure 11.2: A qualitative description of  $v_R(\theta)$  and  $v_\theta(\theta)$

Figure 11.3: A representation of the roots of  $v_\theta(\theta)$  and  $v_R(\theta)$  in the polar plane

**Case 1.** Let the missile be initially at point A shown in Figure 11.3. From 11.2 we immediately see that  $v_{\theta 0} = 0$  and  $v_{R0} < 0$  at this point. But, these are the conditions for a collision course. Thus, right from the beginning the missile is on a collision course with the target. Since the target is a non-maneuvering one, it continues to travel in a straight line; and since  $v_{\theta 0} = 0$ , we have  $\dot{\theta}_0 = 0$ , and so no missile latax is applied. Therefore, the missile also continues to travel in a straight line. Since both the vehicles were initially in a collision course, they continue to be so, and the engagement ends with the missile capturing the target. The relative trajectory in the polar plane is shown in Figure 11.3 in the form of an arrow proceeding from point A towards the target. The corresponding point in Figure 11.2 is A which remains stationary.

**Case 2.** Consider that the missile is at point B in the above figures. From Figure 11.2 we immediately see that  $v_{R0} < 0$  and  $v_{\theta 0} < 0$  at B. This in turn implies that initially  $R$  and  $\theta$  are both decreasing and they continue to decrease. So the point moves in the direction shown. Note however that it is impossible for the point to cross the line denoting  $\theta_{\theta 3}$ . This is so since on the other side of  $\theta_{\theta 3}$ ,  $v_\theta$  is positive and this would force the point back to the side on which B lies. Thus, the missile approaches the target asymptotically along the line  $\theta_{\theta 3}$  from the side on which B lies, and the engagement terminates with the missile capturing the target. In Figure 11.2 the movement of the point is also shown by an arrow. A similar analysis shows that if the missile is initially at B' the missile will again capture the target. But note that the initial values are such that  $\theta$  increases and  $R$  decreases with time.

**Case 3.** Consider that the missile is at point C in the above figures. From (11.2) we immediately see that  $v_{R0} > 0$  and  $v_{\theta 0} < 0$  at C. This in turn implies that initially  $R$  is increasing and  $\theta$  is decreasing. This process continues till the point crosses the  $\theta_{R3}$  line. At the exact point of crossing  $v_R = 0$  and immediately after crossing  $v_R < 0$ . Thus, before crossing the  $\theta_{R3}$  line,  $R$  was increasing with time while it decreases after crossing this line. This implies that the trajectory crosses the  $\theta_{R3}$  line normally (that is, the tangent to the trajectory at the point of crossing is normal to the  $\theta_{R3}$  line). Actually, after crossing the  $\theta_{R3}$  line the point behaves in the same fashion as B in Case 2. Thus, the missile follows a trajectory which approaches the target asymptotically along the  $\theta_{\theta 3}$  line and ultimately captures the target. In Figure 11.2 the movement of the point C is also shown by an arrow. A similar analysis shows that if the missile is initially at C'

the missile will again capture the target. But note that the initial values are such that  $\theta$  increases continuously while  $R$  first increases and then decreases.

*Case 4.* Consider that the missile is at point D in the above figures. From 11.2 we immediately see that  $v_{R0} > 0$  and  $v_{\theta 0} = 0$  at D. This in turn implies that initially  $R$  is increasing while  $\theta$  remains constant. This process continues indefinitely since the missile does not apply any lateral to change its direction of flight. This process is analogous to that mentioned in Case 1, except that here  $R$  increases instead of decreasing. As a result the missile goes farther and farther away from the target and is not able to capture it. Note that even here the corresponding point in Figure 11.2, denoted by D, remains stationary.

From the above discussion it is clear that the missile can capture the target from almost all initial points except a few points at which the initial LOS rate is zero and the missile is initially moving away from the target. This result can be stated more formally as:

**Theorem 11.1.** A missile pursuing a non-manoeuvring target, and following a PPN law with  $\nu > 1$  and  $k\nu > 1$  will be able to capture the target from all initial conditions except those for which  $v_\theta = 0$  and  $v_R > 0$ . □

*Some comments on Figures 11.2 and 11.3*

1. Note that the roots of the  $v_\theta$  and  $v_R$  shown in these two figures are dependent on the initial condition. Thus, for a different initial condition the roots will be different and consequently the curves in Figure 11.2 and the partitioning of the polar plane in Figure 11.3 will also change. To prove the main result (stated in Theorem 11.1) we have shown the missile trajectories starting from each sector in the polar plane in Figure 11.3. In other words, we have addressed the following question in our discussion: *Suppose the initial conditions were such that the missile was initially located in a certain sector in the polar plane, then what kind of trajectory does it follow relative to the target?*. And we have shown that in most cases the missile is able to capture the target no matter where it starts from. However, the point to note here is that when the curves shown in Figure 11.2 and the partitioning of the polar plane in Figure 11.3 is actually carried out for a given initial condition, the same initial

condition will define the initial position of the missile in both figures uniquely, and consequently the trajectory of the missile is also uniquely defined (although in a qualitative sense). In other words, there is only one possible trajectory and it emanates from the given initial condition. Thus, for a given initial condition, the trajectory is restricted to a small region of the polar plane and never enters the other regions.

2. The next point to observe is that given an initial geometry it is always possible to locate the position of the missile in Figure 11.2 and consequently determine the sign of  $\dot{\theta}$ . If we wish to find the final LOS angle (that is the angle at which the missile approaches the target at the point of capture) then all one needs to do is to compute the value of  $\theta$ , nearest to  $\theta_0$  on either side, for which  $v_\theta(\theta) = 0$ . There will be two such values of  $\theta$ , one larger than  $\theta_0$  and the other smaller than  $\theta_0$ . Obviously we choose the larger one if  $V_{\theta 0} > 0$  and the smaller one if  $V_{\theta 0} < 0$ . Once the final LOS angle is known, we can easily determine other terminal quantities like the final closing velocity (which is also the velocity with which the missile hits the target) and the directions of the missile and target velocities relative to the final LOS at the final time. We shall illustrate this in the following example. (look at next example)
3. Note that the analysis proves that the miss-distance is always zero. This is indeed true for the simplified model we have adopted here. Moreover, one of the reasons for high miss-distance in BR and CLOS guidance laws was latax saturation due to the high latax commanded during the terminal phase of the interception. This problem is, to a large extent, taken care of in the PPN guidance law because from Figure (11.3) we see that in the terminal phase the missile approaches the target along a line where  $v_\theta = 0$  and  $v_R < 0$ . In other words, the missile and target trajectories converge to the collision course geometry in the terminal phase. Thus,  $\dot{\theta} \rightarrow 0$  at the terminal phase and so the latax commanded in the terminal phase is small (actually it continues to decrease as the missile approaches the target).
4. The capture region for PPN against a non-maneuvering target covers the whole of the  $(V_\theta, V_R)$ -space except the positive  $V_R$ -axis. This is shown in Figure 11.4.
5. The qualitative analysis approach given here does not help us to obtain the time for interception or the trajectory equations analytically.

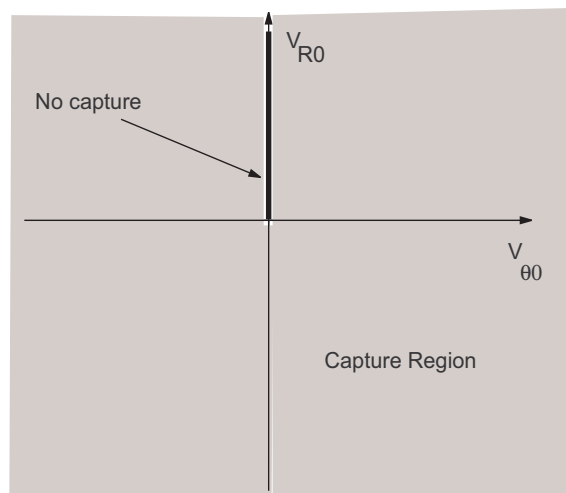


Figure 11.4: Capture region of PPN against non-maneuvering target

## Module 10: Lecture 29 An Illustrative Example

*Solve before going ?*

**Keywords.** PPN, Example

### 11.1.1 An Illustrative Example

Consider the initial missile-target engagement geometry to be as shown in Figure 11.5(a). The reference is chosen as the direction of the target velocity vector and the angles are defined accordingly in keeping with our convention in Figure 11.5(b).

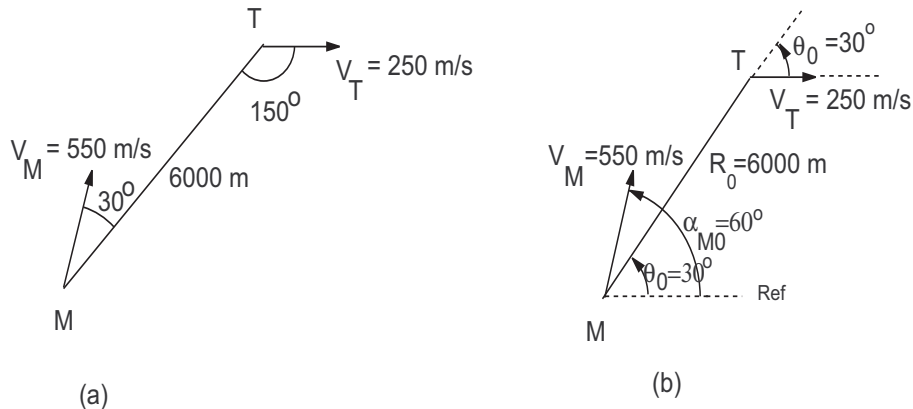


Figure 11.5: (a) Initial geometry (b) Initial geometry in the conventional notation

Note that,

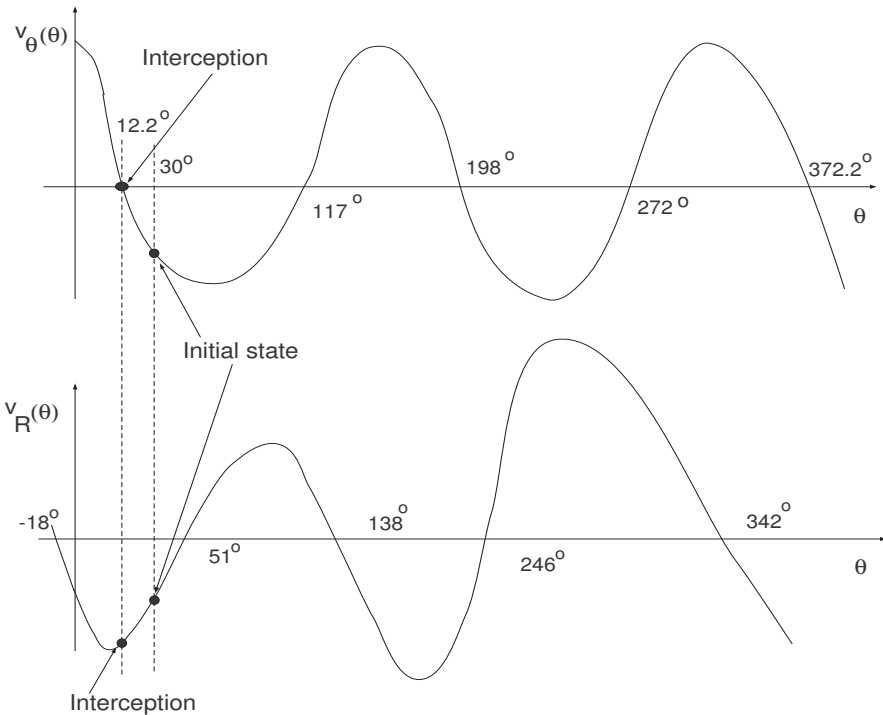
$$\nu = \frac{V_M}{V_T} = \frac{550}{250} = 2.2 > 1$$

$$k\nu = (N - 1)\nu = (3 - 1) \times 2.2 = 4.4 > 1$$

Thus, the conditions on the velocity ratio and the navigation constant are met and we can use the results of Lemmas 11.1 and 11.2 and Theorem 11.1. From the figure we get,

$$\alpha_{M0} = 60^\circ \quad \theta_0 = 30^\circ$$

and therefore,

Figure 11.6:  $v_R(\theta)$  and  $v_\theta(\theta)$  vs.  $\theta$  in the example problem

$$\phi_0 = \alpha_{M0} - N\theta_0 = 60^\circ - 3 \times 30^\circ = -30^\circ$$

Therefore,

$$v_R(\theta) = \cos \theta - 2.2 \cos(2\theta - 30^\circ)$$

$$v_\theta(\theta) = -\sin \theta - 2.2 \sin(2\theta - 30^\circ)$$

The curves  $v_R(\theta)$  and  $v_\theta(\theta)$  as a function of  $\theta$  are shown in Figure 11.6. Note that these two functions satisfy Lemmas 11.1 and 11.2 both. In Figure (11.7) we show the roots of these two functions in the polar plane.

At initial time,

$$v_{R0} = v_R(30^\circ) = -1.039 \quad v_{\theta 0} = v_\theta(30^\circ) = -1.6$$

This point is shown in Figures 11.6 and 11.7. Note that since  $v_{\theta 0} < 0$ ,  $\theta$  goes on decreasing. It continues to decrease till it hits  $\theta_{\theta 3} = 12.2^\circ$ , at which point capture

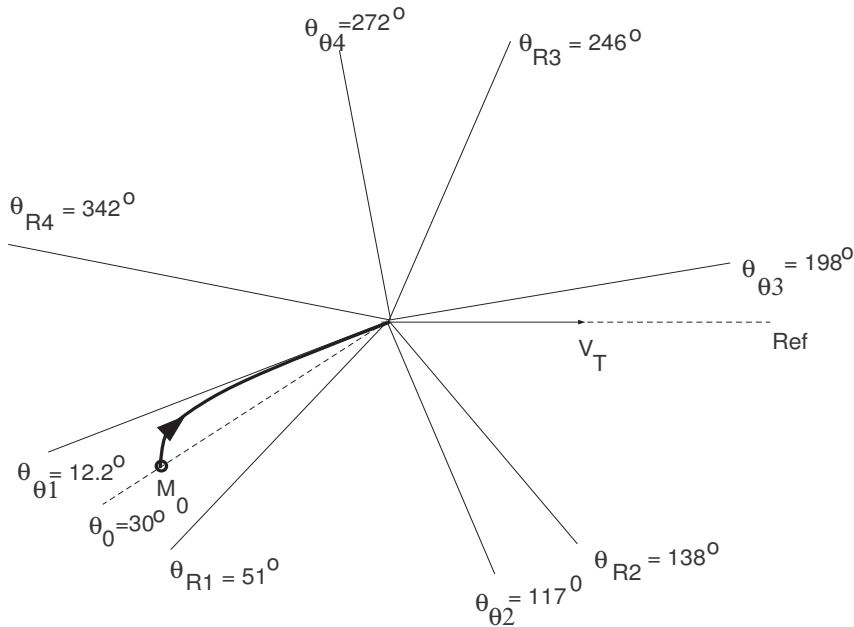


Figure 11.7: Trajectory in the polar plane for the example problem

occurs. Thus, at the point of interception (i.e., final time),

$$v_{Rf} = v_R(12.2^\circ) = -1.212 \quad v_{\theta f} = v_\theta(12.2^\circ) = 0$$

Thus, the final LOS angle  $\theta_f = 12.2^\circ$  and the final closing velocity  $V_{cf} = -v_{Rf} \times V_T = 303$  m/sec. It is also possible to find the direction of the missile velocity at final time. The final geometry is given in Figure (11.8a).

The angle  $\eta$  can be found out from the fact that  $v_{\theta f} = 0$  and  $v_{Rf} < 0$ . Thus, at final time,

$$V_T \sin 12.2^\circ - V_M \sin \eta = 0 \quad \Rightarrow \quad \eta = 5.512^\circ \text{ or } \eta = 174.488^\circ$$

Obviously, the first value is correct since this gives  $v_{Rf} < 0$ , whereas for the second value we get  $v_{Rf} > 0$ .

Based on the above solution in Figure (11.8b) we plot the missile and target trajectories in the plane. Note that these are the actual trajectories of the missile and target whereas in the polar plane (Figure (11.7)) only the missile trajectory relative to the tar-

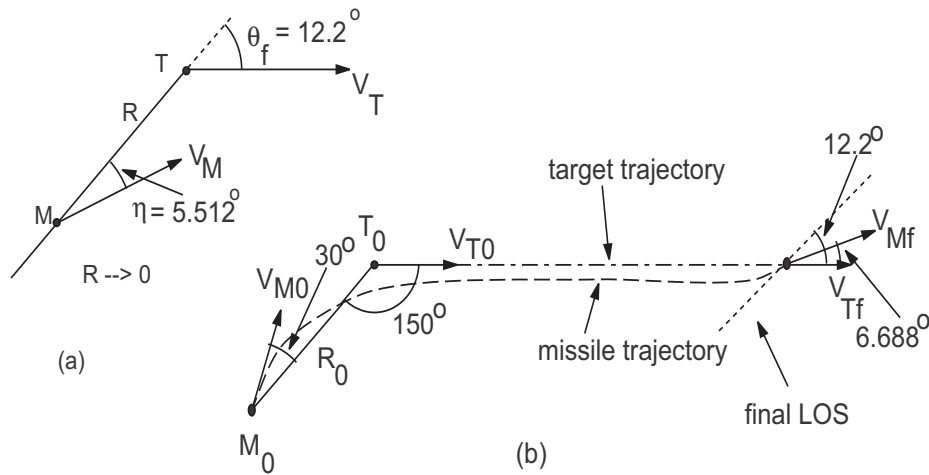


Figure 11.8: (a) The final geometry (b) The initial and final geometry in the plane

get was given.

### 11.1.2 Comments

Although the qualitative analysis given above was slightly more complicated than what we were doing till now, the importance of the exercise lies in its future use. There were a couple of central ideas in the above analysis. One was concerned with the behaviour of the relative velocity components with respect to the LOS angle  $\theta$ , and the other was the behaviour of  $\theta$  itself with respect to time. A qualitative idea of these two behaviours was sufficient for us to get the necessary *capturability* results. In the next section we will see that even though the model becomes more complicated (in order to take into account various realistic behaviour patterns of the target), these two central ideas still play their crucial roles and form the heart of the analysis.

## Module 10: Lecture 30 Maneuvering Target

**Keywords.** PPN, Maneuvering Target

### 11.2 Maneuvering Target

In this section we shall consider a target executing a constant maneuver. That is, it applies a constant latax for all time, thus flying on a circular trajectory. All other assumptions remain the same as in the non-maneuvering target case. The geometry is shown in Figure 11.9. The latax applied by the target is  $a_T$ . Note that here the reference

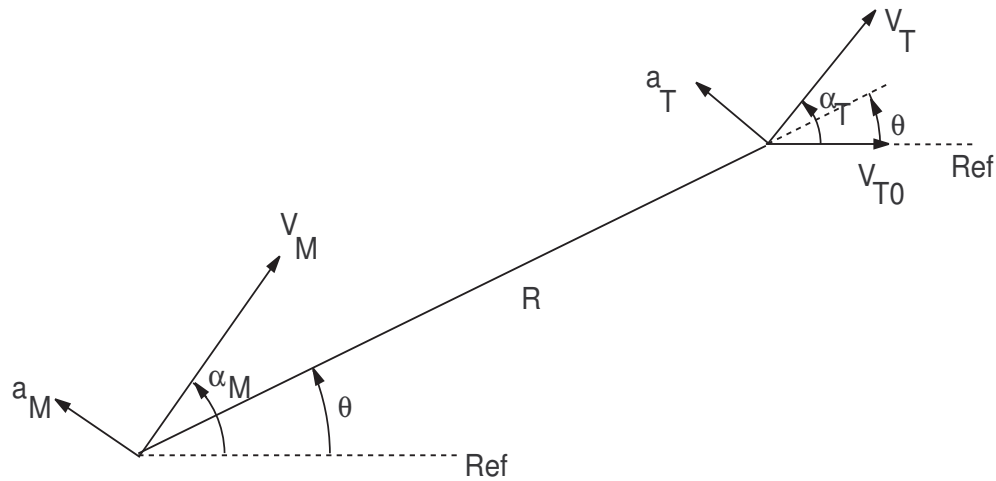


Figure 11.9: Missile-target engagement geometry: Maneuvering target

is taken as the initial direction of flight of the target. Thus, assuming that the initial time at which the engagement begins is  $t_0 = 0$ , the target flight angle  $\alpha_T$  at any instant in time  $t$  is given by,

$$\alpha_T = \left( \frac{a_T}{V_T} \right) t = a_{\nu T} t \quad (11.19)$$

where,  $a_{\nu T} = (a_T/V_T)$  is the normalized latax for the target. It has been normalized with respect to the target velocity. Now we carry out an analysis similar to that in the

non-maneuvering case. The equations of motion are given as,

$$V_R = \dot{R} = V_T \cos(\alpha_T - \theta) - V_M \cos(\alpha_M - \theta) \quad (11.20)$$

$$V_\theta = R\dot{\theta} = V_T \sin(\alpha_T - \theta) - V_M \sin(\alpha_M - \theta) \quad (11.21)$$

Which may be written as,

$$V_R = \dot{R} = V_T \cos(\theta - a_{vT}t) - V_M \cos(\alpha_M - \theta) \quad (11.22)$$

$$V_\theta = R\dot{\theta} = -V_T \sin(\theta - a_{vT}t) - V_M \sin(\alpha_M - \theta) \quad (11.23)$$

A procedure similar to the one in the non-maneuvering case yields an equation identical to (11.7):

$$\alpha_M - \theta = k\theta + \phi_0 \quad (11.24)$$

where,  $k = N - 1$  and  $\phi_0 = -N\theta_0 + \alpha_{M0}$ . Note that  $\phi_0$  is a constant dependent only on the initial conditions. Substituting (11.24) in (11.22) and (11.23), we get the following equations,

$$V_R(\theta, t) = \dot{R} = V_T \cos(\theta - a_{vT}t) - V_M \cos(k\theta + \phi_0) \quad (11.25)$$

$$V_\theta(\theta, t) = R\dot{\theta} = -V_T \sin(\theta - a_{vT}t) - V_M \sin(k\theta + \phi_0) \quad (11.26)$$

Note that here  $V_R$  and  $V_\theta$  are functions of  $\theta$  and  $t$  both. As before, to carry out the qualitative analysis we shall first normalize (11.25) and (11.26) with respect to the target velocity by dividing them by  $V_T$ . This operation yields the following equations,

$$v_R(\theta, t) = \frac{V_R(\theta, t)}{V_T} = \frac{\dot{R}}{V_T} = \cos(\theta - a_{vT}t) - \nu \cos(k\theta + \phi_0) \quad (11.27)$$

$$v_\theta(\theta, t) = \frac{V_\theta(\theta, t)}{V_T} = \frac{R\dot{\theta}}{V_T} = -\sin(\theta - a_{vT}t) - \nu \sin(k\theta + \phi_0) \quad (11.28)$$

where,  $v_R(\theta, t)$  and  $v_\theta(\theta, t)$  are the normalized relative velocities; and  $\nu$  is the missile to target velocity ratio.

In the following we will state a couple of lemmas (similar to Lemmas 11.1 and 11.2) which will aid us in carrying out a qualitative analysis of the equations of motion. However, we will not provide any elaborate proof of the lemmas. For the proofs, see Guelman (1973).

**Lemma 11.3.** For a given  $t$  (say,  $t = t_1$ ), if  $\nu > 1$  and  $k\nu > 1$ , then the roots of the equations,

$$\begin{aligned} v_R(\theta, t_1) &= \cos(\theta - a_{\nu T} t_1) - \nu \cos(k\theta + \phi_0) = 0 \\ v_\theta(\theta, t_1) &= -\sin(\theta - a_{\nu T} t_1) - \nu \sin(k\theta + \phi_0) = 0 \end{aligned}$$

alternate along the  $\theta$  axis. □

Lemma 11.3 has the same connotation as Lemma 11.1. The only difference is that here the value of  $t$  is kept constant when the roots of  $v_R$  and  $v_\theta$  along the  $\theta$  axis are computed. In contrast, In Lemma 11.1,  $t$  did not play any role since the position of the roots did not change with time.

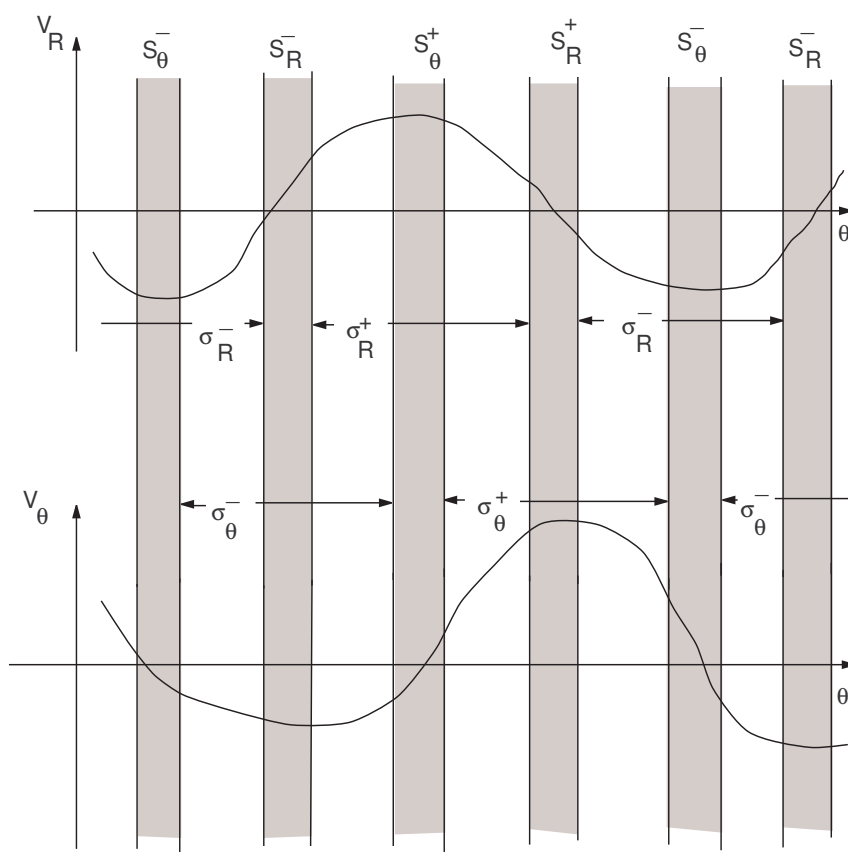
**Lemma 11.4.** For a given  $t$  (say,  $t = t_1$ ), if  $\nu > 1$  and  $k\nu > 1$ ; and  $\theta_\theta$  is a root of the equation  $v_\theta(\theta, t_1) = 0$  then,

$$v_R(\theta_\theta, t_1) \frac{dv_\theta(\theta_\theta, t_1)}{d\theta} > 0 \quad (11.29)$$

□

Lemma 11.4 has the same connotation as Lemma 11.2, but note that the time  $t$  is a constant.

Based on Lemmas 11.3 and 11.4, it is easy to determine the shapes of the  $v_R$  and  $v_\theta$  curves and their relative positions in a qualitative sense, for a constant  $t$ . The curves are similar to those shown in Figure 11.2, but they are drawn for a given constant  $t$ . Another way of understanding these curves is to consider the time axis to be normal to the plane of the paper. If we plot (say)  $v_\theta$  against  $\theta$  and  $t$  we get an undulating surface (or a manifold) over the  $(\theta, t)$  plane. The  $v_\theta$  curve shown in Figure 11.2, is the front view of this undulating surface when it is cut by a plane parallel to the  $(v_\theta, \theta)$  plane. This cutting plane passes through the  $t = t_1$  point on the time axis. This is shown in Figure 11.10. A similar explanation holds for the  $v_R$  curve. From Figure 11.10 and Equations (11.27-11.28), it is evident that as  $t$  changes, the roots of these equations also shift. That is, for a different choice of the cutting plane the points at which the  $v_R$  and  $v_\theta$  curves cross the  $\theta$  axis will be different. Since these roots play a crucial role in the qualitative analysis of the equations of motion, it will be useful to know how these roots behave with change in  $t$ . For this let us consider that  $\theta_\theta$  is a root of  $v_\theta$  for a given  $t$ . Then, we

Figure 11.10: A qualitative description of  $v_R(\theta, t)$  and  $v_\theta(\theta, t)$

can write,

$$-\sin(\theta_0 - a_{\nu T} t) - \nu \sin(k\theta_0 + \phi_0) = 0 \quad (11.30)$$

From which,

$$t = \left( \frac{1}{a_{\nu T}} \right) [\theta_0 - \sin^{-1} \{-\nu \sin(k\theta_0 + \phi_0)\}] \quad (11.31)$$

Let us analyze this equation. Suppose we are given a value of  $\theta_0$  (say,  $\theta_0 = 30^\circ$ ) then this equation enables us to compute the value of  $t$  for which the  $v_\theta$  curve crosses the  $\theta$  axis at  $\theta_0 = 30^\circ$ . For example, suppose we have the following data:

$$k = 2 \quad \nu = 3 \quad \phi_0 = 115^\circ \quad a_{\nu T} = 0.1 \quad \theta_0 = 30^\circ$$

then,  $t$  can be computed to be  $t = 7.88$  seconds. Note that the angles in the above equation should be converted to radians when doing these computations. Thus,  $v_\theta$  becomes zero at  $\theta = 30^\circ$  at 7.88 seconds.

Now, in the same example, let  $\theta_0 = 15^\circ$ . Then,  $\nu \sin(k\theta_0 + \phi_0) = 1.72$  and  $\sin^{-1}(1.72)$  does not exist! Thus, there is no value of  $t$  for which  $v_\theta$  has a root at  $\theta = 15^\circ$ . In other words,  $v_\theta$  never becomes zero at  $\theta = 15^\circ$ .

implies  
there are  
some values  
of  $\theta_0$  where  
 $v_\theta$  can never  
become zero  
given other  
parameters.

## Module 10: Lecture 31 Maneuvering Target (Contd...)

**Keywords.** PPN, Maneuvering Target

The above example tells us that the roots of  $v_\theta$  occur only at certain points or region on the  $\theta$  axis and there are points on the  $\theta$  axis at which they can never occur. It would be natural to ask whether it is possible to identify these regions or not. The answer is yes. From (11.31) it is easily seen that the equation can be evaluated if and only if,

$$|\sin(k\theta_\theta + \phi_0)| \leq \frac{1}{\nu}$$

which can be rewritten as,

$$-\frac{1}{\nu} \leq \sin(k\theta_\theta + \phi_0) \leq \frac{1}{\nu}$$

Note that the following trigonometric relations are true.

$$\begin{aligned} \sin^{-1}(-x) &= -\sin^{-1}(x) \\ -a \leq \sin x \leq a &\Rightarrow -a \leq -\sin x \leq a \Rightarrow -a \leq \sin(n\pi + x) \leq a, \text{ for } n = 0, \pm 1, \pm 2, \dots \end{aligned} \tag{11.32}$$

Using these relations, we can rewrite the above inequality as,

$$-\sin^{-1}\left(\frac{1}{\nu}\right) \leq k\theta_\theta + \phi_0 + n\pi \leq \sin^{-1}\left(\frac{1}{\nu}\right), \quad n = 0, \pm 1, \pm 2, \dots$$

Dividing by  $k$  the above equation can be rewritten as,

$$-\frac{1}{k} \sin^{-1}\left(\frac{1}{\nu}\right) \leq \theta_\theta - \theta_{n0} \leq \frac{1}{k} \sin^{-1}\left(\frac{1}{\nu}\right)$$

where,  $\theta_{n0}$  is a constant, dependent only on the initial condition and the value of  $n$ , and is given by

$$\theta_{n0} = -\frac{\phi_0 + n\pi}{k} \tag{11.33}$$

Now, the inequality, on rearrangement, yields

$$\theta_{n0} - \frac{1}{k} \sin^{-1}\left(\frac{1}{\nu}\right) \leq \theta_\theta \leq \theta_{n0} + \frac{1}{k} \sin^{-1}\left(\frac{1}{\nu}\right) \tag{11.34}$$

For different values of  $n$  this inequality produces different intervals in the  $\theta$  axis inside which the roots of  $v_\theta$  lie. In other words, if we track the migration of a particular root of  $v_\theta$  as  $t$  changes we shall see that the root remains within its appropriate interval. For example, consider the root  $\theta_{\theta 1}$  in Figure 11.2. This is the root of  $v_\theta$  at  $t = 0$  when we consider a maneuvering target. Now if we compute the value of this root for other values of  $t$  we shall see that although the root does change its position, it remains inside the interval given by some  $n$  in the above inequality (11.34).

An exactly similar analysis can be performed for the roots of the  $v_R$  curve as follows:

Let  $\theta_R$  be a root of  $v_R$  for a given  $t$ . Then, we can write,

$$\cos(\theta_R - a_{\nu T} t) - \nu \cos(k\theta_R + \phi_0) = 0 \quad (11.35)$$

From which,

$$t = \left( \frac{1}{a_{\nu T}} \right) [\theta_R - \cos^{-1}\{\nu \cos(k\theta_R + \phi_0)\}] \quad (11.36)$$

From (11.36) it is easily seen that the equation can be evaluated if and only if,

$$|\cos(k\theta_R + \phi_0)| \leq \frac{1}{\nu}$$

which can be rewritten as,

$$-\frac{1}{\nu} \leq \cos(k\theta_R + \phi_0) \leq \frac{1}{\nu}$$

which, in turn, can be written as,

$$-\frac{1}{\nu} \leq \sin\left(\frac{\pi}{2} + k\theta_R + \phi_0\right) \leq \frac{1}{\nu}$$

Using the trigonometric relations given in the previous case, we can rewrite the above inequality as,

$$-\sin^{-1}\left(\frac{1}{\nu}\right) \leq \frac{\pi}{2} + k\theta_R + \phi_0 + m\pi \leq \sin^{-1}\left(\frac{1}{\nu}\right), \quad m = 0, \pm 1, \pm 2, \dots$$

Adding  $\pi/2$  to all the terms and setting  $n = m + 1$ , we obtain

$$\frac{\pi}{2} - \sin^{-1}\left(\frac{1}{\nu}\right) \leq k\theta_R + \phi_0 + n\pi \leq \frac{\pi}{2} + \sin^{-1}\left(\frac{1}{\nu}\right), \quad n = 0, \pm 1, \pm 2, \dots$$

which on dividing by  $k$  and substituting  $\theta_{n0}$  yields,

$$\frac{\pi}{2k} - \frac{1}{k} \sin^{-1}\left(\frac{1}{\nu}\right) \leq \theta_R - \theta_{n0} \leq \frac{\pi}{2k} + \frac{1}{k} \sin^{-1}\left(\frac{1}{\nu}\right)$$

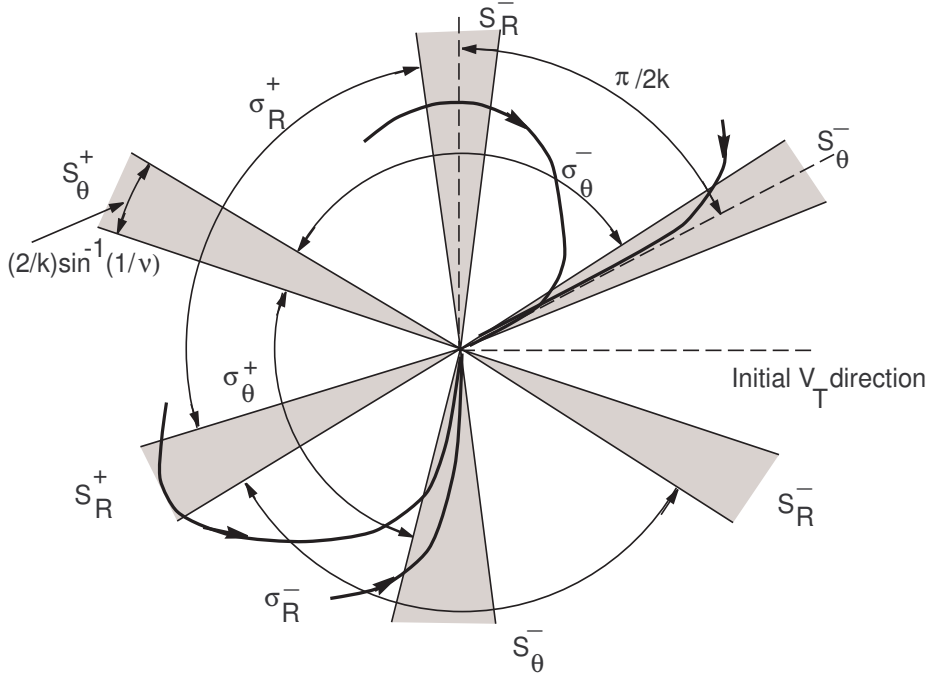


Figure 11.11: A representation of the  $S_\theta$  and  $S_R$  sectors in the target referenced polar plane

Now, the inequality, on rearrangement, yields

$$\theta_{n0} + \frac{\pi}{2k} - \frac{1}{k} \sin^{-1} \left( \frac{1}{\nu} \right) \leq \theta_R \leq \theta_{n0} + \frac{\pi}{2k} + \frac{1}{k} \sin^{-1} \left( \frac{1}{\nu} \right) \quad (11.37)$$

For different values of  $n$  this inequality produces different intervals in the  $\theta$  axis inside which the roots of  $v_R$  lie. One can also see that these intervals have the same span as the intervals in which the roots of  $v_\theta$  occur and are shifted from them by an angle of  $\pi/2k$ . The intervals in which these roots occur are shown in Figure 11.10.

It is possible to represent the roots of  $v_\theta(\theta, .)$  and  $v_R(\theta, .)$  in the polar co-ordinate system as shown in the next figure (Figure 11.11). Note that the intervals here are shown as sectors. Further, these sectors are denoted as  $S_\theta$  and  $S_R$  depending on whether they contain the roots of  $v_\theta$  or of  $v_R$ . From (11.34) and (11.37) the following results are quite obvious:

1. The location of these sectors depend only on the initial conditions and the nav-

igation constant: The  $S_\theta$  sectors are centered around  $\theta_{n0}$  and the  $S_R$  sectors are centered around  $\theta_{n0} + \pi/2k$ , for various integer values of  $n$ .

2. The angular spread of each sector depends only on the velocity ratio and the navigation constant and is given by  $(2/k) \sin^{-1}(1/\nu)$ .
3. The location or the spread of these sectors *do not depend on the target acceleration*.
4. The angular separation between the centerline of two adjacent sectors is given by  $\pi/2k$ .
5. These sectors do not overlap if  $\nu > \sqrt{2}$ .

We will now denote these sectors in both the figures by some special notations:

$$S_\theta^+ = \{\theta : \text{for some real } t, v_\theta(\theta, t) = 0, v_R(\theta, t) > 0\} \quad (11.38)$$

$$S_\theta^- = \{\theta : \text{for some real } t, v_\theta(\theta, t) = 0, v_R(\theta, t) < 0\} \quad (11.39)$$

$$S_R^+ = \{\theta : \text{for some real } t, v_R(\theta, t) = 0, v_\theta(\theta, t) > 0\} \quad (11.40)$$

$$S_R^- = \{\theta : \text{for some real } t, v_R(\theta, t) = 0, v_\theta(\theta, t) < 0\} \quad (11.41)$$

In addition, we can also distinguish four other sectors defined below:

$$\sigma_\theta^+ = \{\theta : v_\theta(\theta, t) > 0, \text{ for all } t\} \quad (11.42)$$

$$\sigma_\theta^- = \{\theta : v_\theta(\theta, t) < 0, \text{ for all } t\} \quad (11.43)$$

$$\sigma_R^+ = \{\theta : v_R(\theta, t) > 0, \text{ for all } t\} \quad (11.44)$$

$$\sigma_R^- = \{\theta : v_R(\theta, t) < 0, \text{ for all } t\} \quad (11.45)$$

Now we have all the necessary elements to perform a qualitative analysis of the missile trajectory during the engagement period.

This qualitative analysis follows the same logic as in the non-maneuvering case discussed in the previous lecture. Using Figures 11.10 and 11.11 we obtain the following result quite easily:

**Theorem 11.2.** A missile pursuing a maneuvering target, and following a PPN law with  $\nu > \sqrt{2}$  and  $k\nu > 1$  will be able to capture the target from all initial conditions lying outside the  $S_\theta^+$  sector. []

It is easy to justify this using arguments similar to those in the non-maneuvering case. The best way to do this is to observe the trajectories given in Figure 11.11. Note that the two central ideas about the behaviour of the relative velocities and of  $\theta$  are used even here to obtain these trajectories.

Further, the  $S_\theta^+$  sector essentially has properties similar to the line  $v_\theta = 0$  and  $v_R > 0$  in the non-maneuvering case. Actually, the sector reduces to a line when the missile does not maneuver. However, unlike in the non-maneuvering case, here it is possible for the missile to capture the target even from inside the  $S_\theta^+$  sector. The basic idea would be to identify those initial conditions for which the missile guidance system generates sufficient latax to take the missile out of the  $S_\theta^+$  sector. The moment the missile is able to leave the  $S_\theta^+$  sector it is now in the domain of the conditions in Theorem 11.2 and this automatically leads to a capture. But, if the initial conditions are such that the missile guidance system cannot generate sufficient latax to enable it to leave the  $S_\theta^+$  sector then the missile continues to be in this sector and goes farther and farther away from the target.

Below, we state the main result without proof.

*Theorem 11.3.* If the initial missile position is inside  $S_\theta^+$  and

1.  $\nu > \sqrt{2}$
2.  $N > 2 + \frac{2V_T}{\sqrt{V_M^2 - V_T^2}} > 1 + \frac{V_T}{V_M}$  (so,  $k\nu > 1$  is automatically satisfied)
3.  $|\dot{\theta}_0| > \frac{|a_T|}{(N-2)\sqrt{V_M^2 - V_T^2 - 2V_T}}$

the missile will leave the  $S_\theta^+$  sector and intercept the target. []

## Module 10: Lecture 32

### Missile Latax

**Keywords.** PPN, Latax

#### 11.2.1 Missile latax

A practical issue in missile guidance is the latax that the missile needs to pull during the engagement. The missile does not have unlimited latax capability and so it is important to have an idea about the maximum latax required by the missile in a typical engagement. The following theorems (stated without proof) give an idea about the latax requirement for PPN guided missiles.

*Theorem 11.4.* If the initial missile position is inside  $S_\theta^-$  and

1.  $\nu > \sqrt{2}$
2.  $N > 2 + \frac{2V_T}{\sqrt{V_M^2 - V_T^2}} > 2 + 2\frac{V_T}{V_M}$  (so,  $k\nu > 1$  is automatically satisfied)

then,

- (a) if  $|a_{M0}| > a_{M1}$ , where

$$a_{M1} = \frac{N}{(N-2)\sqrt{(V_M/V_T)^2 - 1} - 2} \frac{V_M}{V_T} |a_T| \quad (11.46)$$

then  $|a_M|$  will decrease until  $|a_M| \leq a_{M1}$ .

- (b) if  $|a_{M0}| \leq a_{M1}$ , then  $|a_M| \leq a_{M1}$ .

□

For a non-maneuvering target  $a_{M1}$  is zero and so  $a_M$  decreases to zero.

*Theorem 11.5.* If the initial missile position is inside  $S_\theta^-$  and

1.  $\nu > \sqrt{2}$

2.  $N > 1 + \frac{V_M}{V_T}$

then if the entire pursuit is restricted to the rear of the missile (that is,  $-\pi/2 < \alpha_T - \theta < \pi/2$ ) then,

- (a) if  $|a_{M0}| \leq (V_M/V_T)|a_T|$ , then  $|a_M| \leq (V_M/V_T)|a_T|$ .
- (b) if  $|a_{M0}| > (V_M/V_T)|a_T|$ , then  $|a_M|$  will decrease until  $|a_M| \leq (V_M/V_T)|a_T|$ .

[]

A variation on the above result is the following:

*Theorem 11.6.* If the initial missile position is inside  $\sigma_R^- \supseteq S_\theta^-$  and

1.  $\nu > \sqrt{2}$

2.  $N > 4$

then

- (a) if  $|a_{M0}| > a_{Mm}$ , where

$$a_{Mm} = \frac{N}{N-4} \frac{V_M}{V_T} |a_T| \quad (11.47)$$

then  $|a_M|$  will decrease until  $|a_M| \leq a_{Mm}$ .

- (b) if  $|a_{M0}| \leq a_{Mm}$ , then  $|a_M| \leq a_{Mm}|$ .

[]

This theorem when stated for the particular case of a non-maneuvering target is as follows:

*Theorem 11.7.* If the initial missile position is inside  $\sigma_R^-$  (which implies that  $V_{R0} < 0$ ) and

1.  $\nu > \sqrt{2}$

2.  $N > 4$

then  $|a_M|$  is a uniformly decreasing function of time and decreases to zero at interception.  $\square$

Although fairly extensive results were obtained in terms of sufficient conditions for capturability and latax behaviour, results for cases when the  $S_\theta$  and  $S_R$  sectors intersect are not available. Bounds on missile latax outside the  $\sigma_R^-$  sector are also not available.

### 11.2.2 Representation in the LOS referenced frame

In the above, we have obtained the trajectories and the various engagement sectors, in the relative velocity space, based upon a target centered co-ordinate system. Another way, and perhaps a more compact way, of representation of the  $S_R$  and  $S_\theta$  sectors is in the missile centered and LOS referenced co-ordinate system. For this, consider (11.34),

$$\theta_{n0} - \frac{1}{k} \sin^{-1} \left( \frac{1}{\nu} \right) \leq \theta_\theta \leq \theta_{n0} + \frac{1}{k} \sin^{-1} \left( \frac{1}{\nu} \right) \quad (11.48)$$

with

$$\theta_{n0} = -\frac{\phi_0 + n\pi}{k} \quad (11.49)$$

Let the missile flight path angle with respect to the LOS be denoted by  $\alpha$ . Then,

$$\alpha = \alpha_M - \theta = k\theta + \phi_0 \quad (11.50)$$

So,

$$\theta = \frac{\alpha}{k} - \frac{\phi_0}{k} \quad (11.51)$$

For a given root  $\theta_\theta$ , let the corresponding value of the LOS referenced flight path angle be denoted by  $\alpha_\theta$ . So,

$$\theta_\theta = \frac{\alpha_\theta}{k} - \frac{\phi_0}{k} \quad (11.52)$$

Thus,  $\alpha_\theta$  is the LOS referenced flight path angle when  $v_\theta = 0$ . Substituting this in (11.48), we get,

$$-\frac{\phi_0}{k} - \frac{n\pi}{k} - \frac{1}{k} \sin^{-1} \left( \frac{1}{\nu} \right) \leq \frac{\alpha_\theta}{k} - \frac{\phi_0}{k} \leq -\frac{\phi_0}{k} - \frac{n\pi}{k} + \frac{1}{k} \sin^{-1} \left( \frac{1}{\nu} \right) \quad (11.53)$$

From which, we obtain,

$$-n\pi - \sin^{-1} \left( \frac{1}{\nu} \right) \leq \alpha_\theta \leq -n\pi + \sin^{-1} \left( \frac{1}{\nu} \right) \quad (11.54)$$

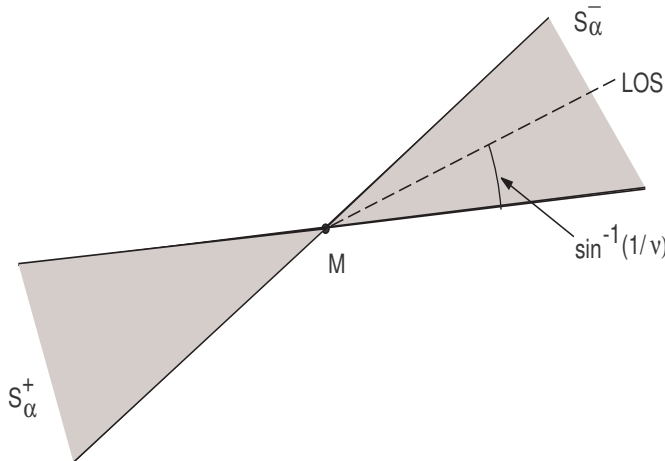


Figure 11.12: A representation of the  $S_\alpha$  sectors in the LOS referenced polar plane

This inequality actually defines the following two sectors when all possible integer values of  $n$  are considered.

$$S_\alpha^- = \{\alpha_\theta : -\sin^{-1}\left(\frac{1}{\nu}\right) \leq \alpha_\theta \leq \sin^{-1}\left(\frac{1}{\nu}\right)\} \quad (11.55)$$

$$S_\alpha^+ = \{\alpha_\theta : -\sin^{-1}\left(\frac{1}{\nu}\right) - \pi \leq \alpha_\theta \leq \sin^{-1}\left(\frac{1}{\nu}\right) = \pi\} \quad (11.56)$$

These sectors are shown in Figure 11.12 in the missile centered coordinate system.

The following observations can be made:

1. The sectors  $S_\alpha$  are independent of initial conditions.
2. The sectors  $S_\alpha$  rotates with the line of sight.
3. If  $V_M$  is within  $S_\alpha^-$  sector then no matter what the orientation of  $V_T$  is, we have  $v_{R0} < 0$ .
4. Since  $S_\alpha^-$  corresponds to the  $S_\theta^-$  sector, by the previous analysis, if  $V_M$  is initially within  $S_\alpha^-$  then it remains within  $S_\alpha^-$  throughout the engagement (this is because the trajectory starting from within the  $S_\theta^-$  sector remains within  $S_\theta^-$  till interception).

The last point is very significant since it implies that the homing head of the missile need not turn by an angle greater than  $\sin^{-1}(1/\nu)$  if initially the missile is within  $S_\alpha^-$ .

## Module 10: Lecture 33

### PPN Capturability in the Relative Velocity Space

**Keywords.** PPN, Capturability, Capture Region

#### 11.2.3 Representation of PPN capturability in the relative velocity space

For this let us use the LOS referenced co-ordinate system as given in the previous section. According to Theorem 11.2, if  $\nu > \sqrt{2}$  and  $k\nu > 1$ , the missile is assured of intercepting the target so long as the initial condition is outside the  $S_\theta^+$  sector. In the LOS referenced co-ordinate system,  $S_\alpha^+$  sector is the equivalent of the  $S_\theta^+$  sector. So, if we identify points in the initial relative velocity space that correspond to the initial conditions being such that the initial velocity vector is outside the  $S_\alpha^+$  sector, then the assured capture region can be identified.

As before, let  $\alpha = \alpha_M - \theta$ . Then, the  $S_\alpha^+$  sector is defined as,

$$-\sin^{-1}\left(\frac{1}{\nu}\right) - \pi \leq \alpha \leq \sin^{-1}\left(\frac{1}{\nu}\right) - \pi \quad (11.57)$$

This is shown in Figure 11.13.

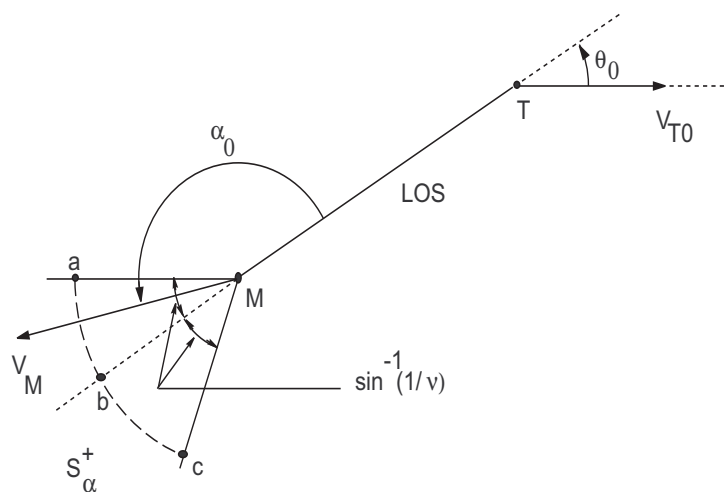


Figure 11.13: The  $S_\alpha^+$  sector and the initial missile velocity vector

For a given  $\theta_0$  we will now identify the values of  $v_{\theta 0}$  and  $v_{R 0}$  that are obtained if the initial  $\alpha_0$  lies in the  $S_\alpha^+$  sector. Excluding these values will give us the assured capture region for PPN against maneuvering targets. Of course, we must also take into account the conditions that  $\nu > \sqrt{2}$  and  $k\nu > 1$ .

The relative velocity equations at  $t = 0$ , obtained from (11.20) and (11.21) normalized with respect to  $V_T$ , are given by,

$$v_{R 0} = \cos(-\theta_0) - \nu \cos \alpha_0 = \cos \theta_0 - \nu \cos \alpha_0 \quad (11.58)$$

$$v_{\theta 0} = \sin(-\theta_0) - \nu \sin \alpha_0 = -\sin \theta_0 - \nu \sin \alpha_0 \quad (11.59)$$

From which,

$$v_{R 0} - \cos(\theta_0) = -\nu \cos \alpha_0 \quad (11.60)$$

$$v_{\theta 0} + \sin(\theta_0) = -\nu \sin \alpha_0 \quad (11.61)$$

Squaring and adding, we get,

$$(v_{R 0} - \cos(\theta_0))^2 + (v_{\theta 0} + \sin(\theta_0))^2 = \nu^2 \quad (11.62)$$

This is the equation of a circle that defines all the possible initial values of  $v_{R 0}$  and  $v_{\theta 0}$ , for a given initial LOS angle  $\theta_0$ , in the initial relative velocity space (normalized with respect to the target velocity). Now, consider the points 'a', 'b', and 'c' in Figure 11.13.

At point 'a',  $\alpha_0 = \pi - \sin^{-1}(1/\nu)$ , and

$$v_{R 0}|_a = \cos \theta_0 + \nu \cos(\sin^{-1}(1/\nu)) \quad (11.63)$$

$$v_{\theta 0}|_a = -(1 + \sin \theta_0) \quad (11.64)$$

At point 'b',  $\alpha_0 = \pi$ , and

$$v_{R 0}|_b = \cos \theta_0 + \nu \quad (11.65)$$

$$v_{\theta 0}|_b = -\sin \theta_0 \quad (11.66)$$

At point 'c',  $\alpha_0 = \pi + \sin^{-1}(1/\nu)$ , and

$$v_{R 0}|_c = \cos \theta_0 + \nu \cos(\sin^{-1}(1/\nu)) \quad (11.67)$$

$$v_{\theta 0}|_c = (1 - \sin \theta_0) \quad (11.68)$$

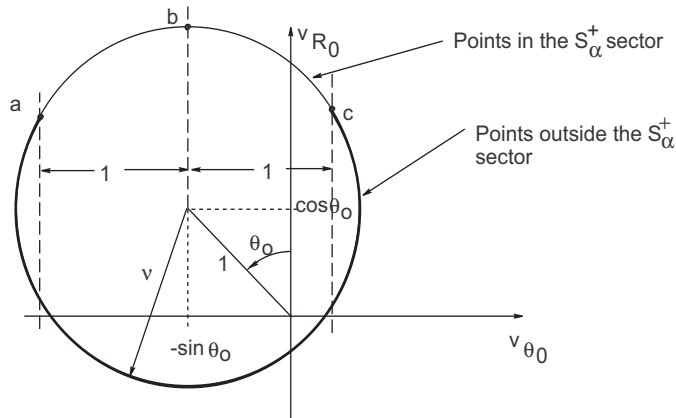


Figure 11.14: The initial points inside and outside of  $S_\alpha^+$  sector mapped onto the initial relative velocity space

Now, look at Figure 11.14. The arc 'abc' represents the initial conditions for which the initial missile velocity vector is in the interior of the  $S_\alpha^+$  sector, and so capture from these points cannot be assured. The other points (shown by the thick line) correspond to initial conditions that correspond to the initial missile velocity vector outside the  $S_\alpha^+$  sector, and hence are candidates for assured capture region. Note that there are two other conditions that need to be met in order to assure capture. These are  $\nu > \sqrt{2}$  and  $(N - 1)\nu > 1$ . Taking these conditions into account, for a given initial LOS angle  $\theta_0$ , the assured capture region for PPN, against a maneuvering target, according to Theorem 11.2, is given as the shaded region in Figure 11.15.

Note that although this capture region is for a maneuvering target, the target latax  $a_T$  itself does not play any role in determining the capture region, and so the assured capture region is independent of the target latax. This immediately leads us to the conclusion that the assured capture region for a non-maneuvering target (with  $a_T = 0$ ) should be the same as shown in Figure 11.15. But, actually we can get a somewhat larger assured capture region for the non-maneuvering target case since the conditions on  $\nu$  and  $k$ , as given in Theorem 11.1 are somewhat less stringent.

The capture region shown in Figure 11.4 for non-maneuvering target is actually incomplete since in that figure, we did not take into account the initial LOS angle and the additional conditions of  $\nu > 1$  and  $k\nu > 1$  as given in Theorem 11.1. If we take

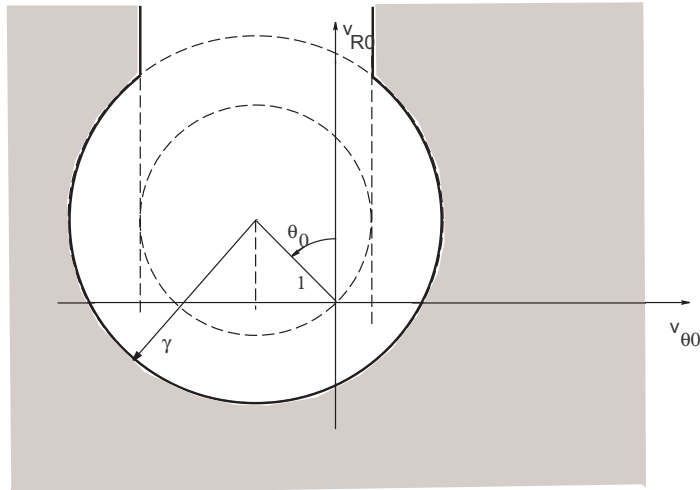


Figure 11.15: The assured capture region for PPN against a maneuvering target in the initial relative velocity space for a given initial LOS angle  $\theta_0$ . When  $N > 1 + 1/\sqrt{2}$ ,  $\gamma = \sqrt{2}$  and when  $1 < N \leq 1 + 1/\sqrt{2}$ ,  $\gamma = 1/(N - 1)$

these into account then for a given initial LOS angle  $\theta_0$ , the assured capture region for PPN, against a non-maneuvering target, according to Theorem 11.1, will be given as the shaded region in Figure 11.16.

### 11.3 Concluding Remarks

In this chapter, the qualitative analysis approach was used to analyze the capturability performance of the PPN law against non-maneuvering and maneuvering targets. In the literature, similar capturability results have been obtained even for arbitrarily maneuvering targets using the qualitative analysis technique.

These results show that, in the absence of closed-form solution for the trajectory equations, the qualitative analysis approach is the ideal choice for obtaining satisfactory solutions to such problems.

However, it should be mentioned that the qualitative analysis approach produces sufficient conditions for capture and not necessary conditions. Hence, it is quite possible that the actual capture region is larger than that obtained from the sufficient condi-

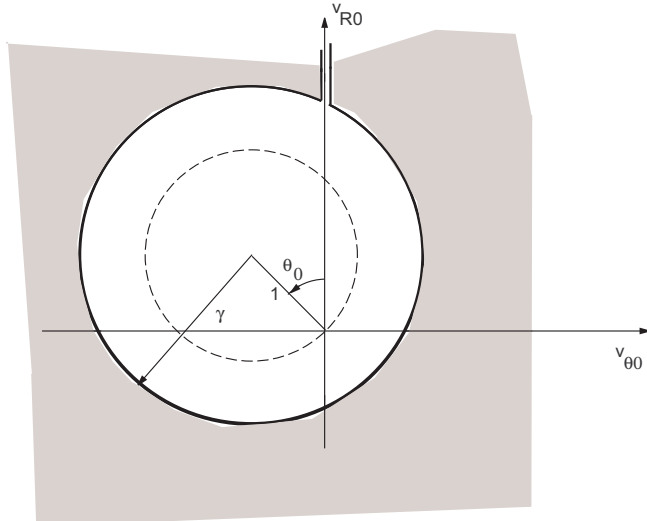


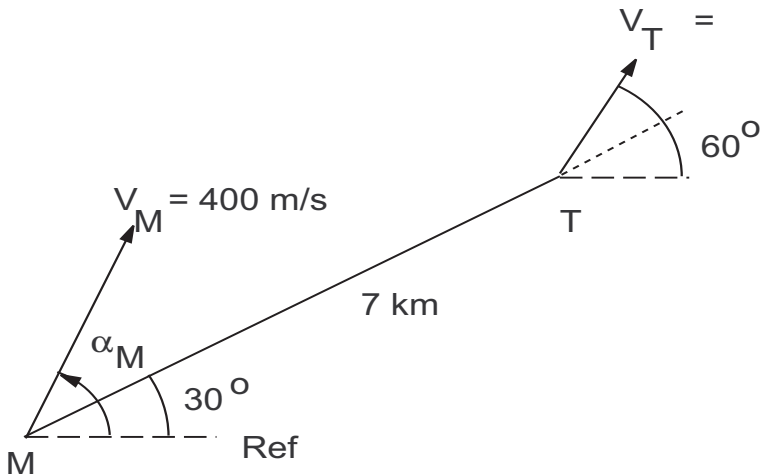
Figure 11.16: The assured capture region for PPN against a non-manoeuvring target in the initial relative velocity space for a given initial LOS angle  $\theta_0$ . When  $N > 2$ ,  $\gamma = 1$  and when  $1 < N \leq 2$ ,  $\gamma = 1/(N - 1)$

tions obtained here.

### Assignment

1. **PPN against non-manoeuvring target.** Consider an initial geometry as given below. Assume that  $V_T$  lies between 0.5 and 0.7 of the value of  $V_M$ . Take the same two values of  $\alpha_{M0}$  that you selected for TPN, in the previous assignment, and answer the following:

- (a) The guidance law is given by  $a_M = NV_M \dot{\theta}$ . Select a value of  $N$  between 3 and 6. Does the missile intercept the target? Find the impact angle at interception.
- (b) Plot  $V_\theta$  vs.  $\theta$  and  $V_R$  vs.  $\theta$  and use them to interpret the results that you get in (a).
- (c) Plot missile target trajectories.
- (d) Draw the missile trajectory with respect to the target in the polar plane and also show the partitioning of the polar plane. Use the results of (b) for this.
- (e) Find the time of interception.



- (f) Plot latax vs. time.
  - (g) Plot trajectories in  $(V_\theta, V_R)$ -space.
2. **PPN against maneuvering target.** Take the same geometry as before. But assume that the target maneuvers with  $a_T = 30 \text{ m/s}^2$  clockwise.
- (a) Same as 2(a) but find the bounds on the impact angle.
  - (b) Same as in 2(b) but remember that when plotting against  $\theta$ , time is also a parameter. So keep time constant at three different values and plot.
  - (c-g) Same as in 2(c-g).
3. Compare the TPN (from the previous assignment) and PPN results. What do you observe?

### References

1. K. Becker: Closed-form solution of pure proportional navigation. *IEEE Transactions on Aerospace and Electronic Systems*, AES-26, 3 (June 1990), 526-533.
2. M. Guelman: A qualitative study of proportional navigation. *IEEE Transactions on Aerospace and Electronic Systems*, AES-7, 4 (Aug. 1971), 637-643.

3. *M. Guelman*: Proportional navigation with a maneuvering target. *IEEE Transactions on Aerospace and Electronic Systems, AES-8*, 3 (June 1972), 364-371.
4. *M. Guelman*: Missile acceleration in proportional navigation. *IEEE Transactions on Aerospace and Electronic Systems, AES-9*, 3 (June 1973), 462-463.
5. *A.S. Locke*: *Guidance*, D. Van Nostrand Co., 1955.

## Chapter 12

# Applications of Guidance

Module 11: Lecture 34  
PN Based Impact Angle Constrained Guidance

**Keywords.** Impact Angle Control, Orientation Guidance

### 12.1 PN Based Impact Angle Constrained Guidance

In many advanced guidance applications (see the list of references at the end of the chapter) it is required to intercept the target from a particular direction, that is, achieve a certain impact angle. In this section we will cover an application of this nature based on the paper by Ratnoo and Ghose (2008).

Lu et al. (2006) have solved the problem of guiding a hypersonic gliding vehicle in the terminal phase to a stationary target using adaptive guidance. In their law, the missile applies maximum lateral acceleration in a sense opposite to the sense of rotation of line of sight and orients itself in a feasible geometry for the PNG to achieve the desired impact angle. In surface-to-surface engagements with high heading errors such an approach is not feasible as applying maximum lateral acceleration in the initial phase of the missile flight will cause immense induced drag. Secondly, due to rotation of the missile velocity vector in a sense opposite to the rotation of line-of-sight will drive the missile away from the collision course and also increase the time of flight.

In this section, a proportional navigation based guidance law is proposed for capturing all possible impact angles in a surface to surface planar engagement against a stationary target. The achievable set of impact angles is derived for pure proportional navigation guidance law with  $N \geq 2$ . To achieve the remaining impact angles an orientation guidance scheme is proposed for the initial phase of the missile trajectory. The orientation guidance law is also proportional navigation with the navigation constant being  $N < 2$  and is a function of the initial engagement geometry and the desired impact angle. After following the orientation trajectory, the missile can switch over to a navigation constant  $N \geq 2$  to achieve the desired impact angle. It is to be noted that varying the value of the navigation constant the proportional navigation guidance law gives a set of impact angles against stationary targets. However, studies on classical proportional navigation guidance (See Shneydor(1998)) reveal that, for  $N < 2$ , the missile lateral acceleration shoots to infinity as the missile-target range goes to zero. But by using  $N \geq 2$  near interception in the proposed guidance law, we avoid the lateral acceleration command to shoot up to infinity and still achieve the desired impact angle.

## 12.2 Impact Angles Against a Stationary Target with PN

Consider the planar engagement scenario as shown in Fig. 12.1 (a). The target is stationary and the guidance objective is to intercept the target along a desired impact angle denoted as  $\alpha_{mf}$ . Here  $\alpha_m$  and  $\theta$  are the missile heading and the line of sight angle, respectively.

Proportional navigation guidance law is defined as,

$$\dot{\alpha}_m = N\dot{\theta} \quad (12.1)$$

Integrating (12.1), and knowing that for successful interception of a stationary target the final missile heading should be toward the target, i.e.,  $\alpha_{mf} = \theta_f$ , we get

$$\frac{\alpha_{mf} - \alpha_{m0}}{\theta_f - \theta_0} = N \quad (12.2)$$

For the successful interception of a stationary target the final missile heading should point towards the target, i.e,

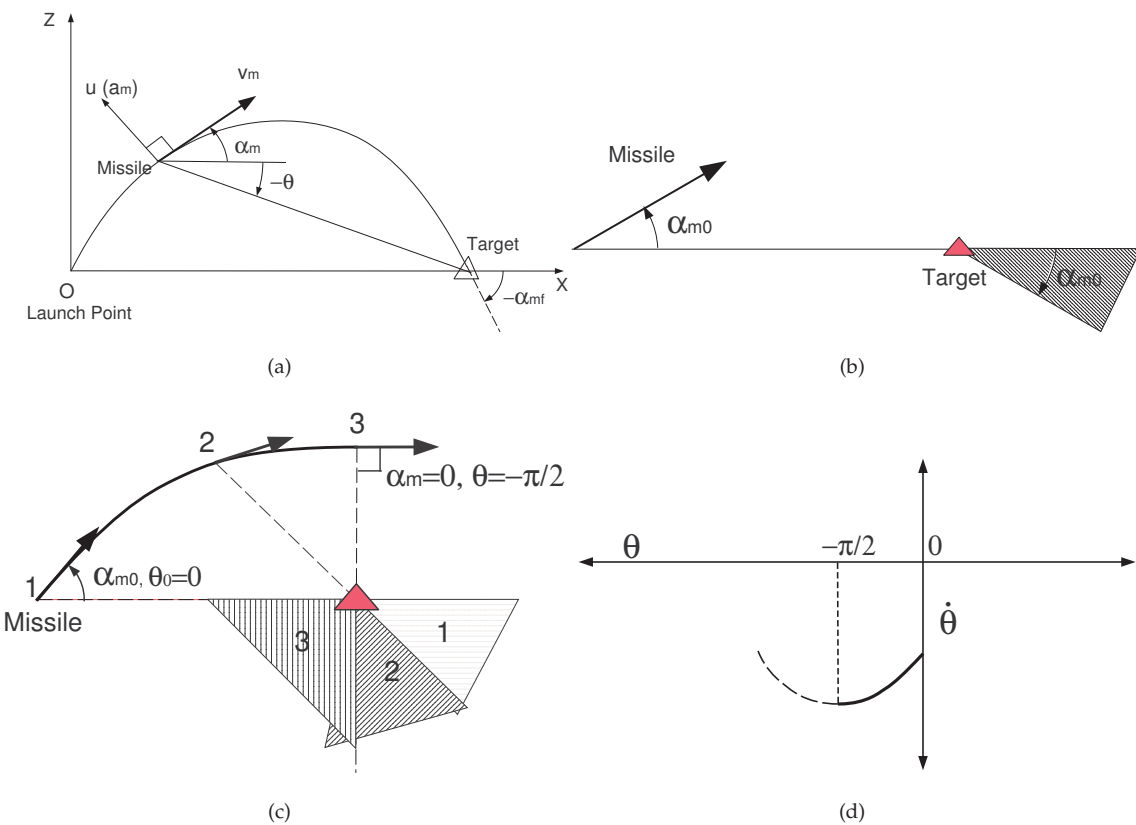


Figure 12.1: (a) Engagement geometry (b) PPN impact angle zone (c) Orientation trajectory (d) Line of sight rate variation on orientation trajectory

$$\theta_f = \alpha_{mf} \quad (12.3)$$

Using (12.2) and (12.3)

$$N = \frac{\alpha_{mf} - \alpha_{m0}}{\alpha_{mf} - \theta_0} \quad (12.4)$$

Solving for the impact angle ( $\alpha_{mf}$ )

$$\alpha_{mf} = \frac{\theta_0}{\left(1 - \frac{1}{N}\right)} - \frac{\alpha_{m0}}{(N-1)} \quad (12.5)$$

Eqn. (12.5) shows that the final impact angle is a function of the navigation constant  $N$ , other parameters being constant for a given initial engagement geometry.

The limiting impact angles using PPN are

$$\alpha_{mf} = \begin{cases} 2\theta_0 - \alpha_{m0} & \text{if } N = 2 \\ \theta_0 & \text{if } N \rightarrow \infty \end{cases} \quad (12.6)$$

that is.,

$$\alpha_{mf} \in [2\theta_0 - \alpha_{m0}, \theta_0], \quad N \geq 2 \quad (12.7)$$

The achievable impact angles using PN guidance for a surface to surface engagement (with  $\theta_0 = 0$ ) lie in the shaded region as shown in Fig. 12.1 (b). Impact angles with  $N < 2$  satisfying (12.4) can not be achieved by PN guidance since the lateral acceleration demand goes to infinity near the interception (See Shneydor (1998)).

### 12.3 Orientation Guidance

In a surface to surface engagement the desired set of impact angles should contain all angles from 0 to  $-\pi$ . As shown above, classical PPN ( $N \geq 2$ ) guidance will not cover the desired range of impact angles completely. For all impact angles outside the range given by (12.7) we propose an orientation guidance for initial phase of the missile flight. The missile follows the orientation trajectory as shown in Fig. 12.1(c) until the value of  $N$  satisfying the following relation becomes equal to 2.

$$\frac{\alpha_{mf} - \alpha_m}{\theta_f - \theta} = N \quad (12.8)$$

After which the missile follows PPN guidance with  $N = 2$ . As shown in Fig. 12.1(c) the achievable impact angle band using PPN guidance at the time of firing the missile is the shaded region 1. As the missile reaches point 2 on the orientation trajectory, the achievable band shifts to the shaded region 2. The purpose of the orientation guidance is to eventually take the missile to the point 3 in Fig. 12.1(c). At point 3,  $\theta = \frac{-\pi}{2}$  and  $\alpha_m = 0$  and thus using (12.7) we find that the impact band covers  $\alpha_{mf} = \frac{-\pi}{2}$  to  $\alpha_{mf} = -\pi$  as shown by the shaded region 3. The union of all shaded impact angle regions formed by tracing the orientation trajectory is  $\alpha_{mf} \in [0, -\pi]$ . The properties of orientation guidance are obtained analytically in the next subsection.

### 12.3.1 Orientation guidance command

For orientation guidance we propose the guidance law

$$a_m = N v_m \dot{\theta} \quad (12.9)$$

To execute the orientation maneuver, i.e., to take the missile from  $\theta = 0$  and  $\alpha_m = \alpha_{m0}$  to  $\theta = \frac{-\pi}{2}$  and  $\alpha_m = 0$ , we choose the navigation constant as

$$N = \frac{\alpha_{m0} - 0}{0 - (-\frac{\pi}{2})} = \frac{2}{\pi} \alpha_{m0} \quad (12.10)$$

Note that

$$N \in (0, 2) \quad \forall \alpha_{m0} \in (0, \pi) \quad (12.11)$$

From (12.9) and (12.10), the orientation guidance command is given by

$$a_m = \frac{2}{\pi} \alpha_{m0} v_m \dot{\theta} \quad (12.12)$$

### 12.3.2 Properties of the orientation trajectory

Using (12.12) we have, on the orientation trajectory

$$\dot{\alpha}_m = \frac{a_m}{v_m} = \frac{2}{\pi} \alpha_{m0} \dot{\theta} \quad (12.13)$$

Integrating with respect to time,

$$\alpha_m = \frac{2}{\pi} \alpha_{m0} \theta + \alpha_{m0} \quad (12.14)$$

Eqn. (12.14) relates the missile heading and the line of sight angle on the orientation trajectory.

**Proposition 1** On the orientation trajectory the line of sight rate  $\dot{\theta} < 0$  and the missile velocity vector rotation rate  $\dot{\alpha}_m < 0$

Proof. For a stationary target

$$\dot{\theta} = -\frac{v_m}{R} \sin(\alpha_{m0} - \theta) \quad (12.15)$$

Using (12.56) in (12.15)

$$\dot{\theta} = -\frac{v_m}{R} \sin \left[ \alpha_{m0} + \left( \frac{2}{\pi} \alpha_{m0} - 1 \right) \theta \right] \quad (12.16)$$

$$\Rightarrow \dot{\theta} < 0, \text{ for all } \theta \in [0 \text{ } - \pi/2], \alpha_{m0} \in (0, \pi) \quad (12.17)$$

With

$$\dot{\theta} = \begin{cases} -\frac{v_m}{R} \sin \alpha_{m0} & \text{if } \theta = 0 \\ -\frac{v_m}{R} & \text{if } \theta = -\frac{\pi}{2} \end{cases} \quad (12.18)$$

The line of sight rate variation with respect to line of sight angle is shown with a solid line in Fig. 12.1(d).

Also, using (12.13)

$$\dot{\alpha}_m = \frac{2}{\pi} \alpha_{m0} \dot{\theta} \quad (12.19)$$

From (12.19) and (12.17)

$$\dot{\alpha}_m < 0, \forall \theta \in [0 \text{ } - \pi/2], \alpha_{m0} \in (0, \pi) \quad (12.20)$$

□

**Proposition 2** On the orientation trajectory,  $\bigcup_{\theta \in [-\pi/2, 0]} [2\theta - \alpha_m, \theta] = [-\pi, 0]$

*Proof.* Let

$$q_1 = 2\theta - \alpha_m \quad (12.21)$$

$$q_2 = \theta \quad (12.22)$$

Differentiating  $q_1$  with respect to time

$$\dot{q}_1 = \dot{\theta} \left( 2 - \frac{\dot{\alpha}_m}{\dot{\theta}} \right) \quad (12.23)$$

Using (12.13) in (12.23)

$$\dot{q}_1 = \dot{\theta} \left( 2 - \frac{2}{\pi} \alpha_{m0} \right) \quad (12.24)$$

Since  $\dot{\theta} < 0$  (Proposition 1) and  $\alpha_{m0} \in (0, \pi)$

$$\dot{q}_1 < 0 \quad (12.25)$$

Similarly for  $q_2$ , using (12.22) and Proposition 1

$$\dot{q}_2 = \dot{\theta} < 0 \quad (12.26)$$

Let  $q_{1i}$  and  $q_{2i}$  be the values of  $q_1$  and  $q_2$  at the initial point (see point 1 on the missile trajectory in Fig. 12.6 (c)) on the orientation trajectory. At the initial point  $\theta = 0$  and  $\alpha_m = \alpha_{m0}$ . Using (12.26) and (12.22), we have

$$q_{1i} = -\alpha_{m0}, q_{2i} = 0 \quad (12.27)$$

Also, let  $q_{1t}$  and  $q_{2t}$  be the values of  $q_1$  and  $q_2$  at the terminal point (see point 3 on the missile trajectory in Fig. 12.6 (c)) on the orientation trajectory. At the terminal point  $\theta = -\pi/2$  and  $\alpha_m = 0$ . Using (12.26) and (12.22), we have

$$q_{1t} = -\pi, q_{2t} = -\pi/2 \quad (12.28)$$

Thus

$$\begin{aligned} \cup_{\theta \in [-\pi/2, 0]} [2\theta - \alpha_m, \theta] &= \cup_{\theta \in [-\pi/2, 0]} [q_1, q_2] \\ &= [q_{1i}, q_{2i}] \cup [q_{2t}, q_{2i}] \cup [q_{1t}, q_{1i}] \quad (\because \dot{q}_1 < 0, \dot{q}_2 < 0) \\ &= [-\alpha_{m0}, 0] \cup [-\pi/2, 0] \cup [-\pi, -\alpha_{m0}] = [-\pi, 0] \end{aligned} \quad (12.29)$$

□

## Module 11: Lecture 35

### Composite Guidance Law



**Keywords.** Impact angle control

#### 12.4 Composite Guidance law

Proposition 2 shows that there exists a point on the orientation trajectory so that if we consider that point as the initial missile position, then PN guidance law with  $N \geq 2$  will achieve any impact angle in  $[-\pi, 0]$ . The proposed composite PN guidance law follows the orientation guidance command given by (12.12) if the value of  $N$  satisfying (12.8) is less than 2 until (12.8) is satisfied with  $N = 2$ . After which PN guidance with  $N = 2$  is used. The proposed composite PN guidance law is given as,

$$a_m = N v_m \dot{\theta} \quad (12.30)$$

For engagement geometries with  $\frac{\alpha_{mf} - \alpha_{m0}}{\theta_f - \theta_0} \geq 2$

$$N = \frac{\alpha_{mf} - \alpha_{m0}}{\theta_f - \theta_0} \quad (12.31)$$

For engagement geometries with  $\frac{\alpha_{mf} - \alpha_{m0}}{\theta_f - \theta_0} < 2$

$$N = \begin{cases} \frac{2}{\pi} \alpha_{m0} & \text{if } \frac{\alpha_{mf} - \alpha_m}{\alpha_{mf} - \theta} < 2 \\ 2 & \text{if } \frac{\alpha_{mf} - \alpha_m}{\alpha_{mf} - \theta} = 2 \end{cases} \quad (12.32)$$

For realistic simulations a gravity compensation term is added to (12.30)

$$a_m = N v_m \dot{\theta} + g \cos \alpha_m \quad (12.33)$$

where  $N$  is given by (12.31) and (12.32).

#### 12.5 Simulations Results

To demonstrate the basic properties of the proposed guidance law we use a constant speed missile model. To prove the applicability of the proposed guidance law in a

realistic scenario we also use a realistic point mass missile model as a point mass flying over a flat non-rotating earth with given aerodynamic and thrust profiles. The detailed model is borrowed from Kee et al. (1998).

### 12.5.1 Constant speed missile model

The missile speed  $v_m = 300 \text{ m/sec}$  with  $(x_{m0}, z_{m0}) = (0, 0)$  and  $(x_{t0}, z_{t0}) = (5000 \text{ m}, 0)$ . Simulations are terminated for  $R < 0.1 \text{ m}$  and the corresponding impact angle errors are  $< 10^{-5} \text{ deg}$ .

**Case 1:**  $\frac{\alpha_{mf} - \alpha_{m0}}{\theta_f - \theta_0} < 2$

In this case we consider engagement geometries with  $\frac{\alpha_{mf} - \alpha_{m0}}{\theta_f - \theta_0} < 2$ . We choose  $\alpha_{m0} = 30^\circ$  and  $\alpha_{mf} = -120^\circ$  for the simulation. The corresponding value of  $\frac{\alpha_{mf} - \alpha_{m0}}{\theta_f - \theta_0} = 1.25$ . Solid lines in Fig. 12.2 (a) and Fig. 12.2 (b) show the missile trajectory and lateral acceleration history respectively. The missile follows the orientation trajectory in the first phase guidance and switches to PN guidance with  $N = 2$  as the value of the expression  $\frac{\alpha_{mf} - \alpha_m}{\theta_f - \theta}$  increases to 2 as shown in Fig. 12.2 (c). Results for classical PN with  $N = 1.25$  are shown in Fig. 12.2 with dashed lines. As expected, the lateral acceleration saturates to the value of  $-15g$  near the end resulting in a miss distance of  $13.05 \text{ m}$  with an impact angle error of  $45.99^\circ$ . The results show that the proposed guidance law achieves impact angles which cannot be achieved by classical PPN guidance. With the same engagement geometry, comparative study is carried out with the proportional navigation based composite impact angle constrained guidance law by Lu et al. (2006). Results are plotted in Fig. 12.2 with dotted lines. Fig. 12.2(a) shows the comparison of the missile trajectories of the two guidance laws. Missile trajectory guided by the existing guidance law applies the maximum possible lateral acceleration of  $15g$  (see Fig. 12.2(b)) to rapidly increase the value of the expression  $\frac{\alpha_{mf} - \alpha_m}{\theta_f - \theta}$  to 2 (see Fig. 12.2(c)). By executing such a maneuver the missile is forced away from the collision course to orient itself to follow PN guidance for the desired impact angle. The proposed PN orientation guidance scheme, on the other hand, applies a guidance command which is of the same sign as the line of sight rate. This keeps the missile closer to the collision course and requires lesser control effort with lesser time of flight. The total control effort  $\int a_m^2 dt$  for the proposed guidance law is 56829 units as against Lu's guidance law that uses 97994 units.

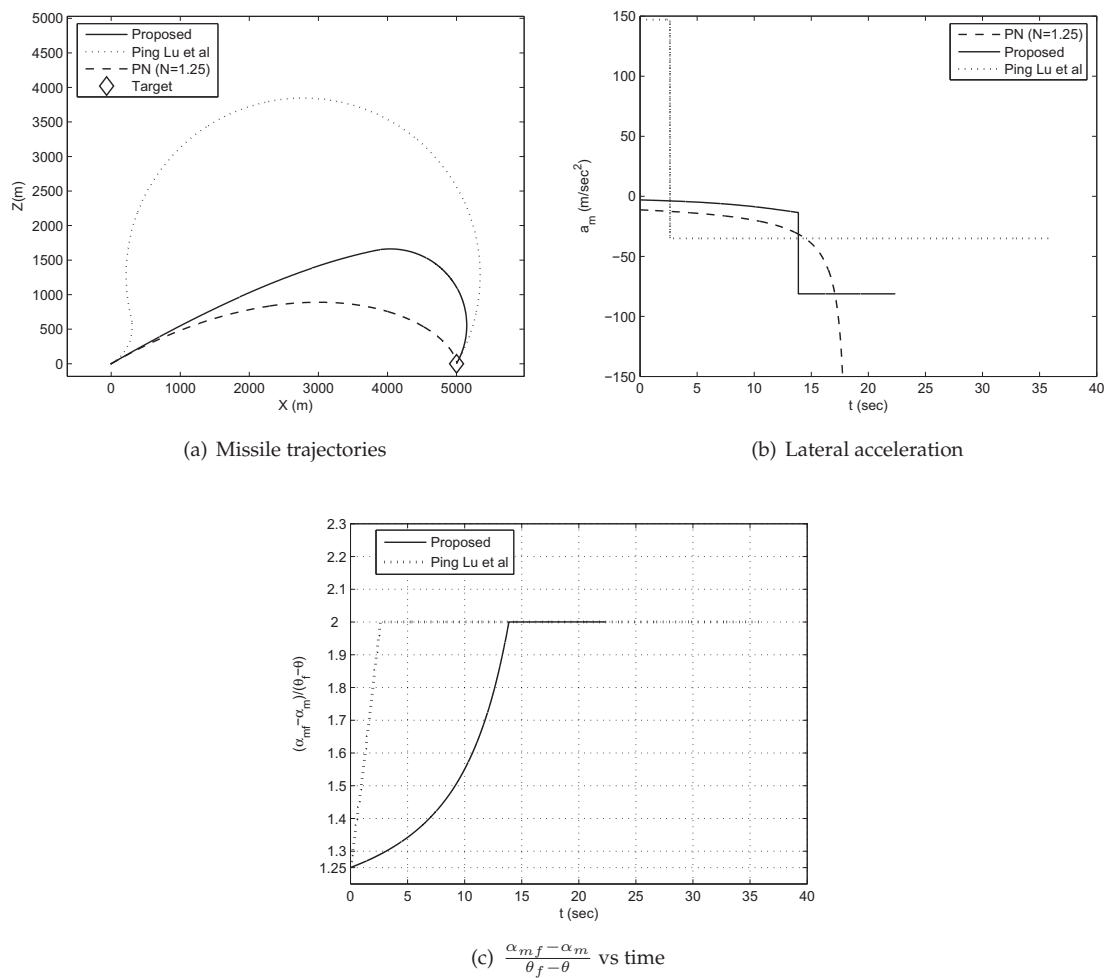


Figure 12.2: Case 1

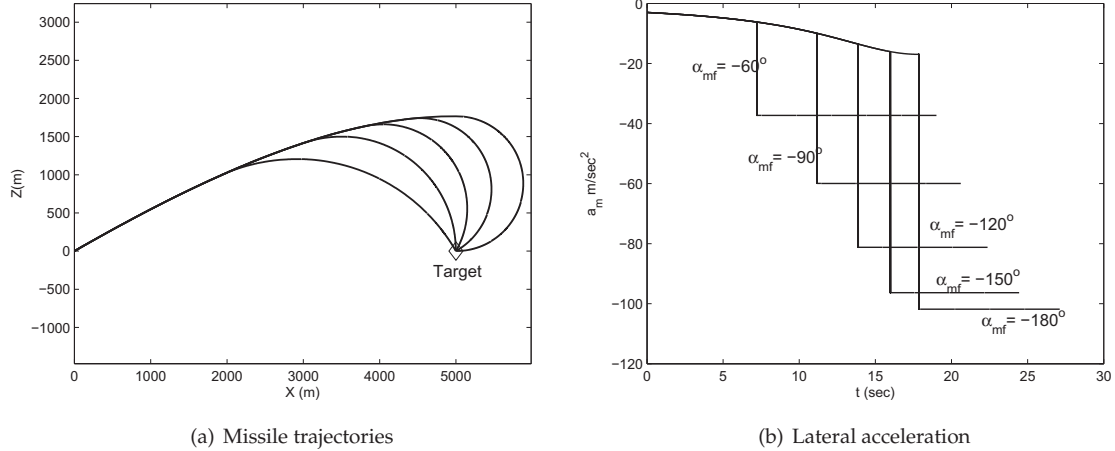


Figure 12.3: Results Case: 2

**Case 2:**  $\frac{\alpha_{mf} - \alpha_{m0}}{\theta_f - \theta_0} < 2$  *With different impact angles*

The engagement parameters for this case are same as in the case 2 with impact angles  $\alpha_{mf} = -60^\circ, -90^\circ, -120^\circ, -150^\circ$ , and  $-180^\circ$ . Missile trajectories and lateral acceleration profiles for the case are plotted in Fig. 12.3 (a) and Fig. 12.3 (b), respectively. The results prove the capability of the proposed guidance law for capturing all impact angles outside the capturability of the classical PPN guidance.

### 12.5.2 Realistic missile model

In this subsection simulations are carried out with the realistic missile model with  $(x_{m0}, z_{m0}) = (0, 0)$  and  $(x_{t0}, z_{t0}) = (10000 \text{ m}, 0)$ . All simulations are terminated for  $R < 0.1 \text{ m}$  and the corresponding impact angle errors  $< 10^{-3} \text{ deg}$ . The model is taken from Kee et al. (1998).

**Case 3:**  $\frac{\alpha_{mf} - \alpha_{m0}}{\theta_f - \theta_0} < 2$

In this study we consider desired impact angles to be outside the capture region of the classical PN guidance law. The missile is fired with  $\alpha_{m0} = 30^\circ$  with desired impact angles  $\alpha_{mf} = -60^\circ, -90^\circ, -120^\circ, -150^\circ$ , and  $-180^\circ$ . As the guidance loop is closed at  $t = 1.5 \text{ sec}$  and  $\theta(t = 1.5) \neq 0$  the orientation command derived from (12.10) is

modified as follows

$$N = \frac{(-0 - \alpha_{mglc})}{(-\frac{\pi}{2} - \theta_{glc})} = \frac{\alpha_{mglc}}{(\frac{\pi}{2} + \theta_{glc})} \quad (12.34)$$

where  $\alpha_{mglc}$  and  $\theta_{glc}$  are the missile heading and line of sight angle respectively at the time of guidance loop closure. The trajectories are plotted in Fig. 12.4 (a) which showing the successful interception of the target. The missile follows the orientation command first (see Fig. 12.4 (b)) and then switches to PPN guidance with  $N = 2$ . The lateral acceleration demand is higher for trajectories with higher overall angular turn. The corresponding speed profiles are plotted in Fig. 12.4 (c). Trajectories with higher lateral acceleration demand have higher induced drag resulting in greater loss of speed. The case study shows that the proposed guidance law achieves all impact angles outside the capture region of the classical PN guidance in a realistic surface to surface engagement scenario.

#### **Case 4: Missile with first order autopilot lag**

The analysis carried out in this chapter is based on Eqn. (12.1). Realistic missile systems have autopilot lag while executing the guidance command and Eqn. (12.1) is no longer valid. The proposed guidance law, in such cases, can be applied in a feedback form as

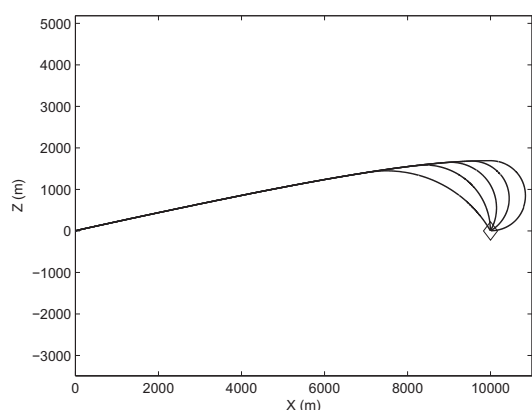
#### **Orientation navigation constant**

$$N = \frac{(-0 - \alpha_m)}{(-\frac{\pi}{2} - \theta)} = \frac{\alpha_m}{(\frac{\pi}{2} + \theta)} \quad (12.35)$$

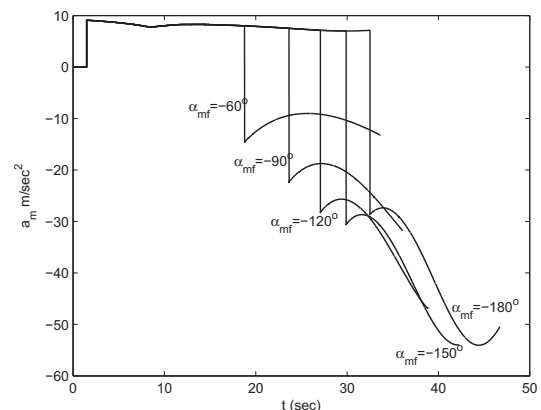
#### **Terminal navigation constant**

$$N = \frac{(\alpha_{mf} - \alpha_m)}{(\alpha_{mf} - \theta)} \quad (12.36)$$

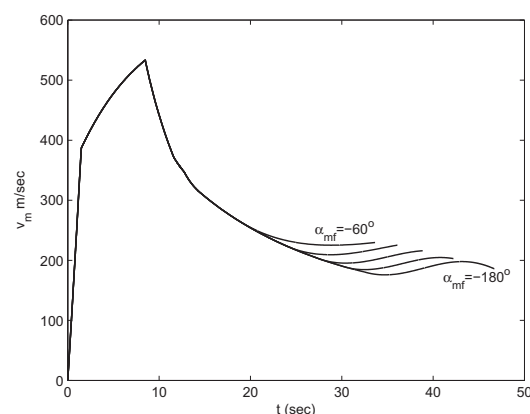
Note that the navigation constants given by (12.35) and (12.36), are no longer constants and are updated every guidance cycle. For simulations we consider a first order autopilot lag with the time constant  $\tau$ . Missile lateral acceleration profiles for  $\alpha_{m0} = 60^\circ$ ,  $\alpha_{mf} = -120^\circ$  and  $\tau = 0.2 \text{ sec}$  is plotted in Fig. 12.5 (a). The error in impact angle is  $0.0488^\circ$ . Impact angle error vs  $\tau$  for different impact angles is plotted in Fig. 12.5 (b). The impact angle errors are lesser than  $0.2^\circ$  for uncompensated first order delays upto  $0.4 \text{ sec}$ . The results show that guidance law can be implemented with autopilot lag with negligible error in any desired impact angle.



(a) Missile trajectories



(b) Lateral acceleration



(c) Missile speed profiles

Figure 12.4: Results: Case 3

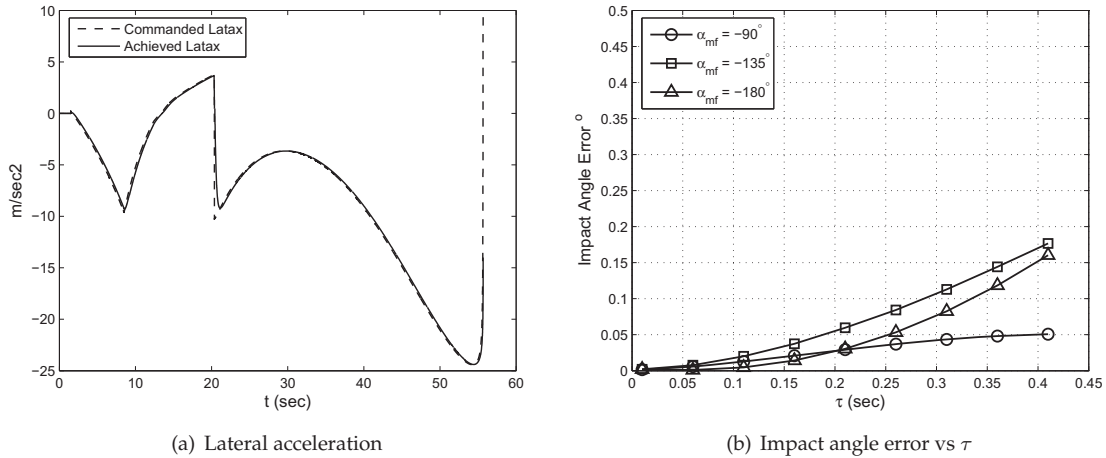


Figure 12.5: Results Case: 4

Here a composite guidance law is proposed for intercepting stationary targets with terminal impact angle constraint. The achievable impact angle set for the conventional PN guidance law with  $N \geq 2$  is limited. The proposed guidance law achieves all possible impact angles in a surface to surface engagement scenario. To obtain the impact angles outside the achievable set of conventional PN guidance law, an orientation guidance strategy is proposed with a navigation constant  $N < 2$ . The orientation navigation constant depends on the initial engagement geometry and the desired impact angle. It is shown mathematically that following the orientation trajectory all impact angles can be achieved. Simulations are carried out for kinematic and realistic missile models separately. The guidance law is implemented in a feedback mode for missiles having autopilot lag with negligible errors in the impact angle and miss distance.

## Module 11: Lecture 36

### Impact Angles Against a Moving Target

**Keywords.** Impact angle control, Orientation guidance

#### 12.6 Impact Angles Against a Moving Target with Proportional Navigation

The problem of achieving all impact angles against moving targets is addressed here. The idea of a two-stage PNG law proposed in the earlier section is further investigated and developed for non-stationary non-maneuvering targets. It is to be noted that for different values of  $N$ , the PNG law results in a set of impact angles against a moving target. However, studies on classical PNG law (Gelman (1971)) reveal that the value of  $N$  should be greater than a minimum value for the terminal lateral acceleration demand to be bounded. The achievable set of impact angles is derived for PNG law with the values of  $N$  satisfying the above mentioned constraint. To achieve the remaining impact angles an orientation guidance scheme is proposed for the initial phase of the interceptor trajectory. The orientation guidance law is also PNG law with  $N$  being a function of initial engagement geometry. It is proven that following the orientation trajectory, the interceptor can switch to  $N = 3$  and achieve any desired impact angle in a surface-to-surface engagement scenario.

Consider a planar engagement scenario shown in Fig. 12.6 (a). The target and the interceptor are constant speed point masses moving in a plane. The target is assumed to be non-maneuvering and the guidance objective is to intercept the target along a desired impact angle, denoted as  $\alpha_{mf}$ . Here  $\alpha_m$ ,  $\alpha_t$  and  $\theta$  are interceptor heading, target heading and line-of-sight angle, respectively. Proportional navigation guidance law is defined as,

$$\dot{\alpha}_m = N\dot{\theta} \quad (12.37)$$

Integrating (12.37) we get

$$\frac{\alpha_{mf} - \alpha_{m0}}{\theta_f - \theta_0} = N \quad (12.38)$$

where  $\theta_f$  is the line-of-sight angle at the time of interception. For interception the target

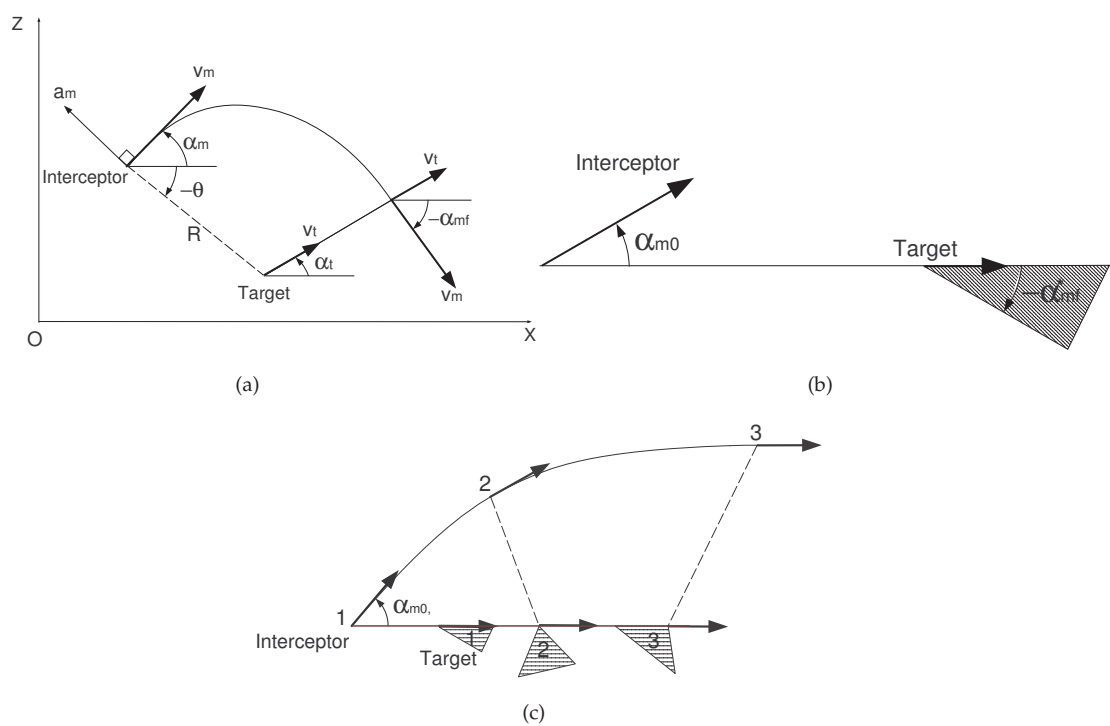


Figure 12.6: (a) Engagement geometry (b) PNG impact angle zone (c) Orientation trajectory

and interceptor velocity components normal to line-of-sight should be equal, that is,

$$v_m \sin(\alpha_{mf} - \theta_f) = v_t \sin(\alpha_t - \theta_f) \quad (12.39)$$

$$\Rightarrow \theta_f = \tan^{-1} \left[ \frac{\sin \alpha_{mf} - \beta \sin \alpha_t}{\cos \alpha_{mf} - \beta \cos \alpha_t} \right] \quad (12.40)$$

where,  $\beta$  is target to interceptor velocity ratio defined as  $\beta = \frac{v_t}{v_m}$ . Using (12.38) and (12.40) we have,

$$N = \frac{\alpha_{mf} - \alpha_{m0}}{\tan^{-1} \left[ \frac{\sin \alpha_{mf} - \beta \sin \alpha_t}{\cos \alpha_{mf} - \beta \cos \alpha_t} \right] - \theta_0} \quad (12.41)$$

Eqn. (12.41) relates the desired impact angle  $\alpha_{mf}$  to the navigation constant  $N$ . The sufficient condition (Guelman (1971)) on  $N$  for the terminal line-of-sight rate and hence the terminal lateral acceleration demand to be bounded is given as

$$N \geq 2(1 + \beta) \quad (12.42)$$

The targets moving on the surface are slower than the interceptor and we assume  $\beta \leq \frac{1}{2}$  in our domain of interest. Using (12.42), with  $\beta \leq \frac{1}{2}$  we have

$$N \geq 3 \quad (12.43)$$

Eqn. (12.43) limits the available set of  $N$  for achieving different impact angles. With this bound on  $N$  we now determine the set of impact angles that can be achieved by the PNG law. Eqn. (12.41) can be rewritten, assuming ground as the frame of reference with  $\alpha_t = 0$ , as

$$\frac{\sin \alpha_{mf}}{(\cos \alpha_{mf} - \beta)} = \tan \left( \frac{\alpha_{mf} - \alpha_{m0}}{N} + \theta_0 \right) \quad (12.44)$$

Solving (12.44) for  $\alpha_{mf}$  as  $N \rightarrow \infty$ , we have

$$\alpha_{mf} = \theta_0 + \sin^{-1}(-\beta \sin \theta_0) \quad (12.45)$$

Which is the collision heading at  $t = 0$ . With  $N \rightarrow \infty$  the interceptor instantaneously attains the collision course. Simplifying (12.44) with  $N = 3$ , we have

$$\frac{\sin \alpha_{mf}}{(\cos \alpha_{mf} - \beta)} = \tan \left( \frac{\alpha_{mf} - \alpha_{m0}}{3} + \theta_0 \right) \quad (12.46)$$

Let  $\alpha_{mf} = \alpha_{mf}^*$  be the solution of (12.46), then the limiting impact angles using PN guidance are given as

$$\alpha_{mf} = \begin{cases} \alpha_{mf}^* & \text{if } N = 3 \\ \theta_0 + \sin^{-1}(-\beta \sin \theta_0) & \text{if } N \rightarrow \infty \end{cases} \quad (12.47)$$

that is,

$$\alpha_{mf} \in [\alpha_{mf}^* \quad \theta_0 + \sin^{-1}(-\beta \sin \theta_0)], \quad N \geq 3 \quad (12.48)$$

Note that  $N \rightarrow \infty$  is the tightest turn possible and a smaller value of  $N$ , say  $N = 3$ , will result in a curved trajectory intercepting the surface target with an angle less than  $\alpha_{mf} < \theta_0 + \sin^{-1}(-\beta \sin \theta_0)$ . The achievable impact angles using PN guidance (with  $\theta_0 = 0$ ) lie in the shaded region as shown in Fig. 12.6 (b). Impact angles with  $N < 3$  satisfying (12.41) cannot be achieved by PN guidance against a non-stationary non-maneuvering target since the lateral acceleration demand may go to infinity near interception.

## 12.7 Orientation Guidance

We consider  $\alpha_{mf} \in [-\pi \ 0]$  as the desired set of impact angles against a surface moving target. As shown in the previous section, the classical PN guidance ( $N \geq 3$ ) does not cover this desired range of impact angles completely. For all impact angles outside the range given by (12.48) we propose an orientation guidance for initial phase of the interceptor flight. The interceptor follows the orientation trajectory as shown in Fig. 12.6 (c) until the value of  $N$  satisfying the following relation becomes equal to 3.

$$N = \frac{\alpha_{mf} - \alpha_m}{\tan^{-1} \left[ \frac{\sin \alpha_{mf} - \beta \sin \alpha_t}{\cos \alpha_{mf} - \beta \cos \alpha_t} \right] - \theta} \quad (12.49)$$

After which the interceptor follows PN guidance with  $N = 3$ . As shown in Fig. 12.6 (c) the achievable impact angle band using PN guidance at the time of firing the interceptor is the shaded region 1. As the interceptor reaches point 2 on the orientation trajectory, the achievable band shifts to the shaded region 2. The purpose of the orientation guidance is to eventually take the interceptor to the point 3 in Fig. 12.6 (c). Point 3 on the orientation trajectory is chosen such that, if the interceptor switches to  $N = 3$ , the resulting impact angle  $\alpha_{mf} = -\pi$ . Thus, the union of all shaded impact angle regions formed by tracing the orientation trajectory is  $\alpha_{mf} \in [0, -\pi]$ . This result is proved in Subsection 12.7.2.

### 12.7.1 Orientation guidance command

For orientation guidance we propose the PN guidance law

$$\dot{\alpha}_m = N\dot{\theta} \quad (12.50)$$

The orientation trajectory takes the interceptor from point 1 to point 3 as shown in Fig. 12.6 (c). At point 3 if the interceptor switches to PN guidance with  $N = 3$  the resulting impact angle is  $\alpha_{mf} = -\pi$ . Using (12.40), with  $\alpha_t = 0$  and  $\alpha_{mf} = -\pi$ , we have  $\theta_f = -\pi$ . Substituting the above values in (12.49), we have at point 3

$$\frac{-\pi - \alpha_m}{-\pi - \theta} = 3 \Rightarrow \alpha_m = 2\pi + 3\theta \quad (12.51)$$

We choose  $\alpha_m = 0$  and  $\theta = -2\pi/3$  satisfying (12.51) for the terminal point on the orientation trajectory. To execute the orientation maneuver, that is, to take the interceptor from  $(\theta, \alpha_m) = (0, \alpha_{m0})$  (see point 1 in Fig. 12.6 (c)) to  $(\theta, \alpha_m) = (-2\pi/3, 0)$  (see point 3 in Fig. 12.6 (c)), the orientation navigation constant is derived as,

$$N = \frac{\alpha_{m0} - 0}{0 - (-\frac{2\pi}{3})} = \frac{3\alpha_{m0}}{2\pi} \quad (12.52)$$

Note that

$$N \in (0, 1.5) \quad \alpha_{m0} \in (0, \pi) \quad (12.53)$$

Using (12.50) and (12.52), the orientation guidance command is given by

$$a_m = \left( \frac{3\alpha_{m0}}{2\pi} \right) v_m \dot{\theta} \quad (12.54)$$

The orientation navigation constant is a function of  $\alpha_{m0}$  and the effect of other engagement parameters like  $v_t$  (the target velocity) is reflected in the orientation command through  $\dot{\theta}$ .

### 12.7.2 Properties of the orientation trajectory

Using (12.54) we have, on the orientation trajectory

$$\dot{\alpha}_m = \frac{a_m}{v_m} = \frac{3}{2\pi} \alpha_{m0} \dot{\theta} \quad (12.55)$$

Integrating with respect to time,

$$\alpha_m = \frac{3}{2\pi} \alpha_{m0} \theta + \alpha_{m0} \quad (12.56)$$

Eqn. (12.56) relates the interceptor heading and the line-of-sight angle on the orientation trajectory.

**Proposition 1** *On the orientation trajectory the line-of-sight rate  $\dot{\theta} < 0$ .*

*Proof.* For a moving target, with  $\alpha_t = 0$ , we have

$$\dot{\theta} = \frac{v_t}{R} \sin(-\theta) - \frac{v_m}{R} \sin(\alpha_m - \theta) \quad (12.57)$$

Using (12.56) in (12.57), we have

$$\dot{\theta} = \frac{v_t}{R} \sin(-\theta) \left[ 1 - \frac{\sin[\alpha_{m0} + (\frac{3}{2\pi}\alpha_{m0} - 1)\theta]}{\beta \sin(-\theta)} \right] \quad (12.58)$$

On the orientation trajectory, that is,  $\theta \in [0, -2\pi/3]$ , we have

$$\sin \left[ \alpha_{m0} + \left( \frac{3}{2\pi}\alpha_{m0} - 1 \right) \theta \right] \in [\sin \alpha_{m0} \quad \sin(2\pi/3)] \quad (12.59)$$

$$\sin(-\theta) \in [0 \quad \sin(2\pi/3)] \quad (12.60)$$

Using (12.59) and (12.60) with  $\alpha_{m0} \in (0, \pi)$ , we have

$$\frac{\sin[\alpha_{m0} + (\frac{3}{2\pi}\alpha_{m0} - 1)\theta]}{\sin(-\theta)} \geq 1 \text{ for all } \theta \in [0, -2\pi/3] \quad (12.61)$$

From (12.61) with  $\beta \leq \frac{1}{2}$ , we have

$$\frac{\sin[\alpha_{m0} + (\frac{3}{2\pi}\alpha_{m0} - 1)\theta]}{\beta \sin(-\theta)} > 1 \text{ for all } \theta \in [0, -2\pi/3] \quad (12.62)$$

Using (12.62) in (12.58), we have

$$\dot{\theta} < 0 \quad (12.63)$$

□

**Proposition 2** *On the orientation trajectory,  $\bigcup_{\theta \in [-2\pi/3, 0]} \left[ \alpha_{mf}^* \theta + \sin^{-1}(-\beta \sin \theta) \right] = [-\pi, 0]$ .*

*Proof.* Let

$$q_1 = \frac{\alpha_{mf}^*}{3} \quad (12.64)$$

$$q_2 = \theta + \sin^{-1}(-\beta \sin \theta) \quad (12.65)$$

Using Eqn. (12.46) and substituting  $\alpha_m^* = 3q_1$  in it, we have on the orientation trajectory,

$$\frac{\sin(3q_1)}{(\cos(3q_1) - \beta)} = \tan\left(\frac{3q_1 - \alpha_m}{3} + \theta\right) \quad (12.66)$$

$$\Rightarrow \frac{\sin 2q_1 \cos q_1 + \cos 2q_1 \sin q_1}{\cos 2q_1 \cos q_1 - \sin 2q_1 \sin q_1 - \beta} = \tan(q_1 + a) \quad (12.67)$$

where,

$$a = \theta - \frac{\alpha}{3} \quad (12.68)$$

Simplifying (12.67), we have,

$$\frac{\sin 2q_1 \cos q_1 + \cos 2q_1 \sin q_1}{\cos 2q_1 \cos q_1 - \sin 2q_1 \sin q_1 - \beta} = \frac{\sin q_1 \cos a + \cos q_1 \sin a}{\cos q_1 \cos a - \sin q_1 \sin a} \quad (12.69)$$

Further simplifying, we have,

$$\frac{2 \sin q_1 \cos^2 q_1 + 2 \cos^2 q_1 \sin q_1 - \sin q_1}{2 \cos^3 q_1 - \cos q_1 - 2 \sin^2 q_1 \cos q_1 - \beta} = \frac{\sin q_1 \cos a + \cos q_1 \sin a}{\cos q_1 \cos a - \sin q_1 \sin a} \quad (12.70)$$

Rearranging and simplifying the terms, after cancelation, we have

$$-\beta \sin q_1 \cos a - \beta \cos q_1 \sin a = \sin 2q_1 \cos a - \cos 2q_1 \sin a \quad (12.71)$$

$$\Rightarrow \frac{-\beta \sin q_1 - \sin 2q_1}{-\cos 2q_1 + \beta \cos q_1} = \tan a \quad (12.72)$$

$$\Rightarrow \frac{\beta \sin q_1 + \sin 2q_1}{-\cos 2q_1 + \beta \cos q_1} = \tan(-a) \quad (12.73)$$

Substituting the value of  $a$  using (12.68) in (12.73), we have

$$\frac{\sin 2q_1 + \beta \sin q_1}{-\cos 2q_1 + \beta \cos q_1} = \tan\left(\frac{\alpha_m}{3} - \theta\right) \quad (12.74)$$

Differentiating (12.74) with respect to  $\theta$ , we have,

$$\frac{(-2 + \beta^2 + \beta \cos 3q_1)}{[-\cos 2q_1 + \beta \cos q_1]^2} \frac{dq_1}{d\theta} = \sec^2\left(\frac{\alpha_m}{3} - \theta\right) \left(\frac{1}{3} \frac{d\alpha_m}{d\theta} - 1\right) \quad (12.75)$$

Differentiating (12.56) with respect to  $\theta$  we have, on the orientation trajectory

$$\frac{d\alpha_m}{d\theta} = \frac{3}{2\pi} \alpha_{m0} \quad (12.76)$$

Using (12.76) in (12.75), we have,

$$\frac{(-2 + \beta^2 + \beta \cos 3q_1)}{[-\cos 2q_1 + \beta \cos q_1]^2} \frac{dq_1}{d\theta} = \sec^2\left(\frac{\alpha_m}{3} - \theta\right) \left(\frac{\alpha_{m0}}{2\pi} - 1\right) \quad (12.77)$$

$$\Rightarrow \frac{dq_1}{d\theta} > 0 \quad (12.78)$$

Since,

$$\frac{(-2 + \beta^2 + \beta \cos q_1)}{[-\cos 2q_1 + \beta \cos q_1]^2} < 0 \text{ for all } \beta \leq 1/2 \quad (12.79)$$

and

$$3 \sec^2 \left( \frac{\alpha_m}{3} - \theta \right) \left( \frac{\alpha_{m0}}{2\pi} - 1 \right) < 0 \text{ for all } \alpha_{m0} \in (0, \pi) \quad (12.80)$$

Differentiating (12.65) with respect to  $\theta$ , we have

$$\frac{dq_2}{d\theta} = \left[ 1 - \frac{\beta \cos \theta}{\sqrt{(\beta \cos \theta)^2 + 1 - (\beta)^2}} \right] > 0 \text{ (since } \beta \leq 1/2) \quad (12.81)$$

Using (12.78) and (12.81), we have

$$\begin{aligned} \bigcup_{\theta \in [-2\pi/3, 0]} [3q_1 \ q_2] = \\ [\min(3q_1(\theta = -2\pi/3), q_2(\theta = -2\pi/3)) \quad \max(3q_1(\theta = 0), q_2(\theta = 0))] \end{aligned} \quad (12.82)$$

At the initial point of the orientation trajectory (see point 1 in Fig. 12.6 (c)) with  $\theta = 0$ , we have, using (12.65)

$$q_2(\theta = 0) = 0 \quad (12.83)$$

which is the maximum possible impact angle is a surface to surface to engagement. Therefore, using (12.83), we have

$$\max(3q_1(\theta = 0), q_2(\theta = 0)) = 0 \quad (12.84)$$

At the terminal point of the orientation trajectory (see point 3 in Fig. 12.6 (c)) we have  $\theta = -2\pi/3$  and  $\alpha_m = 0$ . The values of  $\theta$  and  $\alpha_m$  at this point satisfy (12.66). Therefore, we have

$$3q_1(\theta = -2\pi/3) = \alpha_{mf}(\theta = -2\pi/3) = -\pi \quad (12.85)$$

which is the minimum possible impact angle for a surface to surface engagement. Using (12.85), we have,

$$\min(3q_1(\theta = -2\pi/3), q_2(\theta = -2\pi/3)) = -\pi \quad (12.86)$$

Using (12.84) and (12.86) in (12.82), we have,

$$\begin{aligned} \bigcup_{\theta \in [-2\pi/3, 0]} [3q_1 \ q_2] &= [\min(3q_1(\theta = -2\pi/3), q_2(\theta = -2\pi/3)) \quad \max(3q_1(\theta = 0), q_2(\theta = 0))] \\ &= [-\pi \ 0] \end{aligned} \quad (12.87)$$

□

## Module 11: Lecture 37

### The Proposed Guidance Law

**Keywords.** Impact Angle Control

#### 12.8 The Proposed Guidance law

Proposition 2 shows that for any impact angle in  $[-\pi, 0]$  there exists a point on the orientation trajectory from which the PN guidance law with  $N \geq 3$  results in desired interception. The proposed two stage PN guidance law follows the orientation guidance command given by (12.54) if the value of  $N$  satisfying (12.49) is less than 3 until (12.49) is satisfied with  $N = 3$ . After which  $N = 3$  is used. The proposed guidance law is given as

$$a_m = N v_m \dot{\theta} \quad (12.88)$$

For engagement geometries with  $\frac{\alpha_{mf} - \alpha_{m0}}{\theta_f - \theta_0} \geq 3$

$$N = \frac{\alpha_{mf} - \alpha_{m0}}{\theta_f - \theta_0} \quad (12.89)$$

For engagement geometries with  $\frac{\alpha_{mf} - \alpha_{m0}}{\theta_f - \theta_0} < 3$

$$N = \begin{cases} \frac{3\alpha_{m0}}{2\pi} & \text{if } t < t_s \\ 3 & \text{if } t \geq t_s \end{cases} \quad (12.90)$$

where,  $t_s$  is the switching time when the value of the expression  $(\alpha_{mf} - \alpha_m)/(\theta_f - \theta)$  increases to a value of 3.

#### 12.9 Simulation Results

##### 12.9.1 Constant speed interceptor

To demonstrate the basic properties of the proposed guidance law we use a constant speed interceptor model. We consider  $v_m = 300$  m/sec and  $v_t = 100$  m/sec with  $\alpha_t = 0$ , interceptor initial position  $(x_{m0}, z_{m0}) = (0, 0)$  and target initial position  $(x_{t0}, z_{t0}) = (5000 \text{ m}, 0)$ . Simulations are terminated for a closing range of ( $R < 0.1 \text{ m}$ ).

The interceptor has maximum lateral acceleration limit of  $\pm 15 \text{ g}$ .

### Case 1: A typical surface to surface engagement

We consider  $\alpha_{m0} = 30$  deg and  $\alpha_{mf} = -90$  deg for the simulation. The corresponding value of  $\frac{\alpha_{mf} - \alpha_{m0}}{\theta_f - \theta_0} = 1.1066$  which is outside the capturable impact angle set (see (12.48)) for the classical PNG ( $N \geq 3$ ). Solid lines in Fig. 12.7 (a) and Fig. 12.7 (b) show the interceptor trajectory and lateral acceleration profile, respectively, for the proposed guidance law. The engagement results in successful interception of the target with a negligible impact angle error of 0.034 deg. The variation in  $N$  is plotted Fig. 12.7 (c). The interceptor follows the orientation trajectory in the first phase of the guidance with  $N = 3/(2\pi)\alpha_{m0} = 3/(2\pi)\pi/6 = 0.25$ . With this smaller value of  $N$  the orientation lateral acceleration is also lower (see Fig. 12.7 (b)). On the orientation trajectory the value of  $(\alpha_{mf} - \alpha_m)/(\theta_f - \theta)$  increases from the initial value of 1.1066 (dashed lines see Fig. 12.7 (c)). The interceptor departs from the orientation trajectory as  $(\alpha_{mf} - \alpha_m)/(\theta_f - \theta)$  increases to 3 and switches to  $N = 3$ . Switching to a higher value of  $N$  results in a sudden increase in lateral acceleration (see Fig. 12.7 (b)). After switching to  $N = 3$  the lateral acceleration reduces to zero near interception. As  $(\alpha_{mf} - \alpha_m) \rightarrow 0$  and  $(\theta_f - \theta) \rightarrow 0$  near interception, the value of  $(\alpha_{mf} - \alpha_m)/(\theta_f - \theta) \rightarrow 1$  (see Fig. 12.7 (c)). Dashed lines in Fig. 12.7 (a) and (b) represent the corresponding results for classical PNG with  $N = 1.1066$ . The terminal lateral acceleration demand for PNG increases rapidly as (12.42) is violated and results in an impact angle error of 35.45 deg. We compare the capturability of the proposed guidance law with the existing trajectory shaping guidance law (Zarchan (2002)) which, by linearization, can also be simplified to obtain the optimal impact angle constrained guidance law [Ryoo et al. (2005)]. The trajectory shaping law is given as

$$a_m = 4V_c \dot{\theta} + 2V_c \frac{(\theta_f - \theta)}{t_{go}} \quad (12.91)$$

where  $V_c$  is the closing speed and  $t_{go}$  is the time-to-go. We vary the desired impact angle  $\alpha_{mf}$  and compare the performance in terms of the impact angle error. The comparative results are shown in Fig. 12.7 (d). The proposed guidance law captures all impact angles  $\alpha_{mf} \in [-\pi, 0]$  where as the trajectory shaping guidance law breaks down near head on kind of desired terminal geometries.

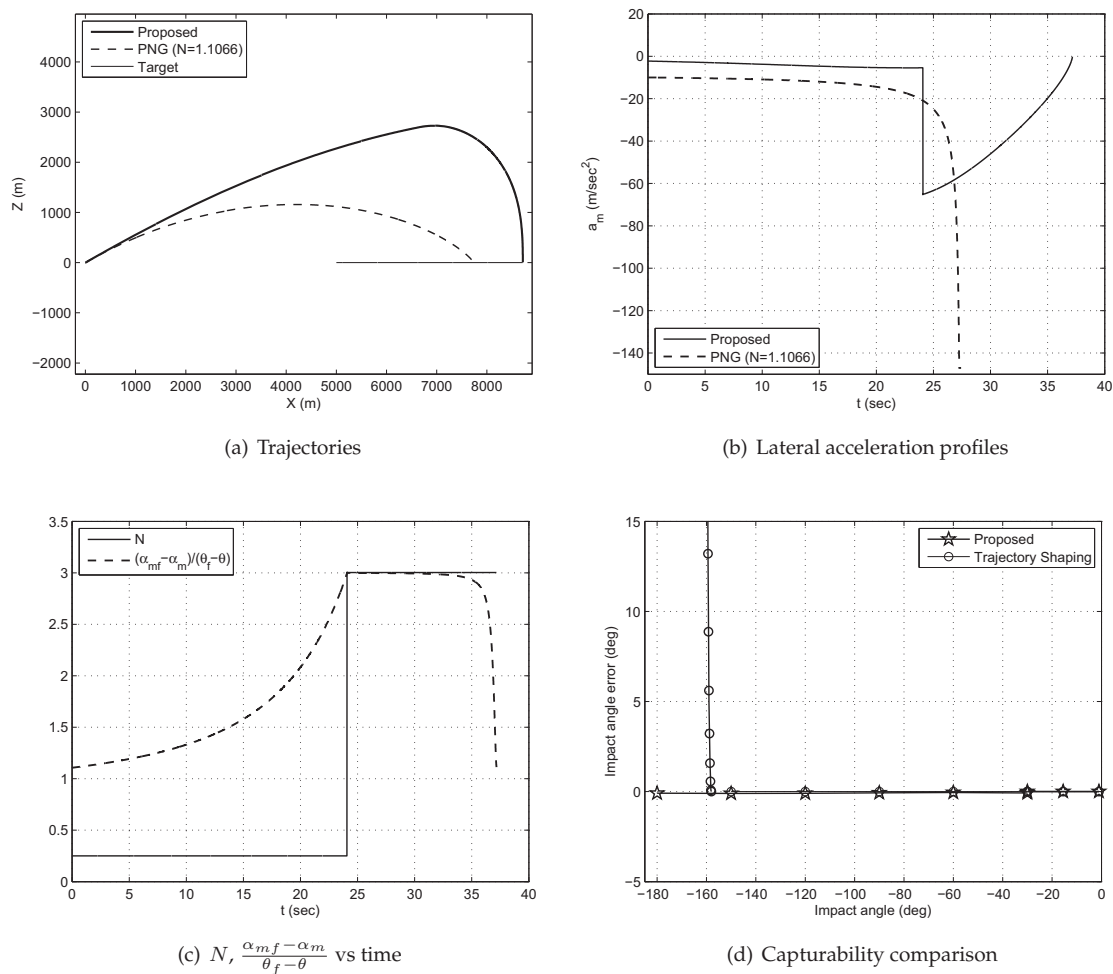


Figure 12.7: Results for Case 1: Constant speed interceptor model

### 12.9.2 Realistic interceptor

To validate the applicability of the proposed guidance law in realistic engagement scenarios we carry out simulations with a realistic interceptor model. The detailed model with vehicle and aerodynamic properties is described in Kee et al. (1998) and is borrowed here. All simulations are terminated for a closing distance of  $R < 0.5 \text{ m}$ . We consider  $\pm 20 \text{ g}$  limit on the maximum lateral acceleration. As the guidance loop is closed after the first boost phase is over the orientation command derived from (12.52) is modified, for realistic engagements, as

$$N = \frac{(-0 - \alpha_{mglc})}{\left(-\frac{2\pi}{3} - \theta_{glc}\right)} = \frac{\alpha_{mglc}}{\left(\frac{2\pi}{3} + \theta_{glc}\right)} \quad (12.92)$$

where  $\alpha_{mglc}$  and  $\theta_{glc}$  are the interceptor heading and line-of-sight angle ,respectively, at the time of guidance loop closure (glc). From (12.40), we see that for a predefined  $\alpha_{mf}$ , the value of  $\theta_f$  varies with interceptor speed. Thus, for realistic engagements, the value of  $\frac{(\alpha_{mf} - \alpha_m)}{(\theta_f - \theta)}$  may deviate from the switching value with variation in interceptor speed and may reduce below the minimum allowable limit of  $2(1 + \beta)$ . We include minimum allowable limit on the navigation constant in the terminal phase for realistic engagements. The modified guidance law, with the gravity compensation, is given as follows,

$$a_m = N v_m \dot{\theta} + g \cos \alpha_m \quad (12.93)$$

For engagement geometries with  $\frac{\alpha_{mf} - \alpha_{m0}}{\theta_f - \theta_0} \geq 3$

$$N = \frac{\alpha_{mf} - \alpha_m}{\theta_f - \theta} \quad (12.94)$$

For engagement geometries with  $\frac{\alpha_{mf} - \alpha_{m0}}{\theta_f - \theta_0} < 3$

$$N = \begin{cases} \frac{\alpha_{mglc}}{\left(\frac{2\pi}{3} + \theta_{glc}\right)} & \text{if } \frac{\alpha_{mf} - \alpha_m}{\theta_f - \theta} < 3, t < t_s \\ \frac{\alpha_{mf} - \alpha_m}{\theta_f - \theta} & \text{if } \frac{\alpha_{mf} - \alpha_m}{\theta_f - \theta} > 2(1 + \beta), t > t_s \\ 2(1 + \beta) & \text{if } \frac{\alpha_{mf} - \alpha_m}{\theta_f - \theta} \leq 2(1 + \beta), t > t_s \end{cases} \quad (12.95)$$

where  $t_s$  is the switching time which is defined as the time when the condition  $(\alpha_{mf} - \alpha_m)/(\theta_f - \theta) = 3$  is satisfied first and the interceptor leaves the orientation

trajectory. Note that the navigation constants in (12.94) and (12.95) are no longer constants and are updated at every guidance cycle.

### **Case 2: Realistic interceptor against a surface moving target**

We consider the desired impact angles to be outside the capture region of the classical PN guidance law ( $N \geq 3$ ) with  $v_t = 50 \text{ m/sec}$ ,  $(x_{m0}, z_{m0}) = (0, 0)$  and  $(x_{t0}, z_{t0}) = (5000 \text{ m}, 0)$ . The interceptor is launched with  $\alpha_{m0} = 30^\circ$ . The desired impact angles are  $\alpha_{mf} = -45, -90, -135$ , and  $-180 \text{ deg}$ . The trajectories are plotted in Fig. 12.8 (a) showing successful interception of the target. The interceptor flies unguided for the first boost phase (1.5 sec) and then follows the orientation command (see Fig. 12.8 (b)) before switching to attain the desired impact angle. The corresponding impact angle errors are less than 1 deg. The proposed guidance scheme is derived using the non-maneuvering target model. However (12.93) is a feedback guidance law that can be used against maneuvering targets. Next, we consider  $\alpha_{mf} = -10, -90, -180 \text{ deg}$  and simulate engagements with different target step acceleration  $a_t$  levels. The impact angle errors are plotted in Fig. 12.8 (c). Impact angle errors for  $\alpha_{mf} = -90, 180 \text{ deg}$  are less than 2 deg and 4 deg, respectively, for target accelerations up to  $4 \text{ m/sec}^2$ . For  $\alpha_{mf} = -10 \text{ deg}$  the target closes to the interceptor early leading to lateral acceleration saturation resulting in higher impact angle errors. To study the robustness of the proposed guidance law we simulate trajectories for values of first order autopilot lag time constant  $\tau$  up to 0.3 sec. The results, as plotted in Fig. 12.8 (d), show less than 2 deg error in impact angle for  $\alpha_{mf} = -90$  and  $\alpha_{mf} = -180 \text{ deg}$ . For  $\alpha_{mf} = -10 \text{ deg}$ , the lateral acceleration saturation causes an error of around 2.4 deg even with no delays and the error increases by 0.2 deg for the considered range of  $\tau$ .

A two stage PNG based guidance law for impact angle constrained interception of non-stationary non-maneuvering targets in a surface-to-surface engagement scenario is presented. The orientation guidance (PNG with a lower  $N$ ) facilitates the interceptor to switch to  $N = 3$  and achieve any desired impact angle for surface-to-surface applications. The feedback implementable form of the guidance law is also presented for realistic engagements. Simulation results show successful achievement of all impact angles for constant speed and realistic interceptor models, respectively. Robustness of the proposed guidance law is verified by realistic simulations with first order autopilot

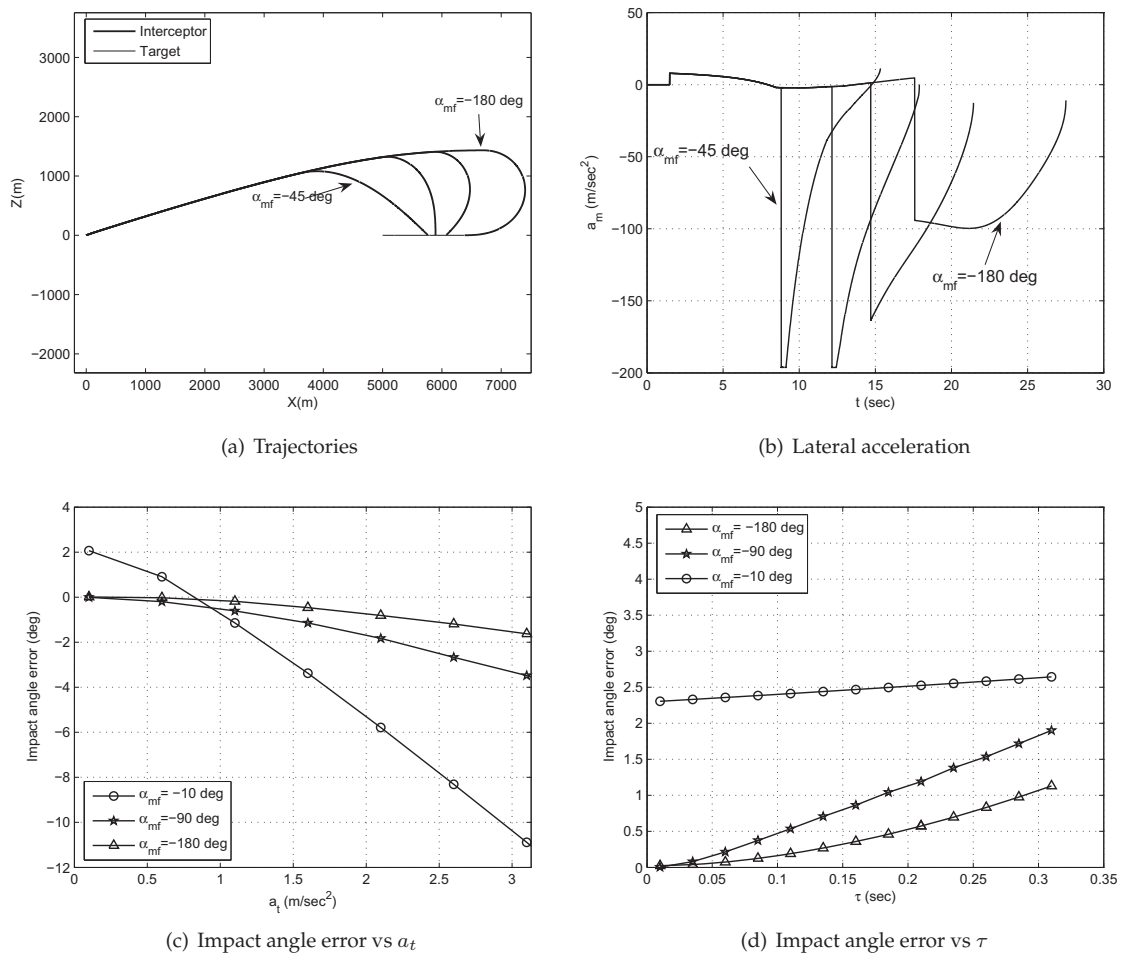


Figure 12.8: Results for Case 2: Realistic interceptor model

lags. Proportional navigation provides the inherent simplicity, robustness and implementation feasibility to the proposed guidance scheme. The impact angle performance is limited by the choice of impact angle in the maneuvering target scenario.

### References

1. M. Kim and K.V. Grider: Terminal guidance for impact attitude angle constrained flight trajectories, *IEEE Transactions on Aerospace and Electronic Systems*, **AES-9**, 6 (Dec.1973), 852-859.
2. R.J. York and H.L. Pastrick : Optimal terminal guidance with constraints at final time, *Journal of Spacecraft and Rockets*, **14** (June 1977), 381-382.
3. B.S. Kim, J.G. Lee and H.S. Han: Biased PNG law for impact with angular constraint, *IEEE Transactions on Aerospace and Electronic Systems*, **AES-34**, 1(Jan.1998), 277-288.
4. C.K. Ryoo, H. Cho and M.J. Tahk: Optimal guidance laws with terminal impact angle constraint, *Journal of Guidance, Control, and Dynamics*, Vol.28 No.4, July-August 2005, 724-732.
5. A. Ratnoo and D. Ghose: Impact Angle Constrained Interception of Stationary Targets, *Journal of Guidance, Control, and Dynamics*, Vol.31 No.6, November-December 2008, pp. 1816-1821.
6. A. Ratnoo and D. Ghose: SDRE based guidance law for impact angle constrained trajectories, *Proceedings of AIAA Guidance, Navigation and Control Conference and Exhibit* Hilton Head Island, SC, Aug 20-23, 2007.
7. P. Lu, D. B. Doman, and J. D. Schierman: Adaptive Terminal Guidance for Hypervelocity Impact in Specified Direction, *Journal of Guidance, Control, and Dynamics*, Vol.29 No.2, March-April 2006, 269-278.
8. N. A. Shneydor, *Missile Guidance and Pursuit*, 1st ed., Horwood Publishing, Chichester, 1998, pp. 104-105.

9. P. E. Kee, L. Dong, and C. J. Siong: Near optimal midcourse guidance law for flight vehicle, *Proceedings of 36th AIAA Aerospace Sciences Meeting and Exhibit*, Reno, NV, January 12-15, 1998.
10. M Guelman: A Qualitative Study of Proportional Navigation, *IEEE Transactions on Aerospace and Electronic Systems*, AES-7, (July 1971), 637-643.
11. Zarchan, P., *Tactical and Strategic Missile Guidance*, 4th ed., Vol. 199, AIAA, Virginia, 2002, pp. 541-568.

## Chapter 13

# Optimal Control Based Guidance Laws

### Module 12: Lecture 38 Linearized Proportional Navigation

**Keywords.** Optimal guidance, APN, Zero Effort miss, Linearized engagement

In this chapter we will formulate the guidance problem as an optimal control problem and use standard (and some non-standard!) techniques to solve them. Note that some of the notations used for the LOS angle, the missile flight path angle, and the target flight path angle, in this chapter are slightly different from those used in the previous chapters. However, this should not create any problems as all the notations are defined at appropriate places.

#### 13.1 Linearized Proportional Navigation

Before we address the problem of formulating the optimal control problem, we look at the linearized analysis of PN, not so as to obtain a solution to the trajectory equation or the lateral acceleration, as to obtain an idea about how the PN philosophy can be extended to get more advanced guidance laws and also for a better understanding of the PN philosophy itself. We will see that these notions will be of some help when we formulate the optimal control problem.

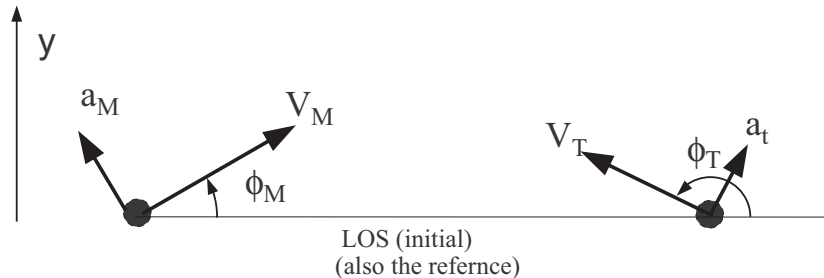


Figure 13.1: Linearized engagement

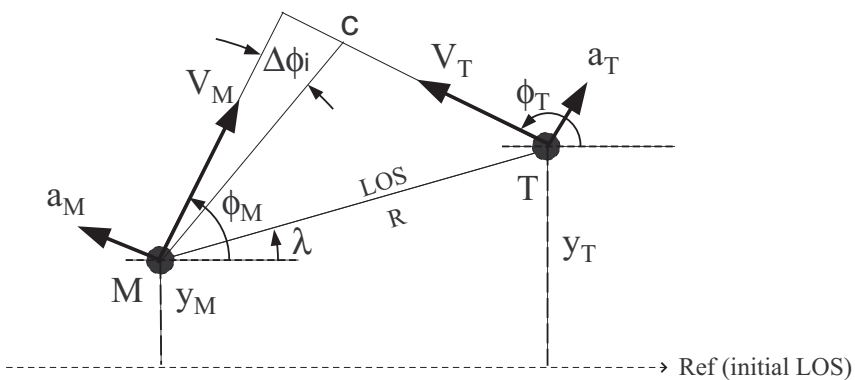


Figure 13.2: Linearized engagement

Consider the following engagement geometry – head-on or tail-chase (see Figure 13.1) in which the small angle approximations are valid.

For all practical purposes one may assume that as  $\phi_M$  is small and  $\phi_T$  is close to  $\pi$  or 0,  $a_M$  and  $a_T$  are also perpendicular to the initial LOS.  $\lambda$  is the LOS angle and is also small. Its initial value is assumed to be zero.

Refer to Figure 13.2. Let

$$y = y_T - y_M$$

where,  $y_T$  and  $y_M$  are the perpendicular displacements of the missile and target  $\perp$  to the initial LOS which is also the reference.

$$y = y_t - y_M \quad (13.1)$$

$$\ddot{y} \simeq a_T - a_M \text{ (small angle approximation)} \quad (13.2)$$

Suppose target does not maneuver, i.e,  $a_T = 0$  then

$$\ddot{y} = -a_M = -N'V_C\dot{\lambda} \quad (13.3)$$

where,  $V_C$  is the closing velocity which, with small angle approximation, is approximately equal to

$$V_C \simeq V_M + V_T \text{ or } V_C \simeq V_M - V_T \quad (\text{constant})$$

Integrating (13.3),

$$\dot{y} = -N'V_C\lambda + C_1 \quad (13.4)$$

But,

$$V_C = \frac{R}{t_f - t} \quad \lambda \simeq \frac{y}{R}$$

Substituting these in (13.4)

$$\dot{y} = -N' \frac{y}{t_f - t} + C_1$$

### 13.1.1 Heading Error

Suppose there is a heading error  $\Delta\phi_i$  then

$$y(0) = 0 \quad (13.5)$$

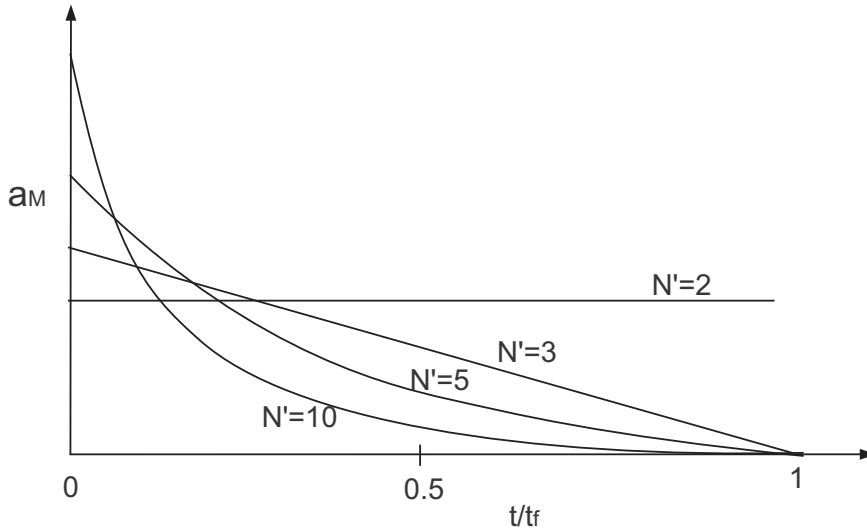
$$\dot{y}(0) = -V_M \sin \Delta\phi_i \simeq -V_M \Delta\phi_i \quad (13.6)$$

$$-V_M \Delta\phi_i = C_1 \quad (13.7)$$

Substituting the above, we get

$$\frac{dy}{dt} + \frac{N'}{t_f - t} y = -V_M \Delta\phi_i \quad (13.8)$$

This is the differential equation for a missile guided by the proportional navigation (PN) law subject to heading error but with a non-maneuvering target. The equation can

Figure 13.3: Variation of  $a_M$  due to non-zero heading error

be solved to obtain an expression for  $y(t)$ ,

$$y(t) = \frac{V_M \Delta \phi_i t_f}{N' - 1} \left(1 - \frac{t}{t_f}\right)^{N'} + K_1 t + K_2 \quad (13.9)$$

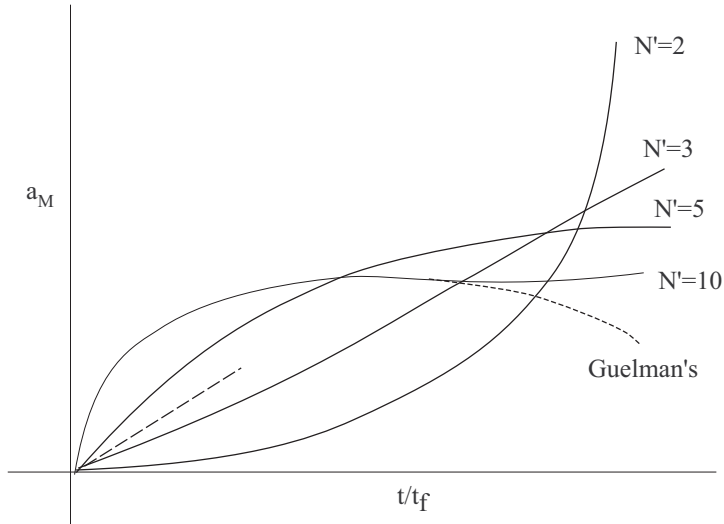
which when differentiated twice gives

$$a_M = \frac{-V_M \Delta \phi_i N'}{t_f} \left(1 - \frac{t}{t_f}\right)^{N'-2} \quad (13.10)$$

From which we also get

$$\begin{aligned} a_M(0) &= \frac{-V_M \Delta \phi_i N'}{t_f} \Rightarrow a_M(0) \propto \Delta \phi_i \\ a_M(0) &\propto \frac{1}{t_f} \\ a_M(0) &\propto V_M \end{aligned}$$

These can be plotted in Figure 13.3. The trend is close to the actual behaviour obtained from nonlinear analysis.

Figure 13.4: Variation of  $a_M$  due to target maneuver

### 13.1.2 Maneuvering target

Suppose heading error is zero, that is,  $\Delta\phi_i = 0$  but the target maneuvers with  $a_T$ . Then the equations become.

$$\ddot{y} = a_T - a_M = a_T - N' V_C \dot{\lambda} \quad (13.11)$$

With initial conditions,

$$\begin{aligned} y(0) &= 0 \\ \dot{y}(0) &= 0. \end{aligned}$$

The solution to this set of differential equations give rise to an expression for  $y(t)$  from which  $a_M$  is found as,

$$a_M = \frac{N'}{N' - 2} \left[ 1 - \left( 1 - \frac{t}{t_f} \right)^{N'-2} \right] a_T \quad (13.12)$$

What happens when  $N' \rightarrow 2$ ? Using L'Hospital's rule

$$\lim_{N' \rightarrow 2} a_M = -2a_T \log \left( 1 - \frac{t}{t_f} \right) \quad (13.13)$$

The results are plotted in Figure 13.4.

### 13.1.3 Zero Effort Miss

Consider the linearized version of the engagement geometry,

$$\begin{aligned}
 a_M &= N' V_C \dot{\lambda} = N' \frac{R}{t_{go}} \frac{d}{dt} \left( \frac{y}{R} \right) \quad \text{where } t_{go} = t_f - t \\
 &= N' \frac{R}{t_{go}} \frac{R\ddot{y} - y\dot{R}}{R^2} \\
 &= \frac{N'}{t_{go}} \left[ \frac{R^2\ddot{y}}{R^2} - \frac{Ry\dot{R}}{R^2} \right] \\
 &= \frac{N'}{t_{go}} \left[ \dot{y} + \frac{y}{t_{go}} \right] \\
 &= \frac{N'}{t_{go}^2} [y + \dot{y}t_{go}]
 \end{aligned}$$

At  $t = t_0$ ,  $y = y_0$ , and  $t_{go} = t_f - t_0$

The expression within the square brackets is called the Zero Effort Miss (ZEM) and is useful in deriving new guidance laws and understanding the philosophy behind PN guidance.

The ZEM is defined as the vertical separation between the missile and target at  $t_f$  if the missile does not use any control effort for the rest of the time-to-go and the target did not maneuver.

### 13.1.4 Augmented proportional navigation

Suppose the target maneuvers then the ZEM must be augmented by an additional term. In which case the ZEM is given by

$$\text{ZEM} = y + \dot{y}t_{go} + \frac{1}{2}a_T t_{go}^2$$

and the corresponding guidance law is given by,

$$a_M = \frac{N'}{t_{go}^2} \left[ y + \dot{y}t_{go} + \frac{1}{2}a_T t_{go}^2 \right]$$

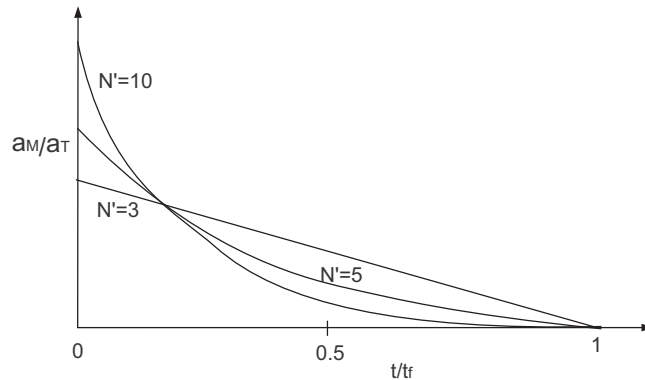


Figure 13.5: Variation of  $a_M$  for APN against a maneuvering target

This is called the augmented proportional navigation (APN) guidance law. It can also be rewritten as,

$$\begin{aligned} a_M &= \frac{N'}{t_{go}^2} [y_o + \dot{y}t_{go}] + \frac{\dot{N}}{2} a_T \\ &= N' V_C \dot{\lambda} + \frac{N'}{2} a_T \end{aligned}$$

The missile acceleration as a function of time for the APN law is given as

$$a_M = \frac{1}{2} a_T N' \left( 1 - \frac{t}{t_F} \right)^{N'-2}$$

This is plotted in Figure 13.5.



## Module 12: Lecture 39 Comparison between PN and APN

**Keywords.** PN, APN, Linearized kinematics

### 13.1.5 Comparison between PN and APN

In the Figures 13.6-13.8 several plots are given for different values of  $N$ .

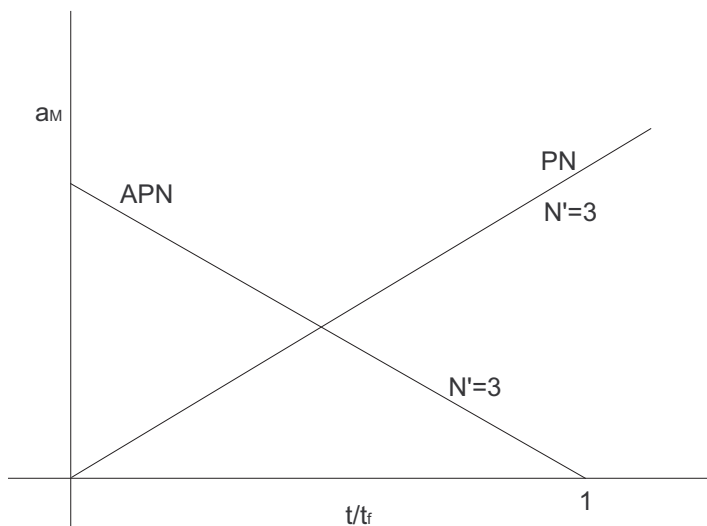
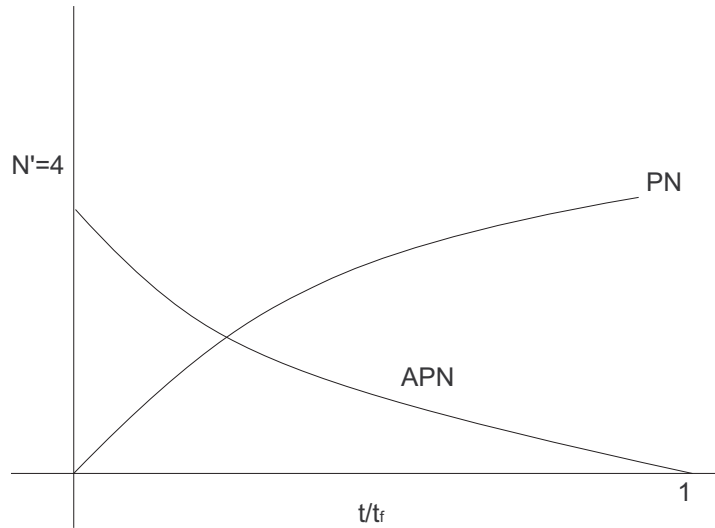
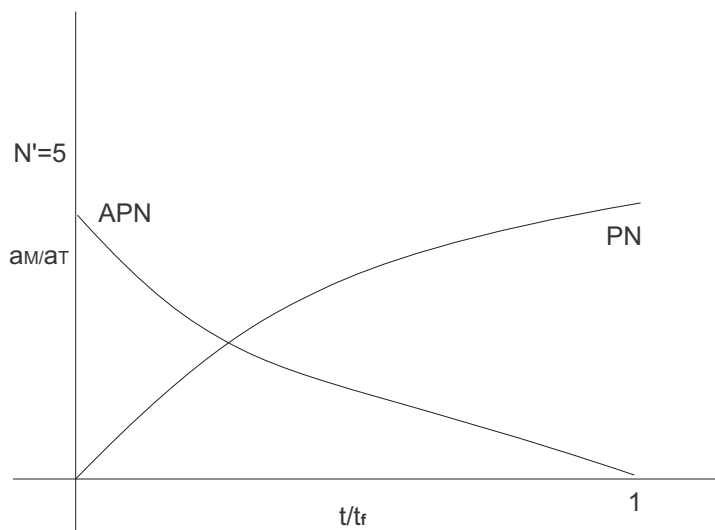


Figure 13.6:  $N' = 3$

APN is considered better so far as acceleration profiles are concerned because

1. Total acceleration needed is less
2. Saturation effect towards the beginning can be compensated later but not the other way.

However, PN has advantage in terms of the input information requirement and implementation.

Figure 13.7:  $N' = 4$ Figure 13.8:  $N' = 5$

The total acceleration effort can be quantized by the area under the acceleration curve. Since the acceleration is positive it can be done. Let us call this MIC ( Manuever Induced Cost)

$$\begin{aligned}\text{MIC}_{|PN} &= \int_0^{t_f} a_M \\ &= \int_0^{t_f} \frac{N' a_T}{N' - 2} \left( 1 - \left( 1 - \frac{t}{t_f} \right)^{N'-2} \right) dt \\ &= \frac{N' a_T t_f}{N' - 1} \\ \text{MIC}_{|APN} &= \int_0^{t_f} \frac{1}{2} a_T N' \left( 1 - \frac{t}{t_f} \right)^{(N'-2)} dt \\ &= \frac{1}{2} \frac{N' a_T t_f}{N' - 1} \\ \text{So, } \text{MIC } |_{APN} &= \left[ \frac{1}{2} \right] \text{MIC } |_{PN}\end{aligned}$$

This is true irrespective of the value of  $N' > 2$

### 13.2 Linear Optimal Control

Thus far only heuristic arguments have been used to “derive” APN guidance laws. It serves the purpose in as so far as the objective is to understand the guidance law but does not help much when a more rigorous analysis is required or when more advanced guidance laws need to be designed. Consider the linearized model shown in Fig. 13.9.

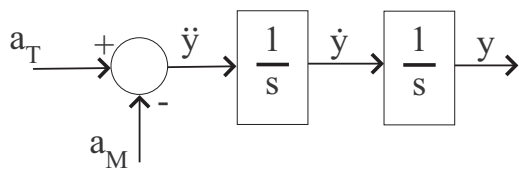


Figure 13.9: Linearized Model

This is a zero-lag model in which the relative acceleration is the difference between the target ( $a_T$ ) and the missile accelerations ( $a_M$ ). We wish to find a guidance law as a function of the system states. But there could be many such guidance laws. How does one choose a suitable guidance law? Obviously by defining what is “suitable”. So we

impose some restrictions and criteria on the performance of the guidance laws and try to find a unique law which satisfies them.

The most important restriction is, of course, that of zero miss-distance. This, after all, is the objective of the missile! But this is not enough.

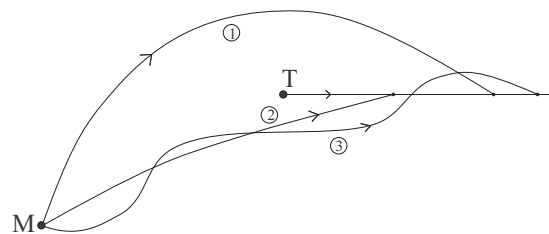


Figure 13.10: An example of different trajectories satisfying zero miss distance

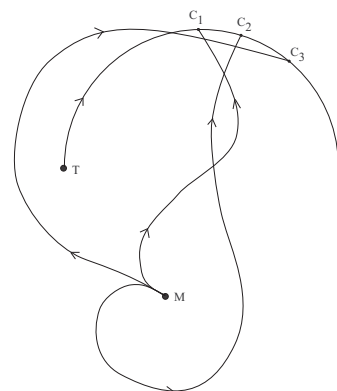


Figure 13.11: Another example of different trajectories satisfying zero miss distance

See the examples given in Figure 13.10 and 13.11. These examples only go to show that several trajectories which satisfy the requirements of zero miss distance are possible but not all of them are satisfactory so far as the total acceleration or time for intercept is concerned. It also tells us that we need to define a suitable performance measure to help us choose a suitable guidance law.

Let us consider one which minimizes the total control effort. The total control effort is now taken as the integral of the square of the commanded acceleration of the missile.

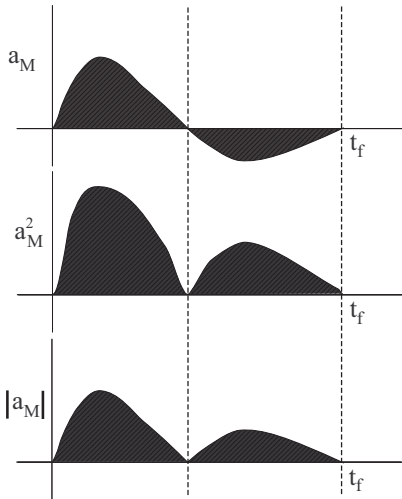


Figure 13.12: Different functions of  $a_M$  which can be used to minimize control effort

Why is the performance measure defined with a square term? See Figure 13.12. In the top figure  $a_M$  is plotted against time, and

$$\int_0^{t_f} a_M dt \simeq 0$$

This obviously does not represent control effort. But the next figure plots  $a_M^2$  against time and

$$\int_0^{t_f} a_M^2 dt > 0$$

Which appears to be a better representation of control effort. There is another justification to this formulation from the point of view of maneuver induced drag. We know that,

$$\begin{aligned} D &= \frac{1}{2} \rho V_m^2 S C_D \\ C_D &= C_{D_0} + C_{D_i} \\ C_{D_i} &= K C_L^2 = K \frac{m^2 a_M^2}{(\frac{1}{2} \rho V_m^2 S)^2} \end{aligned}$$

Thus, one component of the drag is proportional to the square of the maneuver latax, which implies that minimizing this term would lead to less wastage of energy used in

overcoming drag.

A valid question is why not

$$\int_0^{t_f} |a_M| dt$$

This is generally not used since it is not analytically tractable. So this is the third reason for using the integral square control effort since it has a quadratic form which helps in making the optimization problem convex and tractable.

So we formulate an optimal control problem to minimize the following

$$\int_0^{t_f} a_M^2 dt \quad \text{subject to} \quad y(t_f) = 0 \quad (13.14)$$

with state equations in linear form. This gives rise to what is known as a linear quadratic problem in optimal control theory.

Now take a look at the system of equations. (The states are  $y$ ,  $\dot{y}$ , and  $a_T$ )

$$\begin{aligned} \dot{y} &= \dot{y} \\ \ddot{y} &= a_T - a_M \\ \dot{a}_T &= 0 \end{aligned} \quad (13.15)$$

In the state space form it can be written as

$$\begin{bmatrix} \dot{y} \\ \ddot{y} \\ \dot{a}_T \end{bmatrix} = \begin{bmatrix} 0 & 1 & 0 \\ 0 & 0 & 1 \\ 0 & 0 & 0 \end{bmatrix} \begin{bmatrix} y \\ \dot{y} \\ a_T \end{bmatrix} + \begin{bmatrix} 0 \\ -1 \\ 0 \end{bmatrix} a_M(t) \quad (13.16)$$

which is of the form

$$\dot{X} = FX + Gu.$$

If  $t_f$  is known then

$$X(t_f) = \phi(t_f - t)X(t) + \int_t^{t_f} \phi(t_f - \tau)G(\tau)u(\tau)d\tau \quad (13.17)$$

where,  $\phi(t)$  is the state transition matrix given by

$$\phi(t) = \mathcal{L}^{-1} [(sI - F)^{-1}] = \exp^{Ft}. \quad (13.18)$$

Here

$$\begin{aligned}
 \exp^{Ft} &= I + Ft + \frac{F^2 t^2}{2!} + \frac{F^3 t^3}{3!} + \dots \\
 &= \begin{bmatrix} 1 & 0 & 0 \\ 0 & 1 & 0 \\ 0 & 0 & 1 \end{bmatrix} + \begin{bmatrix} 0 & t & 0 \\ 0 & 0 & t \\ 0 & 0 & 0 \end{bmatrix} + \frac{1}{2!} \begin{bmatrix} 0 & 0 & t^2 \\ 0 & 0 & 0 \\ 0 & 0 & 0 \end{bmatrix} \\
 &\quad + \frac{1}{3!} \begin{bmatrix} 0 & 0 & 0 \\ 0 & 0 & 0 \\ 0 & 0 & 0 \end{bmatrix} + \frac{1}{4!} \begin{bmatrix} 0 & 0 & 0 \\ 0 & 0 & 0 \\ 0 & 0 & 0 \end{bmatrix} + \dots \\
 &= \begin{bmatrix} 1 & t & t^2 \\ 0 & 1 & t \\ 0 & 0 & 1 \end{bmatrix}
 \end{aligned} \tag{13.19}$$

Using the above equations we get

$$\begin{bmatrix} y(t_f) \\ \dot{y}(t_f) \\ a_t(t_f) \end{bmatrix} = \begin{bmatrix} 1 & t_f - t & \frac{1}{2}(t_f - t)^2 \\ 0 & 1 & t_f - t \\ 0 & 0 & 1 \end{bmatrix} \begin{bmatrix} y(t) \\ \dot{y}(t) \\ a_t(t) \end{bmatrix} + \int_t^{t_f} \begin{bmatrix} 1 & t_f - \tau & \frac{1}{2}(t_f - \tau)^2 \\ 0 & 1 & t_f - \tau \\ 0 & 0 & 1 \end{bmatrix} \begin{bmatrix} 0 \\ -1(t) \\ 0 \end{bmatrix} a_M(\tau) d\tau \tag{13.20}$$

Considering only the first state

$$\begin{aligned}
 y(t_f) &= y(t) + (t_f - t)\dot{y}(t) + \frac{1}{2}(t_f - t)^2 a_T + \int_t^{t_f} [-(t_f - \tau)] a_M(\tau) d\tau \\
 &= f_1(t_f - t) - \int_t^{t_f} h_1(t_f - \tau) a_M(\tau) d\tau
 \end{aligned} \tag{13.21}$$

where,  $f_1(t_f - t) = y(t) + (t_f - t)\dot{y}(t) + \frac{1}{2}(t_f - t)^2 a_T$  and  $h_1(t_f - \tau) = (t_f - \tau)$ .

But to achieve zero miss-distance one must have  $y(t_f) = 0$  which means

$$f_1(t_f - t) = \int_t^{t_f} h_1(t_f - \tau) a_M(\tau) d\tau \tag{13.22}$$

Note that there could be several  $a_M(\tau)$  functions defined over  $[t, t_f]$  which satisfy this expression. This is where we use the minimum control effort criteria to obtain our result. We use what is known as Schwarz's inequality which is formally stated as follows:

Let  $\mathcal{X}$  be a measure space, with measure  $\mu$ . Let  $f$  and  $g$  be measurable functions on  $\mathcal{X}$ , with range in  $[0, \infty]$ . Then

$$\int_{\mathcal{X}} f g d\mu \leq \left[ \int_{\mathcal{X}} f^2 d\mu \right]^{\frac{1}{2}} \left[ \int_{\mathcal{X}} g^2 d\mu \right]^{\frac{1}{2}}. \tag{13.23}$$

and equality holds when  $f = kg$  where  $k$  is a real number. This is Schwarz inequality. We will use this now.

$$f_1^2(t_f - t) \leq \int_t^{t_f} h_1^2(t_f - \tau) d\tau \int_t^{t_f} a_M^2(\tau) d\tau \quad (13.24)$$

This gives

$$\int_t^{t_f} a_M^2(\tau) d\tau \geq \frac{f_1^2(t_f - t)}{\int_t^{t_f} h_1^2(t_f - \tau) d\tau} \quad (13.25)$$

Our objective was to minimize the left hand side of the inequality. From the inequality, we can see that the minimum possible value that the LHS can take is the value of RHS. That is, when the equality holds.

Again, according to Schwarz inequality, the equality sign holds when

$$a_M(\tau) = kh_1(t_f - \tau) \quad (13.26)$$

That is, one is a multiple of the other, and  $k$  is a constant. Substituting this we have

$$k^2 \int_t^{t_f} h_1^2(t_f - \tau) d\tau = \frac{f_1^2(t_f - t)}{\int_t^{t_f} h_1^2(t_f - \tau) d\tau} \quad (13.27)$$

From which

$$k = \frac{f_1(t_f - t)}{\int_t^{t_f} h_1^2(t_f - \tau) d\tau} \quad (13.28)$$

So

$$\begin{aligned} a_M(\tau) &= kh_1(t_f - \tau) \\ &= \left[ \frac{f_1(t_f - t)}{\int_t^{t_f} h_1^2(t_f - \tau) d\tau} \right] h_1(t_f - \tau) \end{aligned} \quad (13.29)$$

Substituting  $t_{go} = (t_f - t)$ , we get

$$a_M(\tau) = \left[ \frac{y(t) + t_{go}\dot{y}(t) + \frac{1}{2}t_{go}^2a_T}{\int_t^{t_f} (t_f - \tau)^2 d\tau} \right] (t_f - \tau) \quad (13.30)$$

$$= \frac{3}{t_{go}^3} \left[ y(t) + t_{go}\dot{y}(t) + \frac{1}{2}t_{go}^2a_T \right] (t_f - \tau) \quad (13.31)$$

This is the expression for  $a_M(\tau)$  for  $\tau \in [t, t_f]$ . But what is the value of  $a_M$  at current time  $t$ ? This is obtained by substituting  $\tau = t$ .

$$a_M(t) = \frac{3}{t_{go}^2} \left[ y(t) + \dot{y}(t)t_{go} + \frac{1}{2}a_T t_{go}^2 \right]. \quad (13.32)$$

This is the APN guidance law derived from linearized kinematics, and is equivalent to the PN guidance law when  $a_T = 0$ , (again in linearized kinematics framework).

Hence the optimal guidance law in the linearized kinematics is nothing but APN with effective navigation ratio equal to 3.

Remember that the “optimal” guidance law is in this form precisely for the case when the integral square control effort is being minimized. Suppose a different performance criteria (for example, minimum time) had been chosen, we would have obtained a different “optimal” guidance law.

Also note that the optimal guidance law is directly proportional to the ZEM and inversely proportional to  $t_{go}^2$ .

## Module 12: Lecture 40

### Optimal Control Guidance Laws



**Keywords.** Optimal guidance, Hamiltonian, Euler-Lagrange equation

#### 13.3 Optimal Control Based Guidance Laws

In this section we will show how optimal control theory gives rise to a two point boundary value problem, on solving which the guidance law can be obtained for a nonlinear guidance problem. We will consider several cases for this.

##### 13.3.1 Case 1: No terminal constraints; Fixed terminal time

Assumptions:

1. The missile flies for time  $t_f$  no matter what the initial condition geometry is.
2. It is not necessary to meet any terminal constraints.
3. However, to define the mission objective properly we can have a performance index which minimizes the miss-distance . This would be reasonable.

The system equations are

$$\begin{aligned} \dot{x}_1 &= f_1(x, u, t) & x_1(t_0) &= x_{10} \text{ (given)} \\ \vdots & & \vdots & \\ \dot{x}_n &= f_n(x, u, t) & x_n(t_0) &= x_{n0} \text{ (given)} \end{aligned}$$

where,  $x$  is the state vector,  $x = (x_1, \dots, x_n)$  and  $u$  is the control vector,  $u = (u_1, \dots, u_n)$  and  $t_0 \leq t \leq t_f$ ,  $t_f$  is known.

The performance index (to be minimized)

$$\min_u J = \phi[x(t_f), t_f] + \int_0^{t_f} L[x(t), u(t), t] dt$$

From a missile guidance perspective we may have  $\phi[x(t_f), t_f]$  as the miss-distance at  $t_f$  (i.e, the separation between M and T).

$$\int_{t_0}^{t_f} L[x(t), u(t), t] dt = \frac{1}{2} \int_{t_0}^{t_f} a_M^2 dt \quad (13.33)$$

Where,  $u = a_M$  is the guidance or control variable. (This is one dimensional vector,  $m = 1$ ).

Equation 13.33 represents the Integral-Square-Control Effort. Minimization of this also implies minimization of the Maneuver induced drag (MID).

#### The Hamiltonian:

$$H = L + \lambda^T f \quad (13.34)$$

$$= L + \lambda_1 f_1 + \dots + \lambda_n f_n \quad (13.35)$$

where,  $\lambda_1, \dots, \lambda_n$  are the Lagrangian Multipliers (or costates).

#### Euler-Lagrange Equations

#### Costate Equations

$$\begin{aligned} \dot{\lambda}_1 &= -\frac{\partial H}{\partial x_1} \\ &\vdots \\ \dot{\lambda}_n &= -\frac{\partial H}{\partial x_n} \end{aligned}$$

#### Boundary Conditions

$$\begin{aligned} \dot{\lambda}_1(t_f) &= \left. \frac{\partial \phi}{\partial x_1} \right|_{t=t_f} \\ &\vdots \\ \dot{\lambda}_n(t_f) &= \left. \frac{\partial \phi}{\partial x_n} \right|_{t=t_f} \end{aligned}$$

#### The optimal control

$$\begin{aligned} \frac{\partial H}{\partial u_1} &= 0 \\ &\vdots \\ \frac{\partial H}{\partial u_n} &= 0 \end{aligned}$$

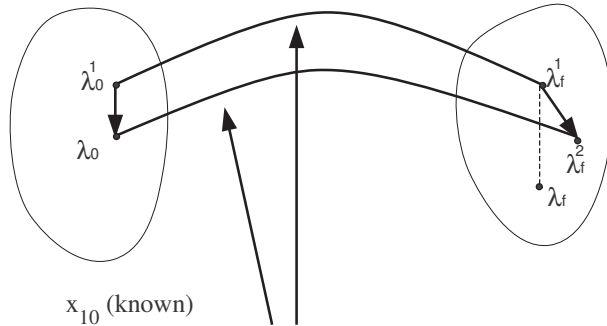


Figure 13.13: A Pictorial representation of solution technique

When we put all these equations along with the state equations together, we obtain what is known as a Two-Point-Boundary-Value-Problem (TPBVP).

Differential equations	Initial condition at $t_0$	Final condition at $t_f$
$\dot{x}_1 = f_1(x, u, t)$	$x_{10}$ (known)	$x_{1f}$ (unknown)
$\vdots$	$\vdots$	$\vdots$
$\dot{x}_n = f_n(x, u, t)$	$x_{n0}$ (known)	$x_{nf}$ (unknown)
$\dot{\lambda}_1 = -\frac{\partial H}{\partial x_1}$	$\lambda_{10}$ (unknown)	$\lambda_{1f}$ (known)
$\vdots$	$\vdots$	$\vdots$
$\dot{\lambda}_n = -\frac{\partial H}{\partial x_n}$	$\lambda_{n0}$ (unknown)	$\lambda_{nf}$ (known)

So the idea is to select the set  $(\lambda_{10}, \dots, \lambda_{n0})$  such that when the  $2n$  differential equations are integrated forward using the optimal control obtained from  $(\frac{\partial H}{\partial u} = 0)$ , we get the specified  $(\lambda_{1f}, \dots, \lambda_{nf})$ . Note that the  $x_{1f}, \dots, x_{nf}$  we obtain are of no consequence here since we do not have any constraints on the final state.

**A pictorial representation of the solution technique:** The iteration continues till we meet the boundary values and this gives the solutions to our problem.

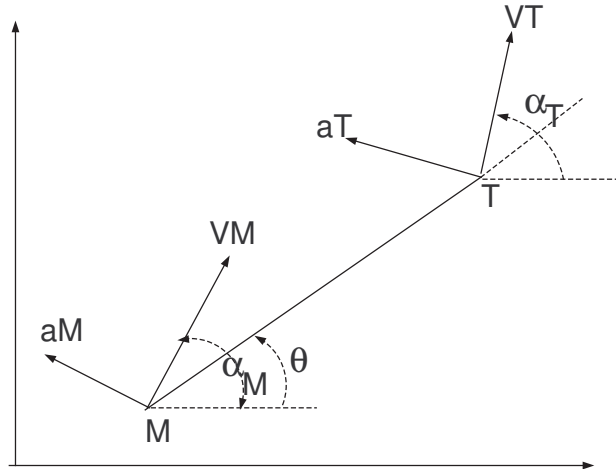


Figure 13.14: The engagement geometry

**An Example:** Consider a missile guidance problem. The control variable ( $a_M$ ) is the latax which is perpendicular to the missile velocity vector. The engagement geometry is given in 13.14:

The state equations are:

$$\begin{aligned}\dot{R} &= V_T \cos(\alpha_T - \theta) - V_M \cos(\alpha_M - \theta) \\ \dot{\theta} &= \frac{1}{R} \{V_T \sin(\alpha_T - \theta) - V_M \sin(\alpha_M - \theta)\} \\ \dot{\alpha}_M &= \frac{a_M}{V_M} \\ \dot{\alpha}_T &= \frac{a_T}{V_T}\end{aligned}$$

State is  $(R, \theta, \alpha_M, \alpha_T)$ .  $V_T$ ,  $V_M$ , and  $a_T$  are all constants over the complete engagement.

Initial time  $t_0 = 0$  and final time  $t_f$  is fixed.

$$\min_{a_M} J = K_1 R(t_f) + \frac{1}{2} K_2 \int_0^{t_f} a_M^2 dt$$

#### The Hamiltonian:

$$\begin{aligned}H &= \frac{1}{2} K_2 a_M^2 + \lambda_1 \{V_T \cos(\alpha_T - \theta) - V_M \cos(\alpha_M - \theta)\} \\ &\quad + \frac{\lambda_2}{R} \{V_T \sin(\alpha_T - \theta) - V_M \sin(\alpha_M - \theta)\} + \lambda_3 \frac{a_M}{V_M} + \lambda_4 \frac{a_T}{V_T}\end{aligned}$$

#### The Euler-Lagrange equations:

**Costate Equations:**

$$\begin{aligned}
\dot{\lambda}_1 &= -\frac{\partial H}{\partial R} = \frac{\lambda_2}{R^2} \{V_T \sin(\alpha_T - \theta) - V_M \sin(\alpha_M - \theta)\} \\
\dot{\lambda}_2 &= -\lambda_1 \{V_T \sin(\alpha_T - \theta) - V_M \sin(\alpha_M - \theta)\} \\
&\quad - \frac{\lambda_2}{R} \{-V_T \cos(\alpha_T - \theta) + V_M \cos(\alpha_M - \theta)\} \\
\dot{\lambda}_3 &= -\frac{\partial H}{\partial \alpha_M} = -\lambda_1 V_M \sin(\alpha_M - \theta) + \frac{\lambda_2}{R} V_M \cos(\alpha_M - \theta) \\
\dot{\lambda}_4 &= -\frac{\partial H}{\partial \alpha_T} = \lambda_1 V_T \sin(\alpha_T - \theta) - \frac{\lambda_2}{R} V_T \cos(\alpha_T - \theta)
\end{aligned}$$

**Boundary Conditions:**

$$\begin{aligned}
\lambda_1(t_f) &= \left. \frac{\partial \phi}{\partial R} \right|_{t=t_f} = K_1 \\
\lambda_2(t_f) &= \left. \frac{\partial \phi}{\partial \theta} \right|_{t=t_f} = 0 \\
\lambda_3(t_f) &= \left. \frac{\partial \phi}{\partial \alpha_M} \right|_{t=t_f} = 0 \\
\lambda_4(t_f) &= \left. \frac{\partial \phi}{\partial \alpha_T} \right|_{t=t_f} = 0
\end{aligned}$$

**The optimal Control:**

$$\begin{aligned}
\frac{\partial H}{\partial a_M} &= 0 \Rightarrow K_2 a_M + \frac{\lambda_3}{V_M} = 0 \\
\Rightarrow a_M &= \frac{\lambda_3}{K_2 V_M}
\end{aligned}$$

Using all these equations we obtain the Two Point Boundary Value Problem (TPBVP)

as:

The Differential Equation	Initial Condition at $t_0$	Final Condition at $t_f$
$\dot{R} = V_T \cos(\alpha_T - \theta) - V_M \cos(\alpha_M - \theta)$	$R_0$ known	$R_f$ unknown
$\dot{\theta} = \frac{1}{R} \{V_T \sin(\alpha_T - \theta) - V_M \sin(\alpha_M - \theta)\}$	$\theta_0$ known	$\theta_f$ unknown
$\dot{\alpha}_M = -\frac{\lambda_3}{K_2 V_M^2}$	$\alpha_{M0}$ known	$\alpha_{Mf}$ unknown
$\dot{\alpha}_T = \frac{a_T}{V_T}$	$\alpha_{T0}$ known	$\alpha_{Tf}$ unknown
$\dot{\lambda}_1 = \dots$	$\lambda_{10}$ unknown	$\lambda_{1f} = K_1$ (known)
$\dot{\lambda}_2 = \dots$	$\lambda_{20}$ unknown	$\lambda_{2f} = 0$ (known)
$\dot{\lambda}_3 = \dots$	$\lambda_{30}$ unknown	$\lambda_{3f} = 0$ (known)
$\dot{\lambda}_4 = \dots$	$\lambda_{40}$ unknown	$\lambda_{4f} = 0$ (known)

If you solve this problem and find the value of  $\lambda_3$  at every moment in time from  $t_0$  to  $t_f$  then you also know the optimal guidance  $a_M$  from 0 to  $t_f$  at every instant in time.

### 13.3.2 Case II: Some state variables specified at a fixed terminal time

Same state equations,  $t_f$  is known (fixed). But, given

$$\min_u J = \phi(x(t_f), t_f) + \int_0^{t_f} L dt$$

#### Terminal Conditions

$$\begin{aligned} x_1(t_f) &= x_{1f} \text{ (known)} \\ &\vdots \\ x_q(t_f) &= x_{qf} \text{ (known)} \end{aligned}$$

$$H = L + \lambda_1 f_1 + \dots + \lambda_n f_n$$

#### Euler Lagrange Equations

#### Costate Equations

$$\begin{aligned} \dot{\lambda}_1 &= -\frac{\partial H}{\partial x_1} \\ &\vdots \\ \dot{\lambda}_n &= -\frac{\partial H}{\partial x_n} \end{aligned}$$

#### Boundary conditions

$$\lambda_{jf}(t_f) = \begin{cases} \lambda_{jf}, & j = 1, \dots, q \text{ (unknown)} \\ \left. \frac{\partial \phi}{\partial x_j} \right|_{t=t_f}, & j = q+1, \dots, n \text{ (known)}. \end{cases}$$

$$\frac{\partial H}{\partial u} = 0 \text{ (given the optimal guidance value).}$$

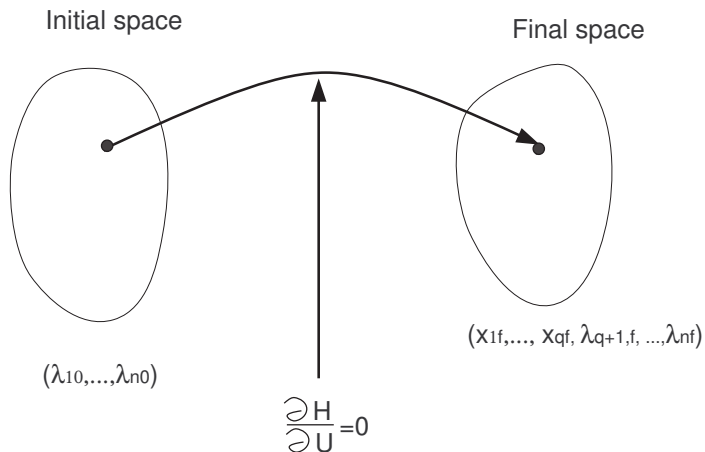


Figure 13.15: A Pictorial representation of solution technique

TPBVP

Differential Equation	Initial Condition at $t_0$	Final Condition at $t_f$
$\dot{x}_1 = f_1(x, u, t)$	$x_{10}$ (known)	$x_{1f}$ (known)
$\vdots$	$\vdots$	$\vdots$
$\dot{x}_q = f_q(x, u, t)$	$x_{q0}$ (known)	$x_{qf}$ (known)
$\dot{x}_{q+1} = f_q(x, u, t)$	$x_{q+1,0}$ (known)	$x_{q+1,f}$ (unknown)
$\vdots$	$\vdots$	$\vdots$
$\dot{x}_n = f_n(x, u, t)$	$x_{n0}$ (known)	$x_{nf}$ (unknown)
$\dot{\lambda}_1 = -\frac{\partial H}{\partial x_1}$	$\lambda_{10}$ (unknown)	$\lambda_{1f}$ (unknown)
$\vdots$	$\vdots$	$\vdots$
$\dot{\lambda}_q = -\frac{\partial H}{\partial x_{q0}}$	$\lambda_{q0}$ (unknown)	$\lambda_{qf}$ (unknown)
$\dot{\lambda}_1 = -\frac{\partial H}{\partial x_{q+1,0}}$	$\lambda_{q+1,0}$ (unknown)	$\lambda_{q+1,f}$ (known)
$\vdots$	$\vdots$	$\vdots$
$\dot{\lambda}_n = -\frac{\partial H}{\partial x_n}$	$\lambda_{n0}$ (unknown)	$\lambda_{nf}$ (known)

### 13.3.3 Case III: Functions of state variables specified at a fixed terminal time

State equations are the same

$$\begin{aligned}\psi_1[x(t_f), t_f] &= 0 \\ &\vdots \\ \psi_q[x(t_f), t_f] &= 0\end{aligned}$$

Same  $J$ . Lagrangian is  $H = L + \lambda^T f$ .

$\frac{\partial H}{\partial u} = 0$  to get the guidance law.

$$\dot{\lambda}^T = -\frac{\partial H}{\partial x}$$

#### Boundary Condition

$$\lambda_j(t_f) = \left( \frac{\partial \phi}{\partial x_j} + \sum_{i=1}^q \gamma_i \frac{\partial \psi_i}{\partial x_j} \right)_{t=t_f}, \quad j = 1, \dots, q$$

Here,  $\gamma_j$  are the unknowns and the  $(n - q)$  known conditions are given through,

$$\begin{aligned}\lambda_1(t_f) &= \frac{\partial \phi}{\partial x_1} + \gamma_1 \frac{\partial \psi_1}{\partial x_1} + \dots + \gamma_q \frac{\partial \psi_q}{\partial x_1} \\ &\vdots \\ \lambda_n(t_f) &= \frac{\partial \phi}{\partial x_n} + \gamma_1 \frac{\partial \psi_1}{\partial x_n} + \dots + \gamma_q \frac{\partial \psi_q}{\partial x_n}\end{aligned}$$

Thus we have  $n$  equations and  $q$  unknowns.

#### TPBVP

Differential Equations	Initial Condition	Final Condition
$\dot{x}_1 = f_1(x, u, t)$	$x_1(t_0) = x_{10}$ (known)	$x_{1f}$ (unknown)
$\vdots$	$\vdots$	$\vdots$
$\dot{x}_n = f_n(x, u, t)$	$x_n(t_0) = x_{n0}$ (known)	$x_{nf}$ (unknown)
$\dot{\lambda}_1 = -\frac{\partial H}{\partial x_1}$	$\lambda_1(t_0) = \lambda_{10}$ (unknown)	$\lambda_1(t_f) = \frac{\partial \phi}{\partial x_1} + \gamma_1 \frac{\partial \psi_1}{\partial x_1} + \dots + \gamma_q \frac{\partial \psi_q}{\partial x_1}$
$\vdots$	$\vdots$	$\vdots$
$\dot{\lambda}_n = -\frac{\partial H}{\partial x_n}$	$\lambda_n(t_0) = \lambda_{n0}$ (unknown)	$\lambda_n(t_f) = \frac{\partial \phi}{\partial x_n} + \gamma_1 \frac{\partial \psi_1}{\partial x_n} + \dots + \gamma_q \frac{\partial \psi_q}{\partial x_n}$

$$\psi_1(x(t_f), t_f) = 0$$

⋮

$$\psi_q(x(t_f), t_f) = 0$$

### 13.3.4 Case IV: Some State Variables specified at an unspecified terminal time (Including minimum time problems)

$x_{1f}, \dots, x_{qf}$  specified. One additional condition

$$\left( \frac{\partial \phi}{\partial t} + H \right)_{t=t_f} = 0$$

This determines  $t_f$ .

For minimum time problem note that

$$\begin{aligned} J &= \phi(x(t_f), t_f) = t_f \implies \phi = t_f \\ \text{or } J &= \int_0^{t_f} dt \implies L = 1 \end{aligned}$$

$$\begin{aligned} H &= \lambda^T f + L \\ \dot{\lambda}^T &= -\frac{\partial H}{\partial x} \end{aligned}$$

$$\lambda_j(t_f) = \begin{cases} \lambda_{jf} & j = 1, \dots, q \text{(unknown)} \\ \frac{\partial \phi}{\partial x_j}_{t=t_f} & j = q+1, \dots, n \end{cases}$$

## 13.4 Conclusions

In this chapter we looked at both the linear and the non-linear formulation of a guidance problem in the optimal control framework. The linear formulation led to closed-form solution which had some similarities with the proportional navigation law. But the non-linear formulation led to a two point boundary value problem which is not easy to solve computationally. In the next chapter we will present a singular perturbation technique to solve such problems.

## References

P. Zarchan: Tactical and Strategic Missile Guidance, 4th ed, AIAA Publishers, 2002.